

# List of contents

|   |           |
|---|-----------|
| <b>Riassunto .....</b>  | <b>1</b>  |
| <b>Introduction.....</b>  | <b>6</b>  |
| <b>Part 1. Tides and tidal power.....</b>   | <b>13</b> |
| <b>1. Tides.....</b>  | <b>14</b> |
| 1.1 Introduction .....  | 14        |
| 1.2 Tidal range variation: springs and neaps.....                                   | 16        |
| 1.3 Tidal amplitude .....   | 17        |
| 1.4 Tidal constituents .....  | 18        |
| 1.5 Tidal phase .....   | 18        |
| 1.6 Tidal physics .....   | 20        |
| 1.6.1 Background.....   | 20        |
| 1.6.2 Tidal forces .....  | 20        |
| 1.6.3 Laplace tidal equation .....  | 22        |
| 1.7 Tidal observations and predictions.....   | 23        |
| 1.7.1 Background.....   | 23        |
| 1.7.2 Timing .....  | 23        |
| 1.8 Tidal analysis .....  | 24        |
| 1.9 Tidal currents .....  | 26        |
| <b>2. Tidal power.....</b>  | <b>28</b> |
| 2.1 Introduction .....  | 28        |
| 2.2 Two ways of generating electricity from tides.....                              | 28        |
| 2.3 Barrage tidal power .....   | 29        |
| 2.3.1 Introduction .....  | 29        |
| 2.3.2 Single-basin two way installation .....                                       | 31        |
| 2.3.3 Energy calculation.....   | 31        |
| 2.3.4 Power output and basin regulation.....  | 32        |
| 2.3.5 Technologies .....  | 33        |
| 2.3.5.1 Introduction.....   | 33        |
| 2.3.5.2 Waterwheel turbines.....  | 33        |
| 2.3.5.3 Kaplan turbines.....  | 35        |
| 2.3.5.4 VLH turbines .....  | 37        |
| 2.3.5.5 Bulb turbines.....  | 38        |
| 2.3.6 Economics.....  | 41        |
| 2.3.7 Social implications.....  | 42        |
| 2.3.8 Environmental aspects .....   | 42        |
| 2.3.9 Prospective sites for tidal energy projects .....                             | 44        |
| 2.3.10 A case study: La Rance power plant.....                                      | 45        |
| 2.4 Tidal stream power.....   | 49        |
| 2.4.1 Introduction .....  | 49        |
| 2.4.2 Energy calculation.....   | 50        |
| 2.4.3 Technologies.....   | 53        |
| 2.4.3.1 Introduction.....   | 53        |
| 2.4.3.2 Darrieus turbine: device description and technical issues .....             | 58        |
| 2.4.3.3 Gorlov helical turbine (GHT): device description and technical issues ..... | 62        |
| 2.4.3.4 Kobold turbine: device description and technical issues .....               | 66        |
| 2.4.5 A case study: the Enermar project.....  | 69        |

|   |            |
|---|------------|
| <b>Part 2. Exploiting tidal energy in Guinea-Bissau .....</b>   | <b>73</b>  |
| <b>3. Guinea-Bissau: a developing country.....</b>  | <b>74</b>  |
| 3.1 Introduction .....  | 74         |
| 3.2 The O.N.L.U.S. Progetto Sviluppo 76 .....   | 74         |
| 3.3 Country background.....   | 75         |
| 3.4 Economy .....   | 77         |
| 3.5 Infrastructures .....   | 77         |
| 3.6 Power Sector .....  | 78         |
| 3.7 The continental watercourses .....  | 80         |
| 3.8 The importance of tides.....  | 81         |
| 3.9 Conclusions .....   | 82         |
| <b>4. Barrage tidal power potential in Guinea-Bissau .....</b>  | <b>83</b>  |
| 4.1 Introduction .....  | 83         |
| 4.2 Single-basin two way installation .....   | 83         |
| 4.2.1 Modelling a single-basin two way generation tidal power plant.....  | 83         |
| 4.2.2 Determination of discharge throughout circular holes.....   | 84         |
| 4.2.3 Propagation through the basin .....   | 85         |
| 4.3 A small size installation: proposal of a power plant near Fanhe.....  | 87         |
| 4.3.1 Site description.....   | 87         |
| 4.3.2 Different regulation laws .....   | 89         |
| 4.3.3 Sluice and no-sluice system.....  | 94         |
| 4.4 A medium size installation: proposal of a power plant near Bissau .....                                       | 98         |
| 4.4.1 Site description.....   | 98         |
| 4.4.2 No-sluice system.....   | 99         |
| 4.4.3 Maximum and minimum tidal amplitude.....  | 101        |
| 4.4.4 VLH turbine installation .....  | 104        |
| 4.5 Preliminary considerations about a big size power plant near Porto Gole .....                                 | 107        |
| <b>5. Tidal stream power in Guinea-Bissau.....</b>  | <b>109</b> |
| 5.1 Introduction .....  | 109        |
| 5.2 Tide propagation in convergent and non-convergent estuaries.....  | 109        |
| 5.3 Formulation of the 1-D problem .....  | 111        |
| 5.3.1 Shallow water equations .....   | 111        |
| 5.3.2 Analytical solution for wide rectangular estuaries with constant width and frictional term negligible ..... | 112        |
| 5.3.3 The resonance phenomenon.....   | 113        |
| 5.3.4 One-dimensional numerical model for wide rectangular convergent and non-convergent estuaries.....           | 113        |
| 5.4 The hydrodynamic of tidal estuaries in Guinea-Bissau .....  | 116        |
| 5.5 The hydrodynamic of Rio Geba.....   | 121        |
| 5.6 The hydrodynamics of Rio Mansoa .....   | 132        |
| 5.7 Power production in the tidal estuaries of Guinea-Bissau .....  | 140        |
| 5.8 Tidal currents in the straits between islands .....   | 146        |
| 5.9 Power production in Bubaque.....  | 148        |
| <b>6. A novel solution: designing artificial inlets connecting tidal estuaries to small inland basins.....</b>    | <b>151</b> |
| 6.1 Introduction .....  | 151        |
| 6.2 Formulation of the problem .....  | 151        |
| 6.2.1 Shallow water equations .....   | 151        |

|   |            |
|---|------------|
| 6.2.2 Analytical solution for inviscid flow in rectangular inlets .....                               | 152        |
| 6.2.3 Resonance in special geometric configurations.....  | 153        |
| 6.2.4 One-dimensional numerical model for rectangular inlets .....                                    | 154        |
| 6.3 The hydrodynamics of tidal inlets in Guinea-Bissau .....  | 156        |
| 6.4 Power production in a tidal inlet of Guinea-Bissau .....  | 162        |
| 6.5 Comparison with a more refined numerical model.....   | 173        |
| <b>7. Preliminary considerations about energy storage and power supply<br/>in Guinea-Bissau .....</b> | <b>174</b> |
| 7.1 Introduction .....  | 174        |
| 7.2 Installation of a storage system .....  | 174        |
| 7.3 Employ of an additional power source.....   | 175        |
| 7.4 Supply of tidal energy in Guinea-Bissau .....   | 176        |
| <b>8. Tentative cost analysis. ....</b>   | <b>177</b> |
| 8.1 Introduction .....  | 177        |
| 8.2 Cost of energy in Guinea Bissau.....  | 177        |
| 8.3 Generic factors influencing the costs of a barrage tidal power plant.....                         | 178        |
| 8.4 Generic factors influencing the costs of a tidal stream power plant .....                         | 178        |
| 8.5 Cost estimates .....  | 179        |
| <b>9. Conclusions.....</b>  | <b>182</b> |
| <b>References.....</b>  | <b>185</b> |
| <b>Ringraziamenti.....</b>  | <b>188</b> |

## List of figures

|  |    |
|--|----|
| Fig. 1.1 - The repeated cycle of sea level due to tidal phenomenon.....  | 15 |
| Fig. 1.2 - Reciprocal positions of Moon, Sun and Earth during spring and neap tides. ..  | 16 |
| Fig. 1.3 - Simple draw of moon at perigee.....   | 17 |
| Fig. 1.4 - The $M_2$ tidal constituent. ....   | 19 |
| Fig. 1.5 - Earth-moon centre of mass and period of rotation (Naval Postgraduate School. Monterey, California).....   | 21 |
| Fig. 1.6 - Tide-producing force as vector addition of centrifugal force and gravitational force due to moon (Naval Postgraduate School. Monterey, California)..... | 22 |
| Fig. 2.1 - Simple draw of the operating condition of a two-ways barrage tidal power plant (Andy Darvill, Broadoak Community School). ....                          | 29 |
| Fig. 2.2 - Simple draw of an undershot waterwheel (Peter Clark et al. Tidal Energy, 2003). ....  | 34 |
| Fig. 2.3 - Simple draw of an overshot waterwheel (Peter Clark et al. Tidal Energy, 2003). ....   | 34 |
| Fig. 2.4 - Simple draw of a breast-shot waterwheel (Peter Clark et al. Tidal Energy, 2003). ....   | 35 |
| Fig. 2.5 - Range of OSSBERGER Kaplan turbine (OSSBERGER, © www-werbeagentur-wie.de).....   | 35 |
| Fig. 2.6 - Kaplan turbine (Martin Roth, ETH Zurich). ....  | 36 |
| Fig. 2.7 - VLH turbine (VLH turbines, MJ2 Technologies S.A.R.L.).....  | 37 |
| Fig. 2.8 - Simple draw of a VLH turbine (VLH turbines, MJ2 Technologies S.A.R.L.).....   | 38 |
| Fig. 2.9 - VLH turbine working condition; from these tables we can estimate their efficiency: $\eta = 79\%$ (VLH turbines, MJ2 Technologies S.A.R.L.).....         | 38 |
| Fig. 2.10 - Bulb turbine (Hitachi, Ltd. 1994, 2005). ....  | 39 |
| Fig. 2.11 - Simple sketch of a rim turbine (Peter Clark et al. Tidal Energy, 2003). ....   | 41 |
| Fig. 2.12 - Prospective sites for tidal energy projects (C. G. Pandya 2006). ....  | 44 |
| Fig. 2.13 - Bulb turbine installed in La Rance power plant. ....   | 46 |
| Fig. 2.14 - A view of the Rance barrage (RSS, 2006). ....  | 48 |
| Fig. 2.15 - Size comparison of a 1 MW wind and tidal turbine ( Marine Current Turbines Ltd.).....  | 50 |
| Fig. 2.16 - Representative relationship between the tip speed ratio ( $\lambda$ ) and the power coefficient ( $\eta$ ) (Bryden et al.1997).....                    | 51 |
| Fig. 2.17 - Power output curve assuming a 10-s rotational period, based upon the $\eta$ - $\lambda$ curve (Bryden et al.1997).....                                 | 52 |
| Fig. 2.18 - Turbine output relative to available power (Clarke et al. 2004).....   | 52 |
| Fig. 2.19- Comparative performance of various turbines in free water currents (Gorlov et al.2001).....   | 54 |
| Fig. 2.20 - Artist's impression of MCT Seagen pile-mounted twin rotor tidal turbine (Marine Current Turbines Ltd).....   | 55 |
| Fig. 2.21 - UEK Twin Turbines prepared for demonstration (Underwater Electric Kite). ....  | 55 |
| Fig. 2.22 - Verdant Power Free-flow Turbine Being Deployed in East River (December 2006). ....   | 56 |

|   |    |
|---|----|
| Fig. 2.23 - Lunar Energy RTT Turbine. One of the different technology options available for tidal in-stream energy conversion (TISEC). .....          | 56 |
| Fig. 2.24 - A gravity base anchors the Open-Centre Turbine to the seabed (OpenHydro). .....   | 57 |
| Fig. 2.25 Davis Hydro vertical-axis turbine (Blue Energy International).....  | 57 |
| Fig. 2.26 - Solid Works image of the tidal rotor (Institute for Energy Systems, university of Edimburgh). .....                                       | 57 |
| Fig. 2.27 - Darrieus wind turbine. ....   | 58 |
| Fig. 2.28 - Darrieus turbine rotor and blades (Alternative Hydro Solutions Ltd).....  | 60 |
| Fig. 2.29 - Darrieus turbine (Alternative Hydro Solutions Ltd). ....  | 60 |
| Fig. 2.30 - Efficiency curves in relation to turbine dimension (Alternative Hydro Solutions Ltd).....   | 61 |
| Fig. 2.31 - Mounting schemes for Darrieus turbine (Alternative Hydro Solutions Ltd). ..   | 61 |
| Fig. 2.32 - Double and triple helical turbine (Lucid energy technologies).....  | 63 |
| Fig. 2.33 - Triple-helix GHT. Diameter: 1m; Length (height): 2.5m. Total weight including steel shaft is about 90 kg (Lucid energy technologies)..... | 63 |
| Fig. 2.34 - Artist's rendition of the floating power plant with helical turbines (Lucud energy technologies). ....                                    | 64 |
| Fig. 2.35 - Power output related to turbine dimension (Lucid energy technologies).....  | 65 |
| Fig. 2.36 - Twin Triple-helix GHT in the Uldolmok Strait (Lucid energy technologies). .....   | 65 |
| Fig. 2.37 - Kobold turbine with floating buoy ( © Turbo Squid ,2008). ....  | 67 |
| Fig. 2.38 - Power output related to water velocities obtained from numerical simulations (Coiro et al). ....  | 68 |
| Fig. 2.39 - The Kobold turbine position in Messina Strait. ....   | 69 |
| Fig. 2.40 - Kobold turbine (left) and floating platform in Messina Strait (right). ....   | 70 |
| Fig. 3.1 - Map of guinea-Bissau (Flash Appeal, 2006).....   | 76 |
| Fig. 3.2 - View of a road in Guinea-Bissau. Its bad conditions remark the difficulty in transport when operating in developing country.....           | 78 |
| Fig. 3.3 - River network of Guinea-Bissau (Extract from the doctoral thesis of G. Pennober). ....   | 80 |
| Fig. 3.4 - Satellite image of Guinea-Bissau with specified in red the tidal stations (©Google 2007). ....   | 81 |
| Fig. 3.5 - Values of maximum and minimum tide amplitude in Guinea-Bissau. ....  | 82 |
| Fig. 4.1 - Simple sketch of the scheme we adopted to model a two-way generation tidal power plant.....  | 83 |
| Fig. 4.2 - Evaluation of the discharge coefficient relating to the ratio between upstream level and the hole diameter (H.R. Henry, 1948). ....        | 85 |
| Fig. 4.3 - Satellite image of the site near Fanhe where we study the feasibility of a small-size power plant (©Google 2007). ....                     | 87 |
| Fig. 4.4 – Quantities characterising the site of Fanhe .....  | 88 |
| Fig. 4.5 - A view of Rio Mansoa near Fanhe. ....  | 88 |
| Fig. 4.6 - Simple sketch of a typical cross-section of an earth fill dam. ....  | 89 |
| Fig. 4.7 - Trend of basin level, sea level and power output over a tide cycle for a hole 0.5 m in diameter.....                                       | 90 |
| Fig. 4.8 - Trend of basin level, sea level and power output over a tide cycle for a hole 1 m in diameter.....   | 91 |

|   |     |
|---|-----|
| Fig. 4.9 - Trend of basin level, sea level and power output over a tide cycle for a hole 3 m in diameter.....   | 92  |
| Fig. 4.10 - Relationship between the hole diameter and the average power output for a basin of 29000 m <sup>2</sup> and a tidal amplitude of 2.2 m. ....  | 93  |
| Fig. 4.11 - Trend of basin level, sea level and power output over a tidal cycle for a hole 1.45 m in diameter.....  | 94  |
| Fig. 4.12 - Trend of surface elevation in the basin, in the sea and power output over a tidal cycle for a basin regulated by sluices. ....  | 95  |
| Fig. 4.13 - Trend of basin level, sea level and power output over a tide cycle for a basin with no sluice regulation system but with a cut in power production in case of head less then 0.8 m.....     | 96  |
| Fig. 4.14 - Working condition of the low head turbine required in the analyzed site (basin surface of 29000 m <sup>2</sup> and tidal amplitude of 2.2 m).....   | 97  |
| Fig. 4.15 - Satellite image of the site near Bissau where we study the feasibility of a medium-size power plant (©Google 2007).....   | 98  |
| Fig. 4.16 – Quantities characterising the site of Bissau .....  | 99  |
| Fig. 4.17 - Trend of basin level, sea level and power output over a tide cycle for a basin with no sluice regulation system but with a cut in power production in case of head less then 0.8 m.....     | 100 |
| Fig. 4.18 - Working condition of the low head turbines required in the analyzed site (basin surface of 1.12 km <sup>2</sup> and tidal amplitude of 1.9 m).....  | 101 |
| Fig. 4.19 - Trend of basin level, sea level and power output over a tide cycle considering the maximum amplitude of 2.5 m . ....  | 102 |
| Fig. 4.20 - Trend of basin level, sea level and power output over a tide cycle considering the minimum amplitude of 1.25 m.....   | 103 |
| Fig. 4.21 - Comparison between the low head turbines working condition operating with the maximum and the minimum amplitude. ....   | 104 |
| Fig. 4.22 - Trend of basin level, sea level and power output over a tide cycle operating with 4 VLH turbines. ....  | 105 |
| Fig. 4.23 - System behaviour for a hole of 3.52 m in diameter compared to the working condition of a VLH turbine 5.6 m in diameter.....   | 106 |
| Fig. 4.24 - Satellite image of the site near Porto Gole where we study the feasibility of a big-size power plant (©Google 2007).....  | 107 |
| Fig. 4.25 – Quantities characterising the site of Porto Gole .....  | 108 |
| Fig. 5.1 - Geometry of the idealized tidal channel assuming a rectangular cross-section and a longitudinal width profile exponentially decreasing (G.Vignoli,2005) . ....                               | 114 |
| Fig. 5.2 - Effect of estuary length on water level: comparison between the results given by the numerical model and the analytical solution in four sections. ....                                      | 116 |
| Fig. 5.3 - Effect of estuary length on water velocity: comparison between the results given by the numerical model and the analytical solution in four sections. ....                                   | 117 |
| Fig. 5.4 - Effect of estuary depth on water level: comparison between the results given by the numerical model and the analytical solution in four sections. ....                                       | 118 |
| Fig. 5.5 - Effect of estuary depth on water velocity assuming an estuary length of 68 Km: comparison between the results given by the numerical model and the analytical solution in four sections..... | 119 |

|   |     |
|---|-----|
| Fig. 5.6 - Effect of estuary depth on water velocity assuming an estuary length of 120 Km: comparison between the results given by the numerical model and the analytical solution in four sections.....  | 120 |
| Fig. 5.7 - Satellite image of the Rio Geba with the five sections taken into consideration (©Google 2007). .....  | 121 |
| Fig. 5.8 - Comparison between the estuary width profile evaluated through satellite image and the exponentially one, calculated assuming $L_b = 47150$ m.....   | 122 |
| Fig. 5.9 - Sediment size distribution of Rio Geba and Rio Mansoa (S. Diop).....   | 123 |
| Fig. 5.10 - Nautical chart of Rio Geba. The red line is the section considered for the evaluation of the equivalent section.....  | 124 |
| Fig. 5.11 - Evaluation of the equivalent section. The brown line is depth referred to the lowest water level (as given by nautical chart) and the blue line is the depth of the equivalent section.....   | 125 |
| Fig. 5.12 - Trend of velocities along the estuary.....  | 126 |
| Fig. 5.13 - Trend of water levels along the estuary considering the effective bottom profile. ....  | 126 |
| Fig. 5.14 - Trend of maximum velocity along the estuary in flood and ebb phase.....   | 127 |
| Fig. 5.15 - Trend of water level and bottom profile along the estuary in comparison with measured values. We remark a good agreement. ....  | 127 |
| Fig. 5.16 - Trend of water level over a tide cycle in 5 significant sections. ....  | 128 |
| Fig. 5.17- Trend of velocity over a tide cycle in 5 significant sections. The flood and ebb maximum velocities given by the 1-D model in Bissau are: $U_{flood} = 1.2$ m/s, $U_{ebb} = -1.25$ m/s; those values are only slightly lower than measured velocities in Bissau: $U_{flood} = 1.25$ m/s, $U_{ebb} = -1.30$ m/s (S. Diop). .... | 129 |
| Fig. 5.18 - Comparison between trend of maximum velocity along the estuary in flood and ebb phase considering maximum and minimum amplitude registered in Bissau. ....  | 130 |
| Fig. 5.19 - Comparison between trend of maximum and minimum water level along the estuary considering maximum and minimum amplitude registered in Bissau. ...   | 130 |
| Fig. 5.20 - Trend of water level over a tide cycle in the section of Porto Gole considering maximum and minimum amplitude registered in Bissau.....   | 131 |
| Fig. 5.21 - Trend of velocity over a tide cycle in the section of Porto Gole considering maximum and minimum amplitude registered in Bissau.....  | 131 |
| Fig. 5.22 - Satellite image of the Rio Mansoa with the five sections taken into consideration (©Google2007).....  | 132 |
| Fig. 5.23 - Estuary width profile evaluated through the satellite image. ....   | 133 |
| Fig. 5.24 - Evaluation of the equivalent section. The red line is depth referred to the lowest water level (as given by nautical chart) and the blue line is the depth of the equivalent section.....   | 134 |
| Fig. 5.25 - Trend of maximum velocity along the estuary in flood and ebb phase. We remark values considerably less than along RioGeba.....  | 135 |
| Fig. 5.26 - Trend of water level and bottom profile along the estuary. ....   | 135 |
| Fig. 5.27 - Trend of water level over a tide cycle in 5 significant sections. ....  | 136 |
| Fig. 5.28 - Trend of velocity over a tide cycle in 5 significant sections. ....   | 136 |
| Fig. 5.29 - Comparison between trend of maximum velocity along the estuary in flood and ebb phase considering maximum and minimum amplitude registered at the mouth of Rio Mansoa.....  | 137 |

|  |     |
|--|-----|
| Fig. 5.30 - Comparison between trend of maximum and minimum water level along the estuary considering maximum and minimum amplitude registered at the mouth of Rio Mansoa. ....  | 138 |
| Fig. 5.31 - Trend of water level over a tide cycle in the section of Fanhe considering maximum and minimum amplitude registered at the mouth of Rio Mansoa.....  | 138 |
| Fig. 5.32 - Trend of velocity over a tide cycle in the section of Fanhe considering maximum and minimum amplitude registered at the mouth of Rio Mansoa.....   | 139 |
| Fig. 5.33 - Theoretical power over a tide cycle for unit of area of the turbine in 5 significant sections of Rio Geba (considering the maximum amplitude registered in Bissau).....  | 140 |
| Fig. 5.34 - Theoretical power over a tide cycle for unit of area of the turbine in 5 significant sections of Rio Mansoa (considering the maximum amplitude of 2.5 m registered at the mouth of Rio Mansoa).....                                  | 141 |
| Fig. 5.35 - Energy output over a tide cycle in Bissau for a Darrieus turbine 3 m in diameter (considering the maximum amplitude of 2.5 m).....   | 142 |
| Fig. 5.36 - Energy output over a tide cycle in Porto Gole for a Darrieus turbine 3 m in diameter (considering the maximum amplitude of 2.5 m registered in Bissau). ...  | 143 |
| Fig. 5.37 - View of Rio Geba in correspondence of Bissau.....  | 144 |
| Fig. 5.38 - Energy output over a tide cycle in Bissau for a Darrieus turbine 6 m in diameter (considering the maximum amplitude of 2.5 m registered in Bissau). ...  | 145 |
| Fig. 5.39 - Satellite image of the narrow body between islands where the village of Bubaque is located (©Google 2007).....   | 146 |
| Fig. 5.40 - Trend of measured velocity over a tide cycle in Bubaque. ....  | 147 |
| Fig. 5.41 - Theoretical power over a tide cycle for unit of area of the turbine in Bubaque. ....   | 148 |
| Fig. 5.42 - View of the jetty situated in the small port of Bubaque. ....  | 149 |
| Fig. 5.43 - Energy output over a tide cycle in Bubaque for a Darrieus turbine 3 m in diameter (considering the maximum amplitude of 2 m registered in site). ....  | 149 |
| Fig. 6.1 - Geometry of the idealized inlet connecting a basin to the open sea or to a tidal estuary. We assume a rectangular cross-section (Tambroni & Seminara).....  | 151 |
| Fig. 6.2 - Effect of the dimensionless parameter $Sk/B$ on inlet speed. ....   | 154 |
| Fig. 6.3 - Effect of inlet depth on velocity assuming a basin surface of $150000 \text{ m}^2$ : comparison between the results obtained for different values of tidal amplitude.   | 157 |
| Fig. 6.4 - Effect of inlet depth on velocity assuming a tidal amplitude of 1.9 m: comparison between the results obtained for different values of the basin surface area. ....   | 158 |
| Fig. 6.5 - Effect of inlet depth on flow speed assuming an inlet width of 4 m, a basin surface area of $150000 \text{ m}^2$ and a tidal amplitude of 1.9 m: comparison between the results obtained for different values of inlet length. ....   | 159 |
| Fig. 6.6 - Effect of inlet depth on inlet speed assuming an inlet length of 10 m, a basin surface area of $150000 \text{ m}^2$ and a tidal amplitude of 1.9 m: comparison between the results obtained for different values of inlet width. .... | 159 |
| Fig. 6.7 - Effect of the parameter $a_0/Y_0$ on dimensionless flood velocity. ....   | 160 |
| Fig. 6.8 - Effect of the parameter $a_0/Y_0$ on the peak dimensionless ebb speed. ....   | 161 |
| Fig. 6.9 - A Gorlov turbine (T) 1 m in height ( $H_T$ ) and 2.5 m in width ( $W_T$ ) in an inlet of dept $Y_0$ and width B. The red line is the horizontal axis of the turbine. ....   | 162 |

|   |     |
|---|-----|
| Fig. 6.10 - Satellite image of the inlet connecting the Rio Geba to an overflow area (© Google 2007).....   | 163 |
| Fig. 6.11 - Trend of inlet speed throughout a tidal cycle assuming an inlet width of 4 m, a basin surface of 150000 m <sup>2</sup> and a tidal amplitude of 1.9 m. .... | 164 |
| Fig. 6.12 - The theoretical power per unit of area of the turbine is plotted as a function of time in a tidal cycle .....   | 165 |
| Fig. 6.13 - Dependence of inlet speed on time in a tidal cycle (red line). The cut in speed of a Gorlov turbine is also shown (blue line).....                          | 166 |
| Fig. 6.14 - Energy output produced by a Gorlov turbine over a tidal cycle for the setting considered herein. ....   | 167 |
| Fig. 6.15 - Dependence of inlet speed on time in a tidal cycle: comparison between the results obtained for different values of tidal amplitude. ....                   | 168 |
| Fig. 6.16 - Dependence of inlet speed on time in a tidal cycle.: comparison between the results obtained for different values of tidal amplitude. ....                  | 169 |
| Fig. 6.17 - Energy output produced by a Gorlov turbine over a tidal cycle considering the maximum tidal amplitude.....  | 170 |
| Fig. 6.18 - Energy output produced by a Gorlov turbine over a tidal cycle considering the minimum tidal amplitude. ....   | 171 |
| Fig. 6.19 - Satellite image of possible overflow areas along the Rio Geba (© Google 2007). ....   | 172 |
| Fig. 6.20 - Comparison between flow speeds obtained by the simplified 1-D model and the 2-D complete model.....   | 173 |
| Fig. 7.1 - Schematic representation of a combined supply/storage system (I.G. Bryden et al., 2000).....   | 175 |
| Fig. 8.1 - Costs for a tidal stream farm (© Verdant Power Canada ULC, 2006).....  | 179 |
| Fig. 8.2 - Quota-weight for each step of project according with its costs for the Enermar project (Ponte di Archimede S.p.A. – 2007).....                               | 180 |

## **Riassunto**

Il presente lavoro è nato da una sollecitazione dell'O.N.L.U.S. Progetto Sviluppo 76 (P.S. 76) ad approfondire la possibilità di produrre energia elettrica negli estuari a marea dalla Guinea-Bissau, paese in cui l'associazione ha avviato negli anni scorsi alcuni progetti di cooperazione appoggiandosi all'associazione locale "Amigos da Guiné-Bissau".

Le precedenti esperienze positive di collaborazione con la facoltà di Architettura nel campo del turismo e con il Dipartimento di Ingegneria dell'Ambiente, delle Costruzioni e del Territorio su un progetto riguardante la produzione di energia dall'olio di palma hanno spinto l'O.N.L.U.S. ad appoggiarsi nuovamente all'Università di Genova, in quanto il settore delle cosiddette energie rinnovabili, tanto attuale quanto ancora inesplorato, ben si prestava ad uno studio nell'ambito di una tesi di laurea.

D'altra parte, l'opportunità di mettere in gioco le nostre competenze tecniche acquisite nel corso degli studi nel campo della cooperazione allo sviluppo è stata da parte nostra colta con entusiasmo in seguito a un cammino di crescita personale, che ci ha portato a maturare la profonda convinzione che solo l'incontro e una reciproca relazione tra la "frenetica" cultura occidentale e quella "lenta" africana possano salvare l'una dal declino in affannata corsa a un successo vuoto e solitario, l'altra da problemi ben più concreti, quali la fame, la mancanza di acqua e la diffusione di malattie.

Inoltre esplorare ed approfondire il tema delle energie rinnovabili, affascinante e discusso, è stato subito individuato come la possibilità di acquisire competenze fondamentali da utilizzare nella nostra futura attività, consapevoli che le energie rinnovabili saranno sempre più necessarie, anche al fine di superare la marcata dipendenza del settore energetico dai combustibili fossili.

Introdotte dunque le motivazioni che hanno dato origine a questa tesi, passiamo ora a descriverne i contenuti.

Le due parti in cui la tesi è suddivisa ben rispecchiano le fasi del lavoro: la prima infatti riassume il processo di apprendimento e acquisizione di conoscenze tecniche sul vasto campo dell'energia in ambienti a marea, la seconda illustra invece varie proposte di applicazioni realizzabili in Guinea-Bissau.

Il primo passo è stato quello di approfondire e analizzare il fenomeno della marea

astronomica, la sua modellazione e le sue caratteristiche.

Successivamente si è reso necessario studiare i diversi metodi che consentono di produrre energia elettrica dalle maree. Il più conosciuto e longevo consiste nella costruzione di una diga che sbarrì una baia o un estuario, in modo da creare un bacino dove il livello oscilla con una legge diversa da quella del mare; si genera dunque un salto. Le turbine, installate lungo la diga, producono energia quando il bacino si riempie o si svuota.

Inoltre, il crescente interesse per le energie rinnovabili e per installazioni con basso impatto ambientale e visivo hanno portato a sviluppare tecnologie in grado di sfruttare direttamente il carico cinetico della corrente. Esistono a questo proposito diversi prototipi di turbine, sia ad asse verticale che orizzontale, che non richiedono la costruzione di opere civili, ma solo una struttura di sostegno, che può essere fissa o galleggiante.

Terminata questa panoramica sulle tecnologie esistenti e su quelle in fase di studio si è passati ad analizzare la realtà particolare della Guinea-Bissau. Questo paese, situato sulla costa occidentale dell' Africa, è caratterizzato da una vasta rete di estuari e canali secondari che si introducono nel continente per centinaia di Km; in essi l'escursione di marea (che già sulle coste assume i massimi valori della zona) si amplifica propagandosi verso monte, raggiungendo all'interno del principale Rio Geba valori di 6.8 m. Nonostante questa enorme risorsa di energia il paese, uno dei 10 più poveri del pianeta, è privo di una rete elettrica (fatta eccezione per la capitale, dove però non funziona da più di 10 anni).

Con queste premesse è evidente la necessità di studiare diverse modalità che sfruttino l'enorme risorsa delle maree per la produzione di energia elettrica.

Usufruendo di un modello numerico e di una serie di valori misurati è stato simulato il comportamento idraulico dei suddetti estuari; in particolare, si sono analizzati il Rio Geba, la cui lunghezza, prossima a quella di risonanza, fa sì che le velocità siano più elevate che negli altri canali, e il Rio Mansoa, sulle cui sponde è situato il villaggio di Fanhé (dove l'associazione P.S. 76 ha avviato alcuni dei progetti citati).

Si sono dunque valutate le ampiezze di marea e le velocità di flusso e di riflusso, con particolare attenzione ad alcune sezioni ritenute più interessanti.

Noto l'andamento nel tempo del livello è stato possibile individuare alcuni siti strategici per la realizzazione di una centrale a marea "con diga" e calcolarne, con un semplice modello numerico, la potenza installata. In particolare:

- vicino al villaggio di Fanhè, dove l'escursione media annua raggiunge i 4.4 m ed è presente un bacino di circa 29000 m<sup>2</sup>, è stata studiata una piccola centrale da 34 KW; in seguito a diverse simulazioni si è inoltre individuato il sistema di regolazione più efficiente (che permette di ottenere la massima energia in un ciclo di marea) e si è valutata la curva caratteristica della turbina da installare;
- nei pressi della capitale Bissau (escursione media di 3.8 m, area del bacino di 1.12 Km<sup>2</sup> e lunghezza dello sbarramento di 150 m) si è analizzata una centrale da 940 KW e si è valutata la produzione di energia nei casi di massima e minima escursione;
- a proposito del tratto più a monte del Rio Geba, dove l'escursione raggiunge il valore massimo di 6.8 m, sono state fatte le prime considerazioni sulla possibilità di sbarrare l'intero Rio con una diga lunga 2 Km; tale opera porterebbe la potenza installata ad un valore di 50 MW, energia che potrebbe di gran lunga soddisfare il fabbisogno dell'intero paese.

Sulla base delle conoscenze acquisite sulle velocità della corrente mareale, si è analizzata la possibilità di produrre energia elettrica con la semplice installazione di una o più turbine "free-flow". Tra le varie tecnologie proposte, si è scelto di adottare una turbina Darrieus di diametro 3 m, in quanto tale prototipo è uno dei pochi già in commercio ed è in grado di sfruttare basse velocità. L'analisi si è rivolta in particolare ai seguenti siti:

- lungo il Rio Geba ciascuna turbina consentirebbe la produzione di 0.67 KW in corrispondenza della capitale Bissau (mediando su un ciclo di marea e considerando la massima escursione) e di 0.71 KW in località Porto Gole, subito a monte di un restringimento naturale;
- lungo il Rio Mansoa le velocità non raggiungono valori elevati (la produzione di potenza raggiungerebbe un valore di 0.37 KW nei pressi di Fanhè), rendendo l'installazione di una turbina free-flow inadeguata;

- nei pressi di Bubaque, in un restringimento naturale determinato da due isole adiacenti, che compongono l'Arquipelago Dos Bijagos, sono stati misurati in sito valori di velocità piuttosto elevati; in questo caso la potenza prodotta con una sola turbina raggiungerebbe 1.26 KW e potrebbe essere sfruttata dai piccoli alberghi della zona.

A proposito di questo tipo di installazioni, la cui potenza prodotta potrebbe a prima vista sembrare di poco interesse, è necessario considerare innanzitutto che tale energia è pulita e priva di alcun costo ambientale; in secondo luogo è da sottolineare la possibilità di installare più turbine (fino a costruire una vera e propria "schiera"), date la larghezza e la profondità elevata delle sezioni considerate.

Infine, si mette in risalto la necessità di effettuare un'accurata campagna di misure sul campo, vista la possibilità di riscontrare in curva o in particolari restringimenti, valori di velocità superiori a quelli ottenuti con simulazioni numeriche.

La parte conclusiva della tesi è infine volta all'analisi di un'idea innovativa che consenta produzione di energia elettrica in misura maggiore che nel caso precedente, ma con lo stesso ridotto impatto ambientale. Si è infatti modellata numericamente l'idraulica di una bocca che connetta un estuario soggetto a marea a una laguna o ad un'area inondabile, caratteristica degli ambienti a marea.

In tal caso, prendendo in esame una bocca profonda 5 m e larga 4 m (reperibile in loco o da realizzare artificialmente) connessa a un bacino di superficie pari a 0,15 Km<sup>2</sup>, con l'installazione di una sola turbina Gorlov (1 m di diametro e 2.5 m in altezza) si produrrebbero mediamente 4 KW con un'escursione di 1.9 m e addirittura 8.4 KW con un'escursione massima di 2.5 m.

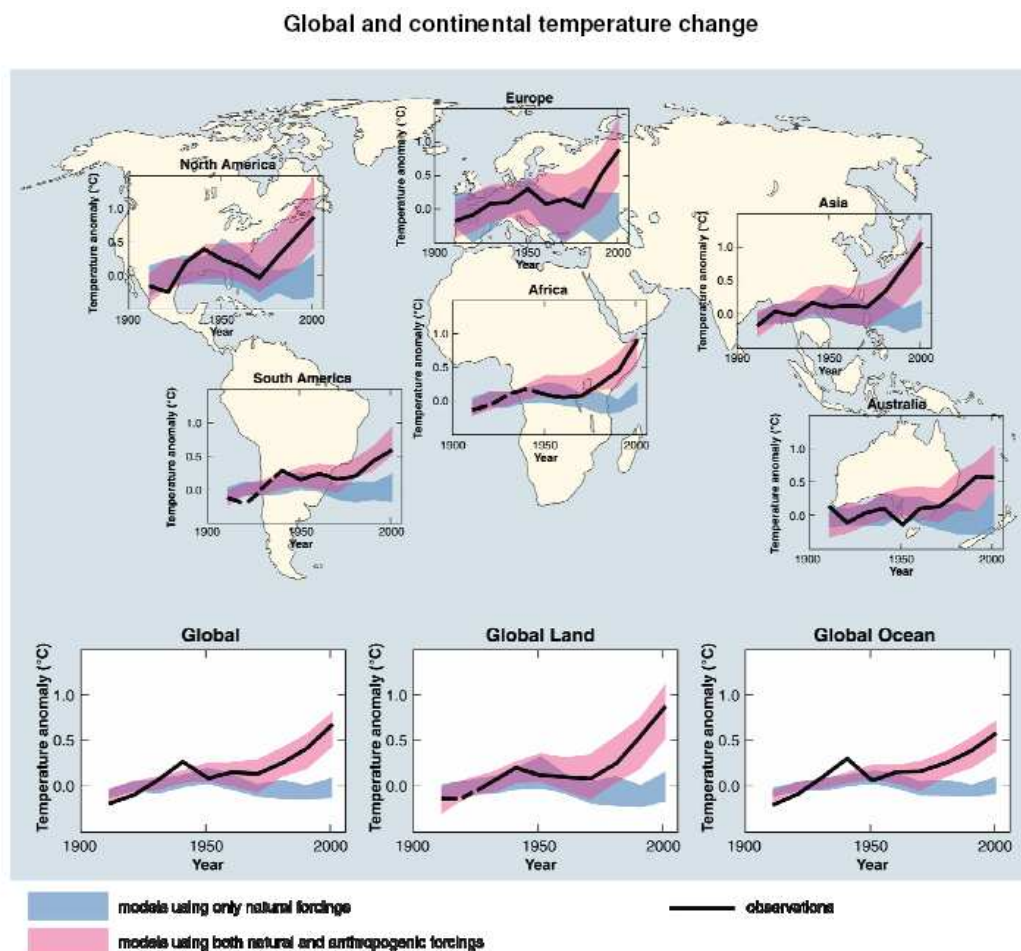
La tesi si conclude con alcune considerazioni sul possibile immagazzinamento dell'energia prodotta e sulla sua distribuzione in una particolare realtà come quella di un paese in via di sviluppo, e con una breve analisi dei costi delle diverse applicazioni.

E' da mettere in luce, infine, la possibilità di accedere ai fondi dell'Unione Europea, la quale, con specifici programmi economici, finanzia progetti di cooperazione nei paesi in

via di sviluppo. Auspichiamo dunque che questo lavoro possa costituire la premessa necessaria per l'acquisizione di finanziamenti che consentano la realizzazione delle opere descritte.

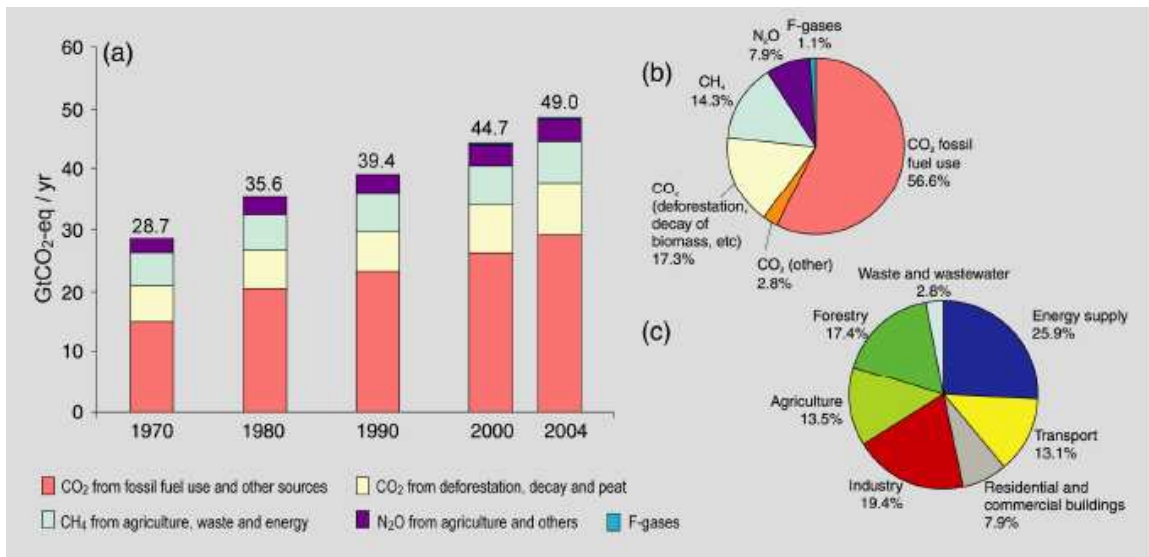
## Introduction

There is increasing consensus in both the scientific and political communities that significant reductions in greenhouse gas emissions are necessary to limit the magnitude and extent of climate change.



Comparison of observed continental (and global) scale changes in surface temperature with results simulated by climate models using either natural or both natural and anthropogenic forcings. Decadal averages of observations are shown for the period 1906-2005 (black line) plotted against the centre of the decade and relative to the corresponding average for the period 1901-1950. Lines are dashed where spatial coverage is less than 50%. Blue shaded bands show the 5-95% range for 19 simulations from 5 climate models using only the natural forcings due to solar activity and volcanoes. Red shaded bands show the 5-95% range for 58 simulations from 14 climate models using both natural and anthropogenic forcings (© Intergovernmental Panel on Climate Change, 2007).

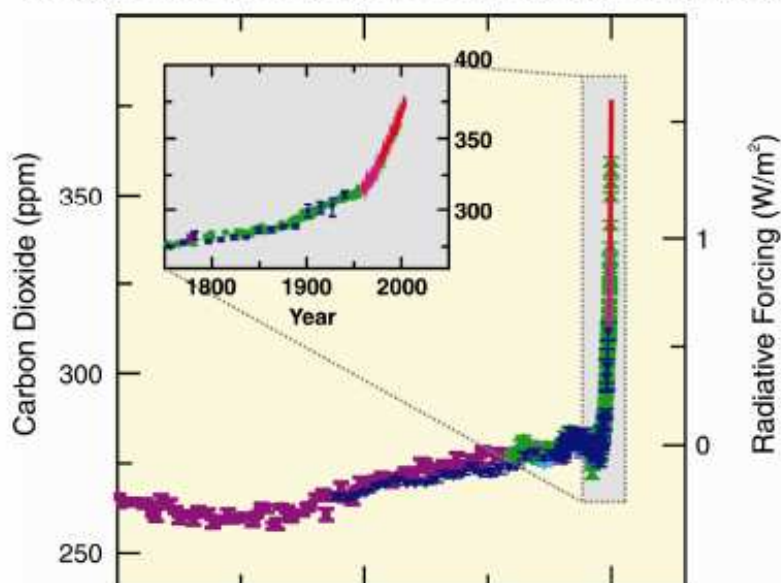
The majority of greenhouse gas (GHG) emissions come from the use of fossil fuels to power a growing world economy.



(a) Global annual emissions of anthropogenic GHGs from 1970 to 2004. (b) Share of different anthropogenic GHGs in total emissions in 2004 in terms of CO<sub>2</sub>-eq. (c) Share of different sectors in total anthropogenic GHG emissions in 2004 in terms of CO<sub>2</sub>-eq. (© Intergovernmental Panel on Climate Change, 2007).

Industrialized countries are responsible for the majority of current and historic emissions, but many developing countries are significantly increasing their share as their economies expand. This is especially true in some of the large emerging economies, such as China and India, that have undergone high economic growth.

## Changes in GHGs from ice core and modern data



*Atmospheric concentrations of CO<sub>2</sub> over the last 10,000 years (large panels) and since 1750 (inset panels). Measurements are shown from ice cores (symbols with different colours for different studies) and atmospheric samples (red lines). The corresponding radioactive forcings relative to 1750 are shown on the right hand axes of the large panels (© Intergovernmental Panel on Climate Change, 2007).*

With the ratification of the Kyoto Protocol, a first step has been taken to reduce the emissions up to 2012, although all emission scenarios indicate that these reductions will not be sufficient to reduce the threat of climate change significantly.

The Kyoto Protocol was intentionally designed as a process with progressively increasing reduction requirements and participation by all countries. How these intentions will be met is the main focus of negotiations for the post-2012 period.

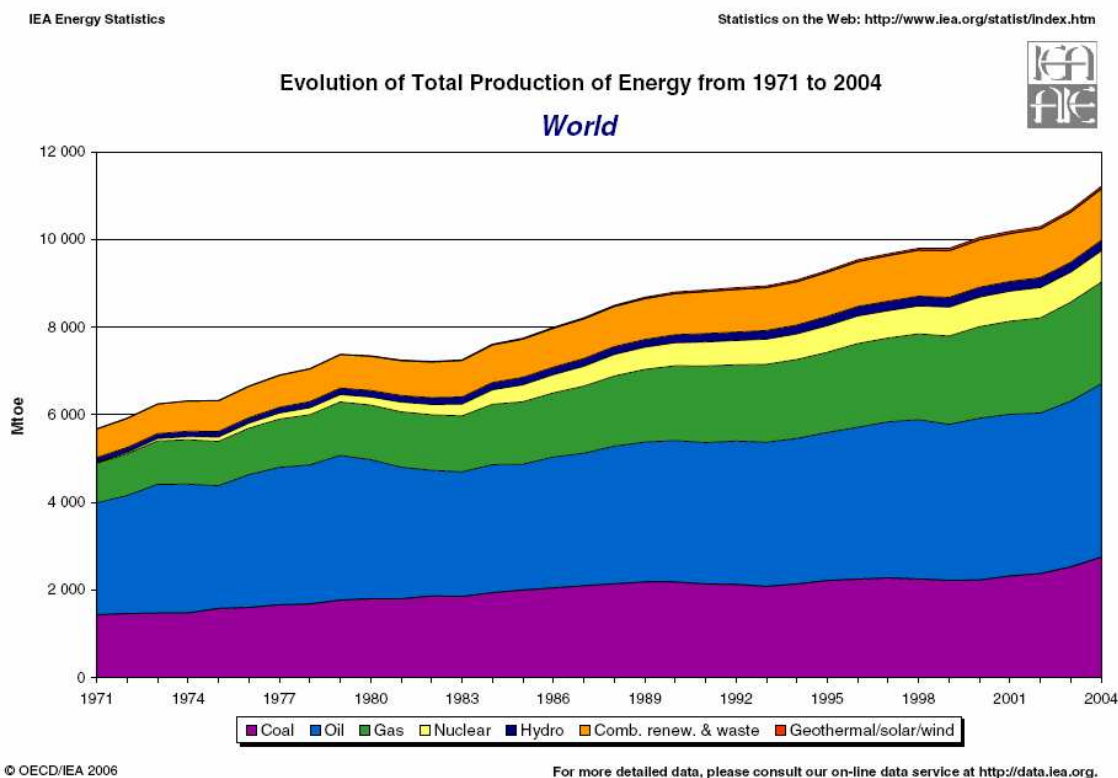
A primary role in this worldwide process will be doubtless played by the renewable energy field.

The expression “renewable energy” covers a number of sources and technologies at different stages of development.

By their nature, renewable energy sources are generally carbon-free or carbon neutral. Many renewable energy technologies have matured over the last decade and moved from being a passion for the dedicated few to a major economic sector attracting large industrial companies and financial institutions.

Renewable energy technologies such as wind power and solar photovoltaic devices have

achieved noticeable cost reductions over the last decades, which are expected to continue in the medium term as large global companies enter new energy markets for hydro, wind, solar and biomass technologies.

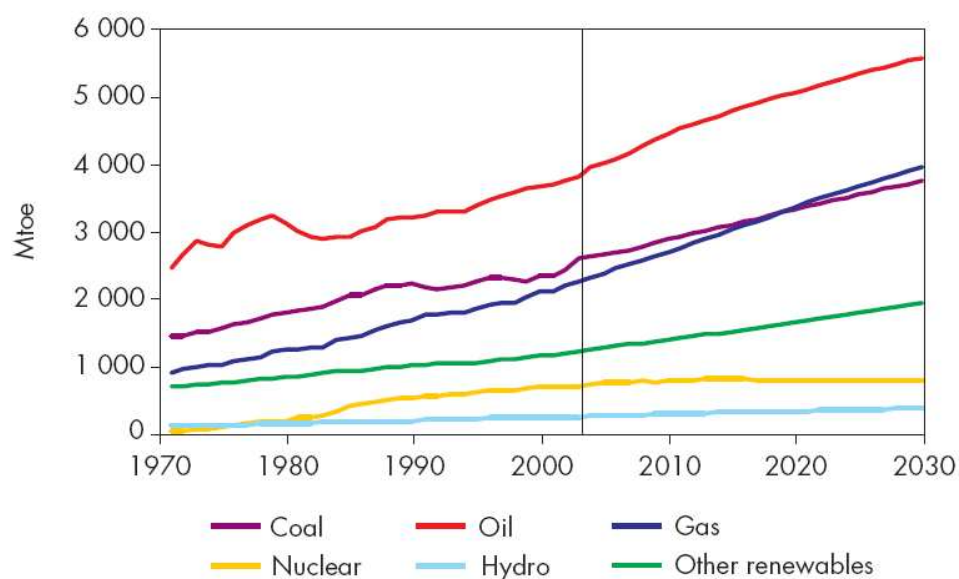


*Historical development in primary energy production. Dominance and increasing importance of fossil fuels in the last decade (© International Energy Agency, 2006).*

Renewable energy can even potentially play an important role in stabilizing greenhouse gas emissions and mitigating climate change. To secure broad public and policy support to promote renewable energy development, it is essential to include not only the climatic aspects, but also other broader economic, environmental, and social benefits in any analysis. Therefore it is not possible to link the global scenario analysis directly to requirements for specific policies at a national level.

Some general forecasts can be attempted:

- global energy demand will continue to grow and is expected to increase approximately 50%-60% by 2030 unless major conservation and efficiency programmes are undertaken;



World primary energy demand (© International Energy Agency 2005).

- with current price expectations and reserve projections, the domination of fossil based technologies will not dramatically change in the next decades unless renewable energy technologies become more cost competitive;
- the atmospheric greenhouse gases concentration of 450-550 ppm (required by the Kyoto Protocol) can only be reached through major reduction of long term emission obtained by either a larger renewable energy penetration, or if significant efforts to increase carbon storage and sequestrations are made;
- renewable energy costs are expected to decline further in the coming decades. This will make most renewable energy technologies cost competitive by the middle of the century.

As regards cost analysis, it is important to notice that the pricing structures of energy markets mostly do not reflect the full costs of producing energy to society, and make

renewable energy less competitive than conventional energy choices. Conventional energy supplies are highly subsidized in many countries, both directly and indirectly.

In fact, the full costs of producing energy from conventional fuels are not normally factored into energy pricing, including external costs such as human health impacts, environmental damage, and the global impacts of climate changes.

In conclusion it is important to consider the special contribution that renewable energy can make in developing countries to both adaptation and mitigation responses. In some cases, renewable energy offers a viable opportunity for developing countries to address energy poverty, mitigate climate change, and develop cleaner, non-fossil based energy systems.

The bulk of rural populations, particularly in developing countries, rely on agricultural activities for their livelihoods. Climate change is expected to exacerbate current problems related to increased variability in temperatures and precipitation, and enhanced extreme events. Decentralized renewable energy options can contribute to addressing current climate-related problems, affording poor communities important breakthroughs, both in terms of climate change adaptation and income generating activities. This is especially relevant in food processing and storage activities that require energy inputs.

Similarly, small-scale hydro and wind generators can reduce greenhouse gas emissions from diesel generators as well as creating power to pump water for irrigation and other agricultural activities. Both agriculture and water are vulnerable resource sectors, yet they are intimately related to rural livelihoods.

It is clear that if renewable energy is to be a serious climate adaptation option, there is a strong need to move from clustered, marginal applications and pilot projects to widespread dissemination, especially within the African continent where climate change might have disproportionate impacts.

| Types of Renewables                                | Application                                      | Mitigative Benefits  | Adaptive Benefits   | Ancillary Benefits  |
|--|--|--|---|---|
| Efficient use of biomass: Shells, peanuts, bagasse | Electricity generation<br>Heat                   | Reduced use of charcoal and woodfuel and less pressure on natural resources  | Reducing the likelihoods of deforestation through continued use of woodfuel and charcoal  | Creation of jobs and livelihood opportunities<br>Reduced drudgery therefore better quality of life<br>Reduction of time spent on fuel collection<br>Reduction of incidents related to indoor air pollution and respiratory infections prevalent with biomass  |
| Wind pumps   | Crop processing<br>Irrigation<br>Water pumping   | Decreased dependence on biomass<br>Avoidance of CO <sub>2</sub> emissions  | Greater resilience to climate related stresses through reduced vulnerability to water scarcity<br><br>More adaptation choices i. e. through irrigated agriculture and not relying solely on rainfed agriculture | Increased access to energy and energy consumption<br>Greater prospects for income generation<br>Improved quality of life<br>Reduced risks of vector borne diseases<br>Improved water supply that is beneficial for agricultural productivity and livestock rearing<br>Improved food security<br>Reduced out migratory fluxes<br>Improved performance and attendance level of school children particularly girls |
| Biogas plants                                      | Production of sludge for fertilisers             | Reduced use of biomass   | Adapting to soil erosion, aridity and environmental degradation   | Environmental sustainability; better prospects of agricultural productivity there more chances to generate income   |
| Solar Home Systems                                 | Water Heating<br>Cooking                         | Reduced consumption of woodfuel, kerosene and dry cell batteries<br><br>Reduced pressure on the environment and natural resources  |   | Improved quality of life<br>Reduced health risks  |
| Solar panels, PVs                                  | Lighting<br>Water pumping<br>Water desalination  | Improved local air quality<br><br>Reduction of CO <sub>2</sub> and reduced dependency on kerosene, woodfuel and dry cell batteries | Build resilience and coping strategies of communities especially during drought periods<br><br>Thus reduced vulnerability to water shortages  | Improved access to water<br>Reduced drudgery for women responsible for water collection<br>Reduced risks of infected water therefore improved sanitation and health   |
| Micro hydro  | Lighting<br>Access to information technology etc | Reduction of GHG<br><br>Protection of land cover   |   | Improved health (indoor air pollution and other respiratory illnesses ) as kerosene lamps are not no longer used<br>Greater school attendance with electrification at school<br>Access to internet facilities with electrification  |

*An attempt to illustrate how different small-scale renewable energy technologies can contribute to both climate change adaptation and mitigation (© United Nations Environment Programme, 2006).*

***Part 1. Tides and tidal power***

# **1. Tides**

## **1.1 Introduction**

The tide is the regular rising and falling of the ocean's surface caused by changes in gravitational forces acting on the Earth. The primary changing gravitational field is associated with the Moon while the secondary field is associated with the Sun.

The repeated cycle of sea level changes in the following stages:

- for several hours the water rises or advances up a beach (flood phase);
- the water reaches its highest level and stops at high tide; tidal currents cease (slack water or slack tide);
- the sea level falls or recedes over several hours (ebb phase);
- the level stops falling at low tide (slack or turning).

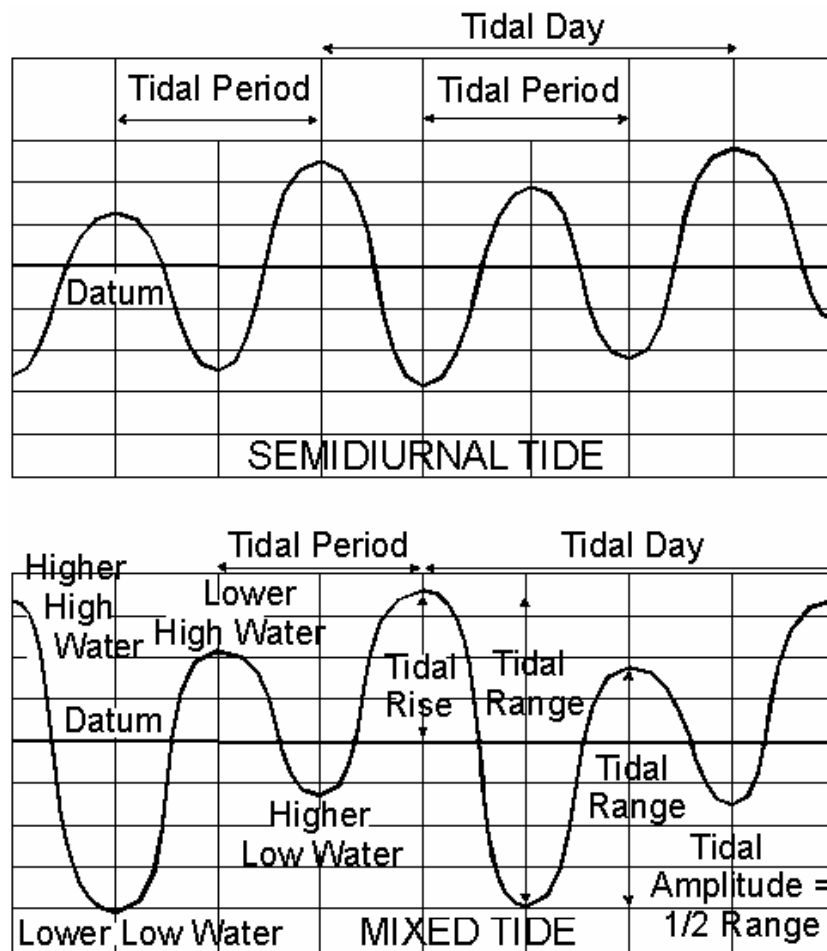


Fig. 1.1 - The repeated cycle of sea level due to tidal phenomenon.

Tides may be semidiurnal (two high tides and two low tides each day), or diurnal (one tidal cycle per day). In most locations, tides are semidiurnal. Because of the diurnal contribution, there is a difference in height (the daily inequality) between the two high tides on a given day; these are differentiated as the higher high water and the lower high water in tide tables. Similarly, the two low tides each day are referred to as the higher low water and the lower low water. The daily inequality changes with time and it is generally small when the Moon is over the equator.

Tides vary on timescales ranging from hours to years, so to make accurate records tide gauges measure the water level over time at fixed stations, which are screened from variations caused by waves shorter than minutes in period. These data are compared to the reference (or datum) level, usually the mean sea level.

## 1.2 Tidal range variation: springs and neaps

The semidiurnal tidal range (the difference in height between high and low tides over about a half day) varies in a two-week or fortnightly cycle. Around new and full moon when the Sun, Moon and Earth form a line (syzygy), the tidal forces due to the Sun reinforce those of the Moon. The tidal range is then maximum: this is called the *spring tide*, or just *springs*. When the Moon is at first quarter or third quarter, the Sun and Moon are separated by  $90^\circ$  when viewed from the Earth, and the forces due to the Sun partially cancel those of the Moon. At these points in the lunar cycle, the tidal range is minimum: this is called the *neap tide*, or *neaps*. Spring tides result in high waters that are higher than average, low waters that are lower than average, slack water time that is shorter than average and tidal currents that are stronger than average. Neaps result in less extreme tidal conditions. There is about a seven day interval between springs and neaps.

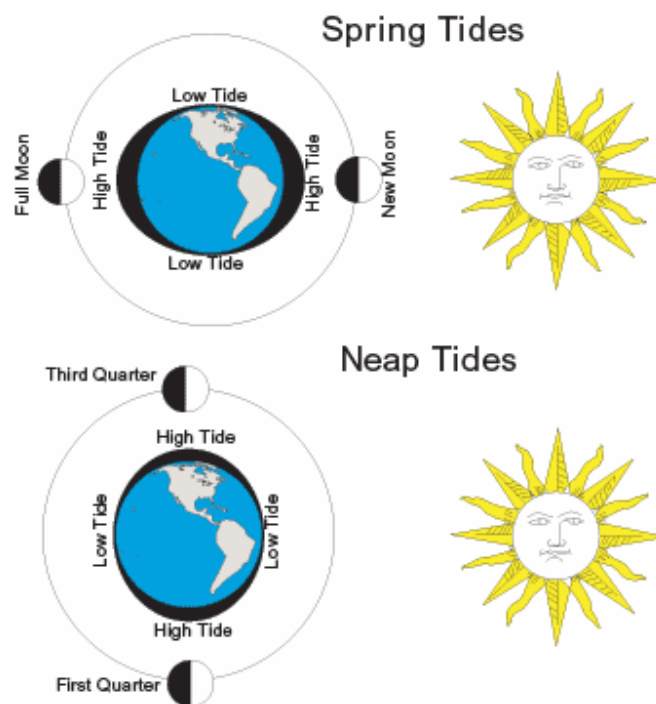
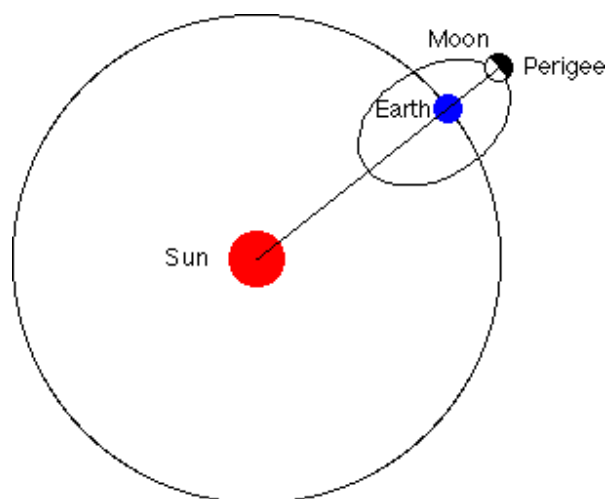


Fig. 1.2 - Reciprocal positions of Moon, Sun and Earth during spring and neap tides.

The changing distance of the Moon from the Earth also affects tide heights. When the Moon is at perigee the range is increased and when it is at apogee the range is reduced.

Every  $7\frac{1}{2}$  lunations, perigee coincides with either a new or full moon causing perigean tides with the largest tidal range. If also a storm happens to be moving onshore at this time, the consequences (in the form of flooding risk) can be especially severe.



*Fig. 1.3 - Simple draw of moon at perigee.*

### 1.3 Tidal amplitude

The theoretical amplitude of oceanic tides due to the Moon is about 54 cm at the highest point, which corresponds to the amplitude that would be reached if the ocean possessed a uniform depth, there were no landmasses, and the Earth were not rotating. The Sun similarly causes tides, of which the theoretical amplitude is about 25 cm (46% of that of the Moon) with a cycle time of 12 hours. At spring tide the two effects add to each other reaching a theoretical amplitude of 79 cm. The total amplitude changes as a result of the varying Earth-Sun and Earth-Moon distances. This causes a variation at neap tide: the theoretical level is reduced to 29 cm. Since the orbits of the Earth about the Sun, and the Moon about the Earth, are elliptical, the tide amplitudes in the tidal force and theoretical amplitude is of about  $\pm 18\%$  for the Moon and  $\pm 5\%$  for the Sun. If both the Sun and Moon were at their closest positions and aligned at new moon, the theoretical amplitude would reach 93 cm.

Real amplitudes differ considerably from the theoretical ones, because of the variations

in ocean depth and of the presence of continents.

#### 1.4 Tidal constituents

The various frequencies of astronomical forcing which contribute to tidal variations are called constituents. In most locations, the largest constituent is the principal lunar semidiurnal ( $M_2$ ). Its period is about 12 hours and 27 minutes, exactly half a tidal lunar day, the average time separating one lunar zenith from the next, and thus the time required for the Earth to rotate once relative to the Moon.

Constituents other than  $M_2$  arise from factors such as the gravitational influence of the Sun, the tilt of the Earth's rotation axis, the inclination of the lunar orbit and the ellipticity of the orbits of the Moon about the Earth and the Earth about the Sun. Variations with periods of less than half a day are called harmonic constituents. Long period constituents have periods of days, months, or years.

#### 1.5 Tidal phase

Because the  $M_2$  tidal constituent dominates in most locations, the stage or phase of a tide, denoted by the time in hours after high tide, is a useful concept. High tide is reached simultaneously along the *cotidal lines* (lines of constant tidal phase) extending from the coast out into the ocean, and cotidal lines (and hence tidal phases) advance along the coast. If one thinks of the ocean as a circular basin enclosed by a coastline, the cotidal lines point radially inward and must eventually meet at a common point, the *amphidromic point*. An amphidromic point is at once cotidal with high and low tides, which is satisfied by zero tidal motion. The rare exception occurs when the tide circles around an island, as it does around New Zealand.

Moreover tidal motion generally lessens moving away from the continental coasts, so that crossing the cotidal lines are contours of constant amplitude which decrease to zero at the amphidromic point. For a 12 hour semidiurnal tide the amphidromic point behaves roughly like a clock face, with the hour hand pointing in the direction of the high tide cotidal line, which is directly opposite the low tide cotidal line. High tide rotates about once every 12 hours in the direction of rising cotidal lines, and away from ebbing cotidal

lines. The difference of cotidal phase from the phase of a reference tide is the epoch.

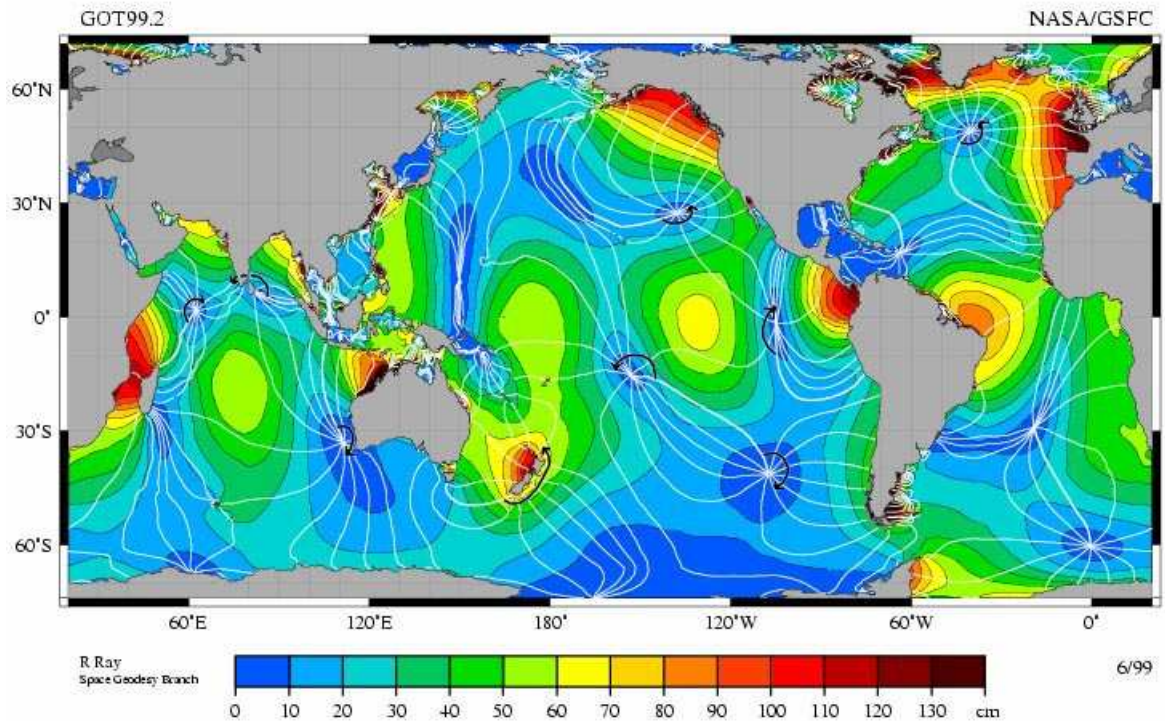


Fig. 1.4 - The  $M_2$  tidal constituent.

Amplitude is indicated by colours; the white lines are cotidal differing by 1 hr. The curved arcs around the amphidromic points show the direction of the tides, each indicating a synchronized 6 hour period. (Y. Accad, C. L. Pekeris, 1978)

The shape of the shoreline and the ocean floor change the propagation behaviour of the tides, so there is no simple, general rule for predicting the time of high tide from the position of the Moon in the sky. Coastal characteristics such as underwater topography and coastline shape mean that individual location characteristics need to be taken into consideration when forecasting tides.

## **1.6 Tidal physics**

### **1.6.1 Background**

Isaac Newton laid the foundations for the mathematical explanation of tides in the *Philosophiae Naturalis Principia Mathematica* (1687). In 1740, the Académie Royale des Sciences in Paris offered a prize for the best theoretical essay on tides. Daniel Bernoulli, Antoine Cavalleri, Leonhard Euler, and Colin Maclaurin shared the prize. Maclaurin used Newton's theory to show that a smooth sphere covered by a sufficiently deep ocean under the tidal force of a single deforming body is a spheroid with major axis directed toward the deforming body. Maclaurin was also the first to write about the Earth's rotational effects on motion. Euler realized that the horizontal component of the tidal force (rather than the vertical) drives the tide. In 1744 D'Alembert studied tidal equations for the atmosphere which did not include the effect of rotation.

The first major theoretical formulation for water tides was proposed by Pierre-Simon Laplace, who formulated a system of partial differential equations relating the horizontal flow to the surface height of the ocean. The Laplace tidal equations are still in use today. William Thomson rewrote Laplace's equations in terms of vorticity which allowed for solutions describing tidally driven coastally trapped waves, which are known as Kelvin waves.

### **1.6.2 Tidal forces**

Tidal forces can be analyzed from the point of view of a reference frame that translates with the centre of mass of the Earth. Consider the tide due to the Moon (the Sun is similar). At first observe that the Earth and Moon rotate around a common orbital centre of mass with a 27.3 day period, as determined by their relative masses. The orbital centre of mass is  $3/4$  of the way from the Earth's centre to its surface.

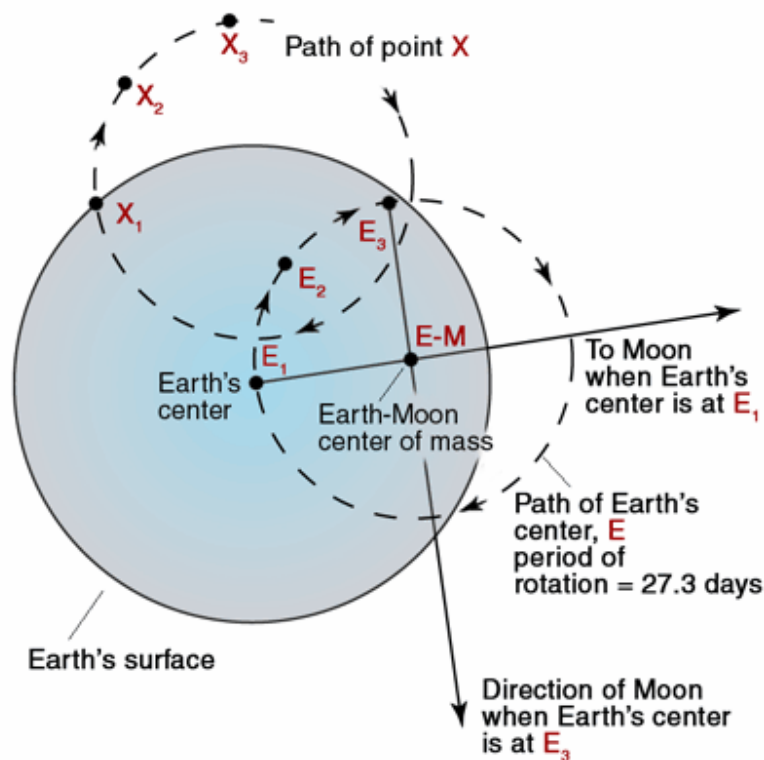


Fig. 1.5 - Earth-moon centre of mass and period of rotation (Naval Postgraduate School, Monterey, California).

The second observation is that the Earth's centripetal motion is the averaged response of the entire Earth to the Moon's gravity and it is exactly the correct motion to balance the Moon's gravity only at the centre of the Earth; but every part of the Earth moves along with the centre of mass and all parts have the same centripetal motion, since the Earth is rigid. On the other hand each point of the Earth experiences the Moon's radially decreasing gravity differently; the near parts of the Earth are more strongly attracted than is compensated by inertia and experience a net tidal force toward the Moon; the far parts have more inertia than is necessary for the reduced attraction, and thus feel a net force away from the Moon.

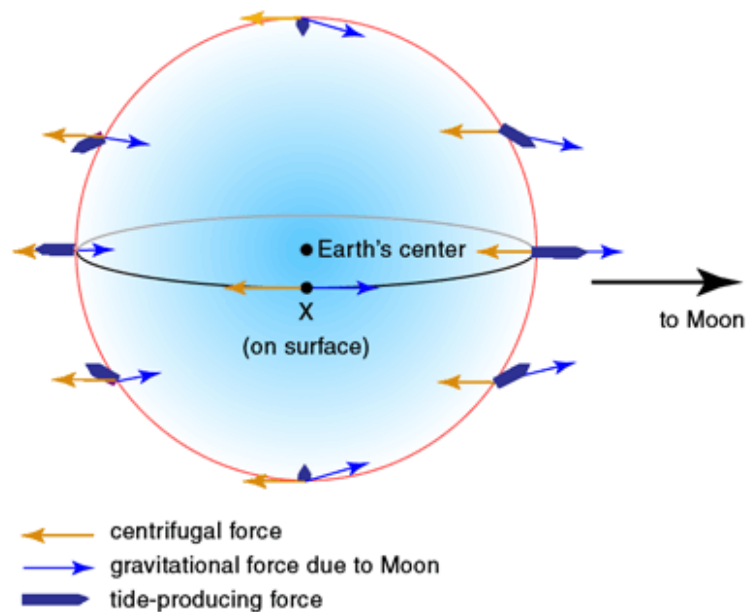


Fig. 1.6 - Tide-producing force as vector addition of centrifugal force and gravitational force due to moon (Naval Postgraduate School, Monterey, California).

The actual tidal acceleration on a particle is only about a ten millionth of gravity acceleration, thus the radial component does not change Earth's gravity significantly. On the contrary, even though the horizontal component of the tidal forces has similar magnitude, it is able to drive a tidal acceleration of the water particles, as it is balanced by shear stresses, that are small because of the high ocean's depth.

### 1.6.3 Laplace tidal equation

The depth of the oceans is much smaller than their horizontal extent; thus, the response to tidal forcing can be modelled using the Laplace tidal equations, which incorporate the following features:

- the vertical (or radial) velocity is negligible, and there is no vertical shear: it's a sheet flow;
- the forcing is only horizontal (tangential);
- the Coriolis effect appears as a fictitious lateral forcing proportional to velocity;
- the rate of change of the surface elevation is proportional to the negative

divergence of velocity multiplied by the depth.

The last feature implies that, as the horizontal velocity stretches or compresses the ocean as a sheet, the volume thins or thickens, respectively. The boundary conditions dictate no flow across the coastline, and free slip at the bottom. The Coriolis effect steers waves to the right in the northern hemisphere and to the left in the southern hemisphere leading to waves being coastally trapped. Finally, a dissipation term can be added which is an analogue of viscosity.

## **1.7 Tidal observations and predictions**

### **1.7.1 Background**

The first known sea-level record of an entire spring–neap cycle was made in 1831 on the Navy Dock in the Thames Estuary, and many large ports had automatic tide gages stations by 1850.

William Whewell first mapped co-tidal lines ending with a nearly global chart in 1836. In order to make these maps consistent, he hypothesized the existence of amphidromes where co-tidal lines meet in the mid-ocean. These points of no tide were confirmed in 1840 by field measurements of Captain Hewett obtained from careful soundings in the North Sea.

### **1.7.2 Timing**

In most places there is a delay between the phases of the Moon and the effect on the tide. Springs and neaps in the North Sea, for example, are two days behind the new/full Moon and first/third quarter. This is called the age of the tide.

The exact time and height of the tide at a particular coastal point is also greatly influenced by the local bathymetry. Southampton in the United Kingdom has a double high tide caused by the interaction between the different tidal harmonics within the region. This is contrary to the popular belief that the flow of water around the Isle of Wight creates two high waters. The Isle of Wight is important, however, as it is responsible for the 'Young Flood Stand', which describes the pause of the incoming tide about three hours after low water.

Because the oscillation modes of the Mediterranean Sea and the Baltic Sea do not coincide with any significant astronomical forcing period the largest tides are close to their narrow connections with the Atlantic Ocean. Extremely small tides also occur for the same reason in the Gulf of Mexico and Sea of Japan. On the southern coast of Australia, because the coast is extremely straight (partly due to the tiny quantities of runoff flowing from rivers), tidal ranges are equally small.

## **1.8 Tidal analysis**

When compared with a periodically varying function, the standard approach is to employ Fourier series. However, for the analysis of tide elevation, the Fourier Series approach is best made more elaborate. While the theorem remains true and the tidal elevation could be analyzed in terms of a single frequency and its harmonics, a large number of significant terms would be required. A much better decomposition for this case involves a basis set having more than one fundamental frequency: specifically, the periods of one revolution of the earth, and one orbit of the moon about the earth are incommensurable (for simplicity in phrasing, this discussion is entirely geocentric, but is informed by the heliocentric model). So, to represent both influences via one frequency would require many harmonics. That is, the sum of two sinusoids, one at the sun's frequency and the second at the moon's frequency, requires those two terms only, while their representation as a Fourier Series having one fundamental frequency and its (integer) multiples would require many terms. For tides then, although the process is still termed Harmonic Analysis, it does not limit itself to harmonics of a single frequency. In other words, the harmonics are multiples of many fundamental frequencies, not just of the one fundamental frequency of the common Fourier series approach.

The study of tide elevation by Harmonic Analysis was initiated by Laplace, Lord Kelvin and George Darwin, it was then rigorously extended by A.T. Doodson who introduced the Doodson Number notation to organise the hundreds of terms that result. This approach has been the international standard ever since, and the complications arise as follows: so far, the tide raising and falling elevation  $h$  [m] is given by:

$$h(t) = a \cos(\omega t + p)$$

where:

- $a$  is the amplitude [m];
- $\omega$  is the angular frequency (usually given in degrees per hour);
- $t$  denotes time;
- $p$  is the phase offset (in degrees) with regard to the astronomical state at time  $t = 0$ .

There is a term for the moon and a second term for the sun. Accordingly, the value of  $a$  is itself varying with time, slightly, about some average figure. Hence, replacing it by  $a(t)$ , it turns out that another sinusoid gives an excellent approximation:

$$a(t) = a_0[1 + a_a \cos(\omega_a t + p_a)]$$

which is to say an average value  $a_0$  with a sinusoidal variation about it of magnitude  $a_a$ , with frequency  $\omega_a$  and phase  $p_a$ . Thus the simple term is now a compound term, the product of two cosine terms:

$$h(t) = a_0[1 + a_a \cos(\omega_a t + p_a)]\cos(\omega t + p)$$

Now, given that

$$\cos(a)\cos(b) = \frac{\cos(a+b) + \cos(a-b)}{2}$$

the following relationship is found:

$$h(t) = a_0 \cos(\omega t + p) + \frac{a_0 a_a \cos(\omega_a t + p_a + \omega t + p)}{2} + \frac{a_0 a_a \cos(\omega_a t + p_a - \omega t - p)}{2}$$

It is clear that a compound term involving the product of two cosine terms each with their own frequency is the same as three simple cosine terms that are to be added, at the original frequency and also at the sum and difference of the two frequencies of the product term.

Consider further that the tidal force on a location depends also on whether the moon (or the sun) is above or below the plane of the equator, and that these attributes have their own periods also incommensurable with a day and a month, and it is clear that many

combinations result. With a careful choice of the basic astronomical frequencies, the Doodson Number annotates the particular additions and differences of them to form the frequency of each simple cosine term.

Remember also that the astronomical tides do not include the effect of weather. Moreover, changes of local conditions (sandbank movement, dredging harbour mouths) can affect the timing and magnitude of the actual tide.

## **1.9 Tidal currents**

The flow pattern due to tidal influence is more difficult to analyse. Moreover, data is more difficult to collect. A tidal height is a simple number, and applies to a wide region simultaneously (often as far as the eye can see), but a flow has both a magnitude and a direction, it can vary substantially over just a short distance due to local bathymetry and it also varies with depth. A flow proceeding up a curved channel is the same flow, even though its direction varies continuously along the channel. Even the obvious expectation that the flood and ebb flows will be in opposite directions is not met, as the direction of a flow is determined by the shape of the channel it is coming from, not the shape where it will shortly be. Likewise, eddies can form in one direction but not in the other.

Nevertheless, the analysis proceeds on the same basis. At a given location in the simple case, the great majority of the flood flow will be in one direction, and the ebb flow in another (not necessarily opposite) direction. Take the velocities along the flood direction as positive, and along the ebb direction as negative, and proceed as if these were tide height figures. In more complex situations, the flow will not be dominated by the main ebb and flood directions, with the flow direction and magnitude tracing out an ellipse over a tidal cycle (on a polar plot) instead of along the two lines of ebb and flood direction. In this case, the analysis might proceed along two pairs of directions, the primary flow directions and the secondary directions at right angles. Alternatively, the tidal flows can be treated as complex numbers, as each value has both a magnitude and a direction.

As with tide height predictions, tide flow predictions based only on astronomical factors do not take account of weather conditions, which can completely change the situation. The tidal flow through Cook Strait between the two main islands of New Zealand is

particularly interesting, as on each side of the strait the tide is almost exactly out of phase so that high tide on one side meets low tide on the other. Strong currents result, with almost zero tidal height change in the centre of the strait. Yet, although the tidal surge should flow in one direction for six hours and in the reverse direction for the following six hours, a particular surge might last eight or ten hours with the reverse surge enfeebled. In especially boisterous weather conditions, the reverse surge might be entirely overcome so that the flow remains in the same direction through three surge periods and longer.

## **2. Tidal power**

### **2.1 Introduction**

Electrification of all aspects of modern civilization has led to the development of various converters for transforming energy from natural power sources into electricity. However, the power plants that use fossil and nuclear fuels create huge new environmental pollution problems, along with the fact that these resources are quickly becoming depleted. Thus, clean renewable energy sources for generating electric power are attracting much attention around the world.

Energy from ocean and tidal currents is one of the best available renewable energy sources. In contrast to other clean sources, such as wind, solar, geothermal etc., tides can be predicted for centuries into the future; thus power outputs can be accurately calculated far in advance, allowing for easy integration with existing electricity grids.

However, this energy, like that from wind and solar, is distributed over large areas that makes it more difficult to economically harness. Moreover tidal power systems do not generate electricity at a steady rate and thus not necessarily at times of peak demand.

### **2.2 Two ways of generating electricity from tides**

There are basically two ways of generating electricity from marine and tidal currents: by building a tidal barrage across an estuary or a bay in high tide range areas, or by extracting energy from free flowing water.

In the first case tidal barrage harnesses the energy in a similar way as run-of-river hydro power plants and was the first ocean energy technology to be used in a large scale project.

The barrage traps a water level inside a basin; this leads to a decrease of tidal range inside the basin or lagoon, implying a reduced transfer of water between the basin and the sea. The reduced transfer of water accounts for the energy produced by the scheme.

The second ocean energy technology is capturing the energy in free flowing water, meaning much less civil engineering work and less environmental impact at the site. A great deal of attention was drawn to marine and tidal currents as a possible source of energy during the oil crisis in the 1970s, but all in all the abundant resources of tidal

energy have remained untapped. However, recent developments in power electronics, in the offshore industry and in wind power technology have brought tidal energy much closer to an introduction on the electricity market. At present, there are a number of promising and more or less innovative concepts for Marine Current Energy Converters.

## 2.3 Barrage tidal power

### 2.3.1 Introduction

A barrage is built across an estuary or a bay that experiences an adequate tidal range. The purpose is to create a basin where water level raises and falls with a time law different from that of the open sea, in order to create a hydrostatic head. The turbines placed along the barrage generate power as water flows in and out the bay. The system is then similar to a low head hydro dam.

The construction of a barrage requires a very long civil engineering project. It will have environmental and ecological impacts, not only during construction, but will change the affected area forever. Just what these impacts will be is very hard to measure as they are site specific, and each barrage is different.

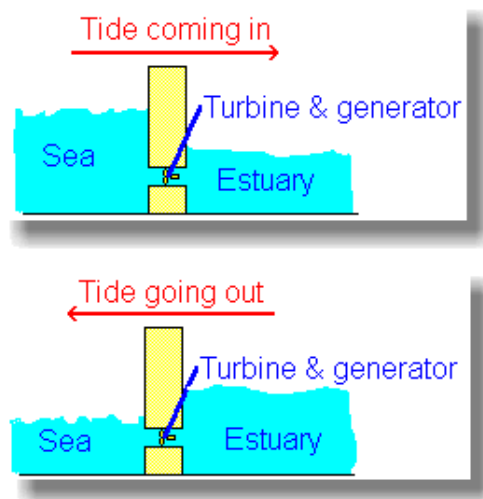


Fig. 2.1 - Simple draw of the operating condition of a two-ways barrage tidal power plant (Andy Darvill, Broadoak Community School).

*Ebb generation:* also known as outflow generation, it takes its name because generation occurs as the tide ebbs. The basin is filled through the sluices until high tide. Then the sluice gates are closed. At this stage there may be pumping to raise the level further. The turbine gates are kept closed until the sea level falls to create sufficient head across the barrage, and then are opened so that the turbines generate until the head is again low. Then the sluices are opened, turbines disconnected and the basin is filled again. The cycle repeats itself.

*Flood generation:* the basin is filled through the turbines, which generate at tide flood. This is generally less efficient than ebb generation, because the volume contained in the upper half of the basin (which is where ebb generation operates) is greater than the volume of the lower half; so the difference in levels between the basin side and the sea side of the barrage, and therefore the available potential energy, is less than it would otherwise be.

*Pumping:* the turbines in the barrage can be used to pump extra water into the basin at periods of low demand. This usually coincides with cheap electricity prices, generally at night when demand is low. The company therefore buys the electricity to pump the extra water in, and generates power at times of high demand when prices are high so as to make a profit. This has been used in Hydro Power, and in that context is known as pumped storage.

*Two way power generation:* electrical power is generated from both the ebb and the flood tides. Ebb generation starts at a basin level that is less than that of a single generation (towards the end of the generating cycle, the sluice gates are opened to allow flow from the basin to the sea and hence drop the water level in the basin). This is necessary to achieve a sufficient difference in water height during the flood generation phase. At low tide, the sea and basin levels become equal and the gates are closed. Once the sea has risen to the optimum height, generation begins by operating the turbine in the opposite direction.

*Two-basin schemes*: another form of energy barrage configuration is that of the dual basin type. With two basins, one is filled at high tide and the other is emptied at low tide. Turbines are placed between the basins. Two-basin schemes offer advantages over normal schemes because generation time can be adjusted with high flexibility and it is also possible to generate almost continuously. In normal estuarine configuration, however, two-basin schemes are very expensive to construct due to the cost of the extra length of barrage. There are some favourable geographical settings, however, which are well suited to this type of scheme.

### **2.3.2 Single-basin two way installation**

All the above schemes were the subject of several studies and all of them present advantages and disadvantages. A single-basin two way installation corresponds best to the natural development of the tide and then leads to the maximum exploitation of the site potential tidal energy; moreover it requires the least degree of regulation.

These are the reasons why this scheme is most suitable in a developing country and is analysed in the present thesis.

### **2.3.3 Energy calculation**

The capacity of tidal power plants (TPP) should not be expressed as a function of head and discharge (which can be calculated after the regulation method has been fixed), but as a function of the basin surface  $S$  [m<sup>2</sup>] and the tidal range  $R$  [m].

Assuming arbitrarily that there is no surface gradient, the work  $L$  [J] performed by the tide during the flood-ebb cycle is the product of the weight of the water raised and lowered by the tide and the height to which the centre of gravity of this mass is lifted:

$$L = \rho gRS \frac{R}{2}$$

where  $\rho$  is the water density ( $\rho = 1000 \text{ kg/m}^3$ ) and  $g$  is the acceleration due to gravity ( $g = 9.81 \text{ m/s}^2$ ).

The work performed each day by the tide is equal to  $L$  multiplied by 3.87 (3.87 being the

number of tidal oscillation per day).

Dividing by the number of seconds per day, the average power potential of the tide  $P$  [W] is:

$$P = 0.9 S \left( \frac{R}{2} \right)^2$$

Finally, following Bernshtein , Gibrat and Mosonyi (1965), the yearly energy reserve  $E$  [KWh/year] is:

$$E = 1.97 S R^2$$

Alternatively, after the regulation method has been chosen or in the case of free flow tidal generation, the energy can be calculated by integrating the power output over a time  $t$ :

$$E = \int_0^t P(\tau) d\tau$$

### 2.3.4 Power output and basin regulation

The power output  $P$  [W] at any instant is given by the following formula:

$$P(t) = \rho g Q(t) \Delta H(t)$$

where  $Q$  [m<sup>3</sup>/s] is the *discharge* flowing through the turbines and  $\Delta H$  is the *head* [m]. In low head sites, where pipes are not too long,  $\Delta H$  is just the difference between upstream and downstream level.

While the tide forces the sea level to vary according to a sinusoidal law, the level in the basin oscillates as a function of the basin filling or emptying conditions. These conditions depend on the number and diameter of turbines (determining the filling rate), on the duration of basin and sea level equalization and on the instants of turbine starting and stopping which are determined by the initial and final heads.

If it is specified that the basin is shut off at high water and low water, the regulation will be called *synchronous*. In this case, water always flows through the turbines in the direction of the tidal wave, and the free surface elevation in the basin is in phase with the

tide.

If a phase shift occurs between TPP operation and tide (such as filling the basin during ebb) the regulation will be called *asynchronous*. Because the rate of sea level variation gradually decreases when approaching high or low water, the replenishment time (the time necessary for the accumulation of the required head in the basin) will be longer with synchronous regulation than if the basin is shut off at some other instant at which the rate of level variation is larger. In order to lengthen the operating interval asynchronous regulation is thus required.

Basin regulation does not need to be based on an infinite sequence of different tides, but it can be based on a single average tidal range for which the optimum conditions have to be determined, with subsequent refinement for extreme ranges.

### **2.3.5 Technologies**

#### **2.3.5.1 Introduction**

There are different types of turbines that can be used for energy production in a tidal barrage system:

- *waterwheels*, which were used since the invention of the tidal mill until the industrial revolution, are suitable for use in a developing country because of their simple construction and working conditions;
- *Kaplan* turbines, widely used in low head power production;
- *Bulb* turbines, which are usually installed in barrage tidal plants.

Moreover, if further tidal schemes will be proposed, additional types of turbines will be tested and implemented.

#### **2.3.5.2 Waterwheel turbines**

The first turbine used was the basic *undershot waterwheel*. This is probably the oldest type of waterwheel dating back over two thousand years. It is mounted vertically on a horizontal axle and it has flat boards located radially around a rim. It is turned by water flowing under the wheel and striking the boards.

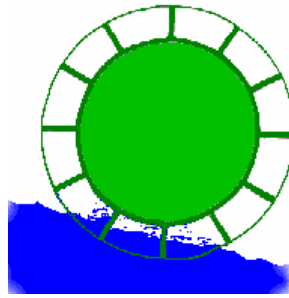


*Fig. 2.2 - Simple draw of an undershot waterwheel (Peter Clark et al. Tidal Energy, 2003).*

The second type of turbine used was an *overshot waterwheel*. The overshot wheel is much more efficient than the undershot wheel. Again, this turbine is mounted vertically on a horizontal axle, but the overshot wheel has buckets mounted around the rim. Water from above flows into the buckets causing one side of the wheel to be heavier. Gravity then acts on the heavier side causing the wheel to turn.

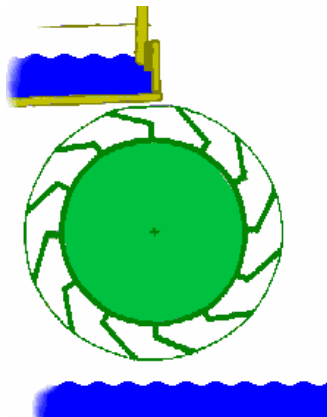


*Fig. 2.3 - Simple draw of an overshot waterwheel (Peter Clark et al. Tidal Energy, 2003).*

The third type of turbine used was a *breast-shot waterwheel*. This type of wheel was developed in the late middle ages and combines the previous two waterwheels. It has buckets on a rim that face the opposite direction of the buckets on the overshot wheel. Water then fills the buckets at the middle of the wheel. Again, gravity acting upon the water in the buckets causes the wheel to turn.

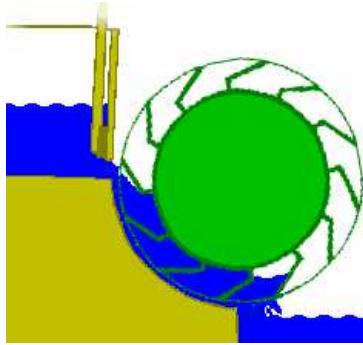


Fig. 2.4 - Simple draw of a breast-shot waterwheel (Peter Clark et al. Tidal Energy, 2003).

### 2.3.5.3 Kaplan turbines

The Kaplan turbine is a propeller-type water turbine that has adjustable blades. It was developed in 1913 by the Austrian professor Viktor Kaplan.

The Kaplan turbine was an evolution of the Francis turbine. Its invention allowed efficient power production in low head applications that was not possible with Francis turbines.

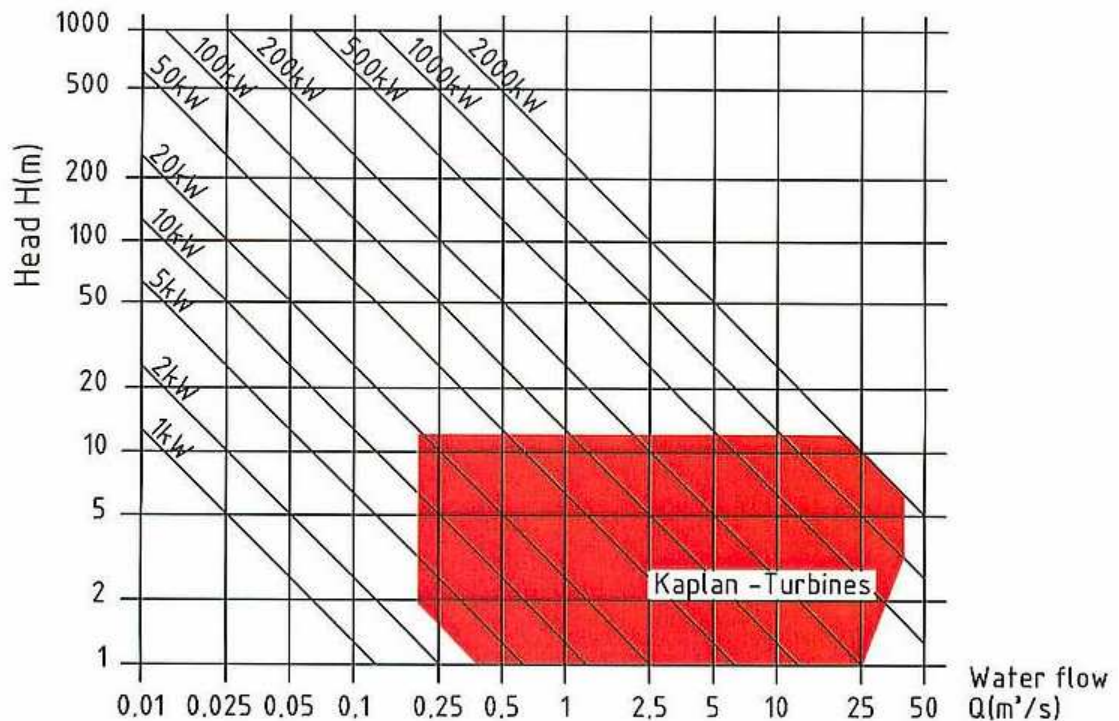
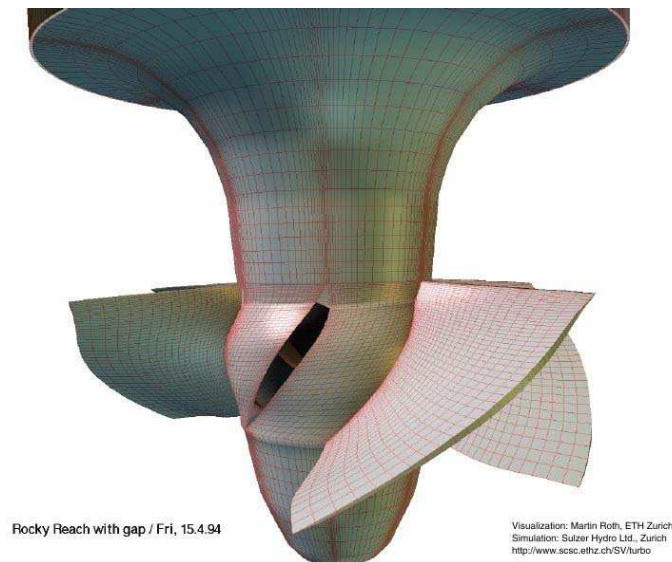


Fig. 2.5 - Range of OSSBERGER Kaplan turbine (OSSBERGER, © www-werbeagentur-wie.de)

Kaplan turbines are now widely used throughout the world in high-flow, low-head power production. The Kaplan turbine is an inward flow reaction turbine, which means that the working fluid changes pressure as it moves through the turbine and gives up its energy. The design combines radial and axial features.



*Fig. 2.6 - Kaplan turbine (Martin Roth, ETH Zurich).*

The inlet is a scroll-shaped tube that wraps around the turbine wicket gate. Water is directed tangentially, through the wicket gate, and spirals on to a propeller shaped runner, causing it to spin. The outlet is a specially shaped draft tube that helps decelerate the water and recover kinetic energy.

The turbine does not need to be at the lowest point of water flow, as long as the draft tube remains full of water. A higher turbine location, however, increases the suction that is imparted on the turbine blades by the draft tube. The resulting pressure drop may lead to cavitation.

Variable geometry of the wicket gate and turbine blades allow efficient operation for a range of flow conditions. Kaplan turbine efficiencies are typically over 90%, but may be lower in very low head applications.

Large Kaplan turbines are very expensive to design, manufacture and install, but operate for decades. Inexpensive micro turbines are manufactured for individual power production with as little as 0.6 m of head.

#### 2.3.5.4 VLH turbines

To make their equipment more competitive, hydraulic turbine constructors have always endeavoured to optimize their product by increasing performances, in particular by a permanent research oriented towards the decrease of the runner diameters. This has led to water intake and outlet structures of sizes such that their economical implementation is impossible when the head is too low.



*Fig. 2.7 - VLH turbine (VLH turbines, MJ2 Technologies S.A.R.L.).*

The basic idea of the VLH concept goes against this tendency by aiming at decreasing, as much as possible, intake and outlet structures by increasing the size of the turbine runner diameter and by integrating therein a self-supporting structure which ensures all the functions of a conventional facility.

The VLH incorporates the following functions:

- standardized Kaplan turbine with 8 blades adjustable according to the level and to the flow rate;
- self-supporting structure enabling complete factory assembly and very fast mounting or dismounting;
- slow direct-drive variable-speed permanent-magnet generator;
- device for stopping and cutting off the flow by closing of the blades on themselves with no power from the system. VLH installations do not require fixed wheel gates to stop the unit;
- distributor used as a protection grid;

- embarked rotating trash rake cleaner;
- electronic speed variator;
- integrated electronic control equipments managing the turbo generator unit and the power electronics equipments;
- withdrawal device enabling taking the unit out of the water for maintenance or for withdrawal in case of a flood.

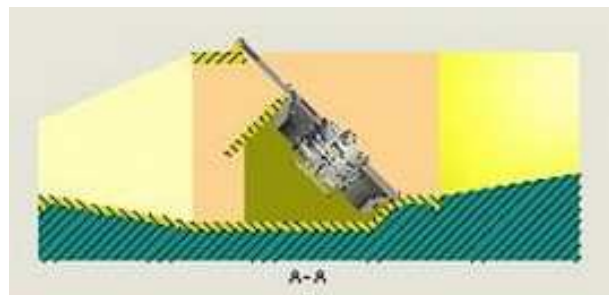


Fig. 2.8 - Simple draw of a VLH turbine (VLH turbines, MJ2 Technologies S.A.R.L.).

|  |      | Runner diameters in mm<br>Diamètres de roue en mm |      |      |      |      |
|--|------|---|------|------|------|------|
|  |      | 3550  | 4000 | 4500 | 5000 | 5600 |
| Net Head in meter<br>Hauteur de chute nette en m | 1,4  | 10,4  | 13,2 | 16,8 | 20,7 | 25,9 |
|  | 1,5  | 10,8  | 13,7 | 17,3 | 21,4 | 26,9 |
|  | 1,6  | 11,1  | 14,2 | 17,9 | 22,1 | 27,7 |
|  | 1,7  | 11,5  | 14,6 | 18,5 | 22,8 | 28,6 |
|  | 1,8  | 11,8  | 15,0 | 19,0 | 23,5 | 29,4 |
|  | 1,9  | 12,1  | 15,4 | 19,5 | 24,1 | 30,2 |
|  | 2,0  | 12,5  | 15,8 | 20,0 | 24,7 | 31,0 |
|  | 2,1  | 12,8  | 16,2 | 20,5 | 25,3 |      |
|  | 2,2  | 13,1  | 16,6 | 21,0 | 25,9 |      |
|  | 2,3  | 13,4  | 17,0 | 21,5 | 26,5 |      |
|  | 2,4  | 13,7  | 17,3 | 21,9 |      |      |
|  | 2,5  | 13,9  | 17,7 | 22,4 |      |      |
|  | 2,6  | 14,2  | 18,0 | 22,8 |      |      |
|  | 2,7  | 14,5  | 18,4 | 23,3 |      |      |
| 2,8  | 14,7 | 18,7  |      |      |      |      |

|  |     | Runner diameters in mm<br>Diamètres de roue en mm |      |      |      |      |
|--|-----|---|------|------|------|------|
|  |     | 3550  | 4000 | 4500 | 5000 | 5600 |
| Net Head in meter<br>Hauteur de chute nette en m | 1,4 | 114   | 145  | 184  | 227  | 284  |
|  | 1,5 | 127   | 161  | 204  | 251  | 315  |
|  | 1,6 | 140   | 177  | 224  | 277  | 347  |
|  | 1,7 | 153   | 194  | 246  | 303  | 380  |
|  | 1,8 | 167   | 211  | 268  | 330  | 414  |
|  | 1,9 | 181   | 229  | 290  | 358  | 449  |
|  | 2,0 | 195   | 248  | 313  | 387  | 485  |
|  | 2,1 | 210   | 266  | 337  | 416  |      |
|  | 2,2 | 225   | 286  | 362  | 446  |      |
|  | 2,3 | 241   | 305  | 386  | 477  |      |
|  | 2,4 | 256   | 325  | 412  |      |      |
|  | 2,5 | 273   | 346  | 438  |      |      |
|  | 2,6 | 289   | 367  | 464  |      |      |
|  | 2,7 | 306   | 388  | 492  |      |      |
| 2,8  | 323 | 410   |      |      |      |      |

Fig. 2.9 - VLH turbine working condition; from these tables we can estimate their efficiency:  $\eta = 79\%$  (VLH turbines, MJ2 Technologies S.A.R.L.).

### 2.3.5.5 Bulb turbines

The bulb turbine is a reaction turbine of Kaplan type which is used for the lowest heads. It is characterised by having the essential turbine components as well as the generator inside a bulb, from which the name is developed. A main difference from the Kaplan turbine is that the water flows with a mixed axial-radial direction into the guide vane

cascade and not through a scroll casing. The guide vane spindles are inclined (normally 60°) in relation to the turbine shaft. Contrary to other turbine types this results in a conical guide vane cascade. The bulb turbine runner is similar to the Kaplan turbine runner, and it may also have different numbers of blades depending on the head and water flow. Bulb turbines are specially indicated for tidal power plants of the barrage type because of their two way working condition.

The bulb turbine consists of the following main components:

- stay cone;
- runner chamber;
- draft tube cone;
- generator hatch;
- stay shield;
- rotating parts;
- turbine bearing;
- shaft seal box;
- guide vane mechanism.

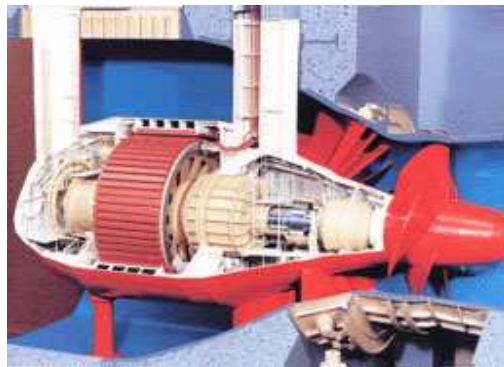


*Fig. 2.10 - Bulb turbine (Hitachi, Ltd. 1994, 2005).*

The water flows axially towards the unit in the centre of the water conduit and passes the generator, the main stays, the guide vanes, runner and draft tube into tail race channel. The general principles for condition control are the same as for the Francis turbines. Further discussion on bulb turbines is therefore connected only to a few specific details:

- the runner should be inspected both from above and below. Particular attention

should be given to possible cavitation erosion and scratches on the blades as well as leaks around the blade flange against the hub;

- the narrow gap between runner and the runner chamber should be checked to verify if foreign objects may have passed through the gap and scratched the chamber;
- for guide vane mechanism with individual vane servomotors on bulb turbines it should be checked that the vanes have an identical movement;
- for bulb turbines at standstill it should be checked that the water does not flow out of the box along the shaft into the turbine bearing;
- generally for bulb turbines special attention should be paid to changes in the sound when the unit is in operation.

Among the large main parts of the bulb turbine it is only the runner which normally needs to be dismantled. The runner chamber is split axially horizontal into two halves. By removing the upper half access to the runner is obtained.

The guide vanes cannot be dismantled without extensive work. Repairs of these and the guide surfaces should be performed at the plant. Bearing and seal box can easily be dismantled. By applying the overhaul seal the seal box may be removed without draining the water canal. Then necessary stairs and floors around the guide vane and the runner chamber may be erected.

The stay shields are adapted against bulb and outer water conduit contour. The shields are mounted as soon as the generator bulb and penstock are completed.

Finally the generator hatch dome plate and cover are installed.

Some further variants of bulb turbine exist.

*Rim turbine:* it is similar to the bulb turbine except for the generator, which is mounted on the periphery of the turbine runner. A seal must be provided to prevent water from entering the generator. This seal is critical to the satisfactory operation of the units. Performance characteristics are similar to those of bulb turbines. Wicket gates can be installed to regulate the flow and both fixed and adjustable pitch blades are available. The rim turbine provides the most compact powerhouse layout of any type of unit in this

head range. However, the limited number of manufacturers that design and build this type of turbine may result in uncompetitive bids.

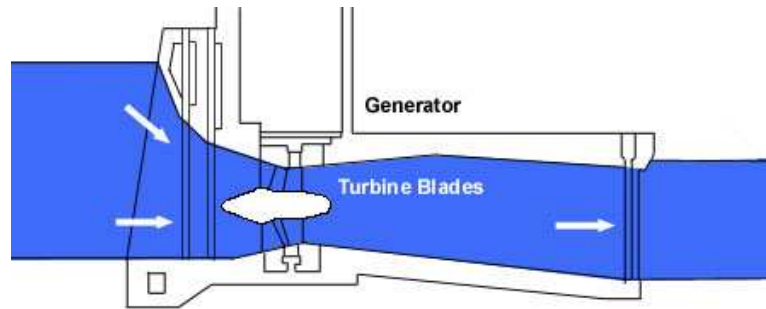


Fig. 2.11 - Simple sketch of a rim turbine (Peter Clark et al. Tidal Energy, 2003).

*Pit turbines* are comparable to bulb turbines in that all mechanical components are located upstream of the runner. The draft tube can therefore be designed to obtain the best hydraulic performance. A further advantage is that the fitting of a gearwheel between the turbine and the generator provides the possibility of selecting a generator with a higher speed. The size of the generator can be reduced by a considerable amount. The pit turbine can be regulated with the help of the wicket gates as well as the adjustable blades of the runner, and shows a similar performance for reduced discharges as in the case of the bulb unit.

### 2.3.6 Economics

The capital required to start the construction of a barrage has been the main stumbling block to barrage tidal power deployment. In fact, it represents a non attractive proposition to an investor due to long payback periods. This problem could be solved by government funding or large organisations getting involved with tidal power. In terms of long term costs, once the construction of the barrage is complete, there are very small maintenance and running costs and the turbines only need replacing once around every 30 years. The life of the plant is indefinite and for its entire life it will receive free fuel from the tide.

The economics of a tidal barrage is very complicated. The major factors in determining the cost effectiveness of such a plant are its size (length and height of the barrage

required) and the difference in height between high and low tides. These factors can be expressed in the *Gibrat ratio* of a site. This is the ratio of length of barrage (in meters) to the annual energy production (in KWh). The smaller is the site Gibrat ratio, the more desirable is the site.

### **2.3.7 Social implications**

Building a tidal barrage can have many social consequences on the surrounding area. During the construction of the barrage, the amount of traffic and people in the area will increase dramatically and will last for a number of years. This will also bring revenue to the area from the tourism and hospitality industry that will accommodate all the different types of visitors that the barrage will bring; this will give a boost to the local economy. The barrage can be used as a road or rail link, providing a time saving method for crossing the bay or estuary. There is also the possibility of incorporating wind turbines into the barrage to generate extra power. The barrage would affect shipping and navigation and provision would have to be made to allow ships to pass through.

The bay would become available for recreation; the waters would be calmer not immediately after the barrage but further in towards the land; this would be another tourist attraction and become a feature of the area.

### **2.3.8 Environmental aspects**

Perhaps the largest disadvantages of tidal barrages are the environmental and ecological impacts on the local area. This is very difficult to predict, each site is different and few projects are available for comparison. The change in water level and possible flooding would affect the vegetation around the coast, having an impact on the aquatic and shoreline ecosystems. The quality of the water in the basin or estuary would also be affected, the sediment levels would change, affecting the turbidity of the water and therefore affecting the animals that live in it and depend upon it such as fish and birds. Fish would undoubtedly be affected unless provision was made for them to pass through the barrage without being killed by turbines. All these changes would affect the types of birds that are in the area, as they will migrate to other areas with more favourable

conditions for them.

These effects are not all bad, and may allow different species of plant and creature to flourish in an area where they are not normally found. But these issues are very delicate, and need to be independently assessed for the area in question.

### 2.3.9 Prospective sites for tidal energy projects

The choice of an attractive site for a barrage tidal power plant has been studied by several authors; the following table shows some of these sites.

| Country      | Location        | Mean tidal range [m] | Basin surface [km <sup>2</sup> ] | Installed capacity [MW] | Yearly energy reserve [TWh/year] | Annual plant load factor <sup>1</sup> [%] |
|--------------|-----------------|----------------------|----------------------------------|-------------------------|----------------------------------|---|
| Argentina    | San José        | 5.8                  | 778                              | 5 040                   | 9.4                              | 21  |
|              | Golfo Nuevo     | 3.7                  | 2 376                            | 6 570                   | 16.8                             | 29  |
|              | Rio Deseado     | 3.6                  | 73                               | 180                     | 0.45                             | 28  |
|              | Santa Cruz      | 7.5                  | 222                              | 2 420                   | 6.1                              | 29  |
|              | Rio Gallegos    | 7.5                  | 177                              | 1 900                   | 4.8                              | 29  |
| Australia    | Secure Bay      | 7                    | 140                              | 1 480                   | 2.9                              | 22  |
|              | Walcott Inlet   | 7                    | 260                              | 2 800                   | 5.4                              | 22  |
| Canada       | Cobequid        | 12.4                 | 240                              | 5 338                   | 14                               | 30  |
|              | Cumberland      | 10.9                 | 90                               | 1 400                   | 3.4                              | 28  |
|              | Shepody         | 10                   | 115                              | 1 800                   | 4.8                              | 30  |
| India        | Gulf of Kutch   | 5                    | 170                              | 900                     | 1.6                              | 22  |
|              | Gulf of Khambat | 7                    | 1 970                            | 7 000                   | 15                               | 24  |
| Korea        | Garolim         | 4.7                  | 100                              | 400                     | 0.836                            | 24  |
| Mexico       | Rio Colorado    | 6.5                  | -                                | -                       | 5.4                              | -   |
| UK           | Severn          | 7                    | 520                              | 8 640                   | 17                               | 23  |
|              | Mersey          | 6.5                  | 61                               | 700                     | 1.4                              | 23  |
|              | Duddon          | 5.6                  | 20                               | 100                     | 0.212                            | 22  |
|              | Wyre            | 6                    | 5.8                              | 64                      | 0.131                            | 24  |
|              | Conwy           | 5.2                  | 5.5                              | 33                      | 0.06                             | 21  |
| USA          | Knik Arm        | 7.5                  | -                                | 2 900                   | 7.4                              | 29  |
|              | Turnagain Arm   | 7.5                  | -                                | 6 500                   | 16.6                             | 29  |
| Russian Fed. | Mezen           | 6.7                  | 2 640                            | 15 000                  | 45                               | 34  |
|              | Tugur           | 6.8                  | 1 080                            | 7 800                   | 16.2                             | 24  |
|              | Penzhinsk       | 11.4                 | 20 530                           | 87 400                  | 190                              | 25  |

Fig. 2.12 - Prospective sites for tidal energy projects (C. G. Pandya 2006).

<sup>1</sup> The load factor is the ratio between the annual average power output and the installed capacity. Following L.B. Bernshtein (1965) tidal power plants may reach a maximum of 34%.

### **2.3.10 A case study: La Rance power plant**

Rance estuary offered a privileged site for the project of a barrage tidal power plant. Firstly, because the tidal amplitude is one of the highest in the world (up to 13.5 meters during equinoctial tides); secondly, because the estuary offers a reservoir of 22 km<sup>2</sup> capable of impounding 180 million m<sup>3</sup> of sea water. At peak periods, 18,000 m<sup>3</sup>/s flow through the estuary, a flow that is ten times larger than that of the Rhone River.

To harness such power, the estuary had to be blocked by a structure 750 metres long and 13 metres high. Twenty-five years of studies and six years of construction works were needed to erect the Rance tidal power plant. Since 1967, this facility, the only full-scale power station of this type in the world, generates 600 million kWh every year, enough to provide energy to 250,000 households.

*Bulb sets.* The tide-driven mills of the past came into action only when the sea withdrew, in other words twice a day. However, for the sake of cost effectiveness, the turbines of the Rance tidal power plant operates both when the basin is filled and when it is emptied, at high tide and low tide.

To do so, Electricité de France developed a new type of turbine, the bulb sets (described in § 2.3.5.5), capable of operating in both directions. The 24 bulb sets in the Rance facility have impressive technical credentials: 5.3 metres in diameter, 470 tonnes in weight and a unit capacity of 10 MW.

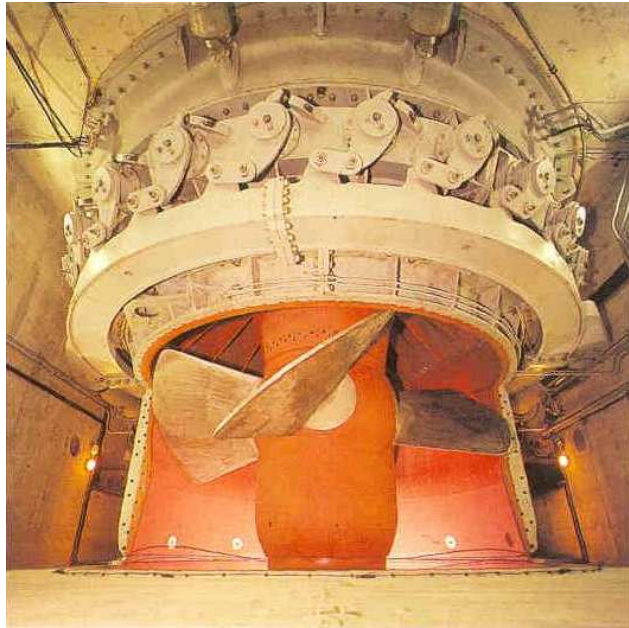


*Fig. 2.13 - Bulb turbine installed in La Rance power plant.*

To increase the power plant operating time further, the bulb sets were designed for use as pumps. Thus, when the sea has almost reached the reservoir level, the filling phase is accelerated by pumping. This supplement serves to increase the volume of water in the reservoir and thus, during the next flow, the turbines will be activated earlier and for a longer time. This pumping-turbining system makes it possible to step up or anticipate generation depending on the electricity requirements of the network.

*The project.* The construction of the Rance tidal power plant was initiated in 1960. The project involved building a dam 330 metres long in which the turbines were to be housed, a lock to allow the passage of small craft, a rockfill dam 165 metres long and a mobile weir with 6 gates to rapidly balance the levels for the emptying and filling of the reservoir.

The first work sites got under way in 1961. For the sake of convenience and safety, it was decided to erect the structure while ensuring that the construction site was dry. This means having to build two temporary dams, one on the sea side and the other on the estuary side, in order to protect the structure from water. The work was to last two years. In July 1963, the Rance was cut off from the ocean and the land dried for the whole

duration of the construction of the dam which was to require another three years of work. Finally, between August 1966 and the end of 1967, the 24 bulb sets of the power plant were connected to the 225 kV transmission network.

*The ecosystem.* Being concerned about preserving the Rance ecosystem, Electricité de France operates the tidal power facility so as to limit its impact on the environment. Regardless of the constraints of the power network, it always endeavours to adjust the high and low tidal level of the reservoir according to the movement of the tides so as not to disturb the biological balance of the aquatic environment.

Research carried out in 1995 by a research laboratory of the National Museum of Natural History showed that the Rance estuary has a rich and varied aquatic, namely benthic life. Furthermore, although the construction of the dam modified the currents in the estuary and, consequently, the geographical distribution of the sediments, the studies available on the sedimentary balance seem to point to a natural evolution. To further enhance its contribution to environmental protection, Electricité de France takes part as a user in the Operation Committee of elected representatives and users of the Rance (C.O.E.U.R.) entrusted with defining and financing projects to preserve the estuary. In 1995, the partners decided to devote three million French francs to support studies and experimentation prior to signing the next Rance bay contract which will concern the quality of water, navigation, banks and marine farms of the estuary. Electricité de France contributed 600,000 French francs to this endeavour.

*Social implication.* Over and above its energy production role, the tidal power plant contributes to the economic, social and tourist development of the region. The power plant has a permanent staff of 58 persons and 30 new jobs were created on the site for the rehabilitation work site which got under way in 1996 on the occasion of the thirtieth anniversary. In addition, as is the case for any industrial facility, Electricité de France pays 14 million French francs in local taxes every year to the neighbouring communes, the department and the Brittany region.

Above all, use was made of the crest of the dam to build a road with two double lanes bringing Saint-Malo and Dinard to within 15 km of each other instead of 45 km as was the case before. Nearly 26,000 motorists use this road every day. The erection of the dam also favoured the rapid development of recreational activities. The Rance estuary

has become a sheltered reservoir covering an area of 22 km<sup>2</sup> which attracts water sports enthusiasts all year round.

Every year, the tidal power plant receives between 300,000 and 400,000 visitors keen on discovering this facility, the only one of its kind in the world. This success puts the Rance power plant in the forefront of French industrial tourist sites.

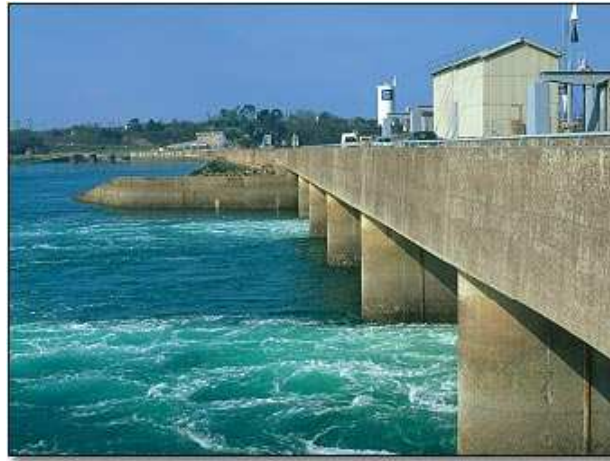


*Fig. 2.14 - A view of the Rance barrage (RSS, 2006).*

*Conclusions.* In November 1996, the tidal power plant celebrated its thirtieth anniversary of operation. The unique forerunner project that started in the 1950's has turned out to be a technical, industrial and economic success.

For 30 years, the 24 turbines of the Rance facility have shown outstanding reliability. The power plant has operated without major incidents or breakdowns for 160,000 hours and generated 16 billion kWh at the price of 18.5 centimes per kWh, a highly competitive price and one that is lower than Electricité de France's average generation costs.

To enable the tidal power plant to operate as well for the next thirty years, Electricité de France has decided to carry out a general and preventive overhaul of all the equipment of the facility. This refurbishment programme will be spread out over a ten-year period at the rate of three bulb sets per year.

## **2.4 Tidal stream power**

### **2.4.1 Introduction**

Useful energy can be generated from marine currents using completely submerged turbines consisting of rotor blades and generator. They are called Water Current Turbines, that are defined as systems that convert hydro kinetic energy from flowing waters into electricity, mechanical power, or other forms of energy, such as hydrogen.

This approach offers many additional advantages:

- it does not require the construction of a dam: hence, it is considered much less costly and more environmentally-friendly; moreover further cost-reductions are realized from not having to dredge a catchment area;
- vertical-axis tidal generators may be stacked and joined together in series to span a passage of water such as a fiord and they offer a transportation corridor (bridge), essentially providing two infrastructure services for the price of one;
- vertical-axis tidal generators may be joined together in series to create a ‘tidal fence’ capable of generating electricity on a scale comparable to the largest existing fossil fuel based, hydroelectric and nuclear energy generation facilities;
- tidal current energy, though intermittent, is predictable (at least its astronomical part) with exceptional accuracy many years in advance. In other words, power suppliers will easily be able to schedule the integration of tidal energy with backup sources well in advance of requirements. Thus, among the emerging renewable energy field, tidal energy represents a much more reliable energy source than wind, solar and wave, which are not predictable;
- present tidal current, or tidal stream technologies are capable of exploiting and generating renewable energy in many marine environments that exist worldwide.

Unfortunately, there are also some disadvantages and limitations in generating power from marine currents: in fact this technology is an intermittent source due to the cyclic nature of the tide. A conventional design, in any mode of operation, would produce power for 6 to 12 hours in every 24 and will not produce power at other times. As the tidal cycle is based on the period of rotation of the Moon (24.8 hours) and the demand for electricity is based on the period of rotation of the earth (24 hours), the energy

production cycle will not be in phase with the demand cycle. This causes problems for the electric power transmission network, as capacity with short starting and stopping times (such as hydropower or gas fired power plants) will have to be available to alternate power production with the tidal power scheme.

#### 2.4.2 Energy calculation

Water turbines work on the same principle as wind turbines: they use the kinetic energy of a moving fluid and transfer it into useful rotational and then electrical energy. The current speed is typically lower than wind speed; however, owing to the higher density of water water turbines are smaller than their wind counterparts for the same installed capacity.



Fig. 2.15 - Size comparison of a 1 MW wind and tidal turbine ( Marine Current Turbines Ltd.).

The energy [W] per second intercepted by a device of frontal area  $A_0$  [ $\text{m}^2$ ] in a current of undisturbed speed  $U$  [m/s] is given by:

$$P(t) = \frac{1}{2} \rho A_0 U(t)^3$$

where  $\rho$  is the water density [ $\text{kg}/\text{m}^3$ ].

The power that can be converted to a useable mechanical form is limited for a device in an open water flow to:

$$P(t) = \frac{1}{2} \rho A_0 U(t)^3 \eta$$

where  $\eta$  is the power coefficient (efficiency). The value of  $\eta$  for a turbine in a flow of incompressible fluid is limited to a maximum theoretical value around 35% (Gorlov et al. 2001). The value of  $\eta$  for a real device is generally a function of the ratio between the speed of the turbine tip and the flow speed, which is commonly known as the *tip speed ratio*.

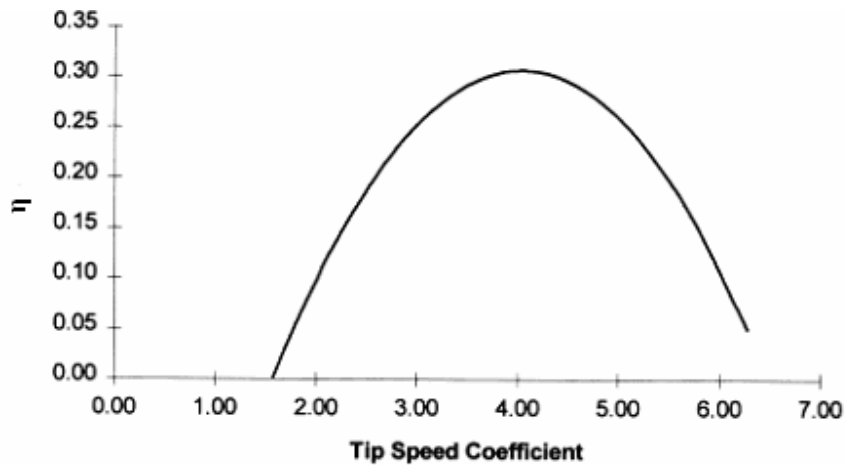


Fig. 2.16 - Representative relationship between the tip speed ratio ( $\lambda$ ) and the power coefficient ( $\eta$ ) (Bryden et al.1997).

The actual shape of this curve is dependent upon the blade shape and the number of blades. Just what should be deemed as "independent design variables" in a system specification is subject to investigation but, in any case, it should include the shape of this curve. If a manufacturer could offer a range of turbines, each with a different  $\eta$ - $\lambda$  curve, then the selection would be within the design specification. Most suggested designs for tidal turbines operate at a constant rotational speed. This allows for a relationship between the flow speed and the power output to be determined.

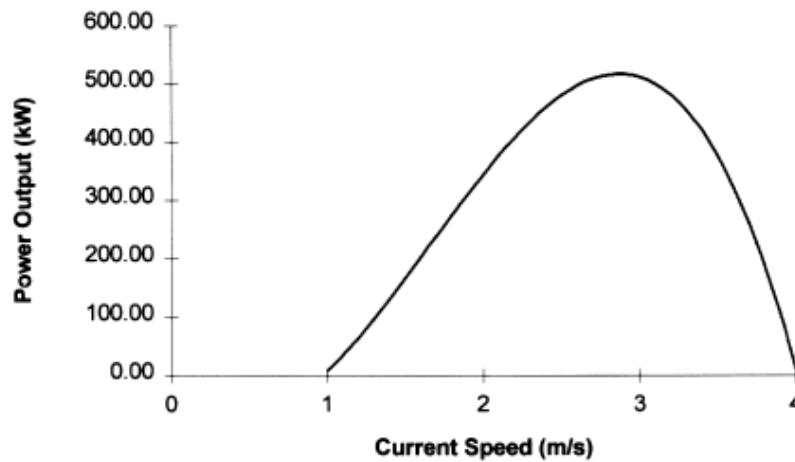


Fig. 2.17 - Power output curve assuming a 10-s rotational period, based upon the  $\eta$ - $\lambda$  curve (Bryden et al. 1997).

As for wind turbines, tidal stream machines are likely to have a cut-in stream velocity, giving rise to a period of enforced idleness at slack water. The chosen velocity will depend on site conditions and turbine design. Wind turbines also have a cut-out speed to avoid damage in storms, but for tidal streams this should not be necessary due to the predictable nature of the flow regime. Shut-down procedures would of course be provided, but would only be executed in emergencies. For some locations, loads caused by wave action under stormy conditions might be severe enough to trigger shut-down.

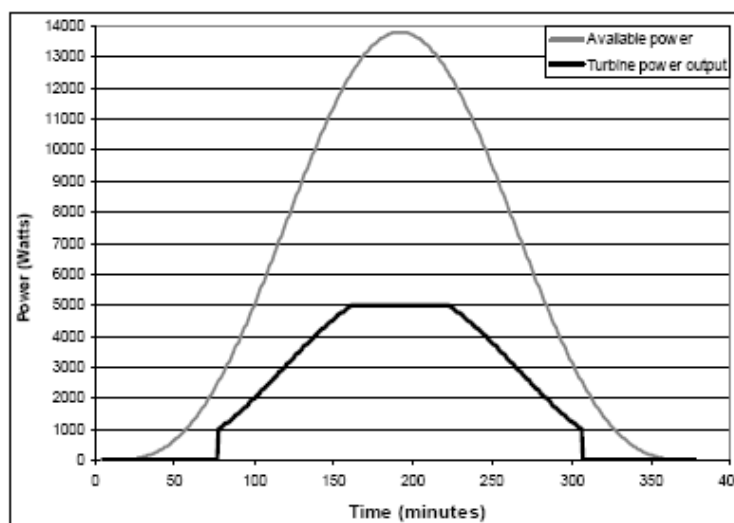


Fig. 2.18 - Turbine output relative to available power (Clarke et al. 2004).

The power produced by the turbine depends upon its power coefficient ( $\eta$ ) and on the control algorithms selected. The above figure shows the variation of the power output with time, for arbitrarily chosen cut-in and rated stream velocities. In the run-up to rated power, the output is determined by the value of  $\eta$ , which in turn depends on the operating conditions: whether the rotor rotates at a fixed or variable speed, and whether the blade pitch angle may be adjusted.

The situation presented here is of course a simplified example. In reality, the assumption of a sinusoidal variation of velocity may be inaccurate. Also, a series of half-cycles may exhibit changes in the value of peak velocity due to the directional properties of the site, and due to the longer spring/neap tidal cycle. Variations in tidal range (and hence stream velocity) between spring and neap tides are very marked in some locations and almost negligible in others. This will have an impact upon the choice of control algorithms, and reinforces the earlier suggestion that tidal turbine systems should be designed such to suit the peculiarities of their particular site.

### **2.4.3 Technologies**

#### **2.4.3.1 Introduction**

Practically all hydraulic turbines that are presently used for hydropower generation have been developed for installation in water dams across streams. This conventional design is the most economical and energy efficient for river hydropower plants because it provides maximum water heads and it forces all the water to flow through the turbines under maximum hydraulic pressure.

However, dams damage the environment and interfere with fish migration.

Also, they cannot be used for power systems extracting energy from such huge potential sources as ocean currents or low grade rivers. Thus, new hydraulic turbines are needed that can operate efficiently in free flow without dams.

For decades scientists and engineers have unsuccessfully tried to utilize conventional turbines for free and low-head hydro. The hydraulic turbines which prove very efficient under high heads become so expensive in applications for low and ultra low-head hydroelectric stations that only very modest developments of this kind are found in

practice.

The principal difference between exploiting high-head or free flow turbines is that the latter need large flow openings to capture as much water masses as possible with low velocities and pressure. Conventional turbines, in contrast, are designed for high pressure and relatively small water ducts where all the water has no chance to escape the turbine installed in the dam body. According to the Bernoulli theorem, the density of potential energy of the flow is proportional to the pressure, while the density of kinetic energy is proportional to the square of velocity. Conventional water turbines utilize mostly the potential component at the expense of the kinetic one. In order to do so, they need so-called “high solidity” where turbine blades cover most of the inside flow passage, resisting water flow and building up the water head. This causes the fluid velocity to fall and the kinetic component of Bernoulli equation to become negligibly small compared to the potential component. This is the reason why the higher water heads correspond to higher efficiency of hydraulic turbines, an efficiency that reaches nearly 90 percent in some cases. However, the situation is completely reversed for free water flows. In this case, the kinetic part dominates, and conventional turbines perform poorly, becoming very expensive.

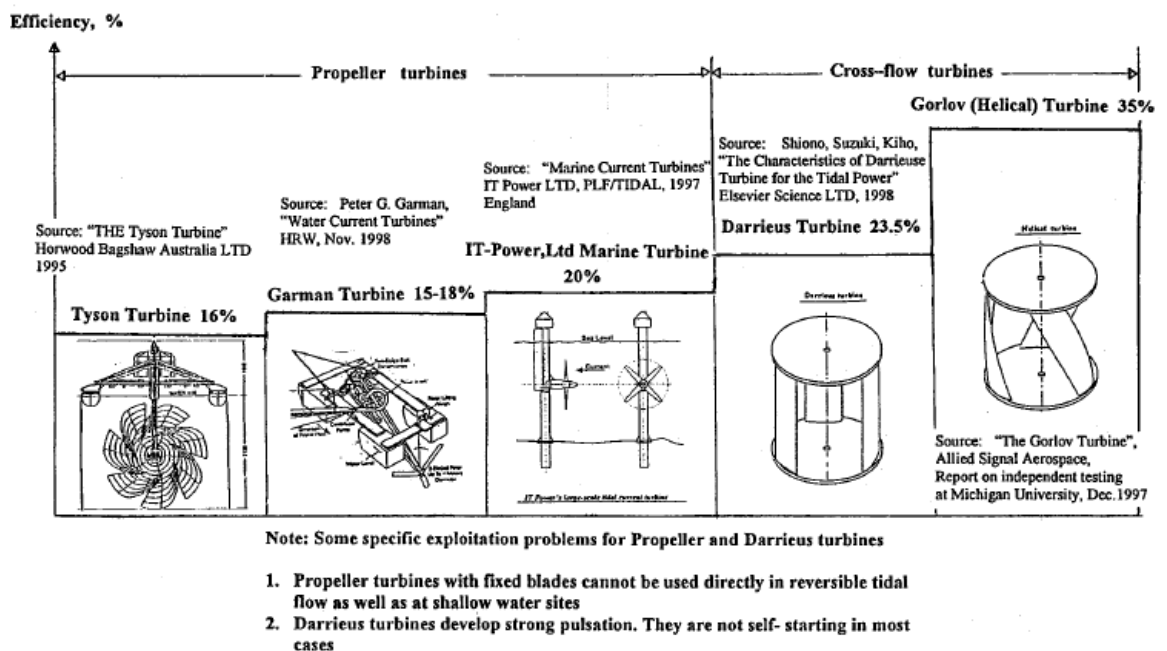
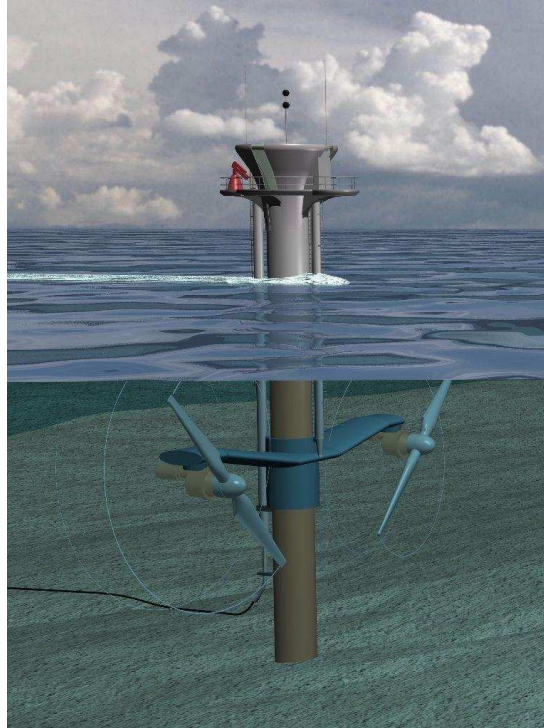


Fig. 2.19- Comparative performance of various turbines in free water currents (Gorlov et al.2001).

Two types of turbines have been so far proposed:

- horizontal axis turbines (axial flow turbine):



*Fig. 2.20 - Artist's impression of MCT Seagen pile-mounted twin rotor tidal turbine (Marine Current Turbines Ltd).*



*Fig. 2.21 - UEK Twin Turbines prepared for demonstration (Underwater Electric Kite).*



*Fig. 2.22 - Verdant Power Free-flow Turbine Being Deployed in East River (December 2006).*

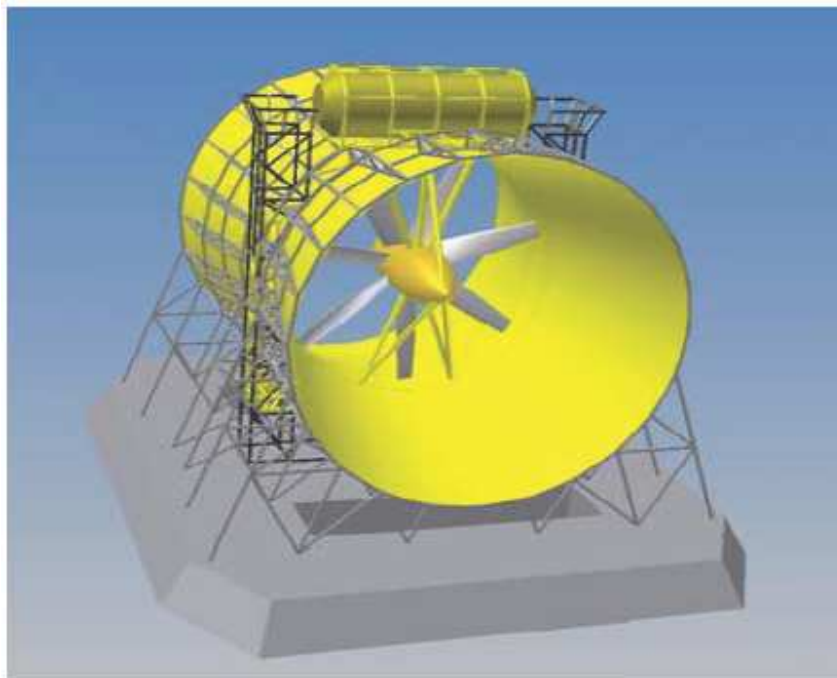


*Fig. 2.23 - Lunar Energy RTT Turbine. One of the different technology options available for tidal in-stream energy conversion (TISEC).*

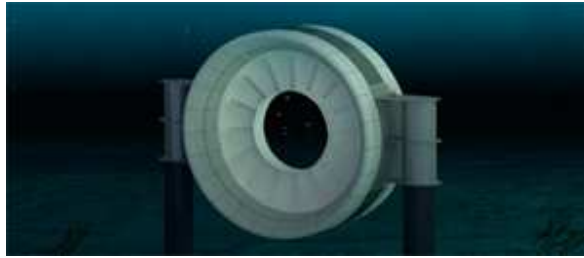


Fig. 2.24 - A gravity base anchors the Open-Centre Turbine to the seabed (OpenHydro).

- vertical axis turbines (cross flow turbine):

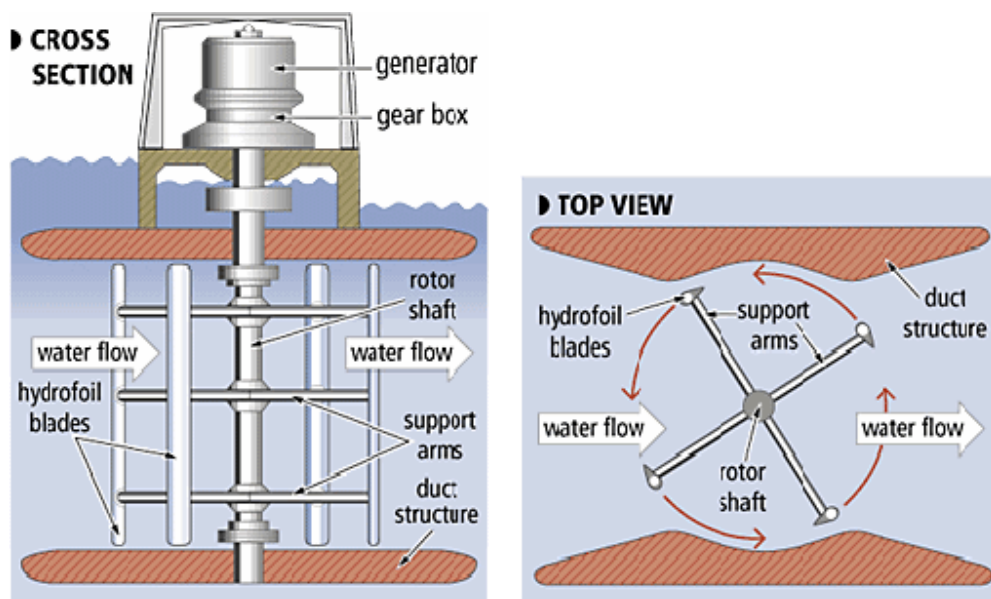


Fig. 2.25 Davis Hydro vertical-axis turbine (Blue Energy International).

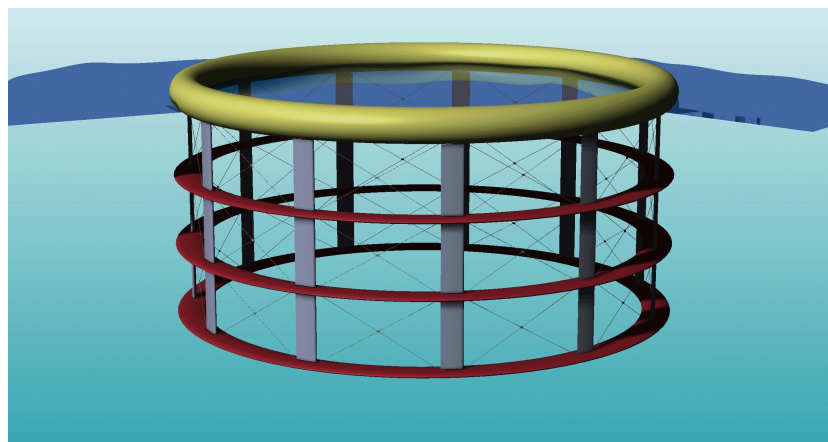


Fig. 2.26 - Solid Works image of the tidal rotor (Institute for Energy Systems, university of Edinburgh).

In the exploration of the possibilities to extract energy from the sea, no technology should be neglected. So, even though the vertical axis turbine is not commonly used for the extraction of wind energy, it is worth being examined in the case of energy extraction from water as the exploitation conditions and the structural forces applied to the turbine are different in the two different fluid media.

#### **2.4.3.2 Darrieus turbine: device description and technical issues**

Darrieus turbine is a vertical axis turbine. It has streamlined blades turning around an axis perpendicular to the flow.

The blades are parallel to the axis. They can be fixed with regards to the axis or they can be articulated and slightly oscillate in order to show always the same line toward the relative flow. They can be straight or curved to diminish the effect of the centrifugal force and to remove the need for links between the axis and the blades. In Darrieus patent, the possibility to use structures to drive the flow on the turbine is also claimed.

Darrieus turbine type converts kinetic energy of the flow into mechanical energy. It uses the hydrodynamic lift on the blades to make the airfoils go faster than the flow around the turbine.



*Fig. 2.27 - Darrieus wind turbine.*

The advantages of Darrieus type vertical axis turbines are:

- it uses the fluid stream whatever the flow direction is;
- in some other vertical axis turbine types, large active areas are needed. Darrieus turbine does not need large blade area to work;
- gearbox and generator can be at one end of the axis. For example, for vertical axis wind turbine, these elements can be laid on the ground.

Introduction of this technology for water turbines has been slower than for wind. Alternative Hydro Solutions Ltd. has taken these concepts and modified them to be more suitable for smaller rivers and tidal currents. A number of design simplifications have been incorporated over the previous designs while maintaining the turbine efficiency.

*Blades.* The turbine blades are custom 6063T5 aluminium extrusions with a solid cross-section in order to provide the required strength. The 6063T5 aluminium offers excellent resistance to corrosion and a smooth surface finish. The profile of arms is typically the same as that of blades in order to reduce the frictional losses. This is not true for the larger turbines as the size of blades increases with the turbine diameter, however, the arms can be made of a smaller airfoil. The mating to the hub is performed with a patentable mechanism, which incorporates a second female extrusion to the arms male. On larger turbines this remains constant, as the arm stays constant between the two diameters of turbines. The shaft is made of stainless steel and is supported by two standard stainless steel pillow block bearings. The frame supporting the two bearings is a standard channel section or flat plate, which may be modified to accommodate a variety of mounting mechanisms. The power is transferred through a flexible coupling to a motor and gearbox combination which allows the motor to run at a higher rpm thereby increasing its efficiency and reducing the torque fluctuations.



*Fig. 2.28 - Darrieus turbine rotor and blades (Alternative Hydro Solutions Ltd).*

*Rotor diameter.* This turbine is available in 4 diameters presently. A 1.25m diameter as well as a 1.5 m diameter and a 2.5m diameter as well as the largest the 3.0m diameter. All are available in various depths.



*Fig. 2.29 - Darrieus turbine (Alternative Hydro Solutions Ltd).*

Rated power: the power output related to water speed is shown in the graph below.

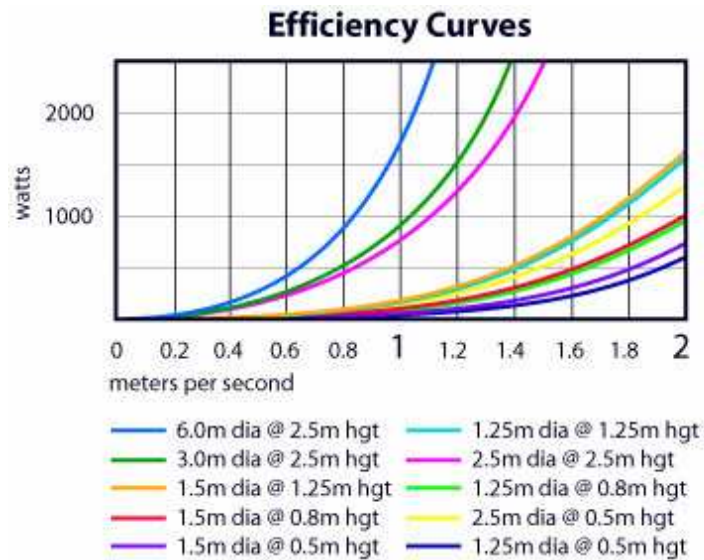


Fig. 2.30 - Efficiency curves in relation to turbine dimension (Alternative Hydro Solutions Ltd).

Foundation - mooring: With the Darrieus turbine the water levels remain effectively the same and the lack of civil structures required make this an environmentally friendly device. Typically these units have been mounted on a pontoon, barge, or small boat, however, for smaller streams other methodologies may be more cost effective. These could include a built-in support beam extending either fully or partially over the river.



Fig. 2.31 - Mounting schemes for Darrieus turbine (Alternative Hydro Solutions Ltd).

*Operation and maintenance:* the amount of debris flowing down the river is also a factor in siting a turbine. If there is a constant flow of heavy debris some protection for the turbine will be required. A "trash rack" to deflect the heavier pieces would provide a safer operating environment.

*Efficiency:* 17% considering also the losses incurred in the transmission of the power to the generator and in the generator itself.

*Environmental impact:* interference with fish should not be viewed as a problem when using a Darrieus turbine. The motion of the blades will tend to deter any fish from going near the turbine and typically the small width of the turbine compared to the large width of the river will allow plenty of area for the fish to migrate without passing through the turbine. Should a fish stray and go through the turbine the low speed of rotation, the blunt leading edge, the openness of the turbine, and the lack of any walls or ducting for the fish to be trapped against would prevent any damage from being done.

#### **2.4.3.3 Gorlov helical turbine (GHT): device description and technical issues**

In 1996, Alexander Gorlov discovered a way to modify and drastically improve the Darrieus design.

The Gorlov turbine is squirrel cage shaped Darrieus turbine with twisted airfoil-shaped blades. Darrieus turbine gives oscillating torque because of the blade accelerations in the higher-pressure zones.

The idea of Gorlov is to have a turbine whose blades always presented an optimally positioned portion in order to decrease the irregular and vibratory behaviour of Darrieus turbine: if Gorlov turbine blades are twisted enough, there is always a blade portion in the upstream part of the turbine.

**Double-Helix Turbine**  
(for underwater installation)



**Triple-Helix Turbine**  
(generator above water)



*Fig. 2.32 - Double and triple helical turbine (Lucid energy technologies).*

The GHT is a cross-flow turbine that provides a reaction thus that can rotate at twice the speed of the water flow. It is self-starting and can produce power from a water current flow as slow as about 1.5 m/s with power increasing in proportion to the water velocity cubed.

Due to his axial symmetry, the GHT always rotates in the same direction , even when tidal currents reverse direction. The standard model GHT (1 m in diameter, 2.5 m in length) can be installed either vertically or horizontally to the water current flow, in waters as shallow as 1.2 m in depth.

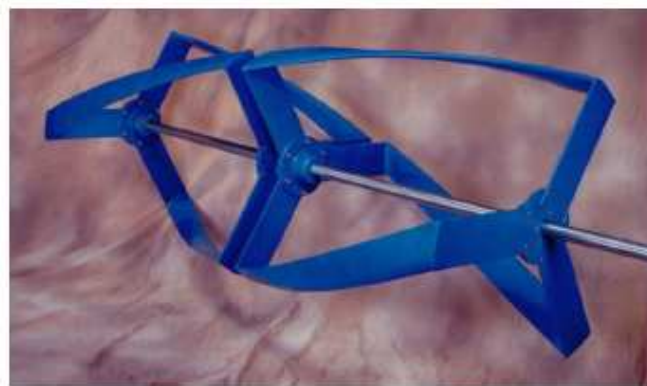


*Fig. 2.33 - Triple-helix GHT. Diameter: 1m; Length (height): 2.5m. Total weight including steel shaft is about 90 kg (Lucid energy technologies).*

It was designed for maximum flexibility, is adaptable for being used in multiple GHT arrays, either in side-by-side arrangements, or with multiple GHTs on the same shaft or boat. This permits the expansion of an initial facility as demand grows without a tremendous amount of additional expense, using a modular approach.



*Fig. 2.34 - Artist's rendition of the floating power plant with helical turbines (Lucud energy technologies).*

The main difference between the GHT and most traditional turbines is its utilization of lift-based propulsion instead of drag-based propulsion. The indicator of the type of propulsion is the tip-speed ratio of the blades. Tip-speed ratio refers to how many times faster the tip of a blade is moving relative to the speed of the current. The GHT has an average tip-speed ratio of 2, meaning in a 5 m/s current the blades are moving at 10 m/s into the current. Traditional fan-shaped turbines operating under a drag-based principle can have tip-speed ratios higher than 7. The speed of the blades relative to the currents in which they are moving can vary along its length and can have adverse effects on the operation of the turbine.

*Blades:* 3, made of aluminium air-foil-shaped extrusion with 140 mm chords.

*Rotor diameter and height:* there are three standard sizes, with diameter of 1 x 2.5 m, 2 x 5 m or 3 x 7.5 m.

*Rated power:* the power output related to water speed is shown in the table below.

| Current Velocity |             |       | Power output by GHT size (KW) |           |             |
|------------------|-------------|-------|-------------------------------|-----------|-------------|
| Meters/Second    | Feet/Second | Knots | 1 x 2.5(m)                    | 2 x 5 (m) | 3 x 7.5 (m) |
| 1.5              | 4.9         | 2.9   | 1.48                          | 5.92      | 13.32       |
| 2                | 6.6         | 3.9   | 3.50                          | 14.00     | 31.50       |
| 2.5              | 8.2         | 4.9   | 7.84                          | 27.36     | 61.56       |
| 3                | 9.8         | 5.8   | 11.81                         | 47.24     | 6.29        |
| 3.5              | 11.5        | 6.8   | 18.76                         | 75.04     | 168.84      |
| 4                | 13.1        | 7.8   | 28.00                         | 112.00    | 252.00      |
| 4.5              | 14.8        | 8.7   | 39.87                         | 159.48    | 358.83      |

*Fig. 2.35 - Power output related to turbine dimension (Lucid energy technologies).*

*Cut in speed:* 0.5 m/s. Due to concerns relating to efficiency of energy conversion GCK does not currently recommend water velocities below 1.5 m/s.

*Foundation-mooring:* the flexibility of the GTH design allows for suspension from a floating structure, such as a barge or from a fixed structure attached to the shore or to the ocean bottom.



*Fig. 2.36 - Twin Triple-helix GHT in the Uldolmok Strait (Lucid energy technologies).*

*Operation and maintenance:* service life of at least 20 yrs. In the absence of catastrophic events the only maintenance would be the re-application of the marine coating, every 2 years and the replacement of the bearings on the GHT shaft and generator refurbishing,

every 5 years.

*Efficiency:* during the 1990s, many tests were made on Gorlov turbines of very different sizes.

Some tests took place in laboratories (Hydro-Pneumatic Power Laboratory at Northeastern University, USA, Hydrodynamic Laboratory of Michigan University), others in natural sites (Cape Cod Canal near Boston, USA, Uldolmok Strait, Korean Peninsula). Some tests show that the turbine efficiency is 35 percent.

*Environmental impact:* GHTs harness energy without interrupting the ecosystem in which they are placed. Because the GHT produces no harmful products by fish, birds, mammals, and plants are not exposed to the types of toxic waste typically produced by other energy producing systems.

#### **2.4.3.4 Kobold turbine: device description and technical issues**

The system, which is called Kobold, is a hydraulic vertical axis turbine; the rotation axis of the rotor is perpendicular to the direction of the flow hitting it. It is able to convert kinetic energy available in the tidal currents of rivers and seas into mechanical rotational energy which in turn is converted into electrical power. The turbine has been designed to achieve the highest possible level of productive efficiency compatible with the need to safeguard the environment as well as to keep construction and (above all) maintenance costs as low as possible.

The Kobold turbine:

- rotates independently of the direction of the current;
- has high torques that permit spontaneous starting even under intense conditions without the need of an ignition device.

*Turbine manufacture.* The construction of the turbine included the assembly of the following parts using the items specified below:

- *blades:* principal material steel (Austenitic Stainless steel used in the aircraft industry. Austenitic grades have excellent corrosion resistance, good formability and can be welded), glass fibre, carbon fibre and resin and a small amount of electricity from a low voltage network;

- *arms*: which serve as blade supports, made using iron, glass fibre and resin plus electricity;
- *transmission shaft*: steel and electricity;
- *gearbox* : steel;
- *synchronous generator*: steel, iron magnet and copper;
- *floating buoy*: supporting sea platform which contains the turbine.

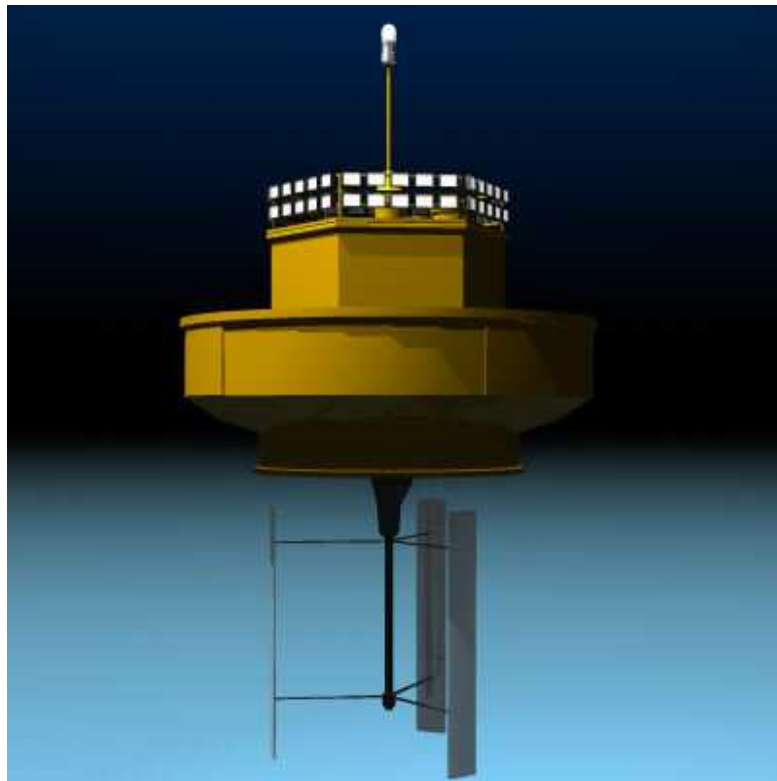


*Fig. 2.37 - Kobold turbine with floating buoy ( © Turbo Squid ,2008).*

*Blades*: after wind-tunnel tests performed on wind-tunnel models and numerical simulations, a study on a real prototype was started. Some analyses and practical considerations on the size of the prototype, led to a choice of a 3 blade turbine with a diameter of 6 meters. The blade height and chord were chosen to be 5 m and 4 m respectively. Each blade had to be supported by two arms and these had to be streamlined using another ad hoc designed airfoil.

*Power output*: the power output related to water speed is shown in the table below.

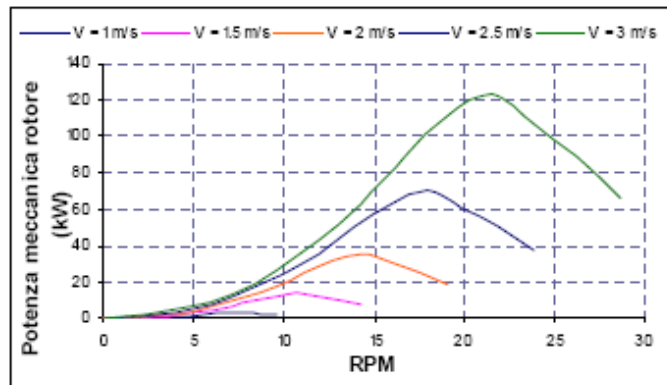


Fig. 2.38 - Power output related to water velocities obtained from numerical simulations (Coiro et al).

*Cut in speed:* 1.2 m/s

Foundation-mooring: the turbine must be securely anchored to the sea bed in order to function effectively. Therefore, the system includes the following components:

- *mooring blocks:* they are concrete made supports laid on the sea bed to hold the turbine in place, ensuring that it is not dragged away by sea currents;
- *chains:* the turbine is attached to the blocks on the sea bed by means of sturdy steel chains.

The sizes of the entire assembly are 10 m in diameter, 2.5 m in height and draws 1.5 m.

*Operation and maintenance.* Maintenance is envisaged at five year intervals with the blades and arms being treated with 8 litres of an anti fouling product to avoid or slow down the formation of algae.

The system is estimated to have a 20-25 year useful life, it was hypothesised that, at the end of this period, all recyclable components would be recovered and put back into the production cycle; this would enable the environmental impact arising from the decommissioning of the turbine to be reduced ,and would allow materials that would otherwise be dumped to be re-used.

*Efficiency.* The global efficiency has been measured to be around 23% which is comparable to figures valid for the well developed wind turbines: hence, these first results can be considered excellent even because on-going improvements in the

mechanical transmission system are likely to rise the global efficiency very soon.

*Environmental impact.* The Kobold turbine environmental impact has been evaluated particularly from the point of view of the compatibility with the sea, flora and fauna. When the turbine is “working” it has virtually no impact on marine resources, namely flora and fauna. In fact, it has been claimed that marine fauna is in no way disturbed by the turbine because it rotates so slowly.

#### 2.4.5 A case study: the Enermar project

The purpose of the ENERMAR project is to demonstrate that the exploitation of the renewable energy contained in the marine currents, by means of a Kobold turbine, is a convenient method if compared with the exploitation of other renewable energy sources. A pilot plant is moored in the Strait of Messina, close to the Sicilian shore, in front of a village called Ganzirri, close to the lake of the same name.

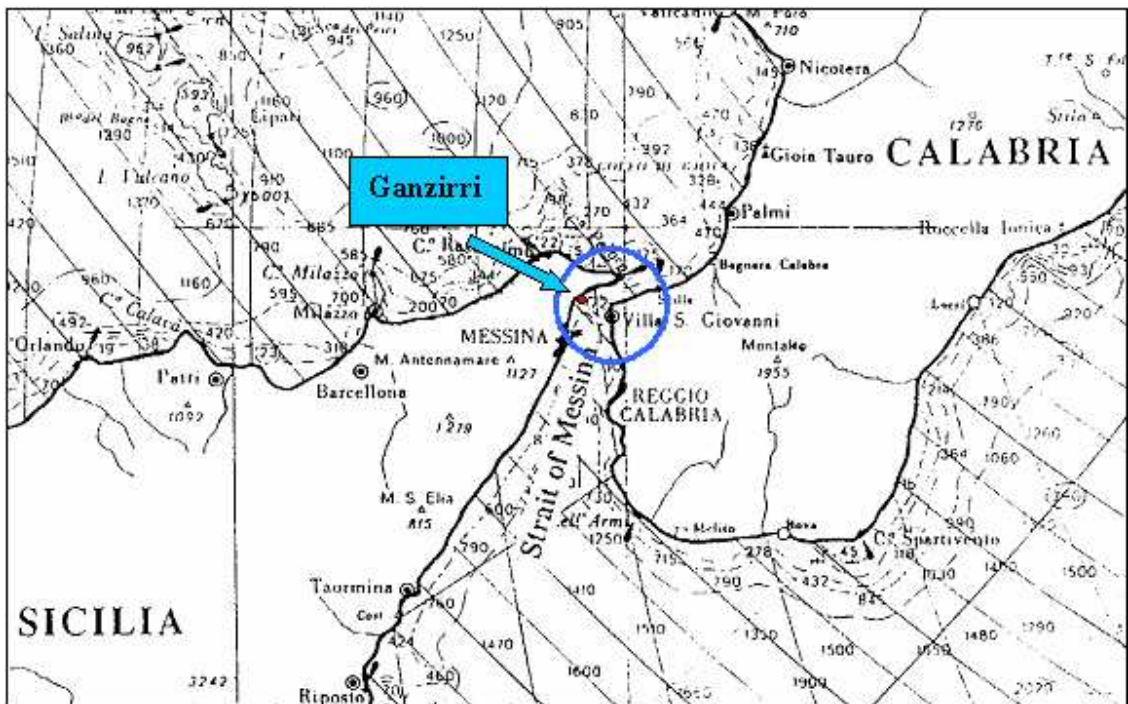


Fig. 2.39 - The Kobold turbine position in Messina Strait.

This plant will be useful to demonstrate on the field the characteristics of limited environmental impact, and the performances of both the system and its components.

In this site the expected current speed is 2 m/s, the sea depth is 20 m and the plant is moored 150 m offshore. The current is never still, its period of inversion is equal to 6 hrs and 12 minutes, the amplitude oscillation has a 14 day period.

The objectives of the Enermar system are the following:

- to test the first pilot plant in the world, consisting of a support floating structure and a patented Kobold turbine, with the necessary devices to produce and manage the electric energy. The whole system has been designed to have characteristics of solidity and high efficiency;
- to optimize the whole system and its single components;
- to promote the industrial development of the ENERMAR project and its commercialisation, once the convenience of the exploitation of marine currents compared with other sources of alternative energy will have been demonstrated.

The ENERMAR plant is composed of the turbine prototype, the design of which has been previously illustrated and an electrical generator. The turbine consists of a transmission shaft, built with special steel, and three couples of radial arms, each of them holding a blade.

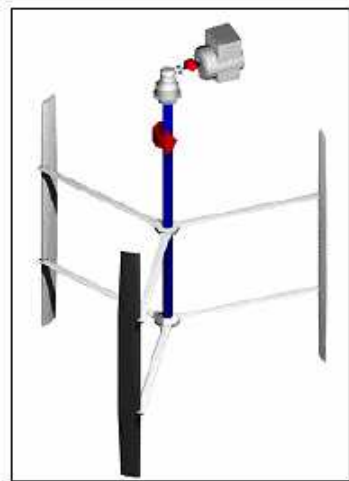


*Fig. 2.40 - Kobold turbine (left) and floating platform in Messina Strait (right).*

From the mechanical point of view, the Kobold turbine has been designed following simple and effective principles, so as to need for its whole useful life very limited maintenance requirements.

The sizes of the main plant are:

- turbine diameter 6 m;
- blade span 5 m;
- chord 4 m;
- number of blades 3;
- Diameter of floating platform: 10 m, depth: 2.5 m;
- draft 1.5 m;
- Mooring's anchoring blocks 4;
- blocks weight (concrete) 350 kN each;
- chain 70 mm;
- water depth 18.25 m.

The generator is brushless, three phases, synchronous, 4 poles, 128 Kw, and is connected to a control unit delivering energy to the network through a gearbox (ratio 90:1) to increase the rotational speed from the 18 rpm of the turbine to the 1500 rpm of the generator shaft (necessary to achieve the frequency of 50 Hz).

The environmental impact of Kobold turbines has been evaluated particularly from the point of view of the compatibility with the sea, flora and fauna.

The environmental impact and compatibility study, carried out by the University of Messina, has reached the conclusion that the environmental impact is negligible.

Moreover, the ENERMAR units are compatible with the Italian rules for the installation and removal of sea structures.

The first set of tests consisted of systematic data collection of the mechanical behaviour of the turbine. Even with a low speed current (1.2 m/s is the cut-in speed), the rotor started rotating very fast, without any external power supply. The global efficiency of the system has been measured as the ratio between the electrical power produced and the theoretical power available in the current relative to the intercepted area  $S$ , defined as the product of the diameter and the blade height ( $S=30 \text{ m}^2$  for a Kobold turbine). The measured global efficiency was estimated around 23%.

Furthermore, the system is equipped with an automatic data acquisition system (including current speed, torque, rpm, voltage, current) which is also employed to perform an automatic control of the loads of the turbine.

Finally, a study has been made to estimate the energy that can be produced in a year from the site where the turbine is currently installed. The result of this study points at a value ranging about 22,000 KWh which can be extracted each year by a plant of this type. Considering the currents available in this area, the total energy potentially extracted might reach values as high as 538GWh per year.

Moreover, a number of studies have been made to identify other sites in Europe suitable for producing electrical energy generated by marine currents. Together with the Institute of Energy Conversion of the Chinese Academy of Sciences, studies regarding the application of the ENERMAR system are currently in progress in the Strait of Jintang (Zhoushan Archipelago), People's Republic of China.

Nowadays Kobold is going to be applied in Indonesian seawaters, Chinese ones and Philippine ones.

The project for Indonesian coast is partially supported by UNIDO (United Nations Industrial Development Organization) funds.

There are several aims linked with this project, such as:

- helping developing countries – as Indonesia – to get electricity energy in a clear way, to improve its economy assuring more independence on energy market, to create new job-position and with new skills;
- helping to test the device in new locations, learn more and consequently get a faster learning rate to decrease future cost of technology;
- helping a sustainable world's growth;
- creating and stimulating interests for ocean energy sectors.

## *Part 2. Exploiting tidal energy in Guinea-Bissau*

### **3. Guinea-Bissau: a developing country**

#### **3.1 Introduction**

Having provided a broad overview of the different tidal power technologies employed worldwide, we now move to investigate the site where our studies are centred: the developing country Guinea-Bissau.

The present thesis was born from a request of the O.N.L.U.S. “Progetto e sviluppo 76” to analyze the possibility of producing electricity from tidal power in Guinea Bissau, where the association is realizing some projects of cooperation in collaboration with the local association “Amigos da Guiné-Bissau”.

Previous experiences of collaboration between the O.N.L.U.S. and the University of Genova, in particular a project concerning the production of power using palm oil and a second project concerning tourism development, had been successful. Thus a new teamwork started to investigate the actual and unexplored field of tidal energy.

#### **3.2 The O.N.L.U.S. Progetto Sviluppo 76**

Progetto Sviluppo 76 is an association of voluntary service born on an initiative of various friends who decided to put on hand their own organizational and entrepreneurial competences in order to promote productive activities in some underdeveloped nations.

Its plans head aim at the development of independent and sustainable productive activities within the framework of market rules, so that those members of the local community who take part and work on a project will become the main actors in the process of exploitation of the outcomes of the project. The association does not mean to act in emergency contexts, field in which many other associations operate successfully.

Development is intended as an interaction between subjects and individuals at the same level:

- Those who come from the developed world bring their own technical, and organizational expertise as well as, if necessary, financial participation;
- Those who live in the less developed nations bring their local acquaintances, the ability to be operative and the availability of “human resources”.

### *3. Guinea-Bissau: a developing country*

The activities are therefore set up and put into effect in cooperation with those individuals who prove to be able to pursue them after a joint start. “ Jointly ” means that development cannot be imported, but can only be constructed through a mutual exchange.

The association statute (which can be found on the web-site [www.ps76.org](http://www.ps76.org)) recognizes the above mentioned formulation and regulates the associative life.

### **3.3 Country background**

Located on the West African coast, Guinea-Bissau is a small country, both in terms of land area, with 36,120 km<sup>2</sup> (including 30 islands forming the Bijagos archipelago) and in terms of population, with 1.472 million inhabitants. It is one of the poorest countries in the world with a per capita gross domestic product (GDP) of USD 900 with more than two-thirds of its population living below the poverty threshold and with under-utilised resources, like fishing, mining, agriculture and tourism.

Other social indicators reflect a dismal picture of pervasive poverty: a life expectancy of 47 years at birth; an under-five year mortality rate of 103 per 1000 live births; a fertility rate of about 5 children born/woman; and an adult literacy rate of 40%. (Central Intelligence Agency).

The capital is Bissau, where about 40 % of the country population lives.

### 3. Guinea-Bissau: a developing country

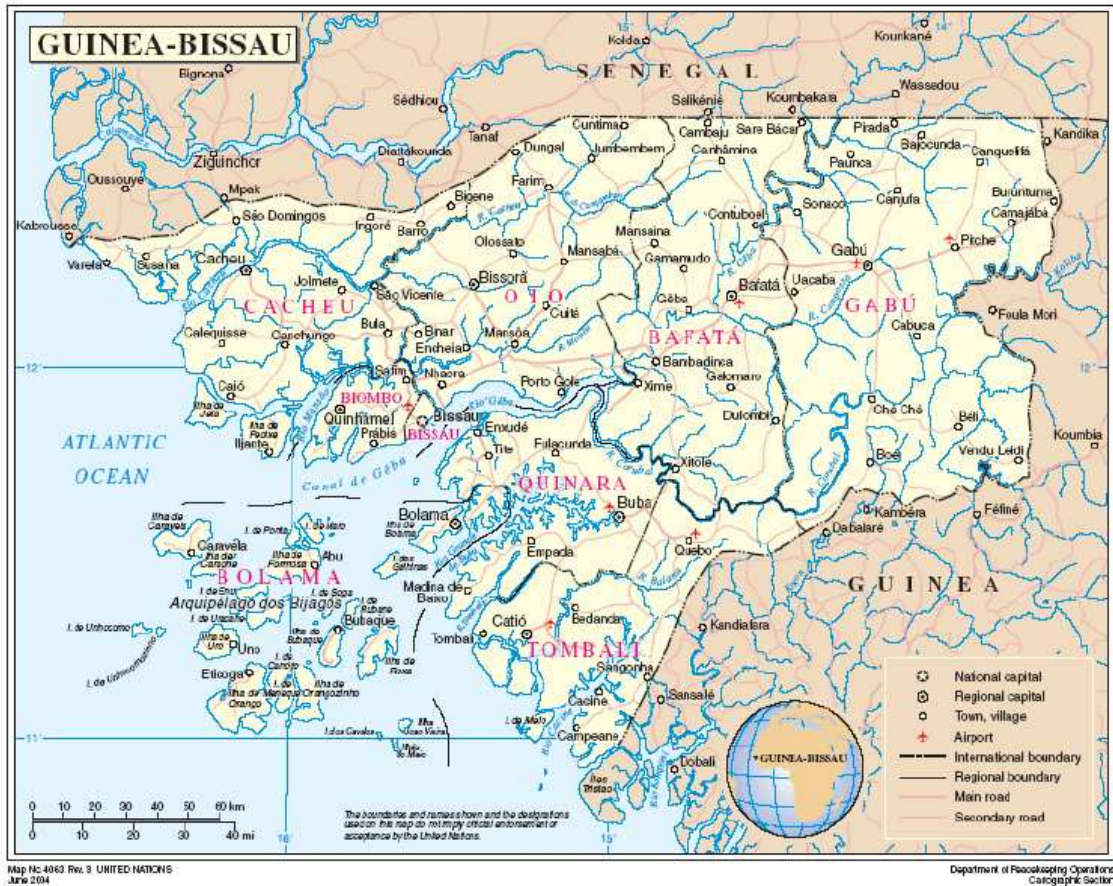


Fig. 3.1 - Map of guinea-Bissau (Flash Appeal, 2006).

Guinea-Bissau gained its independence from Portugal in 1974 after a protracted liberation war that brought tremendous damages to the country’s economic infrastructure. The civil war that took place in 1998 and 1999 and a military coup in September 2003 again disrupted economic activity, leaving a substantial part of the economic and social infrastructure in ruins and intensifying the already widespread poverty. Following the parliamentary elections in March 2004 and the presidential elections in July 2005, the country is trying to recover from the long period of instability despite a still-fragile political situation.

### **3.4 Economy**

The economy is highly dominated by the agricultural sector in which cashew nut represents over 85% of export earnings. However, food self-sufficiency is not reached. Moreover, the insufficiency of transport infrastructure limits substantially the development of new sectors such as bauxite and phosphate mining.

The country sectorial distribution is:

- primary industry (55.8% of GDP and 79% of the working population): cashew nut, rice, cotton seed, sorghum, cassava, wood, fishing;
- manufacturing industry (11.7% of GDP): mainly agro-food, energy;
- services sector (32.5% of GDP): mainly the trade.

### **3.5 Infrastructures**

The road network covers 4,400 km, of which 453 km are asphalt coated. The rehabilitation projects and the road network maintenance projects financed by the European Union (EU) are currently being examined. The main axis crosses the country from West to East, to the city of Buruntuma, at the border with Guinea. A great part of the territory is cut out by the numerous estuaries and the lack of bridges requires that vehicles break bulks and use the fluvial ferries.

### 3. Guinea-Bissau: a developing country



*Fig. 3.2 - View of a road in Guinea-Bissau. Its bad conditions remark the difficulty in transport when operating in developing country.*

The construction of the San Vicente bridge on the Rio Cacheu is in progress, as programmed by the EU, and will enable a faster connection with Senegal. While the country's geographic position is in favour of sea and river transport, infrastructures are few and in a poor condition. The Bissau harbour is silted up and its equipment and maintenance facilities are obsolete. The five estuaries are navigable; the main estuary is Rio Geba, navigable in deep water to Bissau (charge of 120,000 tons). On the Bijagos archipelago, the Bubaque harbour allows for steamers up to 120,000 tons.

#### **3.6 Power Sector**

Guinea-Bissau has one of the lowest electrification rates in Africa, mostly because of corruption and inefficiency. The country is completely dependent on petroleum products, despite its own high energy potential, especially in hydroelectric power.

Electrification covers only 12% of the country, the lowest level of the sub-region, and electric service costs five times more than in Senegal.

The Electricity and Water Company of Guinea Bissau (EAGB) is in charge of electricity

### *3. Guinea-Bissau: a developing country*

supply and distribution in the capital. Peak demand for electricity is estimated to be about 15 MW but the available units in EAGB have the capacity to produce 11.8 MW, about 2/3 of total demand. Production depends on maintenance of the units and steady supplies of spare parts, and, lacking these, EAGB in May 1996 was able to produce a mere 6.85 MW.

This rate of production not only reflects the inefficiency of the system, but is also unable to meet daily average demand for electricity. The consequences are frequent black-outs or load shedding, which can last from several hours to many days. Customer dissatisfaction with the service only serves to exacerbate already existing problems of revenue collection, with the result that EAGB is currently facing a severe cash flow crisis.

The inefficiency of the power sector has disrupted economic activity to the point where many businesses are forced to secure their own generating capacity at high economic cost.

Oil-derived products supply 95% of the country's commercial energy needs. Guinea-Bissau's downstream oil industry is wholly dependent on refined petroleum products imported from neighbouring countries. There has been active exploration offshore Guinea-Bissau since the late 1960's when Esso drilled six wells, but, after the independence from Portugal, exploration has been frequently affected by civil unrest. Offshore exploration has been hampered by a boundary dispute with Senegal, which was not resolved until 1993.

The inefficiency of the power sector has also had a direct negative impact on the water sector: the irregularity of water supply in Bissau is in large part due to frequent power cuts which disrupt pumping of water on a regular basis.

The supply to Guinea Bissau of electric power provided by the power plants built on the Gambia river (in Gambia) and Konkouré in Guinea Conakry is under discussion. Moreover, the studies for the Saltinho dam on the Corubal river (power of 20 MW for an average production of 150 GWh/year) are in progress.

Guinea-Bissau has great potential resources for hydroelectric power development for the domestic market and even for export. The potential production capacity of the Corubal and Geba rivers alone exceeds the country's estimated future need.

### 3.7 The continental watercourses

Guinea-Bissau is covered by a network formed by flowing and stagnating waterways. Estuaries, rivers and their tributaries (the most important, from north to south, being Cacheu river, Mansoa, Geba, Corubal, Rio Grande de Buba, Cumbijã, and Cacine river) belong to the first group. The deep interpenetration of land and the sea, in a distance that varies between 150 and 175 km, introduced salt water further inland, under the influence of tides.

Some lakes and lagoons, including the Cufada lake, which is the largest Limnologic water reserve in the country, belong to the second group.

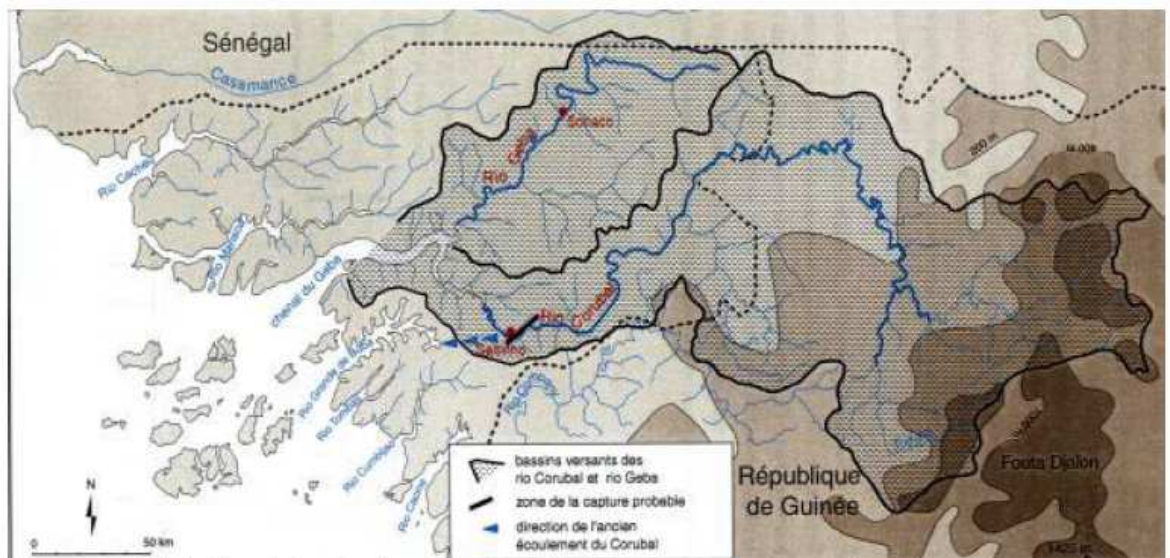


Fig. 3.3 - River network of Guinea-Bissau (Extract from the doctoral thesis of G. Pennober).

Of all the rivers of Guinea-Bissau, only Corubal river has a significant hydroelectric potential, with an average annual flow of nearly  $425 \text{ m}^3/\text{s}$ . With a total basin area of  $23,840 \text{ km}^2$ , it is also the largest fresh water resource in the country. In fact, the rocky thresholds of Cussilutra project the resource from penetration of salt water.

Actually the exploitation of fresh water is limited to a few pumping station employed for irrigation.

### 3.8 The importance of tides.

As we have shown in § 1.5, the tidal range due to the principal lunar semidiurnal constituent  $M_2$  on the coast of Guinea-Bissau is the highest along the west African coast; moreover, the geographic characteristics of the country and the presence of tidal estuaries increase the tidal range to significant values.

The maximum registered tidal range is then 6.80 m in Porto Gole, placed on the bank of Rio Geba.

The tidal station located along the coasts of the country are shown in the image below.



Fig. 3.4 - Satellite image of Guinea-Bissau with specified in red the tidal stations (©Google 2007).

### 3. Guinea-Bissau: a developing country

In the following table typical values of maximum and minimum tide amplitude are listed:

|                   |            | Max Amplitude [m] | Min Amplitude [m] |
|-------------------|------------|-------------------|-------------------|
| <b>Rio Mansoa</b> | Caio       | 1.25              | 0.8               |
| <b>Rio Geba</b>   | Bissau     | 2.5               | 1.25              |
|                   | Jabada     | 2.85              | 1.6               |
|                   | Porto Gole | 3.4               | 1.9               |
| <b>Islands</b>    | Bubaque    | 2                 | 1.1               |

Fig. 3.5 - Values of maximum and minimum tide amplitude in Guinea-Bissau.

### 3.9 Conclusions

The needs for reconstruction, rehabilitation and construction of infrastructures and buildings are of paramount importance for this country. However, the State has insufficient resources for launching big sites required for the development of Guinea Bissau given the public finance status and its debts. The contribution of international donors will be essential to support the reconstruction and development of the country. In this respect, the European Union has programmed within the 9th European Development Fund a financial support amounting to MEUR 82.8. As regards the World Bank, a project portfolio of MEUR 66.7 is active, in which one refers to the rehabilitation of basic urban infrastructures. The African Development Bank and different bilateral aids also give their support.

The large international companies have no local representatives in Guinea Bissau given the political situation of the country in the past years. The political stability and the start-up of new projects financed by the donors should attract international contractors to Guinea-Bissau.

## 4. Barrage tidal power potential in Guinea-Bissau

### 4.1 Introduction

The goal of the second part of the present thesis is to study different types of tidal power plants that could operate in a developing country like Guinea-Bissau.

The first type of plant we consider is a barrage tidal power installation.

### 4.2 Single-basin two way installation

#### 4.2.1 Modelling a single-basin two way generation tidal power plant

As we have already shown in paragraph 2.3.2, a single – basin two way installation is the most suitable in a developing country; the figure below shows the scheme that we adopt in the present thesis.

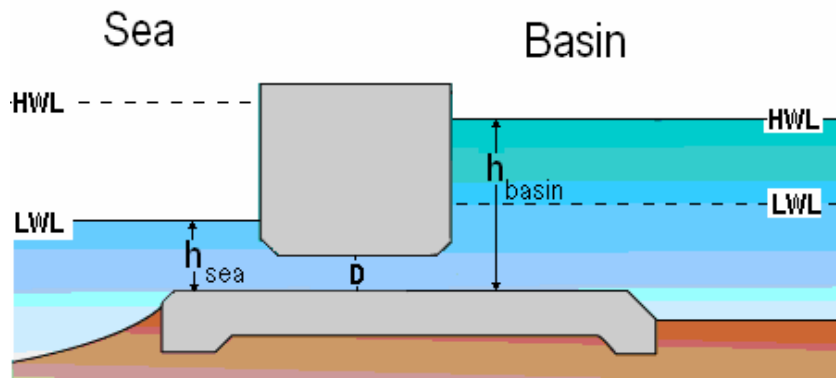


Fig. 4.1 - Simple sketch of the scheme we adopted to model a two-way generation tidal power plant.

The following steps need to be considered:

- the tide makes the sea level  $h_{sea}$  vary according to a sinusoidal law (see § 1.8):

$$h_{sea}(t) = a \cos(\omega t + p)$$

- the discharge  $Q$  flowing through the hole on the barrage is a function of the head  $\Delta h$  (difference between sea and basin level) and of the discharge coefficient  $c_q$  (see § 4.2.2) :

$$Q = c_q A \sqrt{2g\Delta h} ;$$

#### 4. Barrage tidal power potential in Guinea-Bissau

- assuming that the phenomenon is steady over a short time  $\Delta t$  the volume  $\Delta V$  exchanged by the basin with the sea is:

$$\Delta V = Q \Delta t ;$$

- the elevation of the free surface in the basin varies in a “quasi-static” fashion, according to the following law:

$$\Delta h_{basin} = \frac{\Delta V}{S}$$

where  $S$  is the basin surface.

The scheme has been solved numerically; the trend of sea and basin level is thus known and comparisons between different operating conditions in many locations can be performed, in order to seek the best way to maximize the exploitation of tidal power.

#### 4.2.2 Determination of discharge throughout circular holes

For submerged flow conditions the basic head-discharge equation is:

$$Q = c_q A \sqrt{2g\Delta h}$$

where:

- $c_q$  is the discharge coefficient;
- $A$  is the area of the hole;
- $g$  is gravity;
- $\Delta h$  is the head (difference between sea and basin level).

Calibration studies performed by H. R. Henry (1948) have produced the following plot for the determination of the discharge coefficient related to the ratios between the upstream level  $h_1$  and the hole diameter  $D$  and between the downstream level  $h_2$  and the hole diameter<sup>2</sup>.

---

<sup>2</sup> Depending on the direction of the flow throughout the barrage, either sea or basin level may be regarded as the upstream or downstream level.

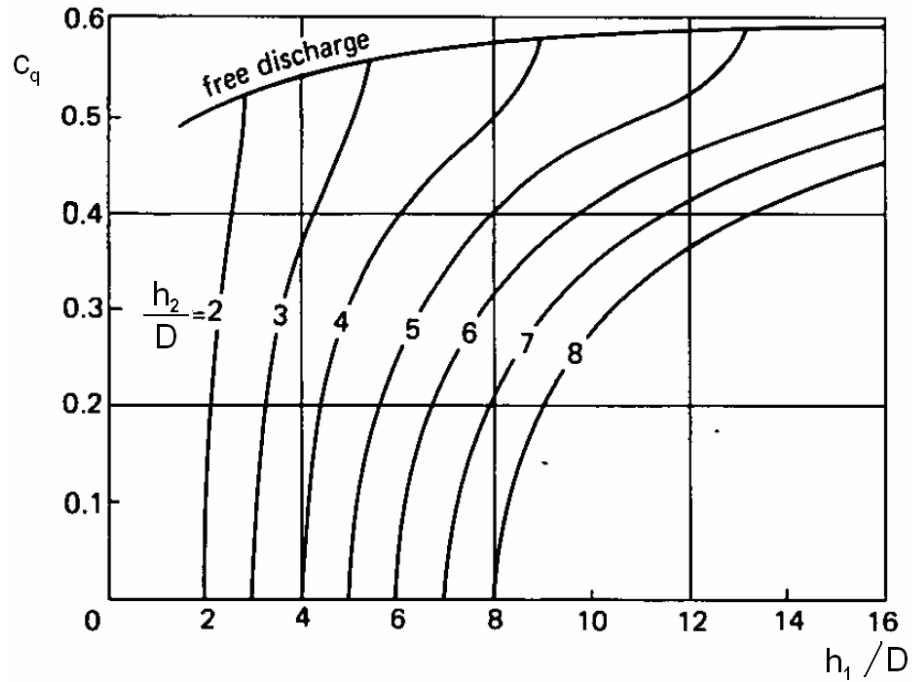


Fig. 4.2 - Evaluation of the discharge coefficient relating to the ratio between upstream level and the hole diameter (H.R. Henry, 1948).

Alternatively a theoretical estimation of the discharge coefficient can be obtained by imposing that the specific energy of the upstream current, calculated ignoring the kinetic head, equals the specific energy of the downstream current, assessed as the sum of elevation head and kinetic head of the submerged jet in the contracted section (thus neglecting the kinetic head of the above current). Follows the equation below, which we employed to model the single-basin two way tidal power plants:

$$c_q = 0.61 \sqrt{1 - \frac{h_{basin}/D}{h_{sea}/D}}$$

#### 4.2.3 Propagation through the basin

Assuming that the level in the basin increases in a quasi-static fashion (thus neglecting propagation through the basin) leads to an excellent modelling of the system behaviour for high depth and wide surface conditions. In a basin characterised by a depth  $Y_0 = 5$  meters, as those we consider later, the propagation speed of very long surface waves  $c_0$  takes a value of about 7 m/s.

#### *4. Barrage tidal power potential in Guinea-Bissau*

We deduce that in 1 minute (adopted as  $\Delta t$ ) the information that the surface elevation has increased propagates a distance of about 420 m: hence, our model is most appropriate for basins having surfaces smaller than roughly 16000 m<sup>2</sup>.

For larger basins and, in particular, for long and narrow channels modelled as basins a more detailed model which takes propagation into account would give more correct results; anyway, considering the low increase of water level at each time step, a good approximation can be performed even assuming a quasi-static approximation.

Finally, we notice that reflective phenomena due to the shores of a particular basin and effects of bottom profile must be evaluated in a more detailed analysis.

### 4.3 A small size installation: proposal of a power plant near Fanhe

#### 4.3.1 Site description

In this section we consider the possibility of applying the scheme described in § 4.2.1 by adopting as a basin one of the minor side channels of the estuary and taking advantage of the increase of tidal range due to landward propagation. As a result the first site we analyze is a small basin on the side of Rio Mansoa, as shown in the figure below.

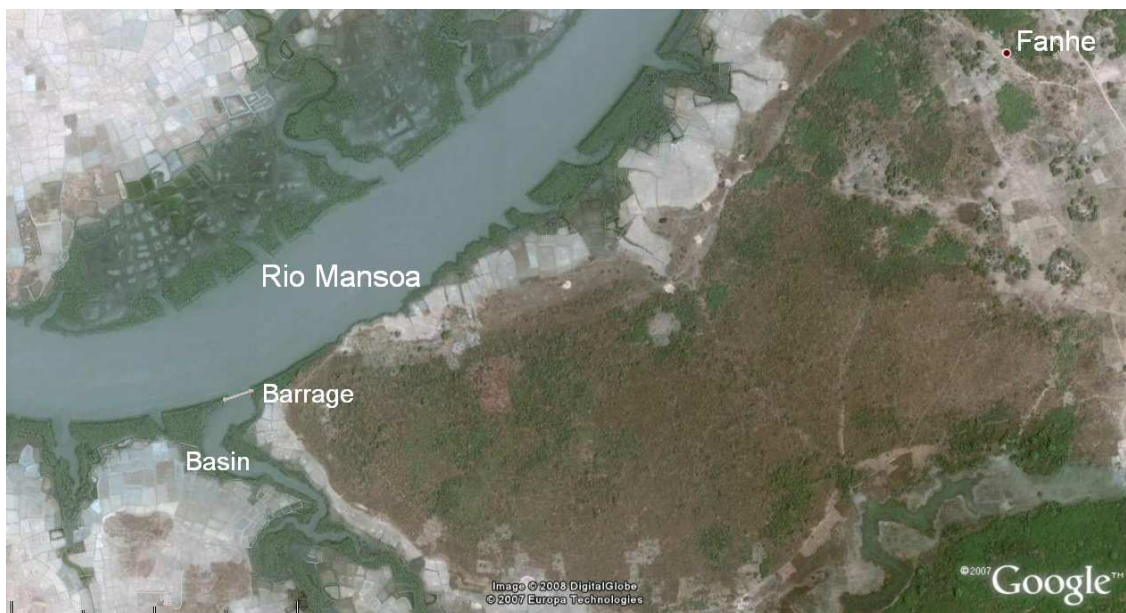


*Fig. 4.3 - Satellite image of the site near Fanhe where we study the feasibility of a small-size power plant (©Google 2007).*

The site is located about 100 km inland from the estuary mouth and it is only 2 km away from the village of Fanhe, where the O.N.L.U.S “Progetto e sviluppo76” is realizing other projects of cooperation. The local values of the tidal amplitude are estimated by a 1-D numerical model (see sect. 5.6), while the length of the barrage and the basin surface are estimated by satellite images. Finally, the average channel depth in the section of the barrage is unknown (because of the lack of nautical charts of the site) but it has been estimated assuming a linear bottom profile along the estuary: anyhow, the latter value is only used to calculate the height of the barrage and does not have any influence on the power output of the system.

#### 4. Barrage tidal power potential in Guinea-Bissau

All the quantities described are reported in the following table.

| <b>TIDE</b>                  |                       |                          |
|------------------------------|-----------------------|--------------------------|
| Annual average amplitude [m] | Minimum amplitude [m] | Maximum amplitude [m]    |
| 2.2                          | 1.6                   | 2.8                      |
| <b>BASIN</b>                 |                       |                          |
| Surface [m <sup>2</sup> ]    | Channel depth [m]     |                          |
| 29000                        | 2                     |                          |
| <b>BARRAGE</b>               |                       |                          |
| Length [m]                   | Height [m]            | Volume [m <sup>3</sup> ] |
| 72                           | 9.1                   | 12400                    |

Fig. 4.4 – Quantities characterising the site of Fanhe

On the basis of the ideas developed in sect. 2.3.3 we can estimate the average diurnal power potential of the tide in this site; a value of 126 KW is found and, assuming that 34 % of potential energy can be utilized, the average power output may reach a value of 43 KW.



Fig. 4.5 - A view of Rio Mansoa near Fanhe.

#### 4. Barrage tidal power potential in Guinea-Bissau

As regards the barrage, the best solution is an embankment dam, in particular an earth fill dam, made up mostly from compacted earth. A cross-section through an embankment dam shows that it is shaped like a levee; most of them have a central section, called the core, made of an impermeable material able to prevent water seepage through the dam. Clayey soils, really abundant in Guinea-Bissau, can be used for the core. A simple sketch of a typical cross-section is shown in the figure below.

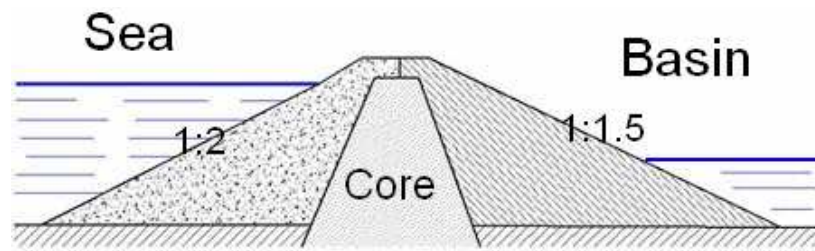


Fig. 4.6 - Simple sketch of a typical cross-section of an earth fill dam.

#### 4.3.2 Different regulation laws

We now simulate the behaviour of the system for different sizes of the holes in the barrage, in order to obtain the maximum exploitation of tidal power. The input data are:

- average amplitude:  $a_0 = 2.2$  m;
- period:  $T = 12.46$  h;
- basin surface:  $A = 29.000$  m<sup>2</sup>;
- efficiency of a common low head turbine:  $\eta = 0.79$  (see § 2.3.5.4);
- number of turbines:  $N = 1$ .

As first we consider the following hole dimension:

| Area [m <sup>2</sup> ] | Diameter [m] |
|------------------------|--------------|
| 0.20                   | 0.5          |

#### 4. Barrage tidal power potential in Guinea-Bissau

In the graph below we show the results for the free surface elevation in the basin, the outer estuary level (sea level) and the power output over a tide cycle of 12.46 hours.

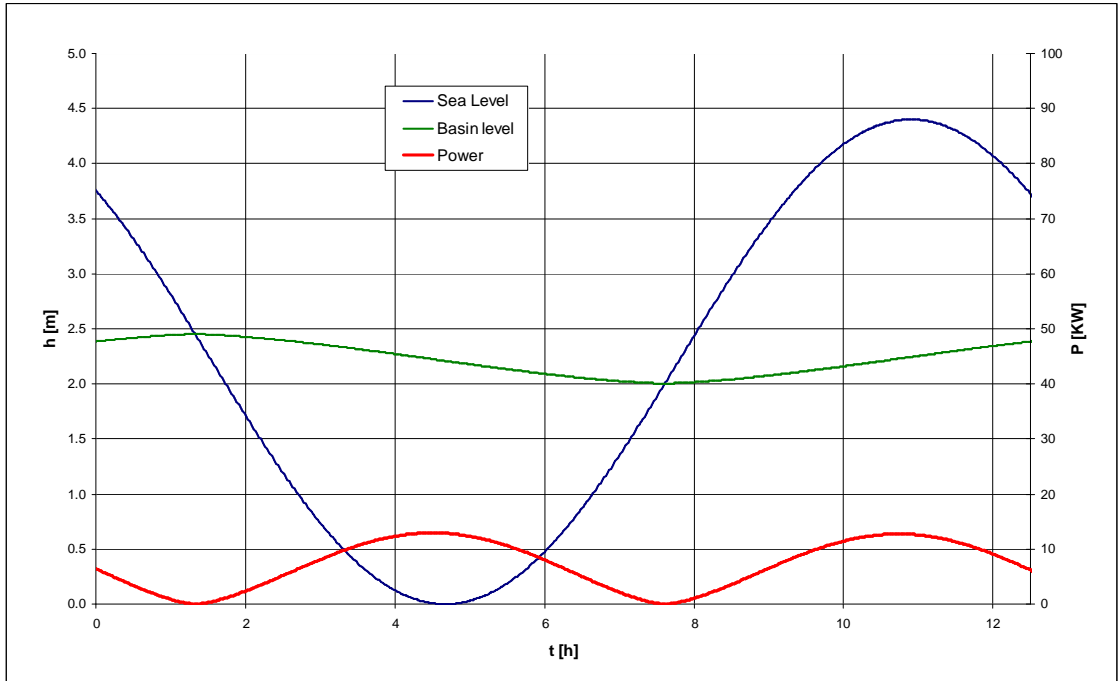


Fig. 4.7 - Trend of basin level, sea level and power output over a tide cycle for a hole 0.5 m in diameter.

We note that the oscillation range in the basin is small, implying high values of head but small discharge values, due to the small hole size. The maximum and the average power output over the cycle are then:

| Maximum power output [KW] | Average power output [KW] |
|---------------------------|---------------------------|
| <b>13.0</b>               | <b>7.1</b>                |

We now consider a larger hole and simulate again the system:

| Area [m <sup>2</sup> ] | Diameter [m] |
|------------------------|--------------|
| 0.785                  | 1.0          |

#### 4. Barrage tidal power potential in Guinea-Bissau

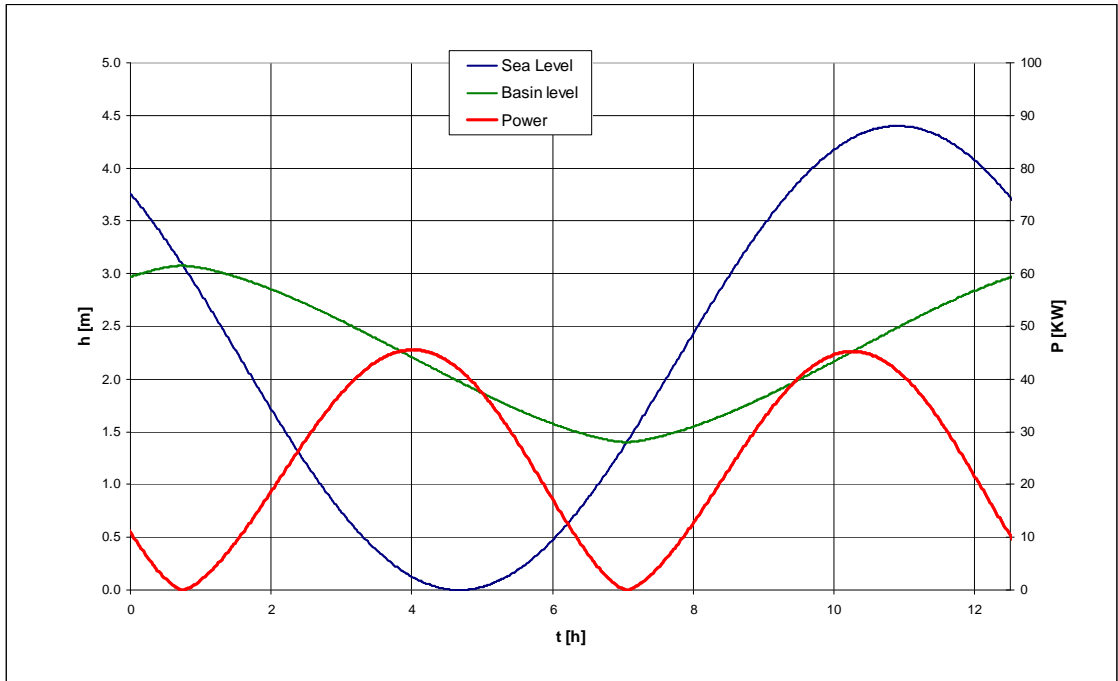


Fig. 4.8 - Trend of basin level, sea level and power output over a tide cycle for a hole 1 m in diameter.

| Maximum power output [KW] | Average power output [KW] |
|---------------------------|---------------------------|
| <b>47.2</b>               | <b>25.1</b>               |

The energy output is higher than in the previous case; then we keep on increasing the hole size, in order to analyse its effects on the power output.

| Area [m <sup>2</sup> ] | Diameter [m] |
|------------------------|--------------|
| 7.07                   | 3.0          |

#### 4. Barrage tidal power potential in Guinea-Bissau

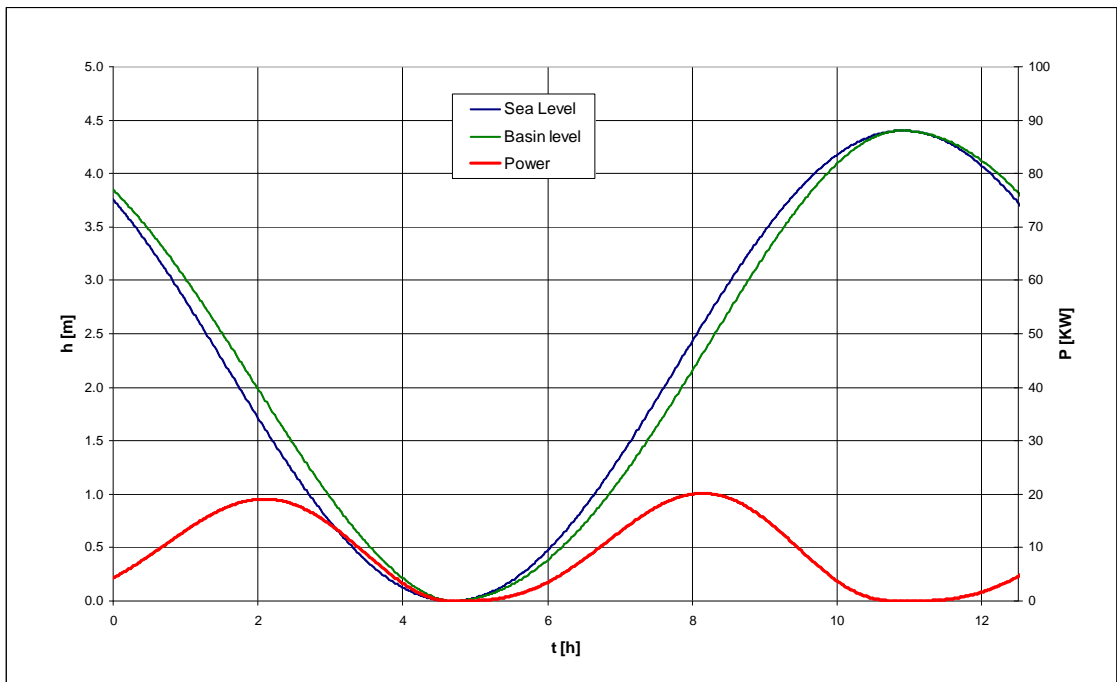


Fig. 4.9 - Trend of basin level, sea level and power output over a tide cycle for a hole 3 m in diameter.

The oscillation in the basin is similar to that of the estuary, implying high discharge values but too low head to generate the maximum power output we are looking for. The resulting outputs are indeed:

| Maximum power output [KW] | Average power output [KW] |
|---------------------------|---------------------------|
| <b>20.2</b>               | <b>8.8</b>                |

#### 4. Barrage tidal power potential in Guinea-Bissau

Therefore, simulating different cases we find the following relationship between the hole diameter and the average power output.

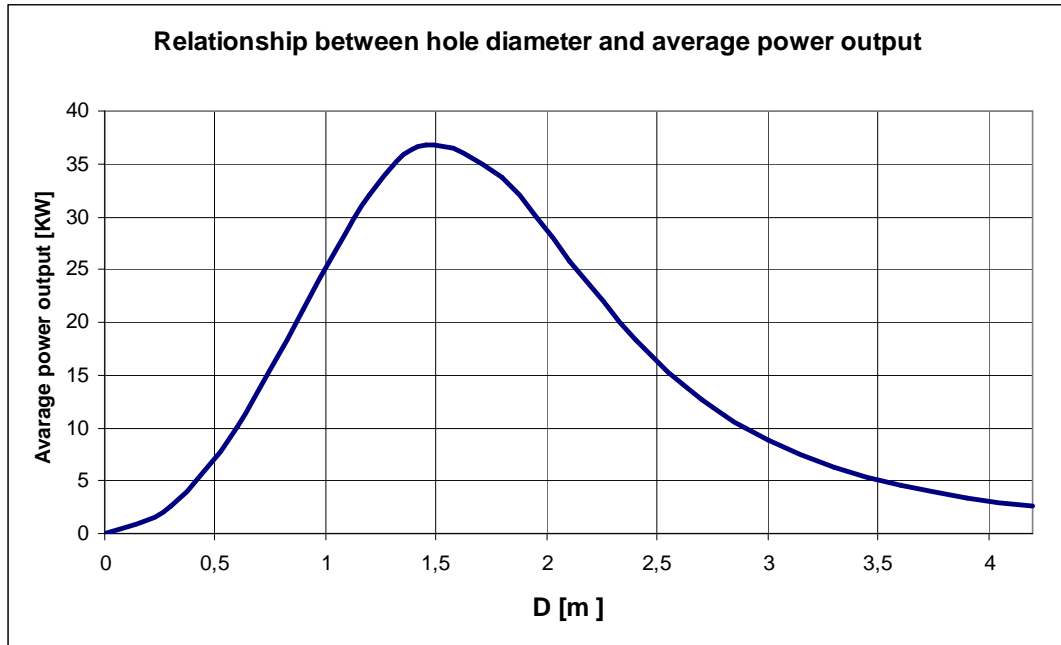


Fig. 4.10 - Relationship between the hole diameter and the average power output for a basin of 29000 m<sup>2</sup> and a tidal amplitude of 2.2 m.

We deduce that there is a hole size that maximizes the energy output in a tidal cycle:

| Area [m <sup>2</sup> ] | Diameter [m] |
|------------------------|--------------|
| 1.65                   | 1.45         |

#### 4. Barrage tidal power potential in Guinea-Bissau

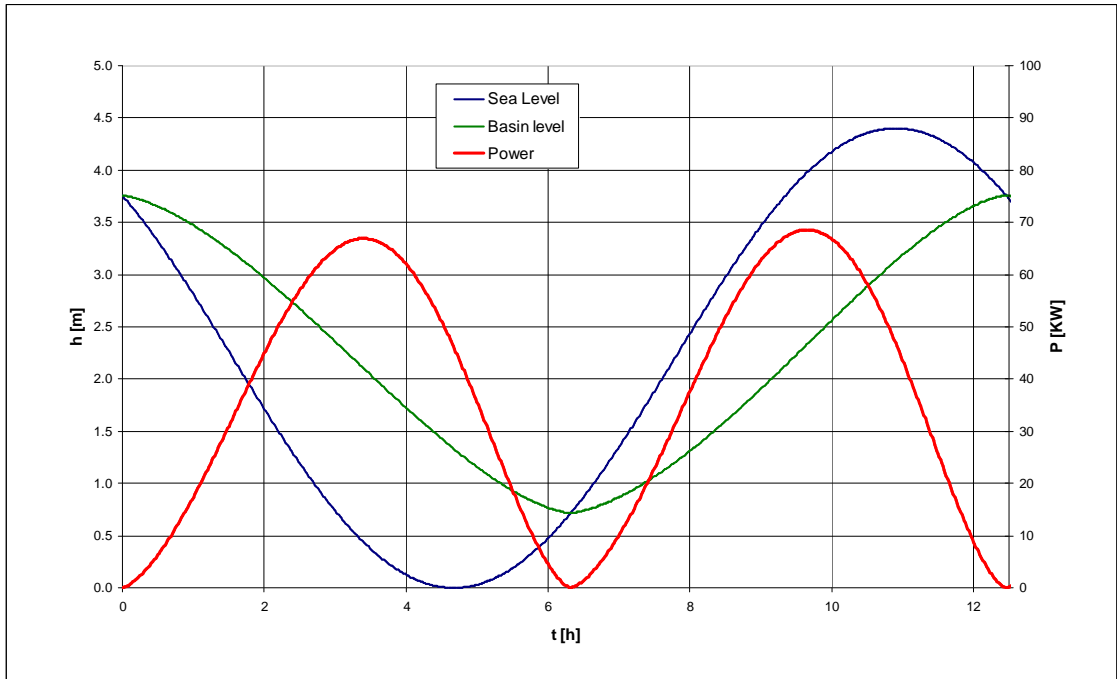


Fig. 4.11 - Trend of basin level, sea level and power output over a tidal cycle for a hole 1.45 m in diameter.

| Maximum power output [KW] | Average power output [KW] |
|---------------------------|---------------------------|
| <b>68.4</b>               | <b>36.8</b>               |

In the present thesis we assume this regulation law as the most effective one, because it gives the maximum energy output. We notice that, in this case, the ratio between the basin oscillation and the estuary tidal range assumes a value of 0.74, as suggested by Garrett and Cummins (2004).

Finally, we remark the slight asymmetry between the trends of flood and ebb power production; this can be explained referring to sect. 4.2.2: the discharge coefficient not only depends on the difference between the elevations of the sea and basin surfaces, but it also varies according to their values, which are higher in the case of maximum amplitude.

#### 4.3.3 Sluice and no-sluice system

Once we have decided the hole size, we need to consider that not all the power output in

#### 4. Barrage tidal power potential in Guinea-Bissau

a cycle is available, because of the too low values that the head reaches in some stages; indeed, even with very low head turbines, it is not possible to obtain good efficiencies under such circumstances.

We then consider a turbine that works under head conditions of at least 0.8 m, as experimented by some prototypes on the Danube river.

Let us analyze the benefits that the system would achieve with the installation of sluices that let us reach higher values of head, allowing the discharge to flow throughout the hole only when the head is higher then 0.8 m.

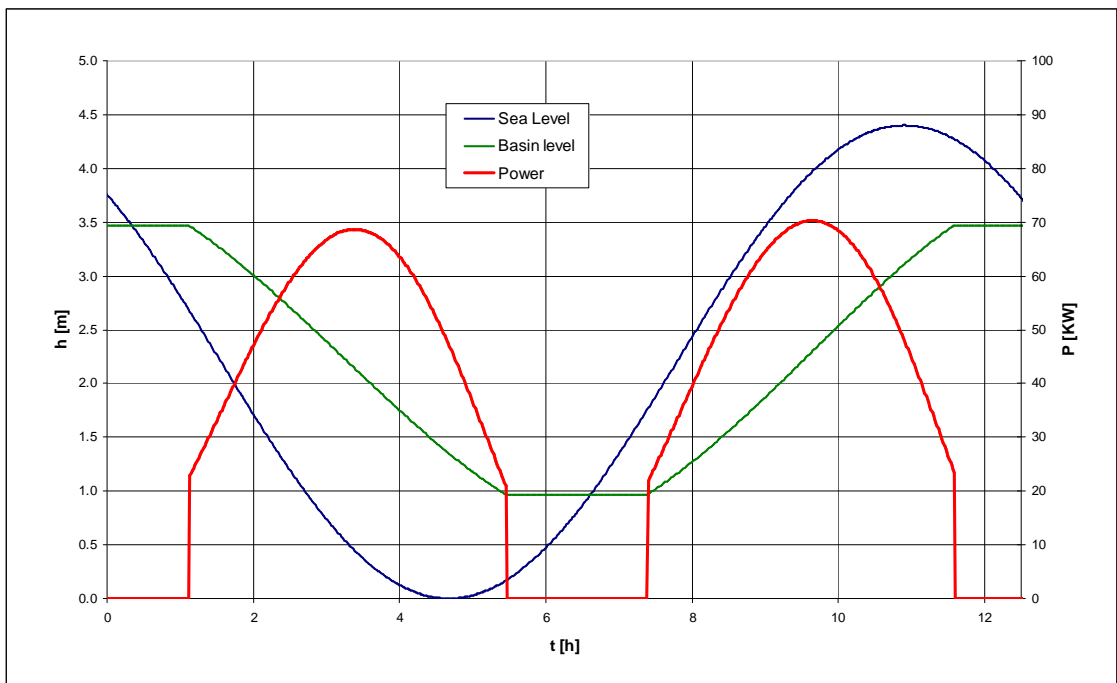


Fig. 4.12 - Trend of surface elevation in the basin, in the sea and power output over a tidal cycle for a basin regulated by sluices.

In this case the maximum power output is larger than in the case of no sluices (because of the increased head) and almost the whole energy cycle is captured.

| Maximum power output [KW] | Average power output [KW] |
|---------------------------|---------------------------|
| <b>70.2</b>               | <b>35.4</b>               |

#### 4. Barrage tidal power potential in Guinea-Bissau

Finally, we consider the possibility to operate without opening and closing the sluices twice in a cycle, in order to avoid the need to regulate continuously the power plant, as in a developing country maintenance and management is not as easy as in developed countries<sup>3</sup>.

Below, we plot the energy output obtained by summing up the energy produced only when the head is larger than 0.8 m, because of the previous consideration about low head turbines.

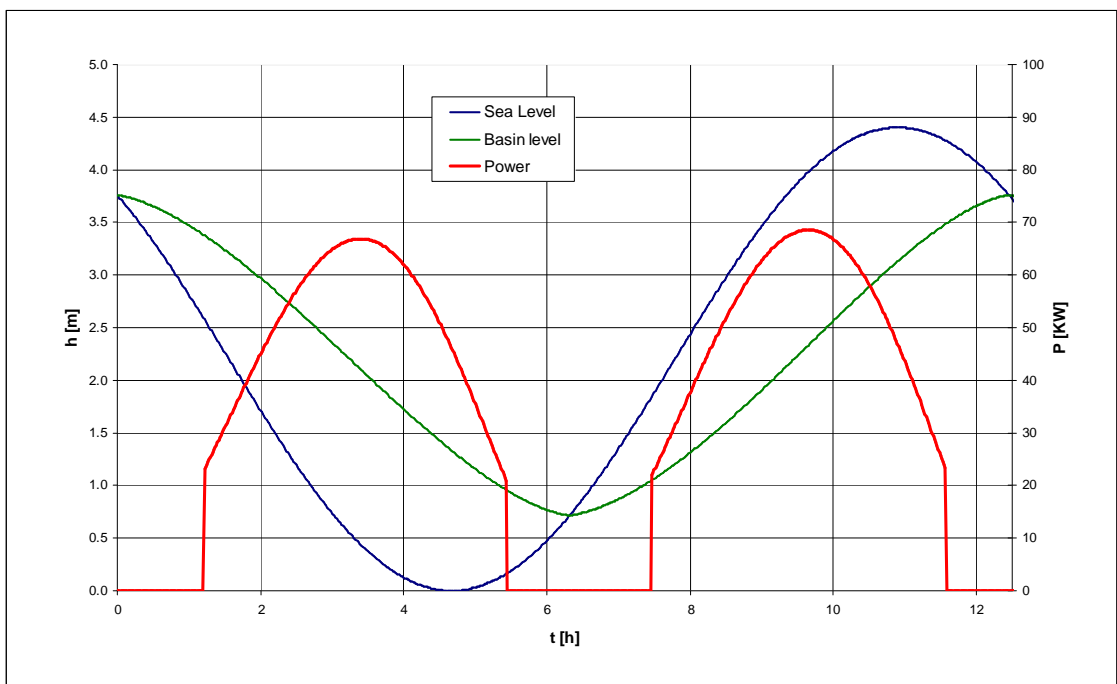


Fig. 4.13 - Trend of basin level, sea level and power output over a tide cycle for a basin with no sluice regulation system but with a cut in power production in case of head less than 0.8 m.

The maximum power output and the average power output over the cycle are then:

| Maximum power output [KW] | Average power output [KW] |
|---------------------------|---------------------------|
| <b>68.4</b>               | <b>33.9</b>               |

<sup>3</sup> Anyway a sluice system will be required for security reason and for maintenance operations.

#### 4. Barrage tidal power potential in Guinea-Bissau

Because of the advantages due to the simplicity of operating without sluices, this type of regulation is evaluated as the most attractive in Fanhe, even though about 4% of the energy produced with sluices is lost. In this case the power plant load factor would assume a value of 27 %, referring to the average diurnal power potential of the tide evaluated in sect. 4.3.1.

The working condition of the turbine over an average cycle is shown in the graph below and summarized in the following table.

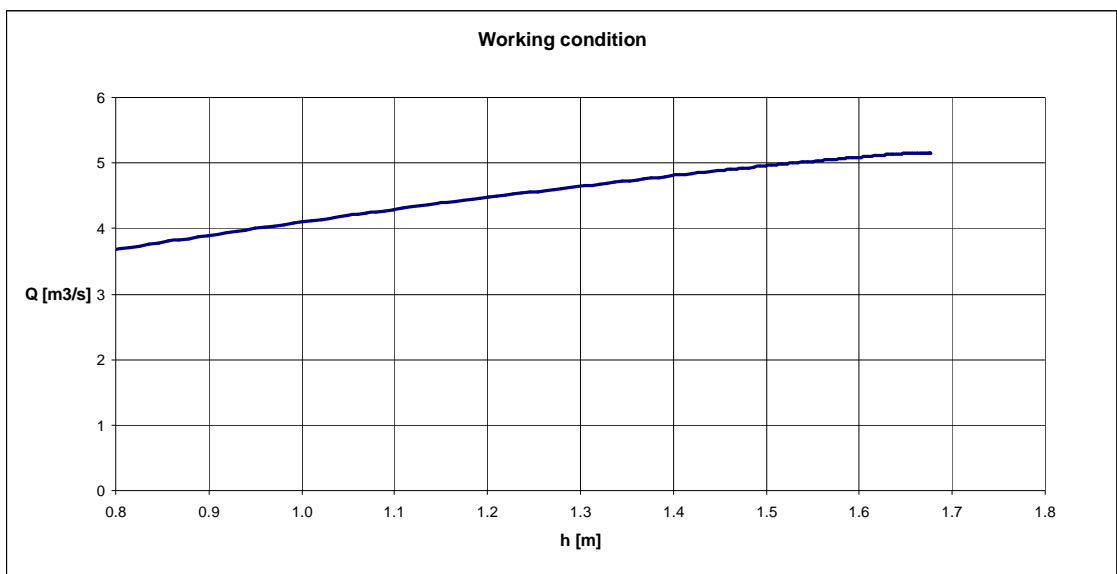


Fig. 4.14 - Working condition of the low head turbine required in the analyzed site (basin surface of 29000 m<sup>2</sup> and tidal amplitude of 2.2 m)

| TURBINE SPECIFICS |                  |                  |                           |                           |
|-------------------|------------------|------------------|---------------------------|---------------------------|
| Efficiency        | Minimum head [m] | Maximum head [m] | Min Q [m <sup>3</sup> /s] | Max Q [m <sup>3</sup> /s] |
| 0.79              | 0.8              | 1.68             | 3.69                      | 5.15                      |

#### 4.4 A medium size installation: proposal of a power plant near Bissau

##### 4.4.1 Site description

We then consider the possibility of installing a bigger tidal power plant near Bissau, adopting as a basin a minor side channel of the Rio Geba, as shown in the figure below.

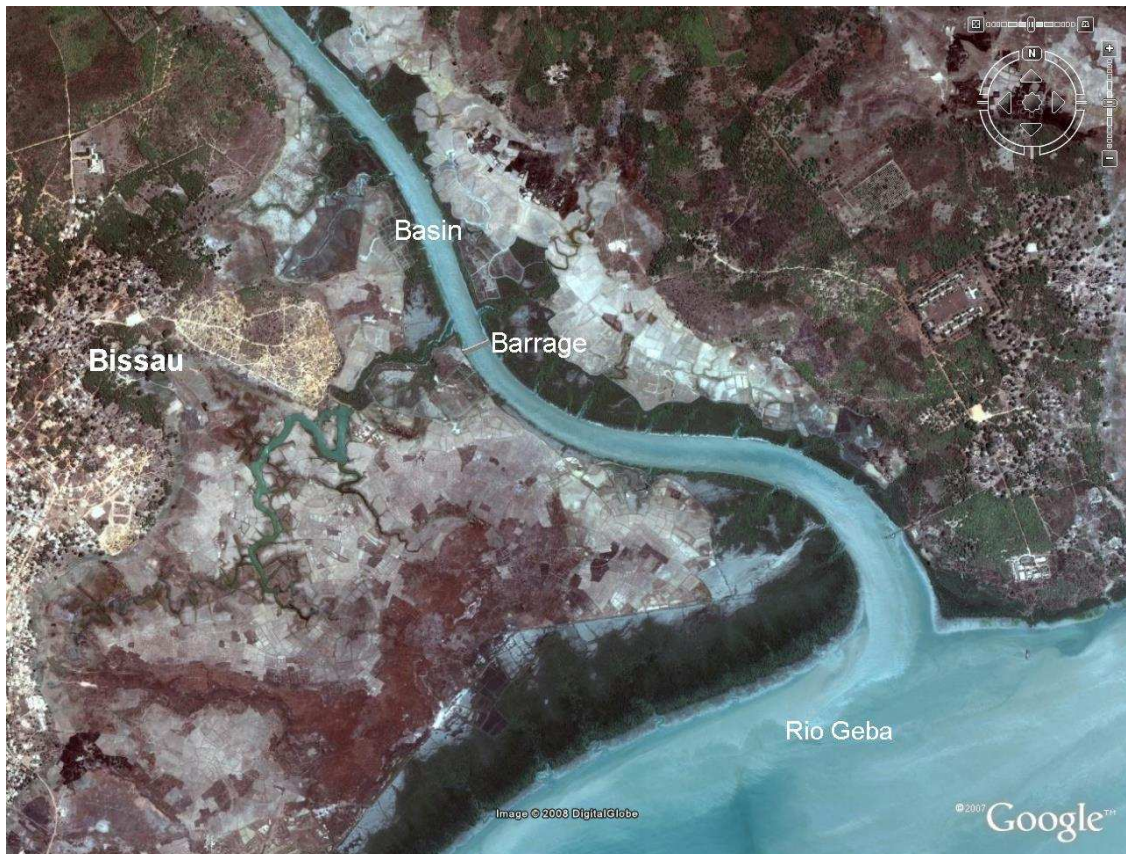


*Fig. 4.15 - Satellite image of the site near Bissau where we study the feasibility of a medium-size power plant (©Google 2007).*

The barrage is located about 1 km inland from the channel mouth, where the width is smaller, in order to reduce to one third its length and decrease the costs. After that the basin surface is diminished, but it is still wide enough, because of the high channel length.

The site would be less than 1 km away from the capital Bissau, so the power produced could be introduced in the city electric network.

Finally, as annual average tidal amplitude is assumed the one of Bissau, estimated by the

#### 4. Barrage tidal power potential in Guinea-Bissau

tidal tables of the Portuguese Instituto Hidrografico, without considering the possible amplification due to tide propagation in the side channel.

All the quantities described above are summarized in the following table.

| <b>TIDE</b>                  |                       |                          |
|------------------------------|-----------------------|--------------------------|
| Annual average amplitude [m] | Minimum amplitude [m] | Maximum amplitude [m]    |
| 1.9                          | 1.25                  | 2.5                      |
| <b>BASIN</b>                 |                       |                          |
| Surface [m <sup>2</sup> ]    | Channel depth [m]     |                          |
| 1.12 x 10 <sup>6</sup>       | 3                     |                          |
| <b>BARRAGE</b>               |                       |                          |
| Length [m]                   | Height [m]            | Volume [m <sup>3</sup> ] |
| 154                          | 9.5                   | 28711.375                |

Fig. 4.16 – Quantities characterising the site of Bissau

As done for the Fanhe case, we can estimate the average diurnal power potential of the tide in Bissau to find a value of 3639 KW.

As far as the barrage is concerned, the same considerations made in sect. 4.3.1 can be repeated.

#### 4.4.2 No-sluice system

Analyzing the Fanhe power plant we have shown that there is a hole size that maximizes the energy output. The same analysis is now repeated with the following input data:

- average amplitude:  $a_0 = 1.9$  m;
- period:  $T = 12.46$  h;
- basin surface:  $A = 1.12$  km<sup>2</sup>;
- efficiency:  $\eta = 0.79$ ;
- number of turbines:  $N = 6$ .

#### 4. Barrage tidal power potential in Guinea-Bissau

In this case we find the size values reported below for each of the 6 holes.

| Area [m <sup>2</sup> ] | Diameter [m] |
|------------------------|--------------|
| 10.17                  | 3.6          |

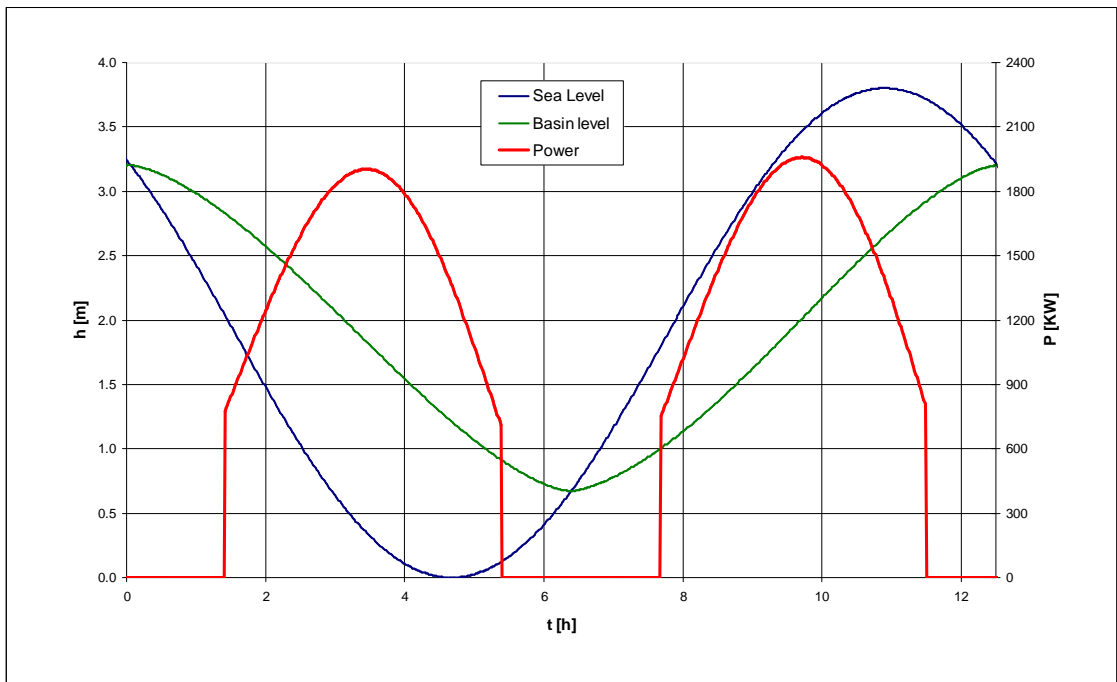


Fig. 4.17 - Trend of basin level, sea level and power output over a tide cycle for a basin with no sluice regulation system but with a cut in power production in case of head less than 0.8 m.

The maximum power output and the average power output over the cycle are:

| Maximum power output [KW] | Average power output [KW] |
|---------------------------|---------------------------|
| <b>1951</b>               | <b>936</b>                |

As we stated in the case of Fanhe, also in Bissau we assume this regulation law as the most effective.

In this site the power plant load factor would assume a value of 26 %, referring to the

#### 4. Barrage tidal power potential in Guinea-Bissau

average diurnal power potential of the tide evaluated in sect. 4.4.1.

The working conditions of the turbines over an average cycle are shown in the graph below and summarized in the following table.

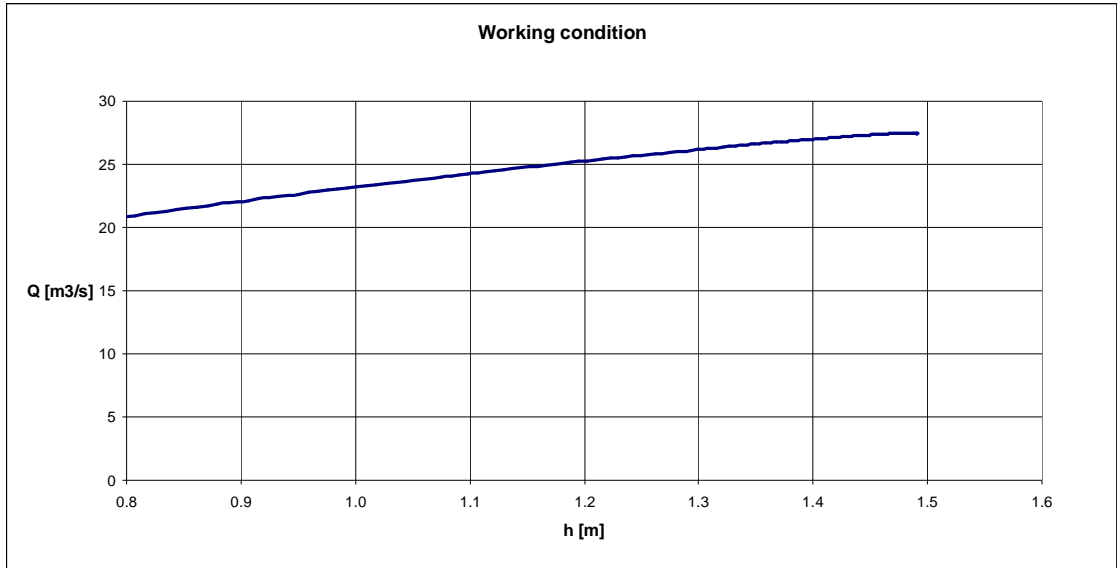


Fig. 4.18 - Working condition of the low head turbines required in the analyzed site (basin surface of 1.12 km<sup>2</sup> and tidal amplitude of 1.9 m)

| TURBINES   |                  | SPECIFICS        |                           |                           |
|------------|------------------|------------------|---------------------------|---------------------------|
| Efficiency | Minimum head [m] | Maximum head [m] | Min Q [m <sup>3</sup> /s] | Max Q [m <sup>3</sup> /s] |
| 0.79       | 0.8              | 1.49             | 20.9                      | 27.4                      |

Values of discharge higher than in Fanhe are found, due to the possibility of the exploitation of a wider basin surface; that would lead to the requirement in Bissau of turbines larger in diameter, as proved by the bigger hole sizes.

#### 4.4.3 Maximum and minimum tidal amplitude

The power output has been calculated so far adopting the annually averaged tidal amplitude at the analyzed site. In this section, we consider the effects of the monthly variation of tidal amplitude due to springs and neaps; we then simulate the two extreme cases of the maximum and minimum amplitudes in order to calculate their influence on

#### 4. Barrage tidal power potential in Guinea-Bissau

power output.

Firstly, we consider the local maximum amplitude ( $a_0 = 2.5$  m); maintaining the previous number and size of turbines we obtain the following results.

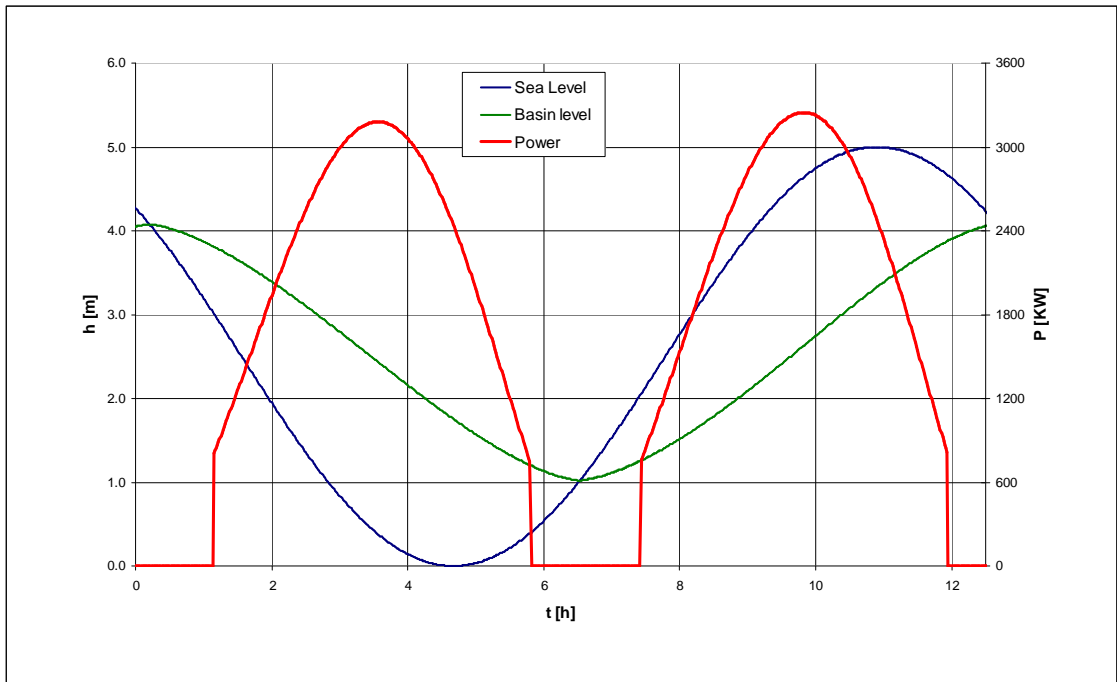


Fig. 4.19 - Trend of basin level, sea level and power output over a tide cycle considering the maximum amplitude of 2.5 m .

| Maximum power output [KW] | Average power output [KW] |
|---------------------------|---------------------------|
| <b>3277</b>               | <b>1676</b>               |

A noticeable increase of power output and production period are shown above.

We now analyze the case of minimum amplitude ( $a_0 = 1.25$  m). Having decreased the head we need to reduce the discharge flowing through the barrage in order to obtain the maximum energy output. To do that we consider only 4 turbines working.

#### 4. Barrage tidal power potential in Guinea-Bissau

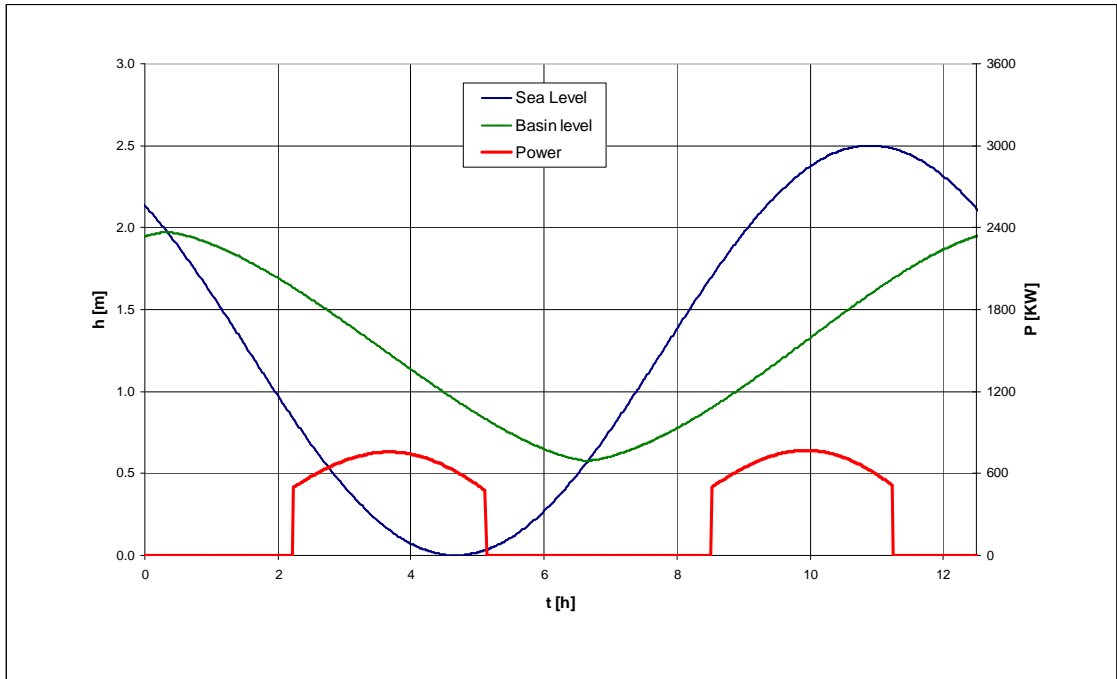


Fig. 4.20 - Trend of basin level, sea level and power output over a tide cycle considering the minimum amplitude of 1.25 m.

| Maximum power output [KW] | Average power output [KW] |
|---------------------------|---------------------------|
| <b>780</b>                | <b>302</b>                |

We obtain in this case a predictable decrease of power output and production period. Note that, due to the non linear dependence of energy on tidal amplitude, the mean value of the power outputs calculated using the maximum and minimum amplitudes reads:

$$\frac{1676 + 302}{2} = 989 \text{ KW}$$

This value is larger than the one calculated based on the annual average amplitude (936 KW).

Consequently, the monthly averaged power output would be slightly larger than the average power output evaluated in sect. 4.4.2 and should be evaluated simulating a period of at least 14 days.

The turbine working conditions of the previous cases are shown in the graph below.

#### 4. Barrage tidal power potential in Guinea-Bissau

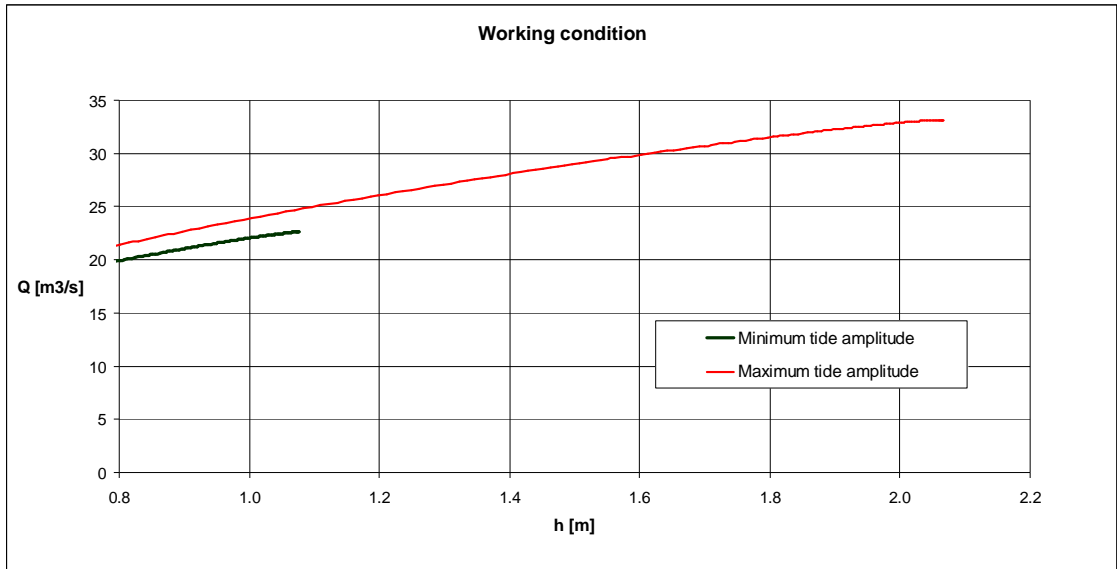


Fig. 4.21 - Comparison between the low head turbines working condition operating with the maximum and the minimum amplitude.

Remarking that discharge values corresponding to the same head are slightly different, we refer to the considerations made in sect. 4.3.2 concerning the power asymmetry.

#### 4.4.4 VLH turbine installation

The turbine type adopted so far in our power estimate, as we have already explained, is a prototype not yet available on the market. Even if a pressing increasing of production and supply of very low head turbines were really predictable that would fit in the studied power plants, we finally analyze the installation of 4 VLH turbines, available on the market and described in sect. 2.3.4.

| N° of turbines | Diameter [m] |
|----------------|--------------|
| 4              | 5.6          |

#### 4. Barrage tidal power potential in Guinea-Bissau

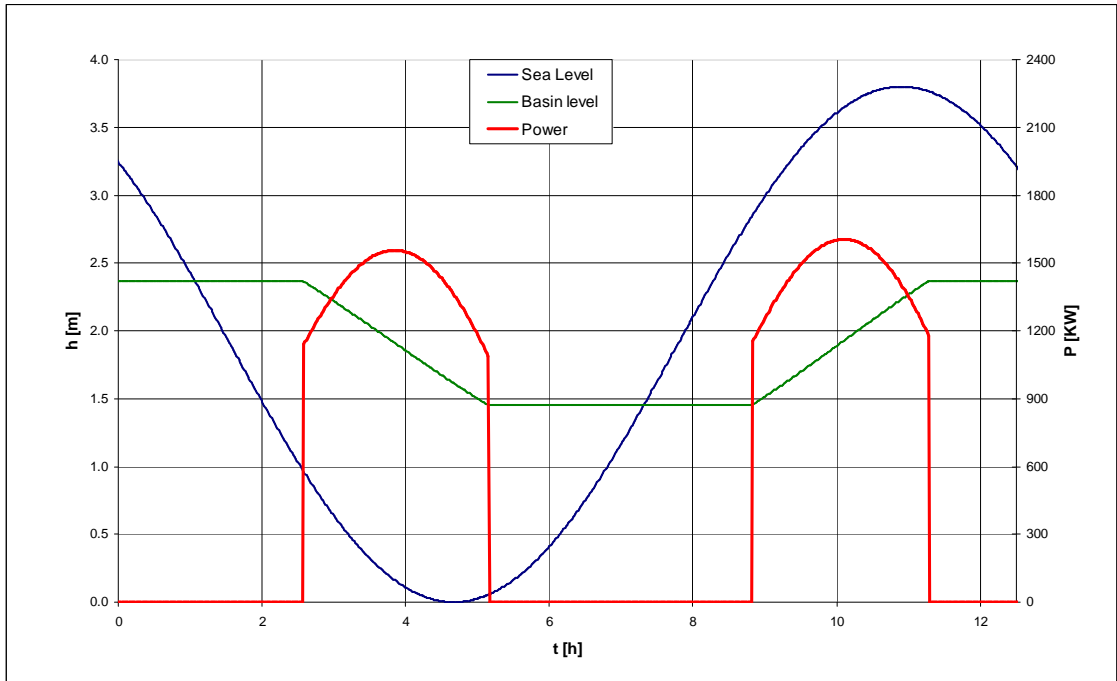


Fig. 4.22 - Trend of basin level, sea level and power output over a tide cycle operating with 4 VLH turbines.

| Maximum power output [KW] | Average power output [KW] |
|---------------------------|---------------------------|
| <b>1601.5</b>             | <b>577.8</b>              |

The resulting energy output is lower than the one estimated previously, because of the higher head required by the VLH turbines ( $\Delta h > 1.4$  m as shown in § 2.3.5.4) and the following shorter period of power production. This final case proves the urgent need of studying and developing specific very low head turbines, in order to collect the large amount of clean energy by oceans.

At last, in the graph and table below we show the working conditions of 4 VLH turbines; comparing them with the relationship between head and discharge that would be set up in the case of free flowing throughout 4 holes 3.52 m in diameter we note the larger dimension required for the turbines for the same discharge values, in order to decrease velocity (and then losses) and produce electric power.

#### 4. Barrage tidal power potential in Guinea-Bissau

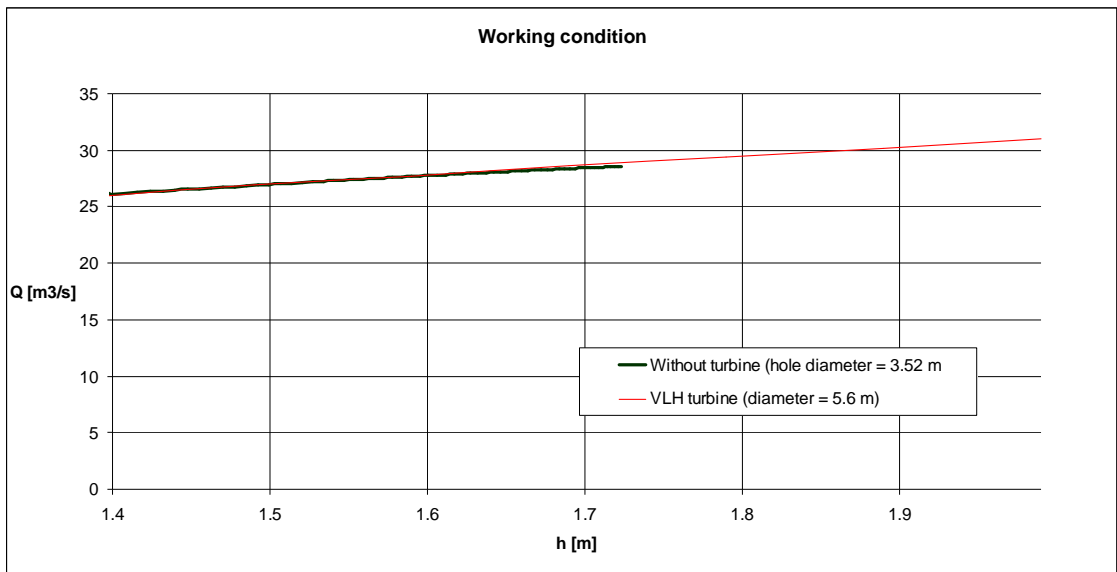


Fig. 4.23 - System behaviour for a hole of 3.52 m in diameter compared to the working condition of a VLH turbine 5.6 m in diameter.

| TURBINES   |                  | SPECIFICS        |                           |                           |
|------------|------------------|------------------|---------------------------|---------------------------|
| Efficiency | Minimum head [m] | Maximum head [m] | Min Q [m <sup>3</sup> /s] | Max Q [m <sup>3</sup> /s] |
| 0.79       | 1.4              | 2.0              | 25.9                      | 31.0                      |

#### 4.5 Preliminary considerations about a big size power plant near Porto Gole

The best location where to install a barrage tidal power plant is the one with the greatest tidal range. Around Guinea Bissau the locality where we find the maximum measured tidal amplitude is Porto Gole, as we show in sect. 3.8. According to this consideration, we analyze a site located 8 km away from Porto Gole and 76 from Bissau, on the landward share of Rio Geba.

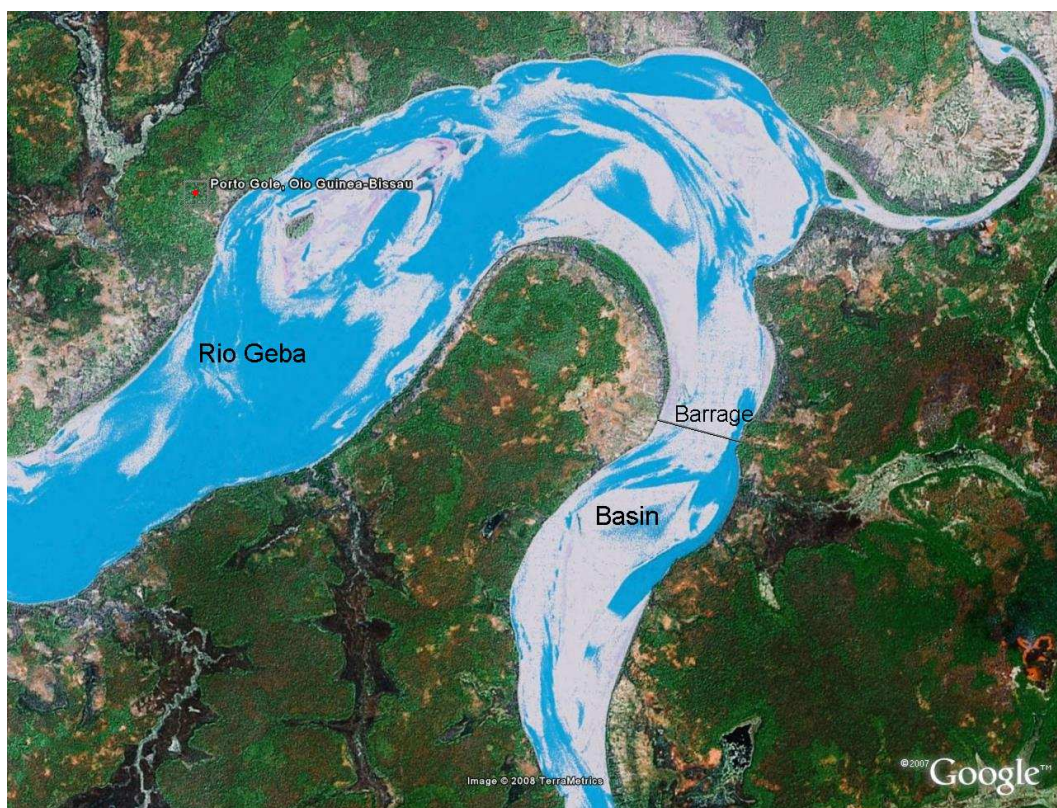


Fig. 4.24 - Satellite image of the site near Porto Gole where we study the feasibility of a big-size power plant (©Google 2007).

As shown in the above figure, the barrage is located in a narrow section, in order to reduce its length and then decrease the costs. We next consider the possibility of adopting as a basin the wide landward share of Rio Geba.

Taking into account the distance from the capital Bissau, we need to consider an extra cost to install a power line connecting the power plant to the city.

#### 4. Barrage tidal power potential in Guinea-Bissau

Finally, we remark the likely increase of tidal amplitude after the construction of the barrage, which would act as a reflective wall. Anyway, in order to perform a preliminary analysis, we do not take into account this potential increase of the amplitude.

All the quantities characterising the site are summarized in the following table.

| <b>TIDE</b>                  |                       |                          |
|------------------------------|-----------------------|--------------------------|
| Annual average amplitude [m] | Minimum amplitude [m] | Maximum amplitude [m]    |
| 2.7                          | 1.9                   | 3.5                      |
| <b>BASIN</b>                 |                       |                          |
| Surface [m <sup>2</sup> ]    | Channel depth [m]     |                          |
| 22.5 x 10 <sup>6</sup>       | 1.5                   |                          |
| <b>BARRAGE</b>               |                       |                          |
| Length [m]                   | Height [m]            | Volume [m <sup>3</sup> ] |
| 2030                         | 10                    | 416150                   |

Fig. 4.25 – Quantities characterising the site of Porto Gole

Due to the high tidal range and the wide basin surface, the average diurnal power potential of the tide assumes a value of 148 MW. Considering that a maximum of 34 % of potential energy can be utilized, the average power output may reach 50.2 MW. This great amount of clean and predictable energy, more than twice as large as the capacity installed by the construction of the Saltinho dam on the Corubal river (on which studies are in progress), deserves a more detailed analysis and a specific measurement campaign.

Nevertheless, due to the small size of the turbines considered so far (comparable with the enormous values that the discharge would assume in this case) and to the many variables which must be taken into account when designing these big power plants, we think that these results should be considered with caution.

## 5. Tidal stream power in Guinea-Bissau

### 5.1 Introduction

In this chapter we investigate the possibility of exploitation of estuary tidal power in order to produce electricity without the construction of any barrage.

Following Perillo (1995) an estuary is a semi-enclosed coastal body of water that extends to the effective limits of tidal influence, within which sea water entering from one or more free connections with the open sea, or any other saline coastal body of water, is significantly diluted with fresh water derived from land drainage, and can sustain euryhaline (i.e. able to tolerate a wide range of salinity) biological species from either part or the whole of their life cycle.

In particular, tide dominated estuaries are those in which tidal currents play a dominant role, while density driven circulations are nearly absent because strong tidal effects are able to destroy vertical stratification. Tide dominated estuaries are usually funnel-shaped and characterized by the presence of sand waves, intertidal flats and salt marshes. The periodic tidal currents can store large volumes of water in the estuary at high tides, which are followed by drainage at low tides.

### 5.2 Tide propagation in convergent and non-convergent estuaries

It is essential in particular to describe the role of several basic factors (length of the estuary, friction, channel convergence, bed altimetry, river discharge) on the properties of the tidal wave.

The morphodynamic behaviour of tide dominated estuaries depends strongly on upstream propagation of the tide. The celerity  $c_0$  at which tide moves along the estuary is governed by the shallow water equations and is therefore an increasing function of water depth ( $c_0 = \sqrt{gY_0}$ ).

As a result of this depth dependence, tides are deformed during their propagation: flood velocities are generally larger than ebb velocities and the flood-phase is shorter than the ebb-phase. The upstream decrease of the cross sectional area (depth and width of the channel) forces the tide to increase its amplitude during upstream propagation; however,

frictional dissipation tends to counteract this effect, decreasing the amplitude of tidal wave. “Hypersynchronous” estuaries are those where the effect of channel convergence is dominant and the wave is amplified; around the world many examples of such systems, like those of Guinea-Bissau analyzed in this thesis, can be found.

Besides the geometrical characteristics of tidal channels, the hydrodynamics of estuaries is strongly affected by many other elements, like the presence of short waves coming from the sea or due to wind action. Moreover, in some cases the river discharge at the landward end of the channel plays an important role and may induce stratification phenomena and density driven circulations.

Here, we restrict the analysis to a widespread class of tidal inlets, namely the well-mixed estuarine channels. This kind of morphological elements includes those estuaries and lagoon channels where the tidal forcing is so strong that stratification does not occur. The absence of a salt wedge allows one to consider a constant water density and to describe the flow field using the usual equations of single-phase fluid.

Tidal waves are driven by water oscillations imposed at the channel mouth, which is connected to the outer sea. Almost all the non-linear terms appearing in the governing equations for the flow field are proportional to the ratio between the tidal amplitude  $a_0$  and the average water depth  $Y_0$ , where the subscript 0 denotes the values at the channels mouth:

$$\varepsilon = \frac{a_0}{Y_0}$$

We may notice that  $\varepsilon$  ranges between 0 and 1 and in many real estuaries it can reach relatively large values.

Notice that a tidal wave generates over-tides along its propagation. For the sake of simplicity, in the present work we neglect the effect of external over-tides and force the system by a purely sinusoidal semi-diurnal  $M_2$  tide at the mouth of the estuary. Over-tides, like the quarter-diurnal  $M_4$ , occur at the mouth of estuaries when the offshore shelf is relatively wide and flat; moreover the presence of a wider wave spectrum at the channel inlet may affect the overall hydrodynamics of the system, while increasing the number of degrees of freedom in the analysis. Accounting for the effects of over-tides is beyond the aim of the present analysis.

### 5.3 Formulation of the 1-D problem

#### 5.3.1 Shallow water equations

The standard one-dimensional partial differential equations describing the unsteady water flow in a wide rectangular channel are the classical shallow water equations of mass and momentum conservation, which read:

$$\frac{\partial Q}{\partial t} + \frac{\partial}{\partial x} \left( \frac{Q^2}{\Omega} \right) + g\Omega \frac{\partial h}{\partial x} + g\Omega j = 0$$

$$\frac{\partial \Omega}{\partial t} + \frac{\partial Q}{\partial x} = 0$$

where:

- $t$  is time;
- $x$  the longitudinal coordinate;
- $Q$  is the water discharge;
- $\Omega$  is the area of the cross section;
- $h$  is the water surface elevation;
- $g$  is gravity.

The frictional term is evaluated in the following form:

$$j = \frac{Q|Q|}{g\Omega^2 C_h^2 R_h}$$

having denoted with  $C_h$  the dimensionless Chézy coefficient and with  $R_h$  the hydraulic radius:

$$R_h = \frac{BY_0}{B + 2Y_0}$$

Two boundary conditions to be imposed one at each side (the mouth of the channel and its landward end) are required.

The seaward boundary condition is given by the sea level, which is assumed to be determined by the tidal oscillation without any influence of the internal response of the estuary:

$$h(t) = a_0 \cos(\omega t)$$

where:

- $\omega$  is the angular frequency:

$$\omega = \frac{2\pi}{T} = kc_0$$

- $k$  is the wave number:

$$k = \frac{2\pi}{L}$$

- $L$  is the tide wave length:

$$L = c_0 T$$

The landward boundary condition is given by a totally reflective wall:

$$U_{(x=L_e)} = 0$$

where  $L_e$  is the estuary length.

The shallow water equations can be solved in two different ways:

- seeking analytical solutions;
- using numerical models.

### 5.3.2 Analytical solution for wide rectangular estuaries with constant width and frictional term negligible

The hypothesis under which the solutions of the shallow water equations can be found analytically are the following:

- the width  $B$  of the channel is constant;
- the cross sections are rectangular;
- the bottom is horizontal;
- $\varepsilon$  is small enough for its effect to be negligible;
- the frictional term is insignificant;
- the river discharge at the landward end of the channel is negligible.

Combining the two 1-D equations under the mentioned hypothesis and applying the previously defined boundary conditions, the following analytical solutions can be found

( $x$  axis directed landward, starting from the reflective wall section):

$$h = \frac{a}{\cos(kL_e)} [\cos(kx) \cos(\omega t)]$$

$$U = \frac{a}{Y_0} c_0 \frac{1}{\cos(kL_e)} [\sin(\omega t) \sin(kx)]$$

### 5.3.3 The resonance phenomenon

Basing on solutions found in the previous paragraph it is possible to determine a condition in which water level and velocity assume values that go to infinity.

The ratio between the water level in the final section and that imposed in the mouth of the estuary reads:

$$\frac{h_{\max}(x=0)}{h_{\max}(x=-L_E)} = \frac{1}{\cos(kL)}$$

The above fraction goes to infinity if:

$$kL_E = \frac{\pi}{2}(2n+1) \Rightarrow \frac{L_E}{L} = \frac{1}{4}$$

It means that for specific values of estuary length ( $L_E = L/4$ ), the reflective wall that closes the estuary gives rise to an amplification of the forcing wave; such increase of water level and velocity in reality is attenuated by energy losses across entrance shoals and frictional dissipation at the sandy bed.

### 5.3.4 One-dimensional numerical model for wide rectangular convergent and non-convergent estuaries

We investigate now the propagation of the tidal wave through a one-dimensional cross-sectional averaged model, with the longitudinal coordinate  $x$  directed landward, starting from the mouth of the estuary (M. Bolla Pittaluga, "Long term morphodynamic equilibrium of tidal channels", Università degli Studi di Padova, 2003). We also assume that a rectangular cross-section is suitable to describe, as a first approximation, the behaviour of a real section of the channel.

The above assumptions may be rather strong, since they imply that the model is unable

to account for topographically driven effects on the flow field as well as to include the role of shallow areas adjacent to the main channel.

The sketch of the geometry of the idealized tidal channel adopted in the present analysis is given below:

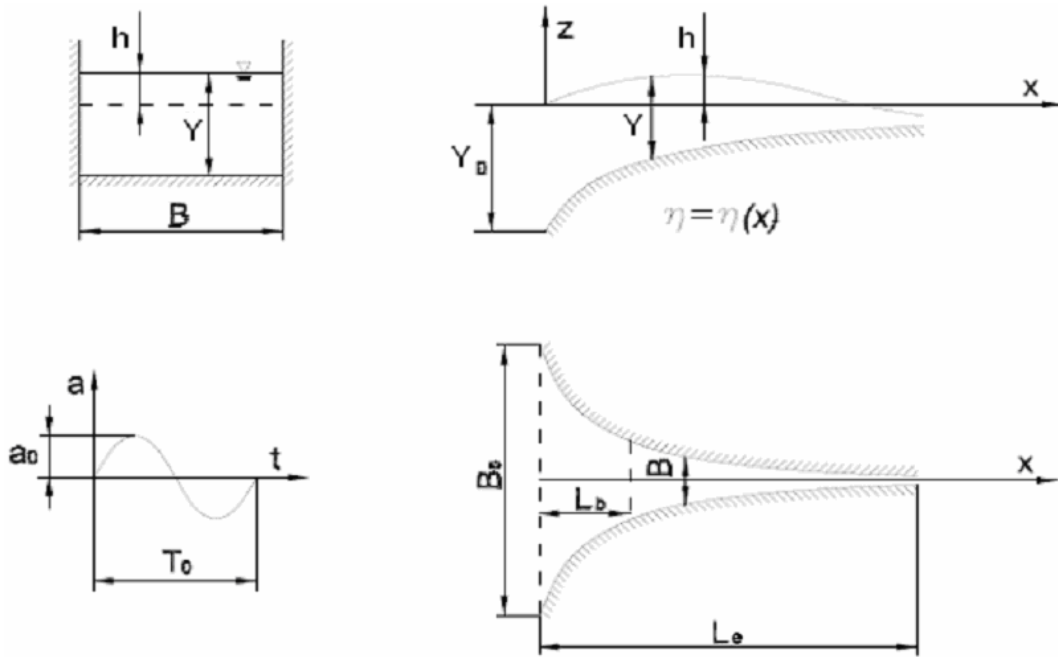


Fig. 5.1 - Geometry of the idealized tidal channel assuming a rectangular cross-section and a longitudinal width profile exponentially decreasing (G.Vignoli,2005) .

A typical funnel shape is assumed and represented employing an exponentially decreasing function of the longitudinal coordinate  $x$ , as assumed by many authors in the past (Friedrichs and Aubrey, 1994; Lanzoni and Seminara, 1998), according to the relationship:

$$B(x) = B_0 \exp\left(-\frac{x}{L_b}\right)$$

where  $L_b$  is the convergence length.

Alternatively, either a constant width or the estuary effective width trend can be assumed. In the present thesis both the above options are taken into consideration in order to study the influence of the longitudinal profile on the hydrodynamic behaviour of the channel.

### *5. Tidal stream power in Guinea-Bissau*

As for the longitudinal profile, it is commonly observed that in tidal estuaries the flow depth decreases landward. In the first steps of our work we assume the bed to be horizontal in order to reduce the number of independent variables; in the following steps the bottom profile will be chosen linear or evaluated through nautical charts.

### 5.4 The hydrodynamic of tidal estuaries in Guinea-Bissau

We focus now on the main hydrodynamic properties of Guinea-Bissau tidal estuaries.

Therefore we need to define some properties which characterize the watercourses network of the country; as annual average tidal amplitude is assumed that of the capital Bissau, extracted from the tidal tables of the Portuguese Instituto Hidrografico:  $a_0 = 1.9$  m.

In the first steps we assume the bed to be horizontal and the average water depth to be  $Y_0 = 10$  m (consequently:  $\varepsilon = 0.19$ ), in order to analyze the effects of the estuary length on water levels and velocities.

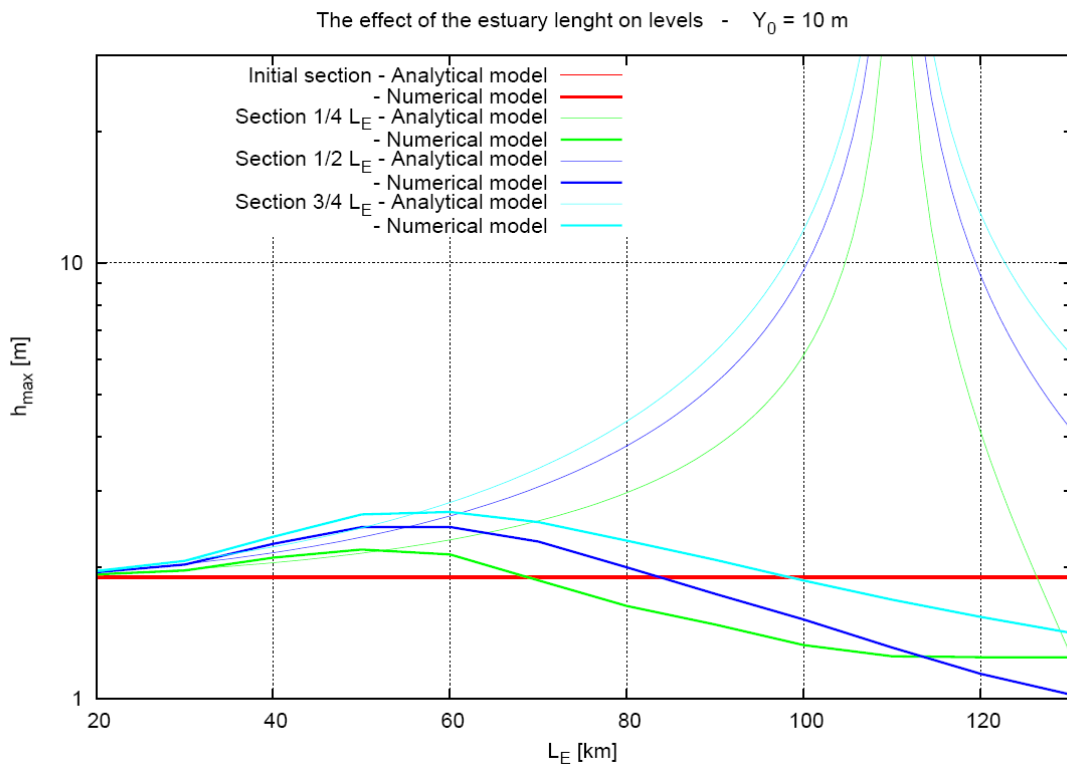


Fig. 5.2 - Effect of estuary length on water level: comparison between the results given by the numerical model and the analytical solution in four sections.

The shallow nature of the channels promotes tidal resonance which is counter-balanced by energy losses across entrance shoals and frictional dissipation at the sandy bed.

In the non dissipative analytical model the resonant peak, identified by values of maximum high water level which reach infinity, is located in correspondence of an

## 5. Tidal stream power in Guinea-Bissau

estuary length of about 110 km.

On the contrary the results given by the fully non-linear numerical model shows a softening of the resonant peak due to the dissipative effects; moreover the length giving rise to a maximum tidal amplification is lower than the analytical one, being about 55 km.

Similar consideration can be drawn about the effects of the estuary length on the maximum flood velocities.

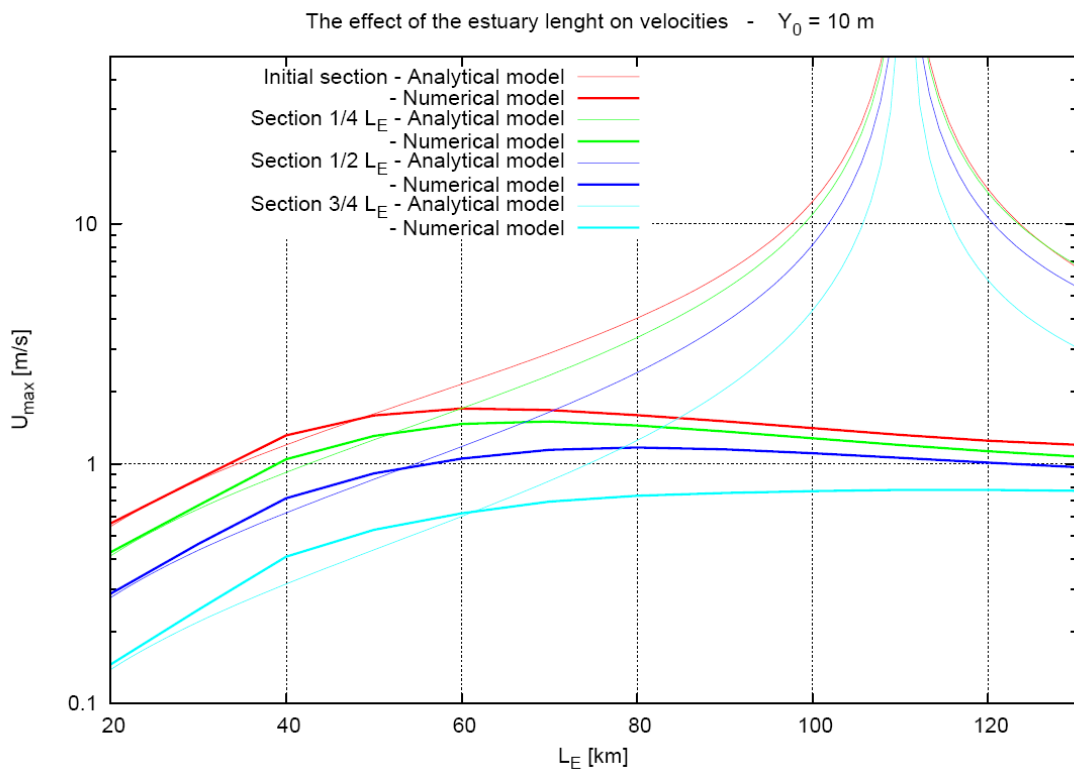


Fig. 5.3 - Effect of estuary length on water velocity: comparison between the results given by the numerical model and the analytical solution in four sections.

## 5. Tidal stream power in Guinea-Bissau

Among the many channels around Guinea-Bissau we focus now on the Rio Geba, because its length of 68 Km (considering the distance between Bissau and a sharp bend which can be considered as a reflective wall) is close to the non linear resonance length.

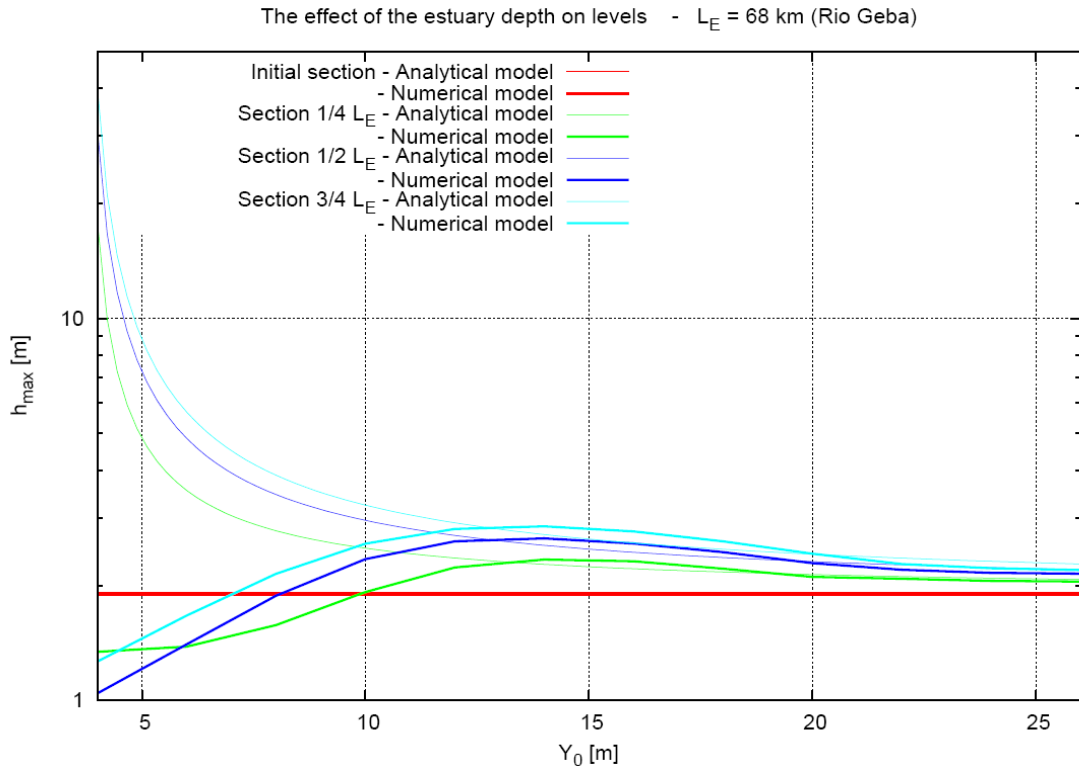


Fig. 5.4 - Effect of estuary depth on water level: comparison between the results given by the numerical model and the analytical solution in four sections.

## 5. Tidal stream power in Guinea-Bissau

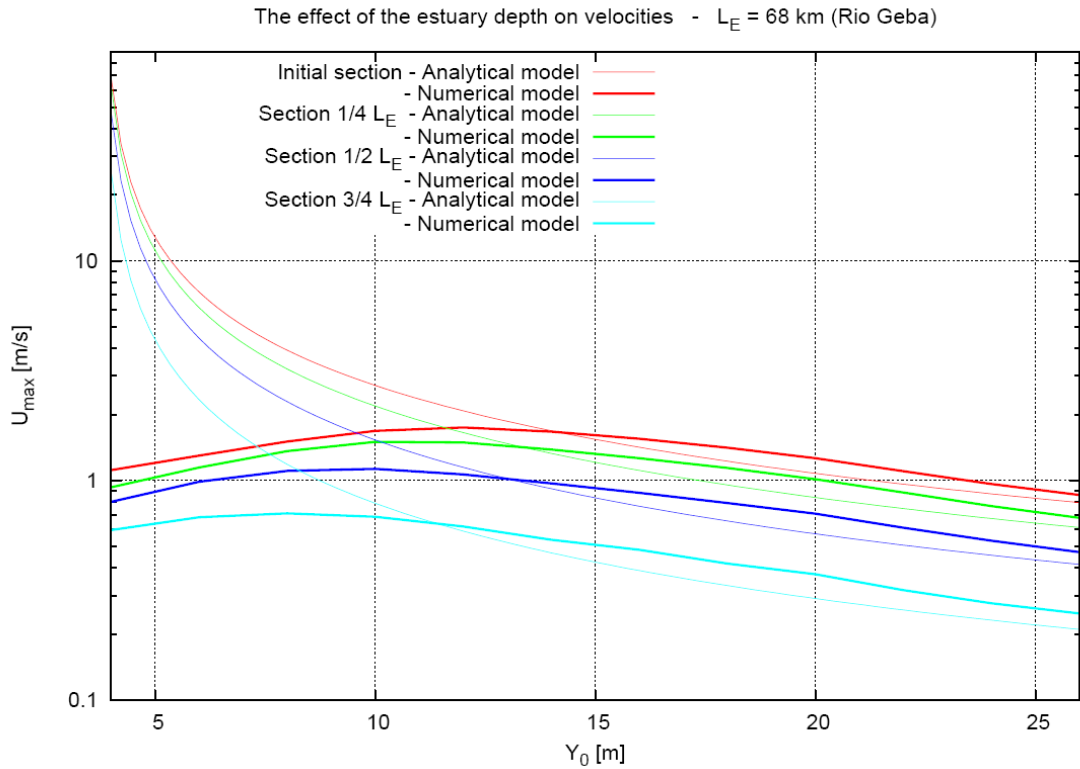


Fig. 5.5 - Effect of estuary depth on water velocity assuming an estuary length of 68 Km: comparison between the results given by the numerical model and the analytical solution in four sections.

It is important to observe that for small values of depth ( $Y_0 < 10$  m) the maximum water level and velocities obtained by the numerical model are much smaller than those given by the analytical model because in this range of depths dissipative effects are significant. On the contrary for large depths ( $Y_0 > 10$  m) the curves are closer and in both graphs the values given by the numerical model are higher than the analytical ones.

We also analyze the Rio Mansoa because on its banks the little village of Fanhe, where the O.N.L.U.S “Progetto e sviluppo76” is realizing some projects of cooperation, is located.

## 5. Tidal stream power in Guinea-Bissau

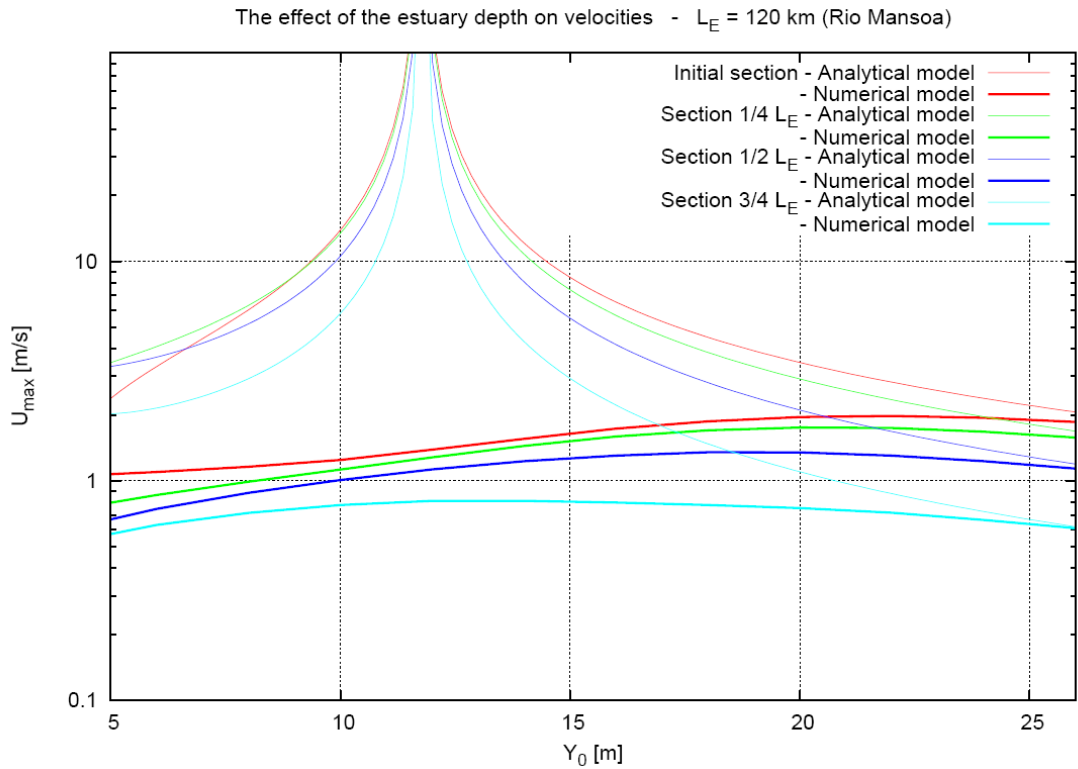


Fig. 5.6 - Effect of estuary depth on water velocity assuming an estuary length of 120 Km: comparison between the results given by the numerical model and the analytical solution in four sections.

Observing the graph above we can draw the same conclusion obtained in the case of Rio Geba about the effects of the estuary depth on the analytical and numerical maximum velocities. Moreover, the dependence of the resonant peak on the relationship between estuary length and average depth emerges: in fact, in the case of Rio Mansoa ( $L_E = 120$  km) the peak is associated with a depth of 12 m, while in the Geba estuary ( $L_E = 68$  km) it was associated with a depth smaller than 5 m.

Hence, a fully non-linear hydrodynamic model is required to capture the most relevant elements about the behaviour of Guinea-Bissau tidal estuaries, whose average depth assume values of about 10m.

## 5.5 The hydrodynamic of Rio Geba

In order to analyze the hydrodynamics of Rio Geba we consider the following configuration.

### *Longitudinal width profile*



*Fig. 5.7 - Satellite image of the Rio Geba with the five sections taken into consideration (©Google 2007).*

The information about the longitudinal width profile is extracted from satellite images. In the figure above we show some significant sections that are specially considered, because of their particular configuration or because of their location next to the villages and towns where we are investigating the possibility of producing tidal stream power.

## 5. Tidal stream power in Guinea-Bissau

The resulting width profile is shown in the following graph.

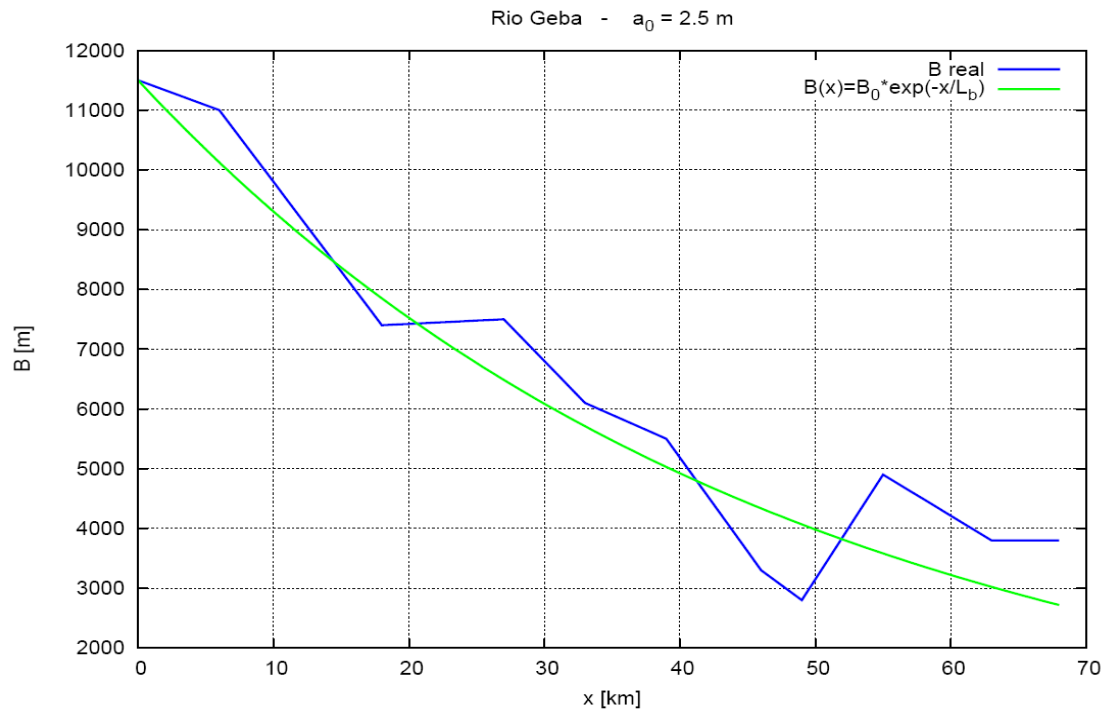


Fig. 5.8 - Comparison between the estuary width profile evaluated through satellite image and the exponentially one, calculated assuming  $L_b = 47150$  m.

*Sediment size distribution*

To evaluate the effect of roughness on water velocities it is important to know the grain size distribution of sediments lying on the estuary bottom.

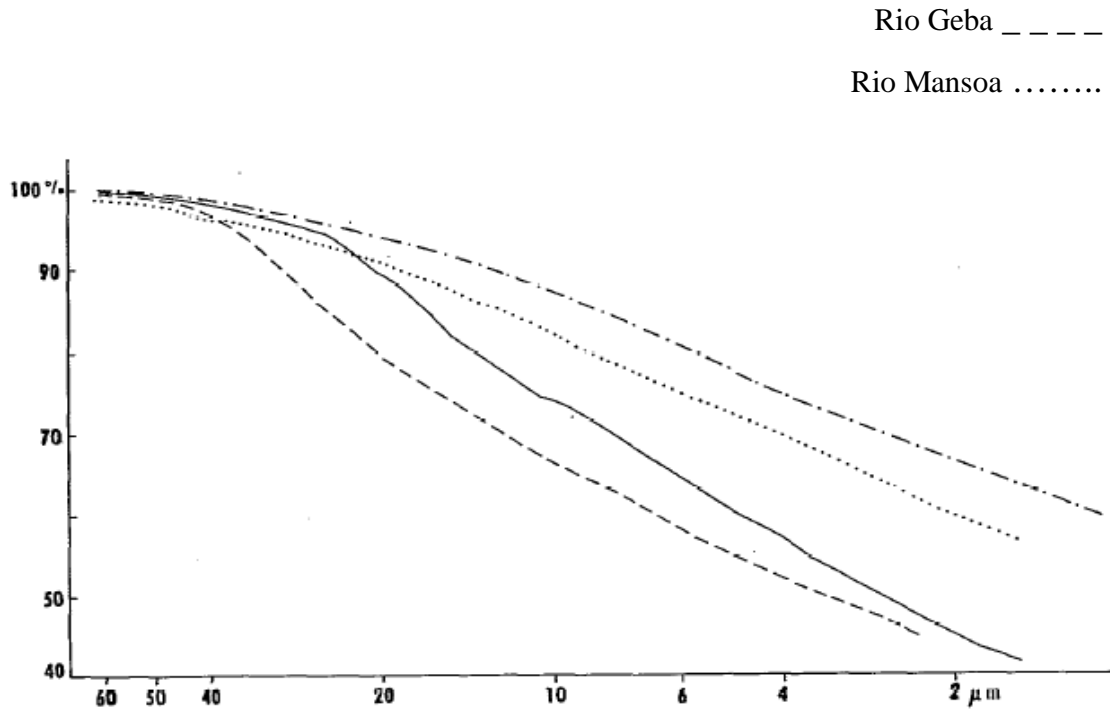


Fig. 5.9 - Sediment size distribution of Rio Geba and Rio Mansoa (S. Diop).

Assuming for Rio Geba  $d_{50} = 0.003$  mm we can define the conductance coefficient  $C$  from the Van Rijn formula (1984).

## 5. Tidal stream power in Guinea-Bissau

### *Longitudinal bottom profile*

To calculate more realistic values of velocities we consider a bottom profile obtained by the analysis of nautical chart; as we show in the figure below, we calculate the average depth in many section along the estuary.

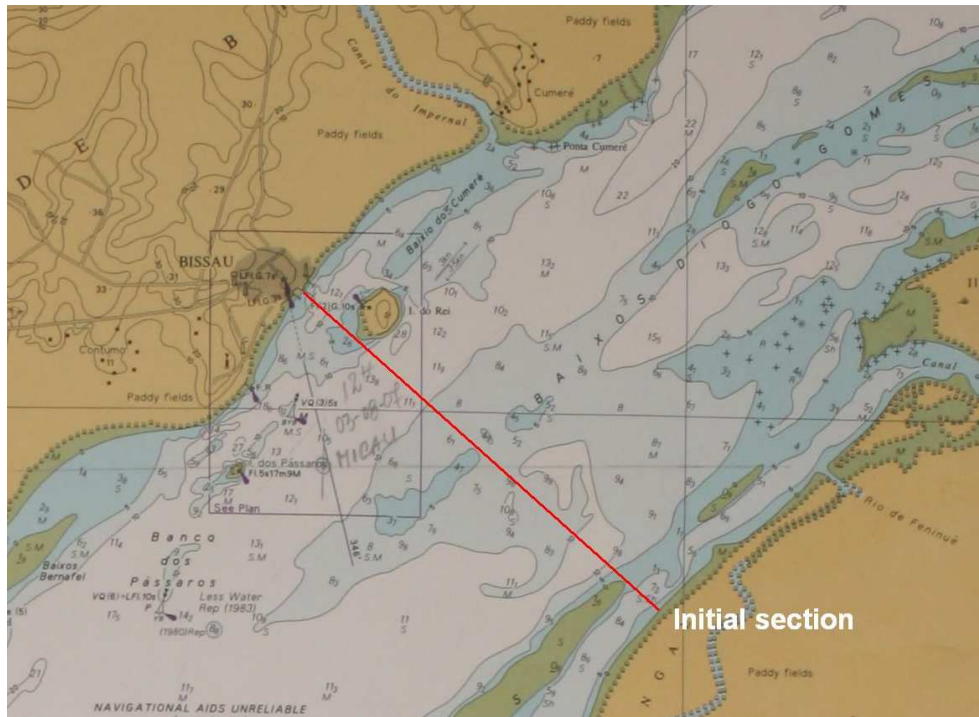


Fig. 5.10 - Nautical chart of Rio Geba. The red line is the section considered for the evaluation of the equivalent section.

In particular in the initial section we estimate the average depth considering the equivalent section.

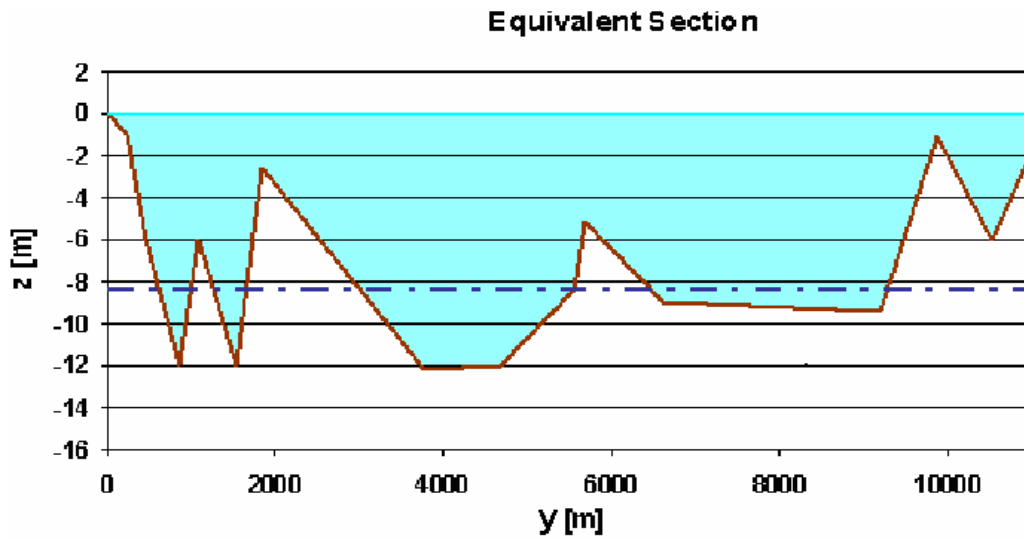


Fig. 5.11 - Evaluation of the equivalent section. The brown line is depth referred to the lowest water level (as given by nautical chart) and the blue line is the depth of the equivalent section.

Using all the previous data, we performed several simulations using the 1-D numerical model described in § 5.3.3. With a maximum amplitude of 2.5 m we obtain the following results.

## 5. Tidal stream power in Guinea-Bissau

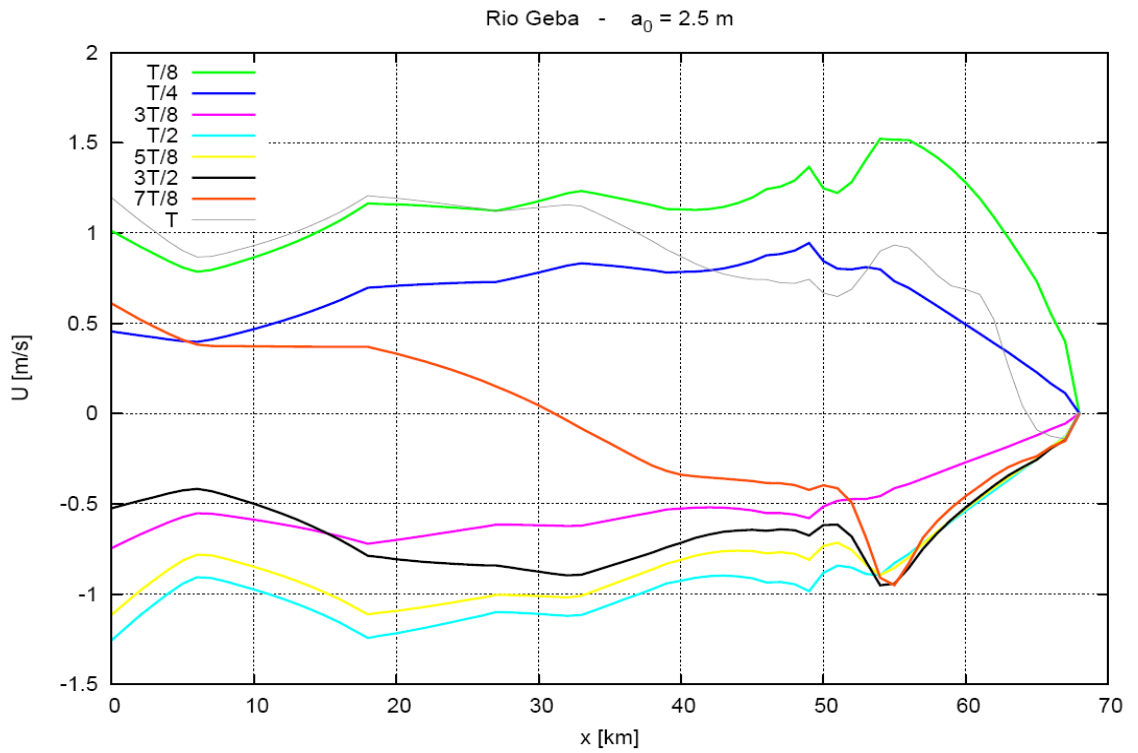


Fig. 5.12 - Trend of velocities along the estuary.

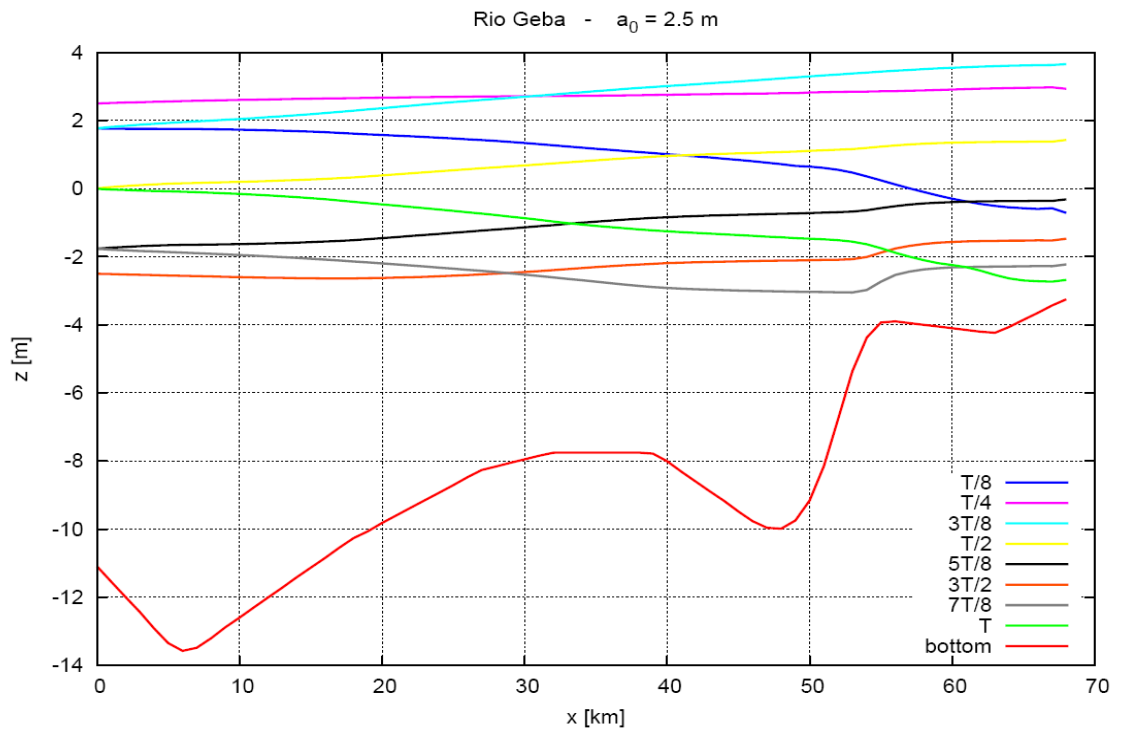


Fig. 5.13 - Trend of water levels along the estuary considering the effective bottom profile.

## 5. Tidal stream power in Guinea-Bissau

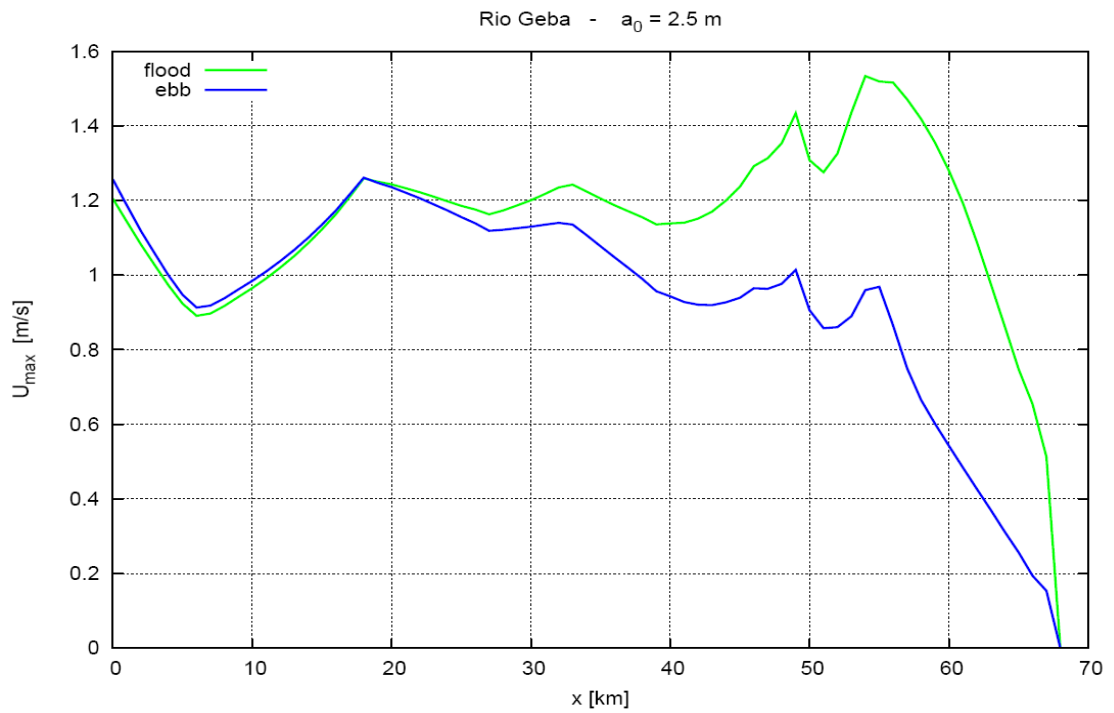


Fig. 5.14 - Trend of maximum velocity along the estuary in flood and ebb phase.

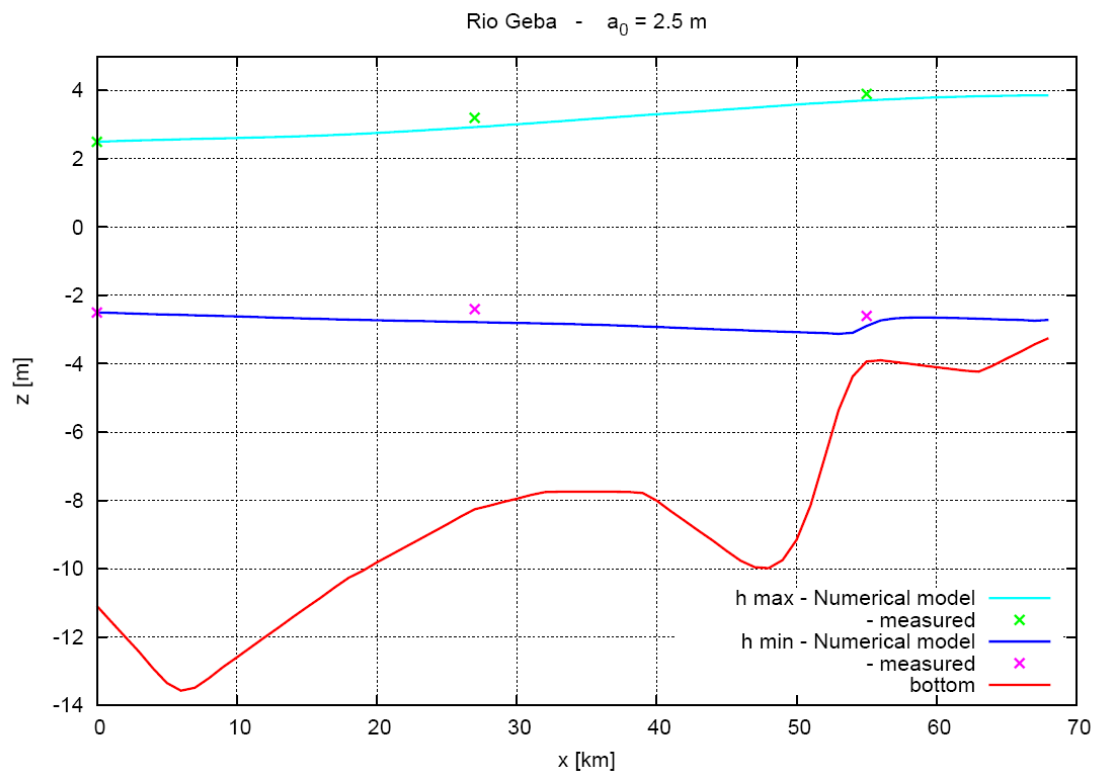


Fig. 5.15 - Trend of water level and bottom profile along the estuary in comparison with measured values. We remark a good agreement.

5. Tidal stream power in Guinea-Bissau

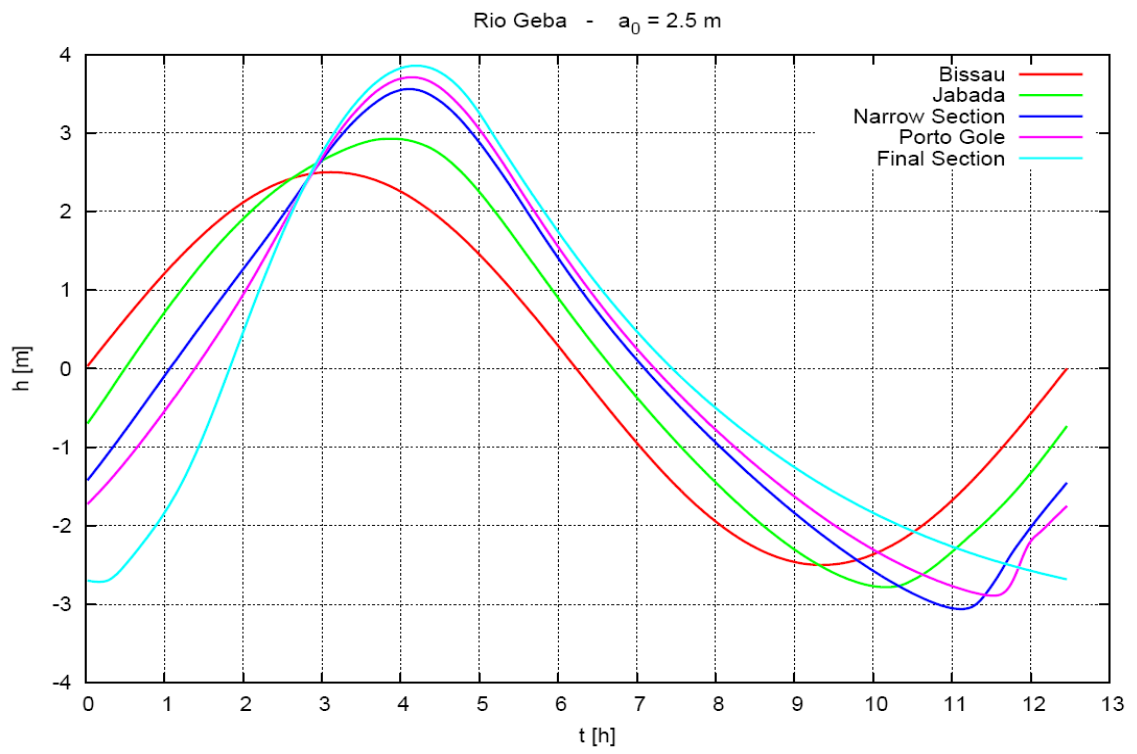


Fig. 5.16 - Trend of water level over a tide cycle in 5 significant sections.

## 5. Tidal stream power in Guinea-Bissau

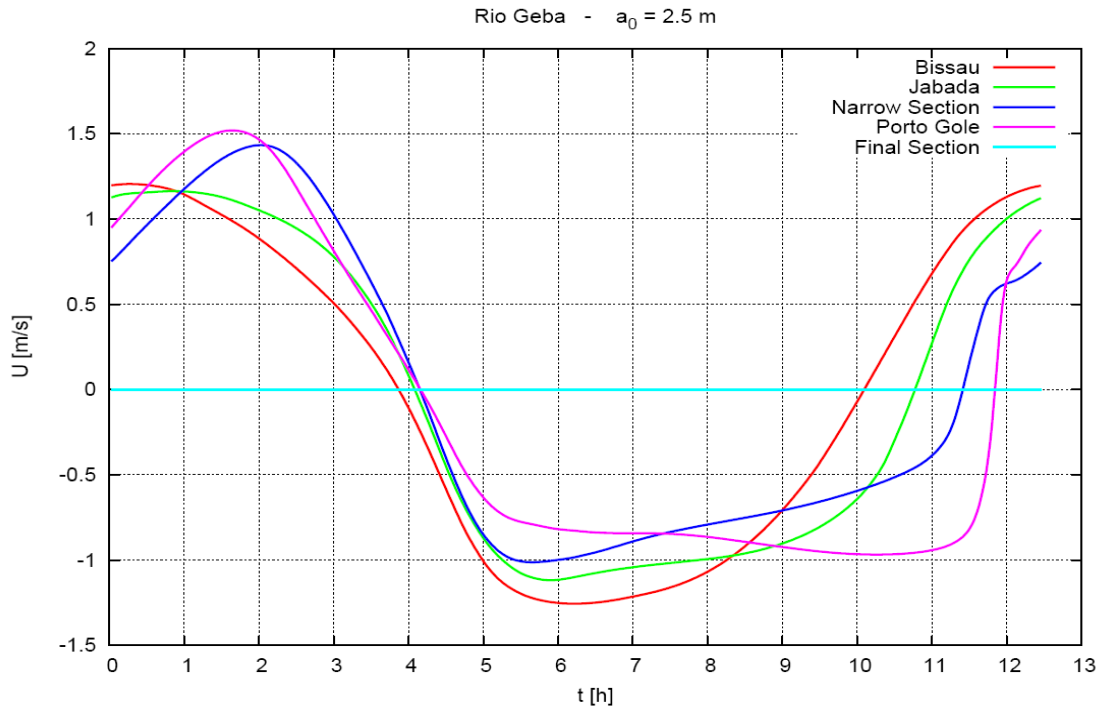


Fig. 5.17- Trend of velocity over a tide cycle in 5 significant sections. The flood and ebb maximum velocities given by the 1-D model in Bissau are:  $U_{flood} = 1.2$  m/s,  $U_{ebb} = -1.25$  m/s; those values are only slightly lower than measured velocities in Bissau:  $U_{flood} = 1.25$  m/s,  $U_{ebb} = -1.30$  m/s (S. Diop).

We also performed simulations using a minimum amplitude of 1.25 m; a comparison between the hydrodynamic behaviour in the two extreme cases is shown in the following graphs.

## 5. Tidal stream power in Guinea-Bissau

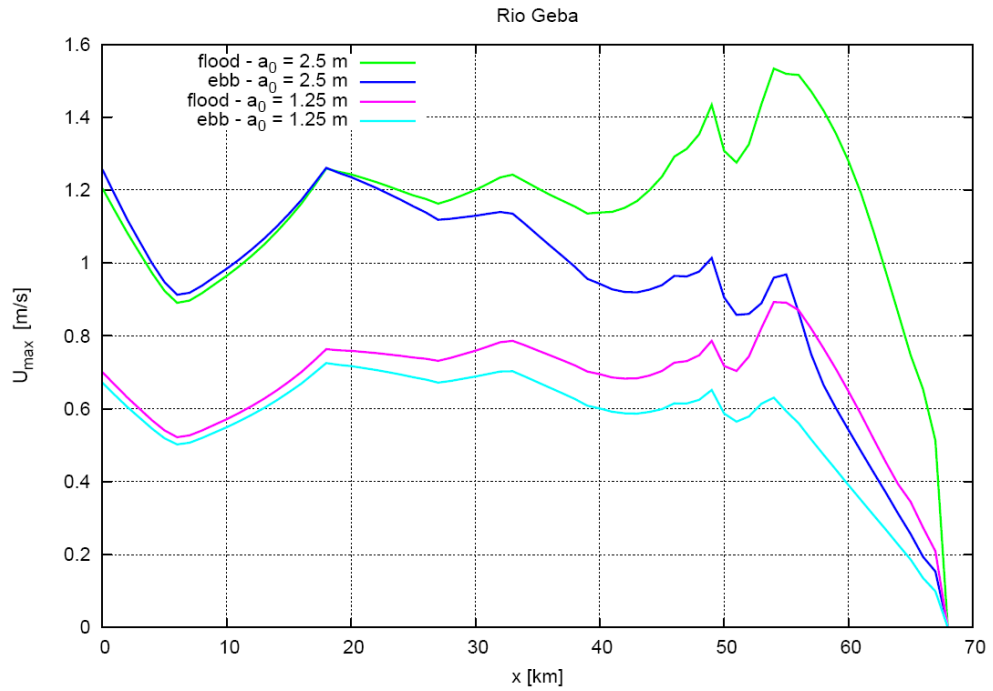


Fig. 5.18 - Comparison between trend of maximum velocity along the estuary in flood and ebb phase considering maximum and minimum amplitude registered in Bissau.

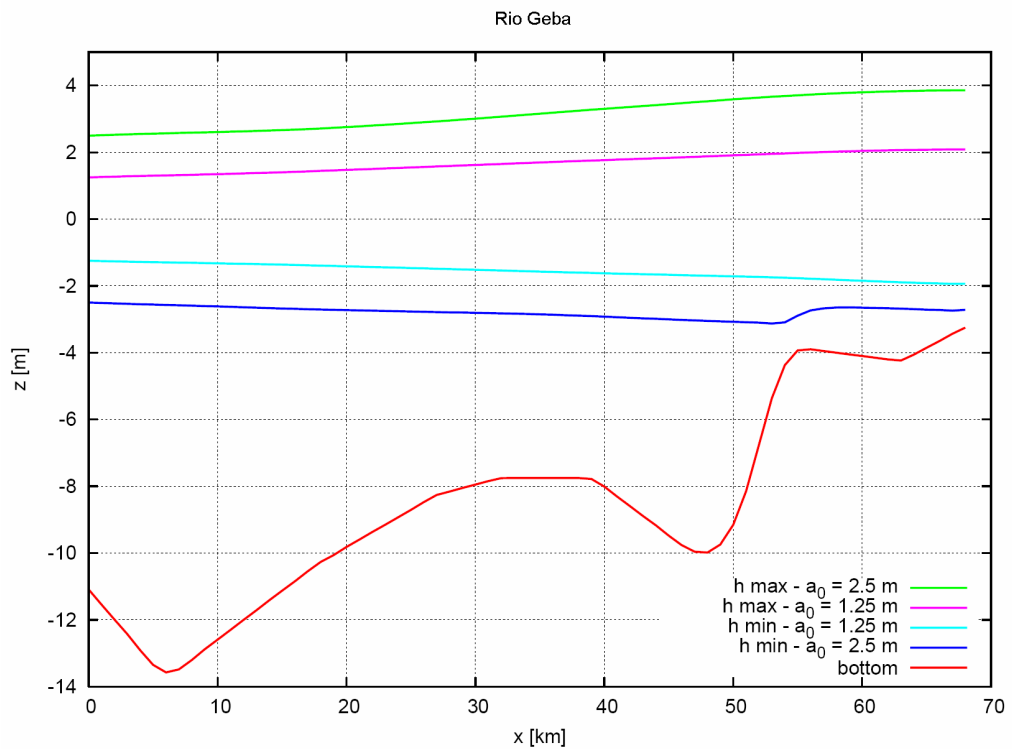


Fig. 5.19 - Comparison between trend of maximum and minimum water level along the estuary considering maximum and minimum amplitude registered in Bissau.

## 5. Tidal stream power in Guinea-Bissau

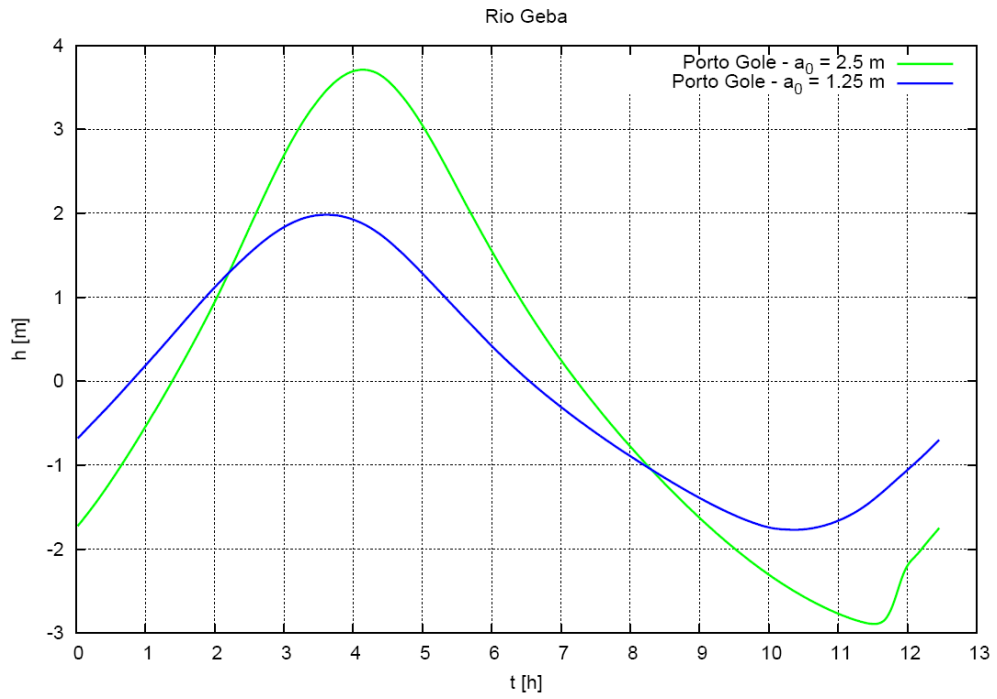


Fig. 5.20 - Trend of water level over a tide cycle in the section of Porto Gole considering maximum and minimum amplitude registered in Bissau.

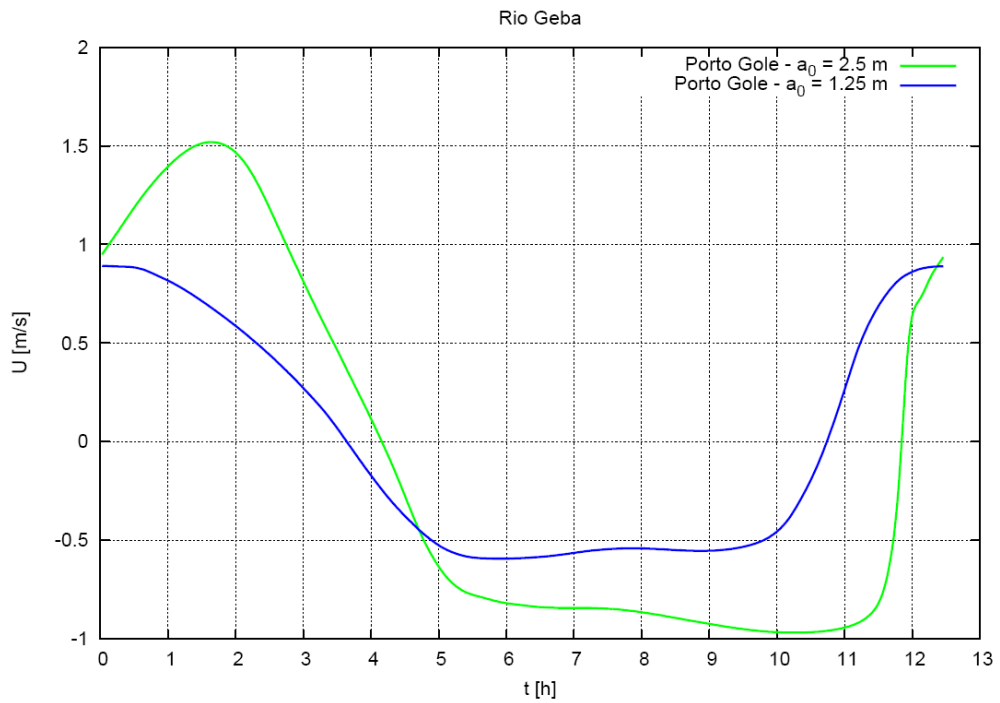


Fig. 5.21 - Trend of velocity over a tide cycle in the section of Porto Gole considering maximum and minimum amplitude registered in Bissau.

## 5.6 The hydrodynamics of Rio Mansoa

We next analyze the hydrodynamics of Rio Mansoa considering the following data.

### *Longitudinal width profile*



*Fig. 5.22 - Satellite image of the Rio Mansoa with the five sections taken into consideration (©Google2007).*

The information about the longitudinal width profile is extracted from satellite images. In the figure above we show some significant sections that are specially considered, because of their particular configuration or because of their location next to the villages and towns where we are investigating the possibility of producing tidal stream power.

The resulting width is shown in the following graph.

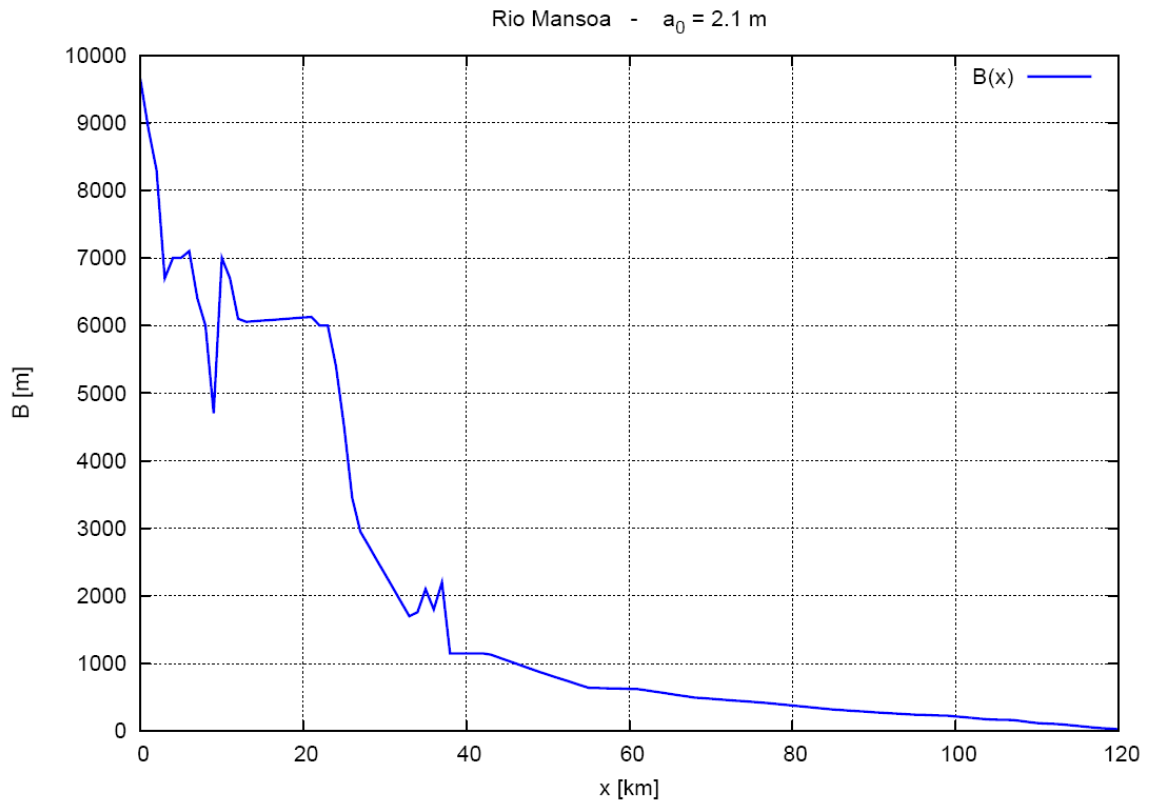


Fig. 5.23 - Estuary width profile evaluated through the satellite image.

*Sediment size distribution*

Taking into consideration the sediment size distribution shown in sect. 5.5 we assume for Rio Mansoa  $d_{50} = 0.001$  mm.

*Longitudinal bottom profile*

In this case we consider a linear bottom profile because of the lack of reliable nautical charts of Rio Mansoa.

Only in the initial cross section we are able to estimate the average depth.

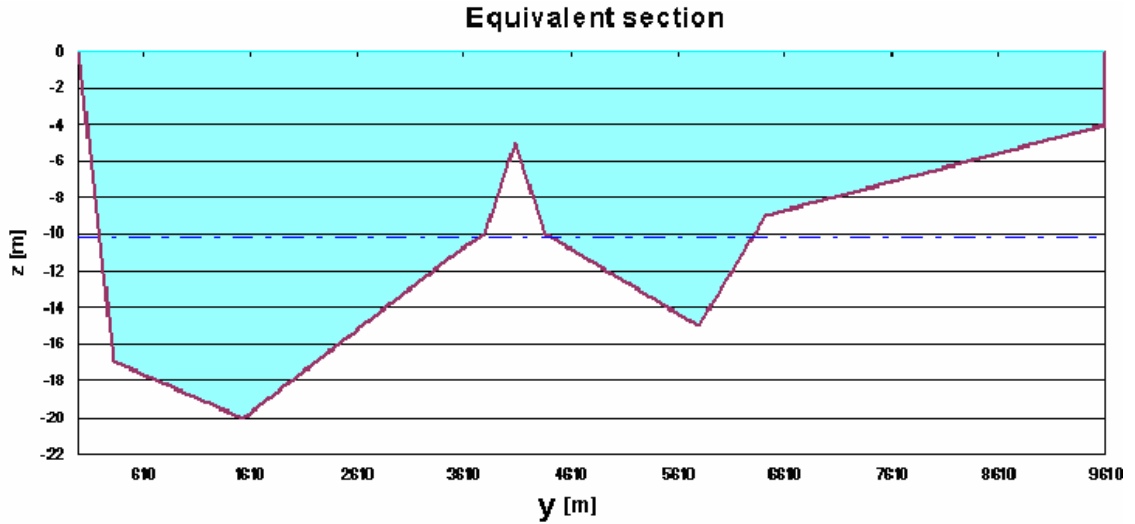


Fig. 5.24 - Evaluation of the equivalent section. The red line is depth referred to the lowest water level (as given by nautical chart) and the blue line is the depth of the equivalent section.

Using all the previous data, we have performed several simulations using the 1-D numerical model described in sect. 5.3.3. With a maximum amplitude of 2.1 m we obtain the following results.

5. Tidal stream power in Guinea-Bissau

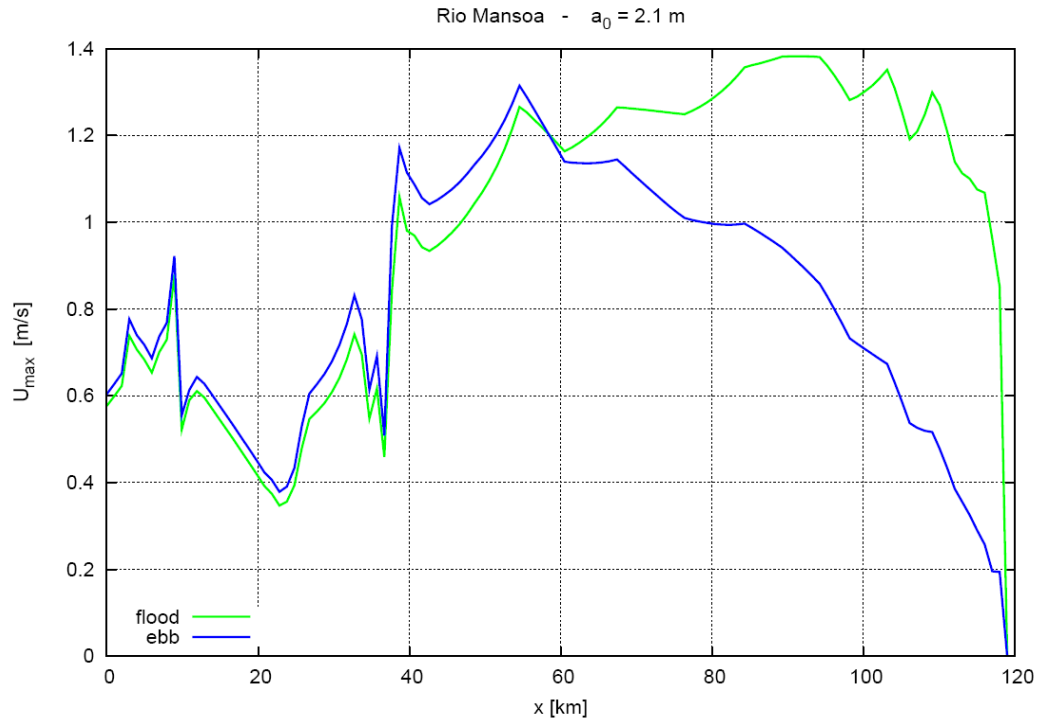


Fig. 5.25 - Trend of maximum velocity along the estuary in flood and ebb phase. We remark values considerably less than along RioGeba.

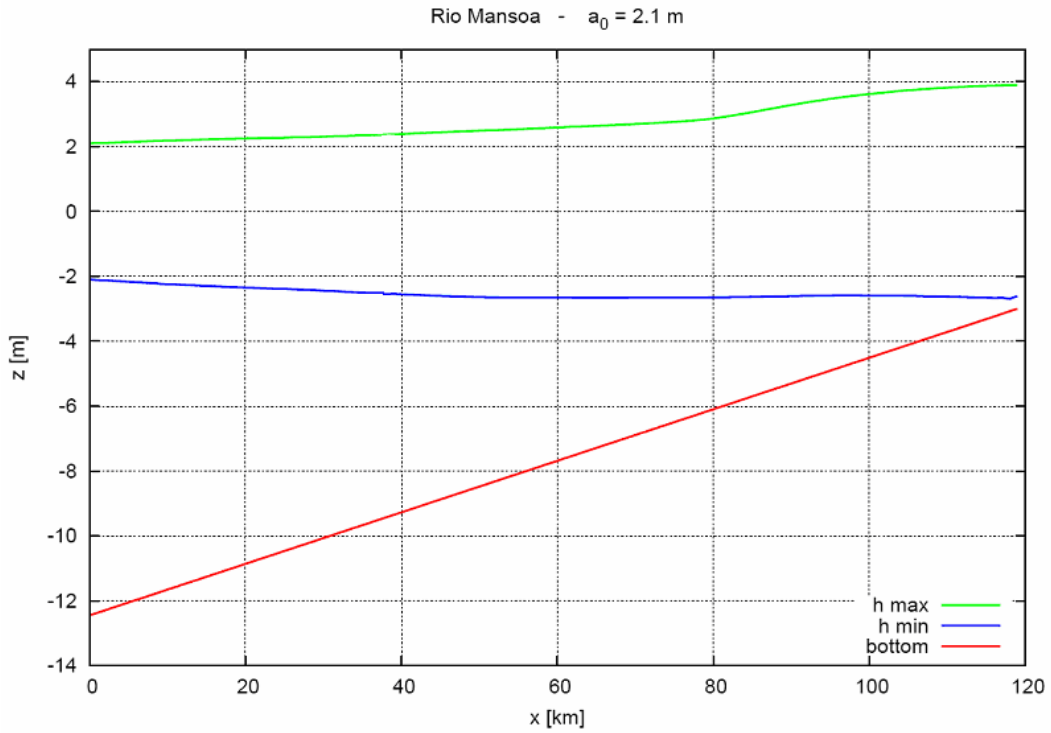


Fig. 5.26 - Trend of water level and bottom profile along the estuary.

5. Tidal stream power in Guinea-Bissau

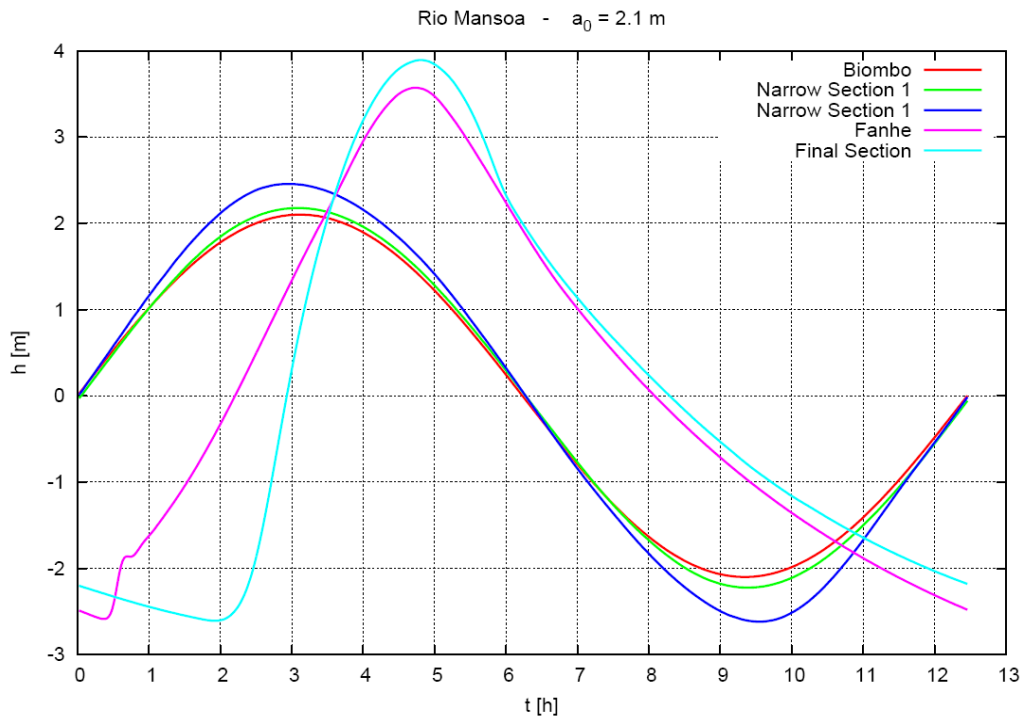


Fig. 5.27 - Trend of water level over a tide cycle in 5 significant sections.

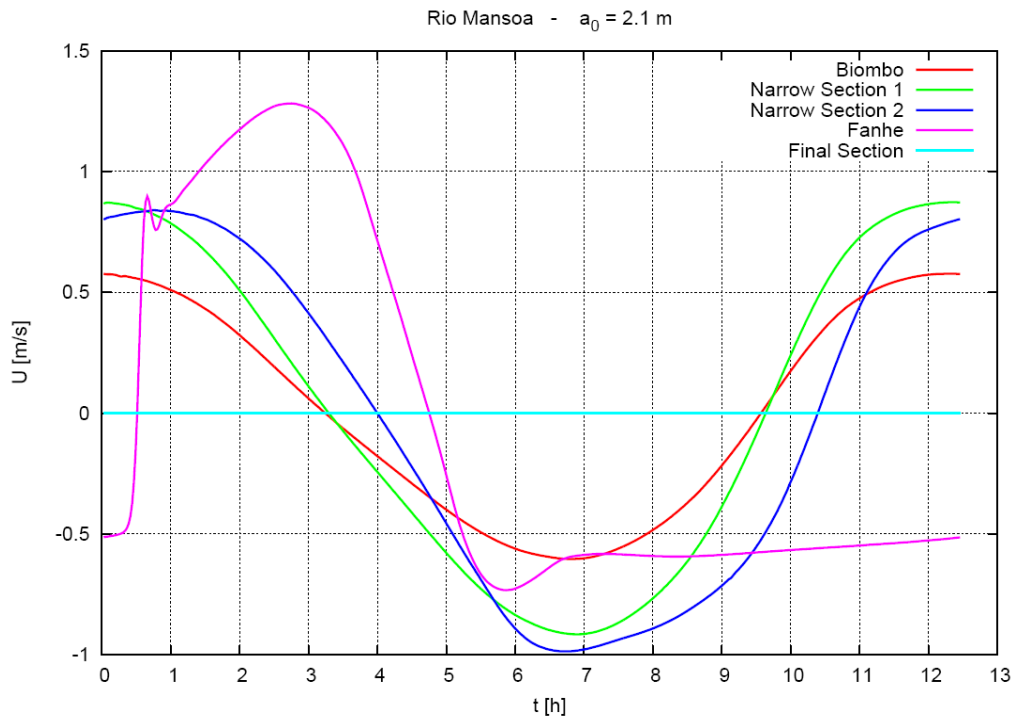


Fig. 5.28 - Trend of velocity over a tide cycle in 5 significant sections.

## 5. Tidal stream power in Guinea-Bissau

We also performed simulations with minimum amplitude of 0.8 m; a comparison between the hydrodynamic behaviour in the two extreme cases is shown in the following graphs.

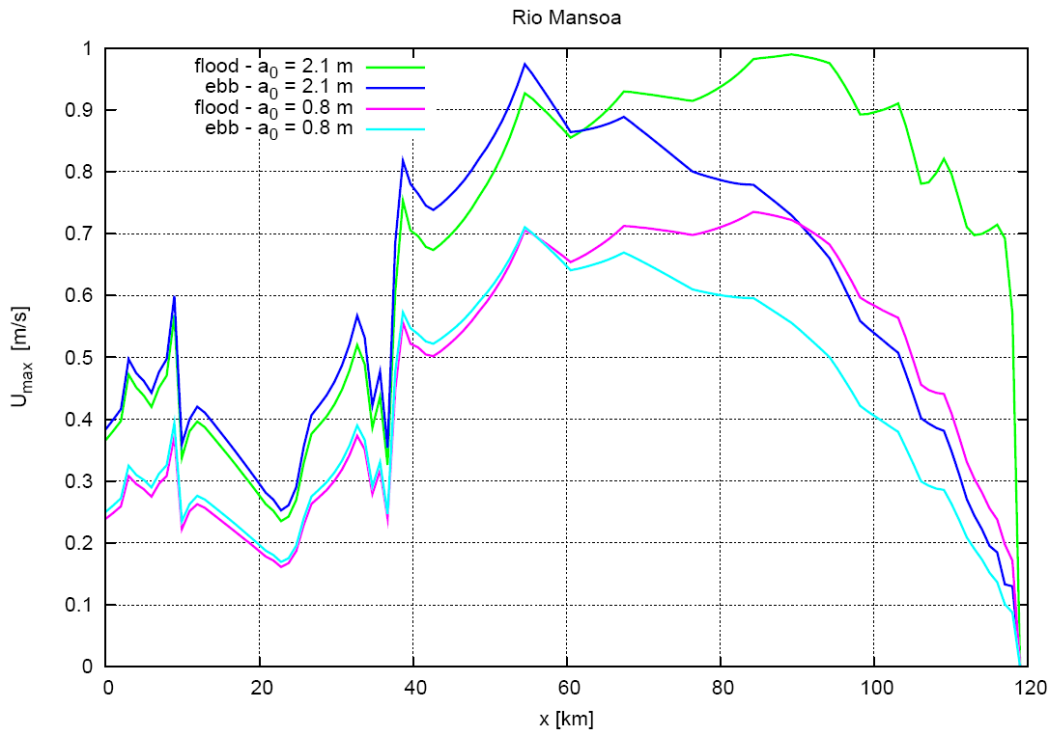


Fig. 5.29 - Comparison between trend of maximum velocity along the estuary in flood and ebb phase considering maximum and minimum amplitude registered at the mouth of Rio Mansoa.

5. Tidal stream power in Guinea-Bissau

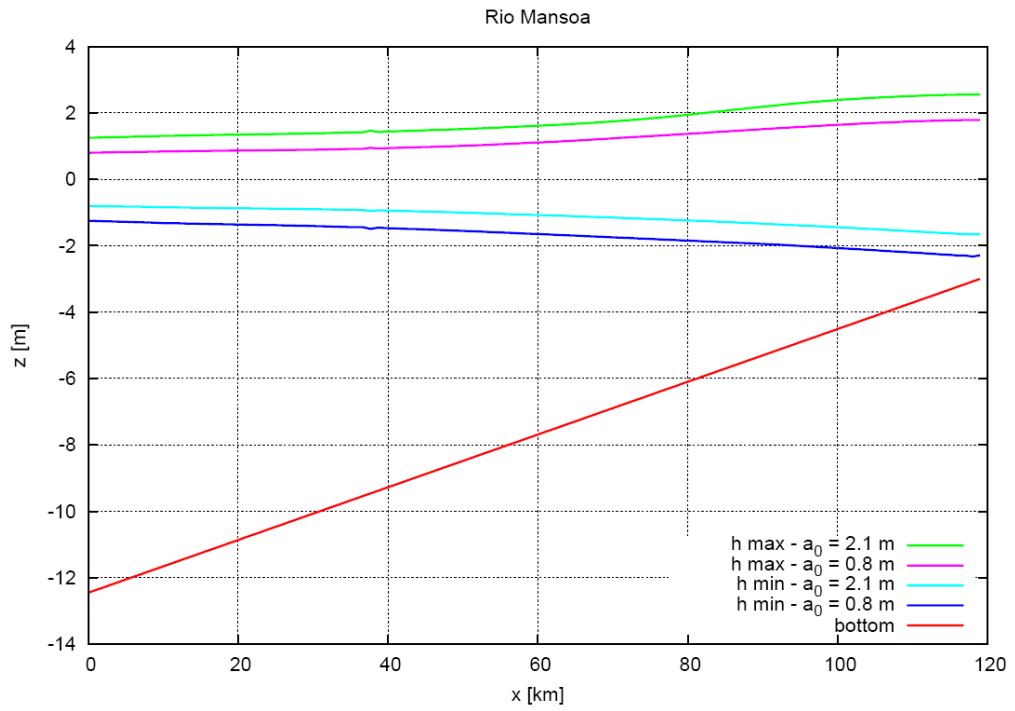


Fig. 5.30 - Comparison between trend of maximum and minimum water level along the estuary considering maximum and minimum amplitude registered at the mouth of Rio Mansoa.

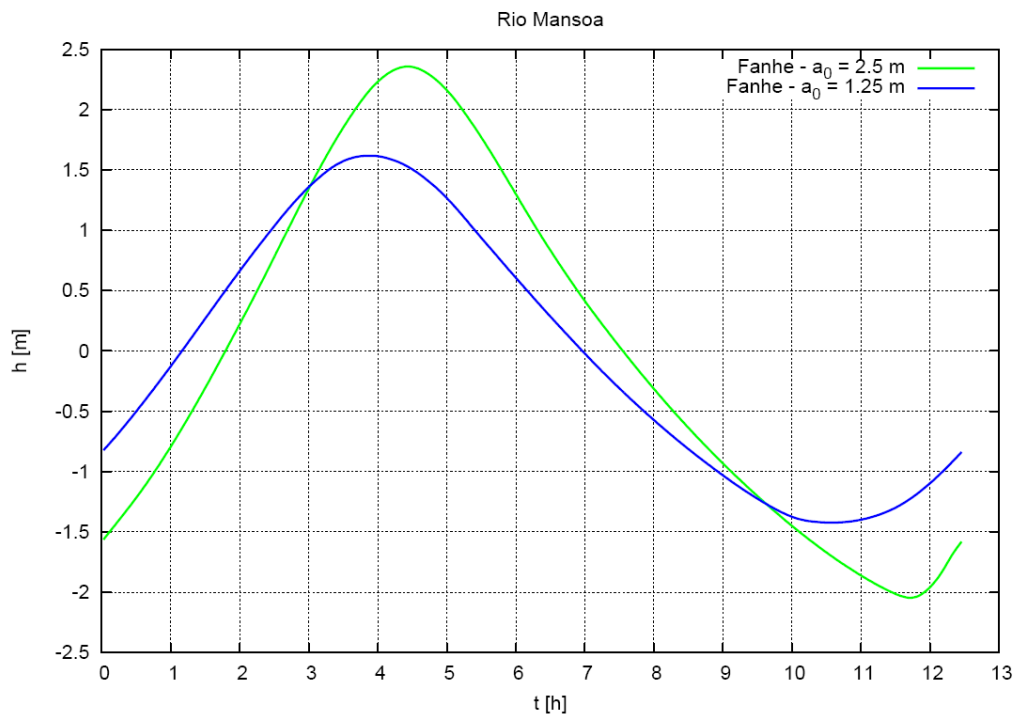


Fig. 5.31 - Trend of water level over a tide cycle in the section of Fanhe considering maximum and minimum amplitude registered at the mouth of Rio Mansoa.

## 5. Tidal stream power in Guinea-Bissau

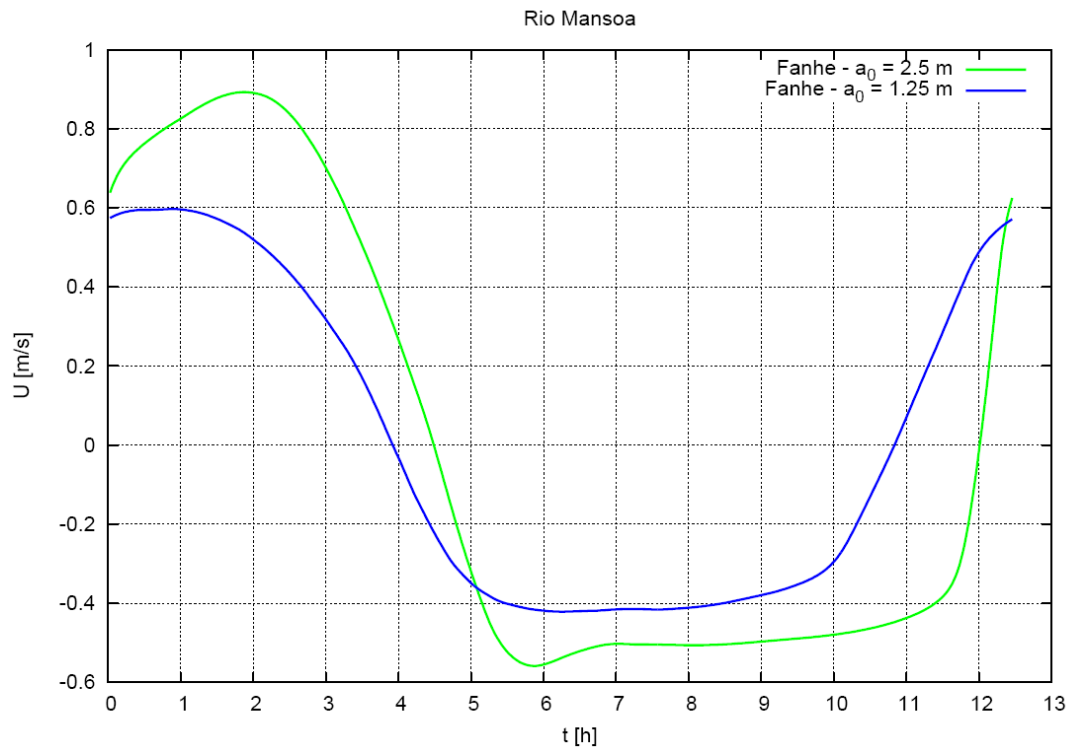


Fig. 5.32 - Trend of velocity over a tide cycle in the section of Fanhe considering maximum and minimum amplitude registered at the mouth of Rio Mansoa.

### 5.7 Power production in the tidal estuaries of Guinea-Bissau

In this paragraph we study the energy output potentially available in different cross sections obtained by the analysis of water velocities previously shown.

As a first step, we calculate the theoretical power for unit area of the turbine:

$$P_{TEOR}(t) = \frac{1}{2} \rho U(t)^3$$

where  $\rho$  is water density and  $U$  is water velocity.

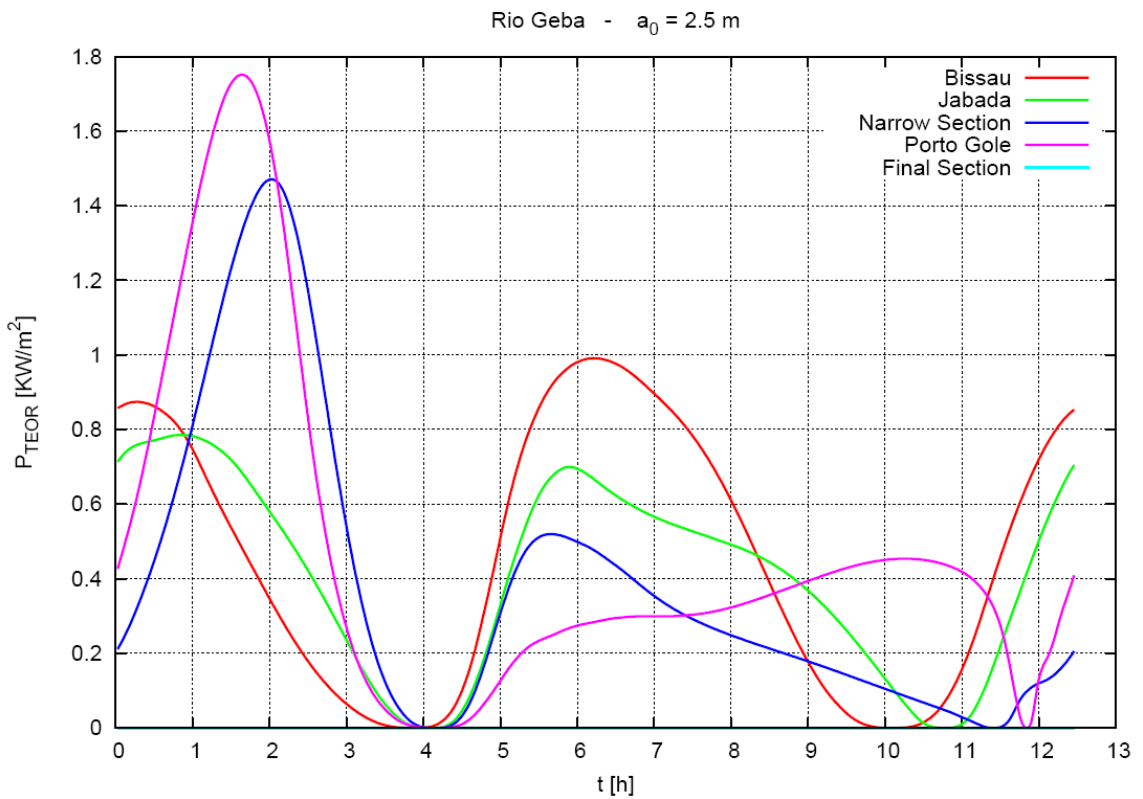


Fig. 5.33 - Theoretical power over a tide cycle for unit of area of the turbine in 5 significant sections of Rio Geba (considering the maximum amplitude registered in Bissau).

## 5. Tidal stream power in Guinea-Bissau

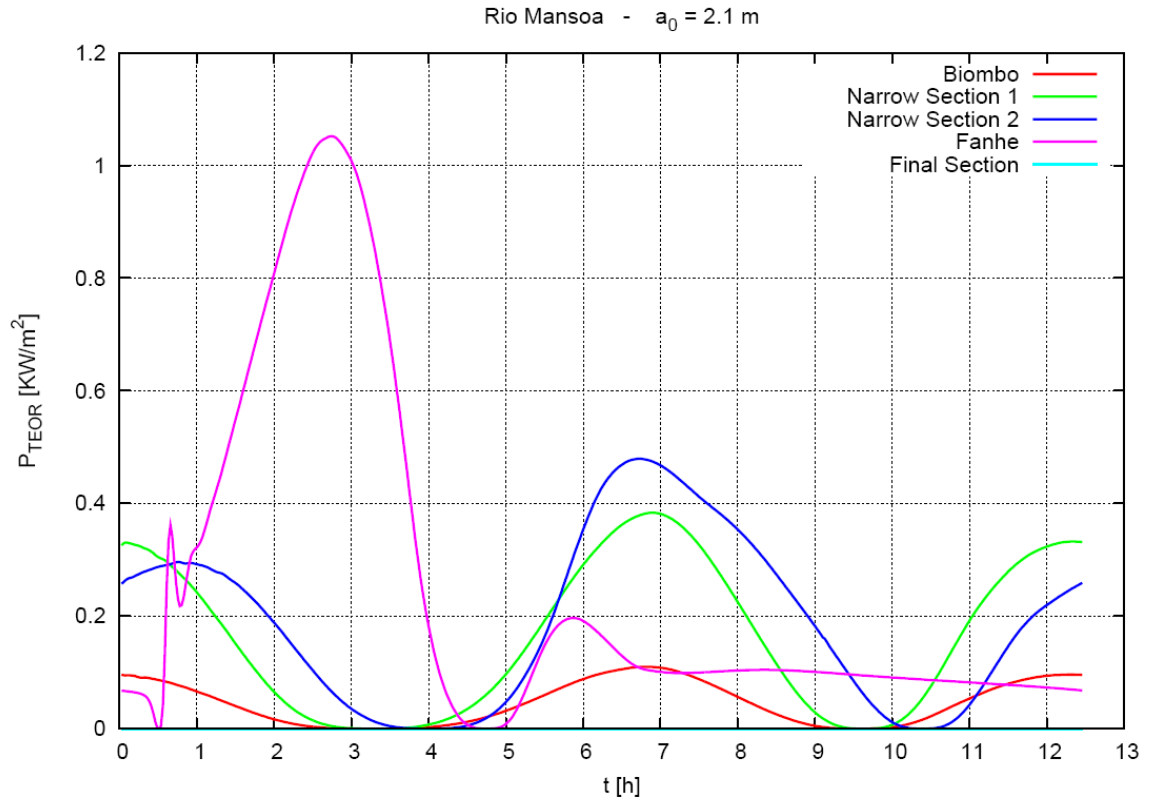


Fig. 5.34 - Theoretical power over a tide cycle for unit of area of the turbine in 5 significant sections of Rio Mansoa (considering the maximum amplitude of 2.5 m registered at the mouth of Rio Mansoa).

Note that the theoretical power in Rio Mansoa is lower than the one in Rio Geba, so from now on we consider only the 2 cross sections in which power is significant, namely Bissau and Porto Gole.

Among the many type of free flow turbines described in sect. 2.4, we refer now to a Darrieus prototype, because it is the only one that can work in the present conditions of velocity and depth.

We can now estimate the effective power output given by the installation of a Darrieus device:

$$P_{EFF}(t) = \eta \frac{1}{2} \rho A U(t)^3$$

Where:

- $A = 7.5 \text{ m}^2$  for a turbine of 3.0 m in diameter and 2.5 m in height;
- $\eta = 0.2$  is the total system efficiency.

### 5. Tidal stream power in Guinea-Bissau

It is then possible to integrate the power in time to find the energy output [KWh] during a tidal cycle of 12h.

in the graph below, we show the energy output obtained using only one turbine in the case of maximum amplitude in the two more significant cross sections along the Rio Geba.

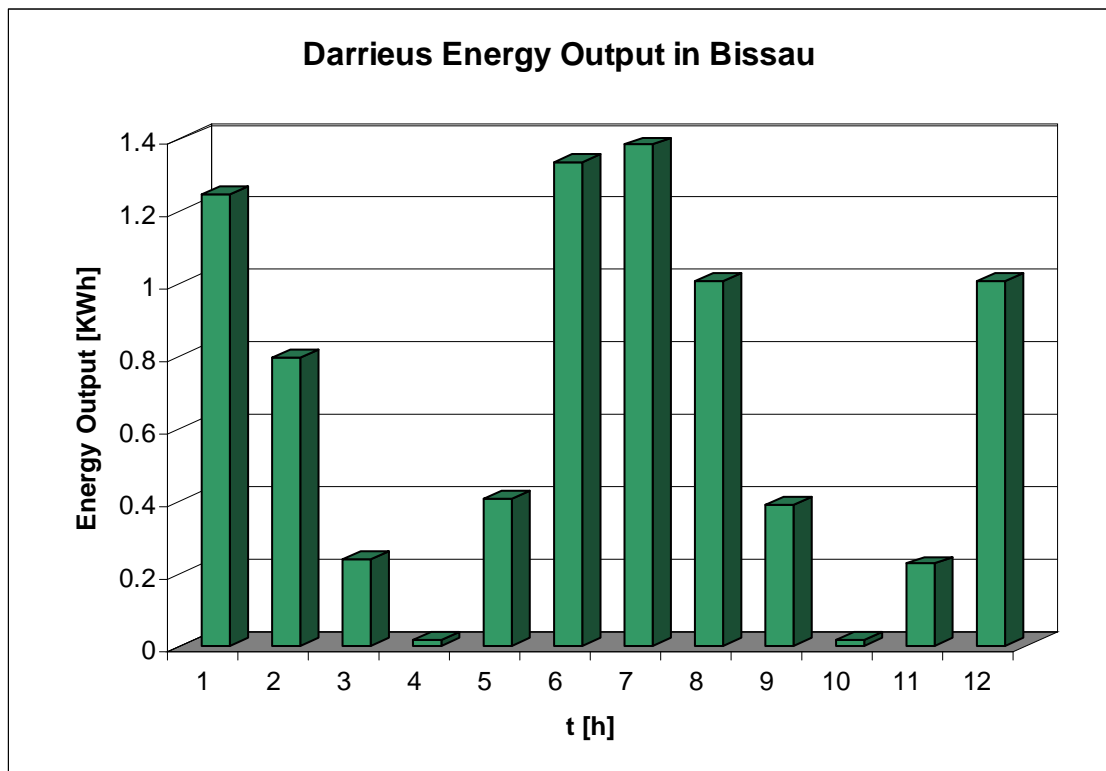


Fig. 5.35 - Energy output over a tide cycle in Bissau for a Darrieus turbine 3 m in diameter (considering the maximum amplitude of 2.5 m).

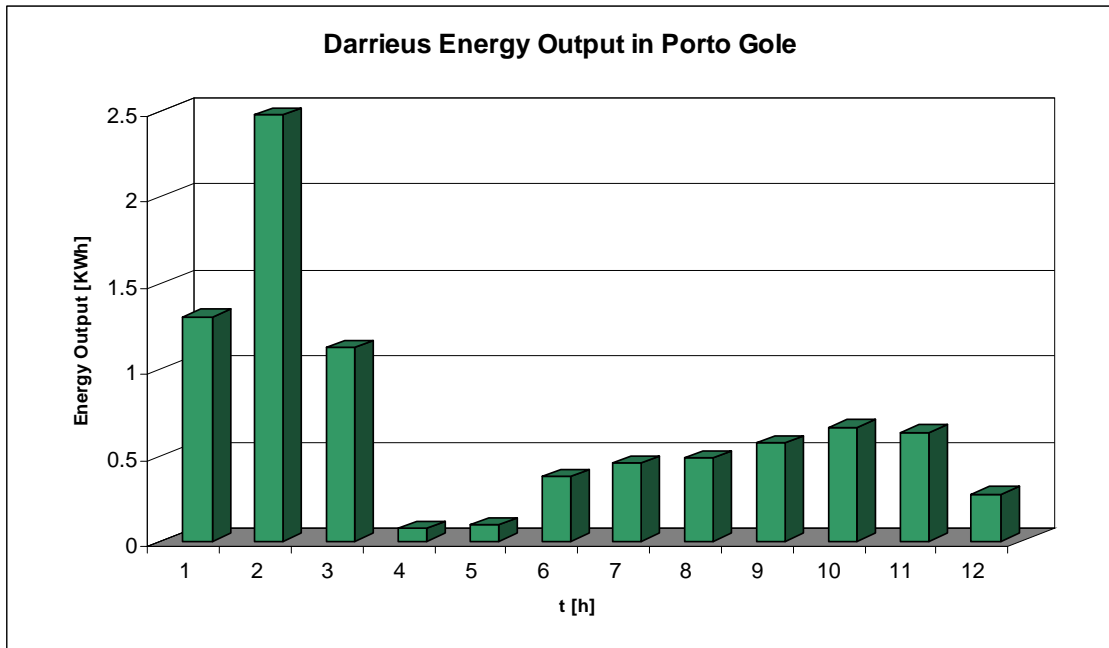


Fig. 5.36 - Energy output over a tide cycle in Porto Gole for a Darrieus turbine 3 m in diameter (considering the maximum amplitude of 2.5 m registered in Bissau).

|            | Average Energy Output<br>[KWh] | Energy output<br>In a Cycle [KWh] |
|------------|--------------------------------|-----------------------------------|
| Bissau     | 0.67                           | 8.1                               |
| Porto Gole | 0.71                           | 8.5                               |

Finally, let us note that:

- during a tidal cycle there are some short periods corresponding to flow reversal when the energy output is negligible: it will be important in the future to analyze some efficient method of energy storage in order to account for the problem of energy variability;
- in this computation we do not take into consideration the cut-in speed of the turbine, even if Darrieus turbine works for very low speed;
- these values are obtained for a fixed amplitude (the maximum), so this power output cannot be considered as constant throughout the year;
- the values of velocities adopted to estimate the energy output arise from 1-D numerical simulations and are then averaged over the cross section: hence,

### 5. Tidal stream power in Guinea-Bissau

velocities could be locally greater because of the morphological configuration of the estuary, for example at a bend;

- the power output is small, but it's durable, predictable and without any environmental and visual impact;
- to increase the power output it is possible to increase the number of turbines, even creating a wall (see fig. 2.34). The picture shows the section of Rio Geba close to Bissau (11 km in width and 8 m in average depth); in this case the maximum kinetic power of the flow crossing the entire section reaches a value of 50 MW.



*Fig. 5.37 - View of Rio Geba in correspondence of Bissau.*

- to increase the power output it is also possible to increase the frontal area of the turbine, by installing a bigger one.

### 5. Tidal stream power in Guinea-Bissau

In fact, considering a turbine of 6.0 m in diameter and 2.5 m in height, the energy output increases sharply, as shown in the figure below.

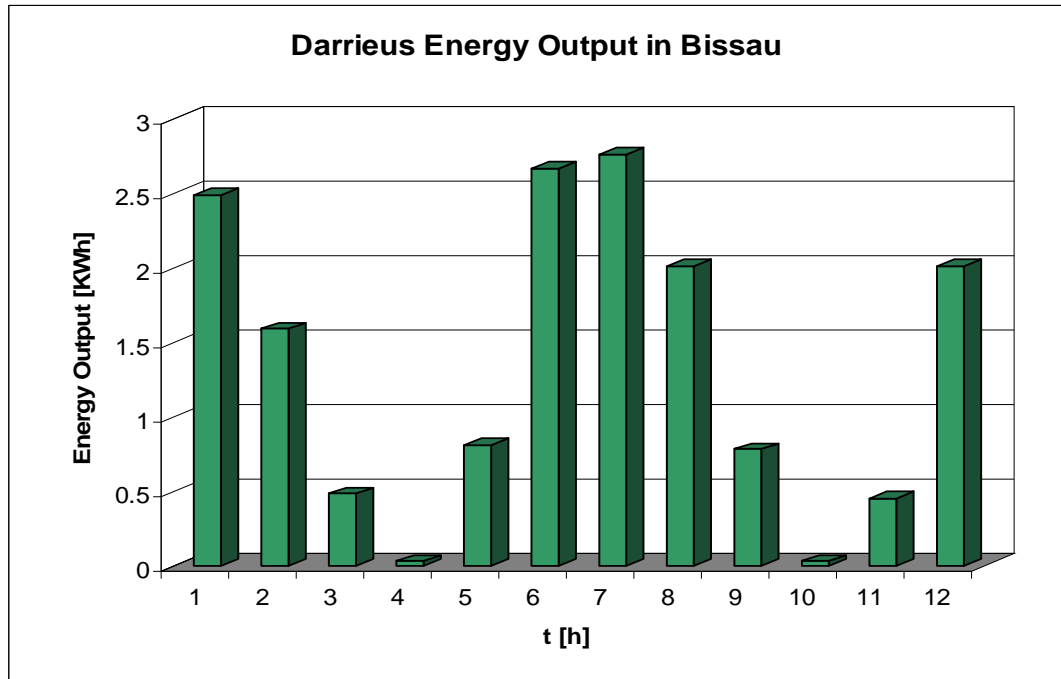


Fig. 5.38 - Energy output over a tide cycle in Bissau for a Darrieus turbine 6 m in diameter (considering the maximum amplitude of 2.5 m registered in Bissau).

|        | Average Energy Output<br>[KWh] | Cycle Energy output<br>[KWh] |
|--------|--------------------------------|------------------------------|
| Bissau | 1.35                           | 16.2                         |

### 5.8 Tidal currents in the straits between islands

Higher velocities can be found in narrow straits between islands, such as the one near the village of Bubaque, in the Arquipelago dos Bijagos, along the coast of Guinea-Bissau.



*Fig. 5.39 - Satellite image of the narrow body between islands where the village of Bubaque is located (©Google 2007).*

## 5. Tidal stream power in Guinea-Bissau

In order to investigate the possibility of producing electricity to supply the village of Bubaque, the O.N.L.U.S. Progetto Sviluppo 76 provided us with measured velocities taken in a preliminary field measurement campaign corresponding to a local maximum amplitude of 2 m.

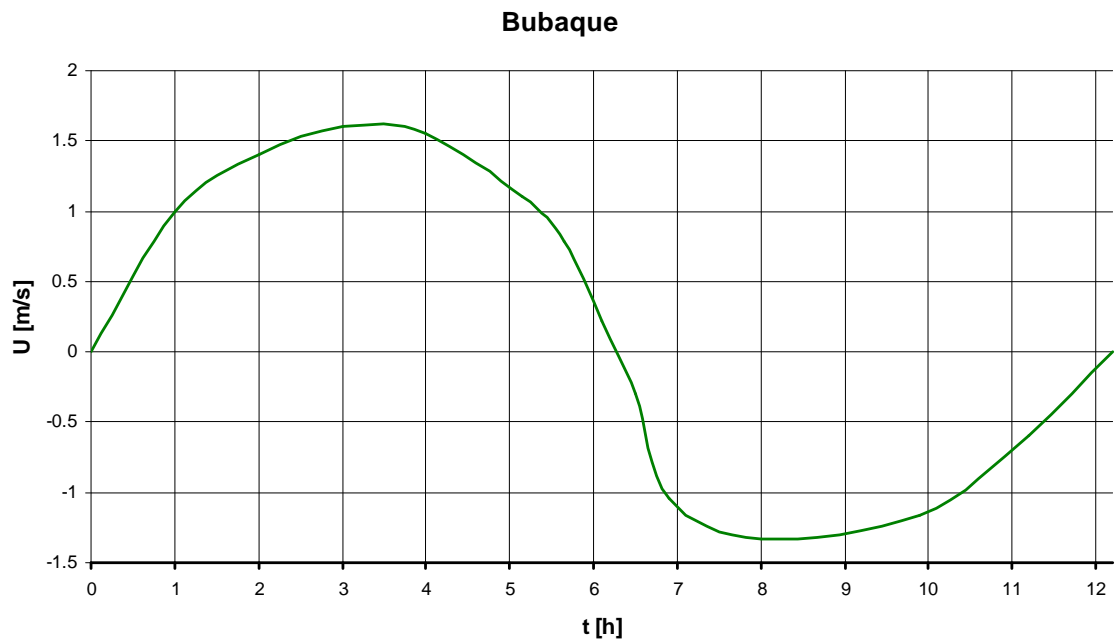


Fig. 5.40 - Trend of measured velocity over a tide cycle in Bubaque.

### 5.9 Power production in Bubaque

Employing the previous relationship between water velocity and theoretical power for unit of area of the turbine we obtain the following plot.

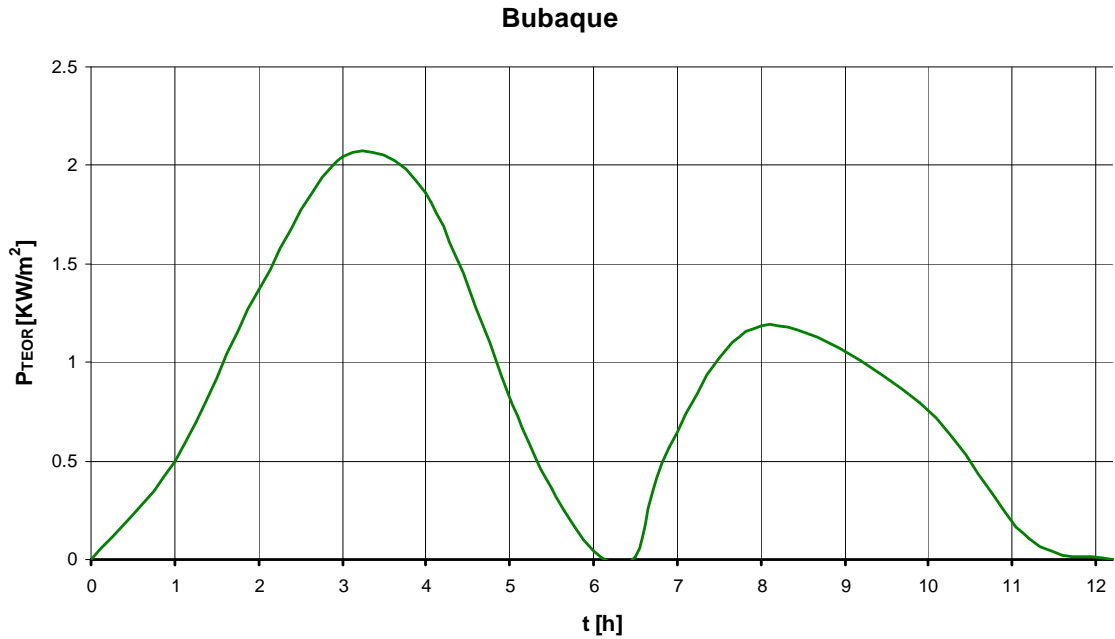


Fig. 5.41 - Theoretical power over a tide cycle for unit of area of the turbine in Bubaque.

As in the case of tidal estuaries, we analyze the installation of a Darrieus turbine 3 m in diameter and 2.5 m in height.

Such turbine sizes are justified by the opportunity to use a jetty located in the small port of Bubaque as supporting structure, thus reducing the installation costs.

## 5. Tidal stream power in Guinea-Bissau



Fig. 5.42 - View of the jetty situated in the small port of Bubaque.

The resulting energy output over a tidal cycle is shown in the graph below.

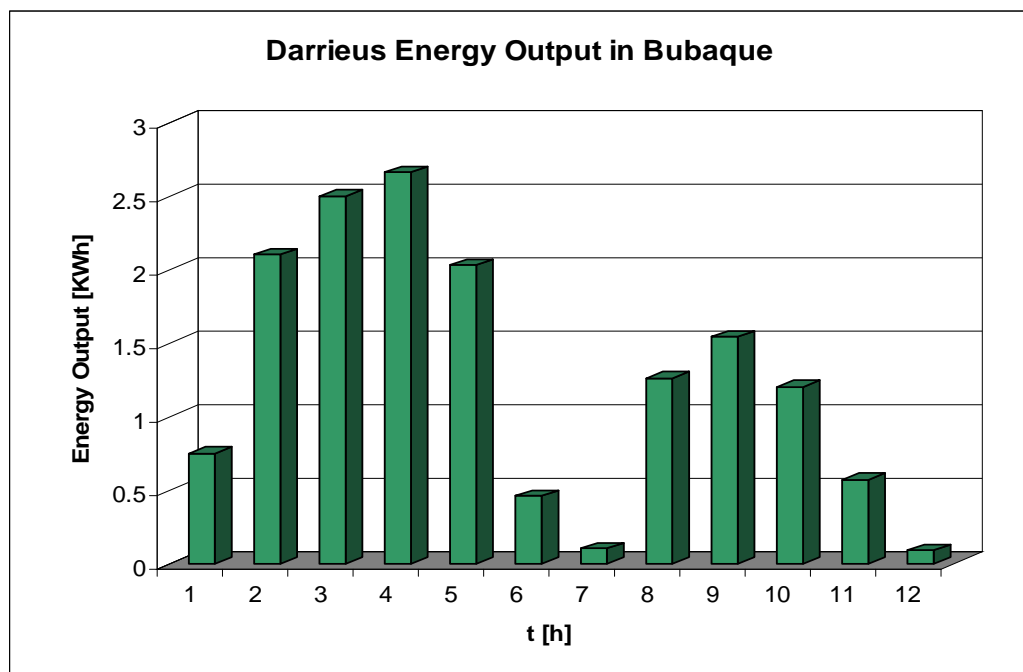


Fig. 5.43 - Energy output over a tide cycle in Bubaque for a Darrieus turbine 3 m in diameter (considering the maximum amplitude of 2 m registered in site).

### 5. Tidal stream power in Guinea-Bissau

|         | Average Energy Output<br>[KWh] | Energy output in a Cycle<br>[KWh] |
|---------|--------------------------------|-----------------------------------|
| Bubaque | 1.26                           | 15.13                             |

The average power output of a single turbine is not large, but the previous considerations about the power output in Bissau and Porto Gole (see sect. 5.7) can be repeated here. On the basis of a preliminary cost evaluation (see sect. 8.5) the installation analysed here turns out to be reasonable.

## 6. A novel solution: designing artificial inlets connecting tidal estuaries to small inland basins

### 6.1 Introduction

We now investigate the possibility to extract tidal power from natural or suitably designed artificial inlets connecting a body of water subject to tidal oscillations to a basin. To this aim we will first analyse the general characteristics of inlet hydrodynamics, with particular attention to the influence of inlet geometry on flow speed in order to determine the configuration that could optimize power production.

### 6.2 Formulation of the problem

#### 6.2.1 Shallow water equations

We model the inlet as a straight rectangular channel with length  $L_i$ , constant width  $B$  and mean flow depth  $Y_0$  relative to a flat and fixed bottom. The channel connects a basin with surface area  $S$  to an open sea.

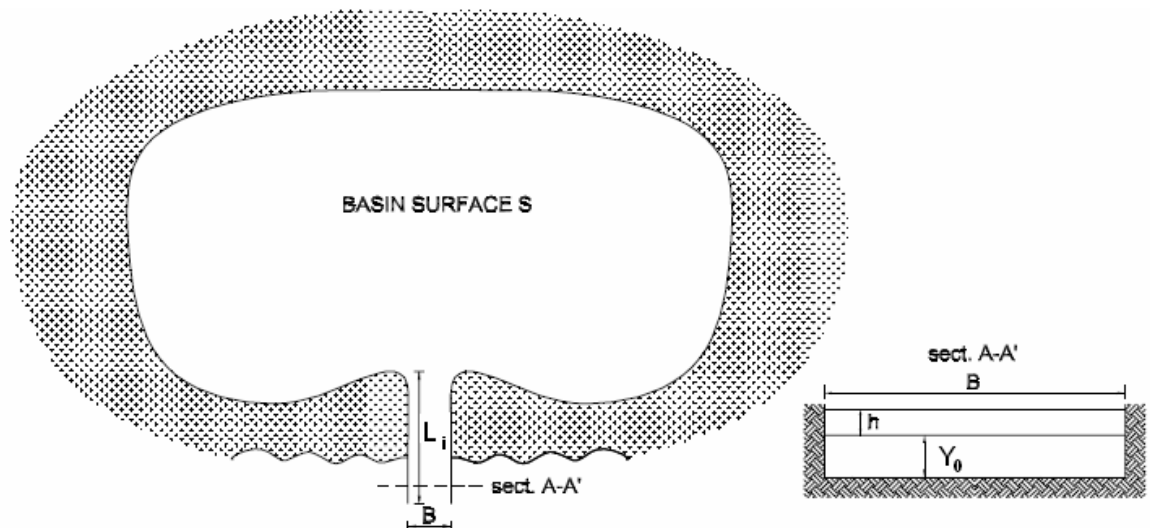


Fig. 6.1 - Geometry of the idealized inlet connecting a basin to the open sea or to a tidal estuary. We assume a rectangular cross-section (Tambroni & Seminara).

The basic one-dimensional partial differential equations describing the unsteady water flow in the rectangular channel are the equations of mass and momentum conservations, seen in § 5.3.2.

## 6. A novel solution: designing artificial inlets connecting tidal estuaries to small inland basins

The equations are to be solved with two appropriate boundary conditions.

At the inlet mouth we assume that the free surface oscillation is determined by the a simple  $M_2$  forcing tide, characterized by an amplitude  $a_0$  as for the analysis of estuaries.

At the inner boundary we impose a continuity condition, whereby the flow discharge through the end cross section of the channel gives rise in a quasi-static fashion to variations of the mean free surface elevation in the basin:

$$BUY_0 = S \frac{dh}{dt}$$

where:

- $U$  is the instantaneous velocity averaged over the cross section;
- $h$  is the water surface elevation relative to the still water level;
- $t$  denotes time.

As we have already seen, the shallow water equations can be solved either analytically or numerically.

### 6.2.2 Analytical solution for inviscid flow in rectangular inlets

A set of assumptions under which a simple solution of the shallow water equations can be found analytically are:

- the width  $B$  of the inlet is constant;
- the inlet cross section is rectangular;
- the bottom is horizontal;
- $\varepsilon = \frac{a_0}{Y_0}$  is small 'enough';
- no dissipation.

Combining the 1-D equations under the above hypotheses and applying the previously defined boundary conditions, the following analytical solution can be found:

$$h = a_0 \cos(\omega t) \frac{\cos(kx) + \frac{Sk}{B} \sin(kx)}{\cos(kL_i) + \frac{Sk}{B} \sin(kL_i)}$$

6. *A novel solution: designing artificial inlets connecting tidal estuaries to small inland basins*

$$U = \frac{a_0}{Y_0} c_0 \sin(\omega t) \frac{\sin(kx) - \frac{Sk}{B} \cos(kx)}{\cos(kL_i) - \frac{Sk}{B} \sin(kL_i)}$$

where  $x$  is the longitudinal axis pointing landward and centred at the inner boundary and  $k = \frac{2\pi}{L}$  is the wave number of the tidal wave characterized by the wavelength  $L$ .

### 6.2.3 Resonance in special geometric configurations.

As in the case of rectangular channel that ends with a totally reflective wall at the inner boundary, also in the case of inlets connecting tidal estuaries to overflow areas it is possible to induce the resonance phenomenon due to the pure reflection that occurs in the basin. In fact, if the quantity  $\frac{Sk}{B}$  takes a value such that  $\cos(kL_i) - \frac{Sk}{B} \sin(kL_i) = 0$  the speed tends to infinity, obviously in the context of a non dissipative scheme.

Let us then attempt to exploit this idea for conditions that apply to Guinea-Bissau. We then assume the following characteristics:

- annual average tidal amplitude  $a_0 = 1.9$  m;
- inlet length  $L_i = 100$  m;
- inlet depth  $Y_0 = 6$  m;
- inlet width  $B = 8$  m.

6. A novel solution: designing artificial inlets connecting tidal estuaries to small inland basins

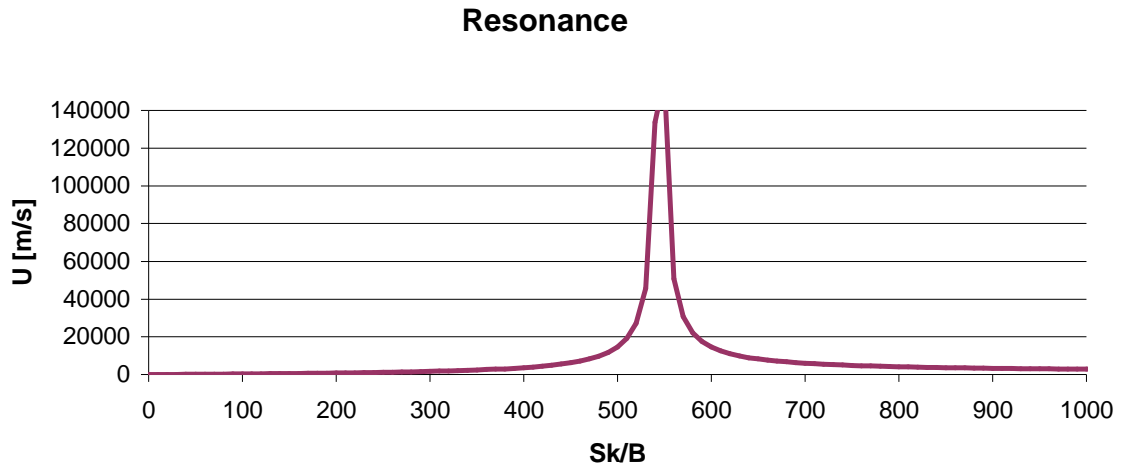


Fig. 6.2 - Effect of the dimensionless parameter  $Sk/B$  on inlet speed.

The resonant peak is located at  $\frac{Sk}{B} = 550$ , meaning that a basin surface of  $240 \text{ km}^2$  would be necessary in this particular case. This requirement can hardly be met in Guinea-Bissau. However this simplified solution suggests that there should be a particular configuration which maximizes the speed at the inlet, hence power output.

#### 6.2.4 One-dimensional numerical model for rectangular inlets

We then employ a simple model (which revisits the analytical formulation of Marchi, 1990), essentially based on the application of a 1-D model to the inlet (N. Tambroni and G. Seminara, 2006). Let us briefly summarize it.

Since the length scale characteristic of each basin as well as the lengths of inlet channels are small compared with the tidal wavelength, we assume that the free surface in the basin is effectively horizontal.

With this assumption, following a 1-D approach, we obtain a known equation governing the temporal development of the free surface oscillation  $\tilde{h}_2$  in the basin, subject to the tidal forcing at the seaward end cross section, where the temporal development of the free surface oscillation  $\tilde{h}_1$  is imposed.

This equation, in dimensionless form, reads:

6. A novel solution: designing artificial inlets connecting tidal estuaries to small inland basins

$$\tilde{h}_1 - \tilde{h}_2 = \delta_1 \frac{d^2 \tilde{h}_2}{d\tilde{t}^2} + \delta_2 \frac{d\tilde{h}_2}{d\tilde{t}} \left| \frac{d\tilde{h}_2}{d\tilde{t}} \right|$$

where the variables of the problem are scaled as follows:

$$\tilde{h} = \frac{h}{a_0}$$

$$\tilde{t} = t\omega$$

Moreover,  $\delta_1$  and  $\delta_2$  are dimensionless parameters measuring the relative role played in the momentum equation by local inertia and dissipation compared with gravity:

$$\delta_1 = \frac{\omega U_0 L_i}{g a_0}$$

$$\delta_2 = \frac{U_0^2 L_i}{g a_0 C_0^2 Y_0}$$

where:

- $t$  denotes time;
- $h$  is the water surface elevation relative to the still water level ;
- $\omega$  is the angular frequency of the tidal wave;
- $Y_0$  is the average flow depth;
- $a_0$  is a characteristic tidal amplitude;
- $C_0$  is the characteristic scale for the flow conductance:

$$C_0 = \frac{k_{se}}{\sqrt{g}} R_h^{1/6}$$

- $U_0$  is the characteristic scale for the average channel speed:

$$U_0 = \frac{S\omega a_0}{B Y_0}$$

Note that  $k_{se}$  is an “effective” Strickler coefficient, accounting for the effects of both the energy losses concentrated at the end cross sections and the distributed losses associated with channel roughness.

The energy losses concentrated at the inlet entrance  $\Delta E_e$  and at its outlet  $\Delta E_o$  can be written in the form:

6. A novel solution: designing artificial inlets connecting tidal estuaries to small inland basins

$$\Delta E_e + \Delta E_o = (\lambda_e + \lambda_o) \frac{U|U|}{2g}$$

with  $\lambda_e$  and  $\lambda_o$  suitable loss parameters.

The total energy loss  $\Delta E$  may then be expressed in terms of the effective Strickler coefficient  $k_{se}$  or in terms of an effective length of the inlet  $L_e$  as follows:

$$\Delta E = (\lambda_e + \lambda_o) \frac{U|U|}{2g} + \frac{U|U|}{k_s R_h^{4/3}} L = \frac{U|U|}{k_{se} R_h^{4/3}} L = \frac{U|U|}{k_s R_h^{4/3}} L_e$$

### 6.3 The hydrodynamics of tidal inlets in Guinea-Bissau

We then apply the above model to study the hydrodynamic behaviour of tidal inlets with particular attention on the influence of inlet geometry.

We assume the following general characteristics:

- tidal amplitude  $a_0 = 1.9$  m;
- basin surface area  $S = 150000$  m<sup>2</sup>;
- inlet length  $L_i = 10$  m;
- inlet width  $B = 4$  m;
- Strickler coefficient  $k_s = 30$  m<sup>1/3</sup>/s.

6. A novel solution: designing artificial inlets connecting tidal estuaries to small inland basins

We use the numerical model of Tambroni & Seminara (2006) to determine the maximum speed as a function of the flow depth at the inlet for different values of the amplitude  $a_0$  and of the basin surface area  $S$ .

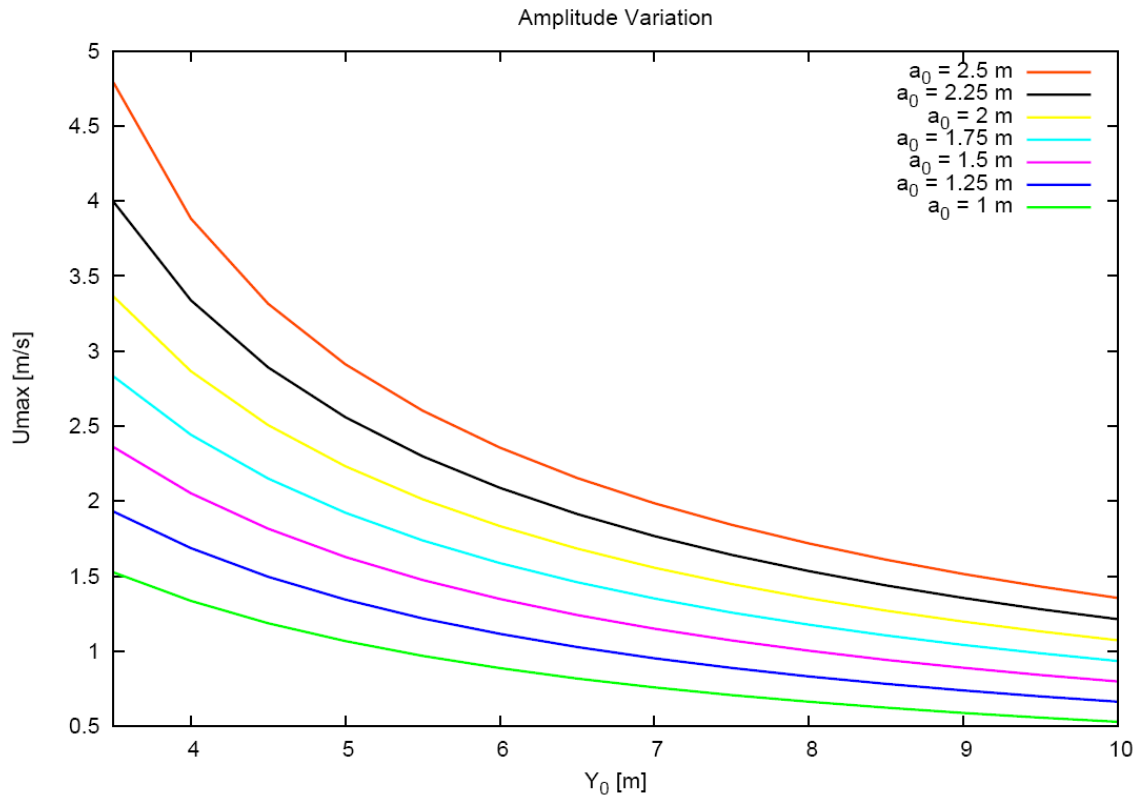


Fig. 6.3 - Effect of inlet depth on velocity assuming a basin surface of  $150000 \text{ m}^2$ : comparison between the results obtained for different values of tidal amplitude.

6. A novel solution: designing artificial inlets connecting tidal estuaries to small inland basins

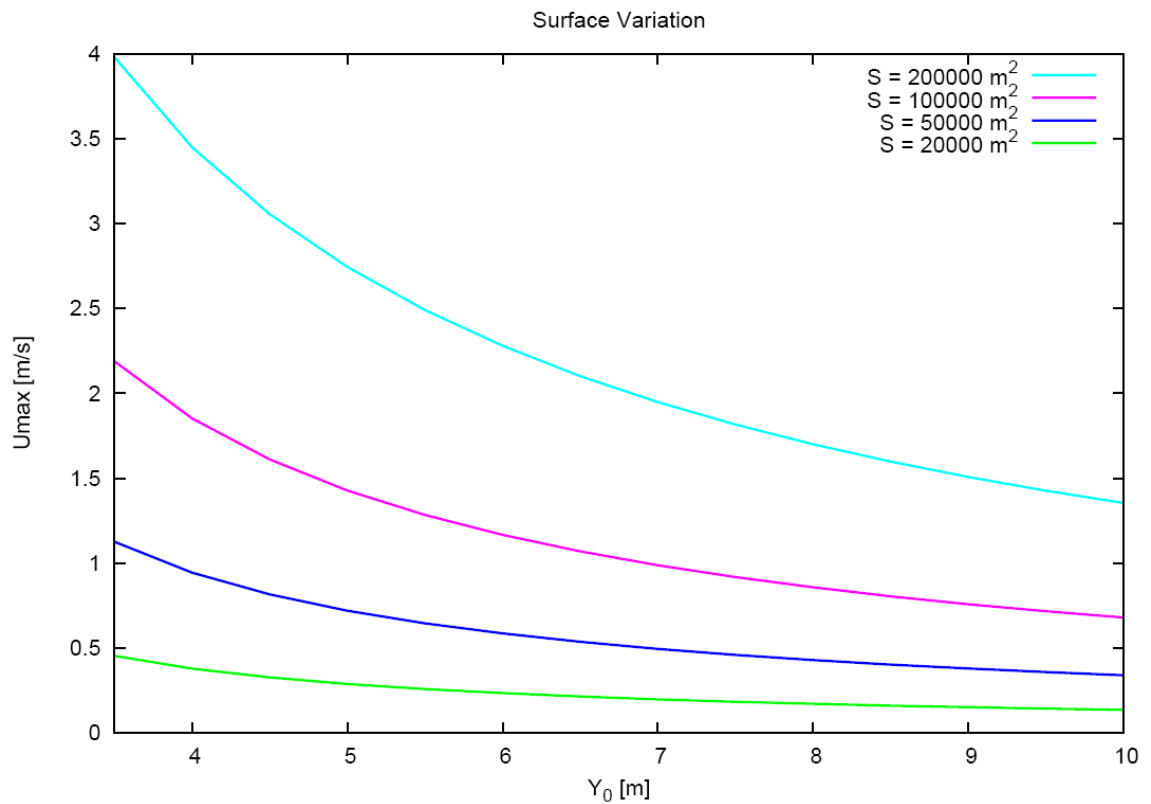


Fig. 6.4 - Effect of inlet depth on velocity assuming a tidal amplitude of 1.9 m: comparison between the results obtained for different values of the basin surface area.

Note that the maximum speed decreases as  $Y_0$  increases while it increases as  $a_0$  or  $S$  increase.

We next determine the maximum inlet speed as a function of the flow depth at the inlet for different values of the inlet length  $L_i$  and of the inlet width  $B$ .

6. A novel solution: designing artificial inlets connecting tidal estuaries to small inland basins

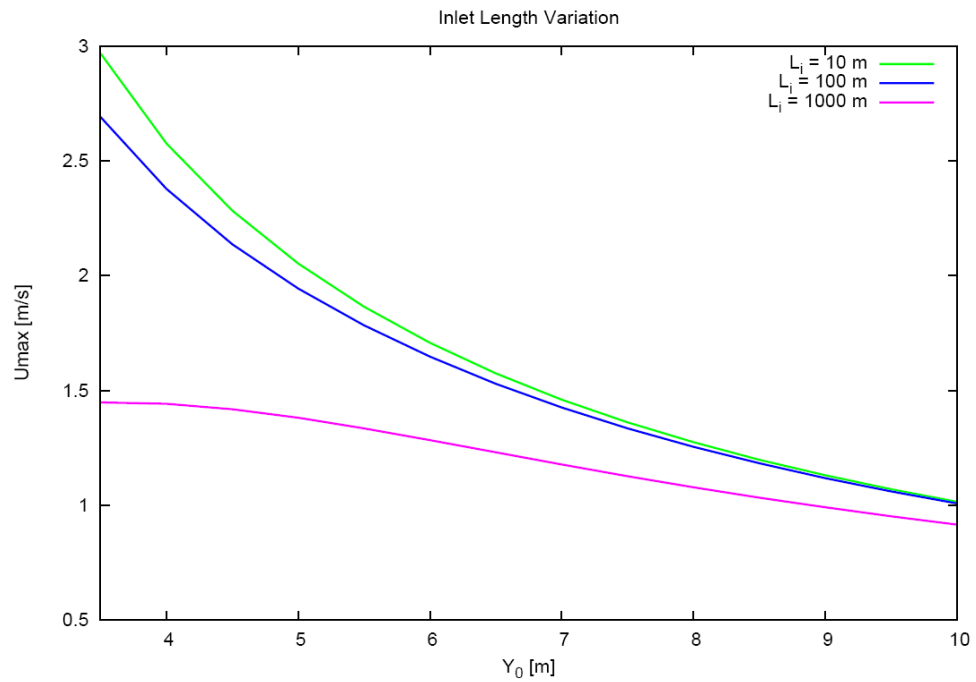


Fig. 6.5 - Effect of inlet depth on flow speed assuming an inlet width of 4 m, a basin surface area of 150000 m<sup>2</sup> and a tidal amplitude of 1.9 m: comparison between the results obtained for different values of inlet length.

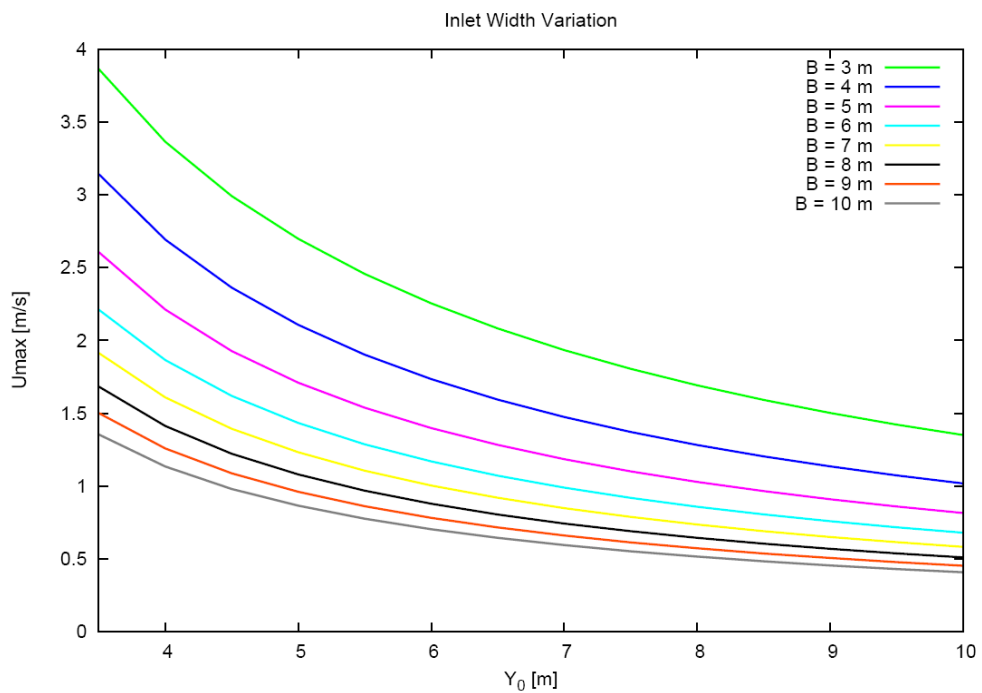


Fig. 6.6 - Effect of inlet depth on inlet speed assuming an inlet length of 10 m, a basin surface area of 150000 m<sup>2</sup> and a tidal amplitude of 1.9 m: comparison between the results obtained for different values of inlet width.

6. A novel solution: designing artificial inlets connecting tidal estuaries to small inland basins

Note that the maximum speed decreases as  $Y_0$  increases, as previously seen, and decreases as  $B$  or  $L_i$  increase.

Moreover, if the dimensionless speed is defined as:

$$U^* = \frac{U}{U_0}$$

all the curves collapse, as shown in the figure below.

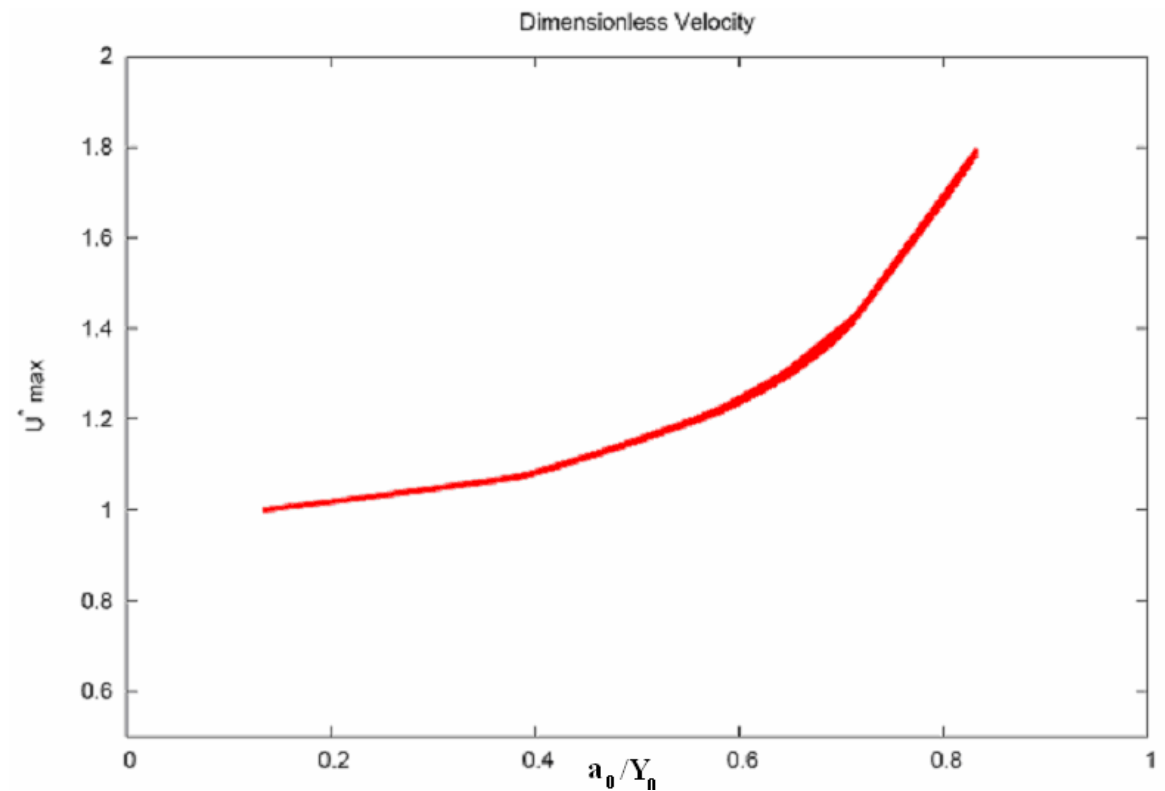


Fig. 6.7 - Effect of the parameter  $a_0/Y_0$  on dimensionless flood velocity.

6. A novel solution: designing artificial inlets connecting tidal estuaries to small inland basins

As regards the ebb speed, it follows the same trend as the flood speed when varying the geometric parameters, though it is typically slightly larger. This is due to the dependence of friction on the flow depth.

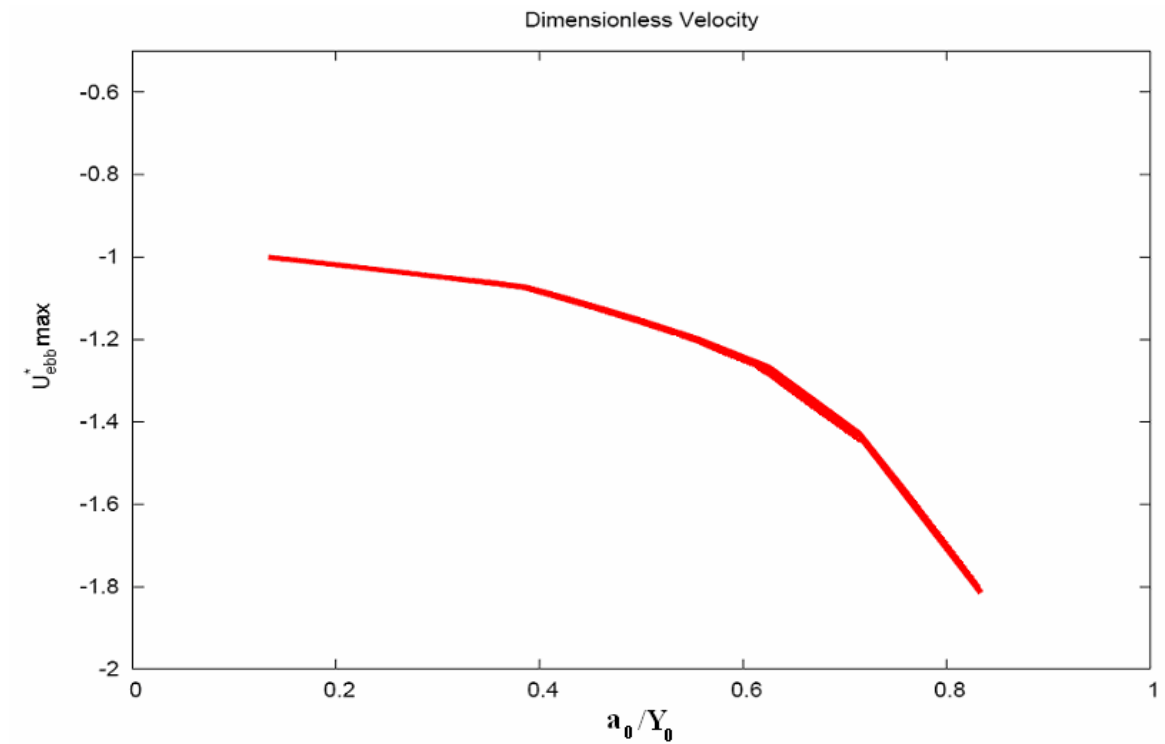


Fig. 6.8 - Effect of the parameter  $a_0/Y_0$  on the peak dimensionless ebb speed.

6. A novel solution: designing artificial inlets connecting tidal estuaries to small inland basins

### 6.4 Power production in a tidal inlet of Guinea-Bissau

Analysing the previous graphs we can determine the optimal conditions for tidal power production. In particular, we obtain:

- tidal amplitude  $a_0 = 1.9$  m, a value fairly typical of tidal events near Bissau
- basin surface area  $S = 150000$  m<sup>2</sup>
- inlet length  $L_i = 10$  m
- inlet depth  $Y_0 = 5$  m
- inlet width  $B = 4$  m
- Strickler coefficient  $k_s = 30$  m<sup>1/3</sup>/s

The cross section of the inlet is small enough to obtain high speed values, but it is large enough to install a Gorlov turbine 1 m in height and 2.5 m in width, as shown in the following sketch.

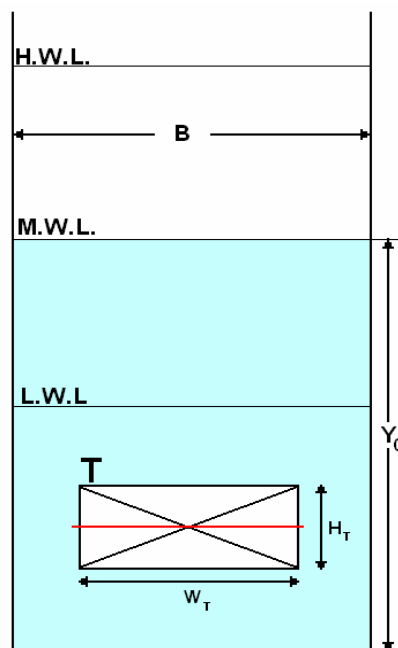


Fig. 6.9 - A Gorlov turbine ( $T$ ) 1 m in height ( $H_T$ ) and 2.5 m in width ( $W_T$ ) in an inlet of dept  $Y_0$  and width  $B$ . The red line is the horizontal axis of the turbine.

We remark that we can neglect the effect of the turbine on the hydraulic behaviour of the inlet considered because it takes away only 35 % of the kinetic head on a frontal area of 2.5 m<sup>2</sup> out of 20 m<sup>2</sup> of the section (4 % of the kinetic head of the flow).

6. A novel solution: designing artificial inlets connecting tidal estuaries to small inland basins

Moreover, the basin surface is sufficiently wide to find the desired speeds and it is of the size of many overflows areas that can be found in Guinea-Bissau, like the one shown in the figure below.



Fig. 6.10 - Satellite image of the inlet connecting the Rio Geba to an overflow area (© Google 2007).

Finally, as a first step we consider the annual average amplitude of 1.9 m and next we study the behaviour of the power output under the effects of the monthly variation of tidal amplitude due to springs and neaps.

6. A novel solution: designing artificial inlets connecting tidal estuaries to small inland basins

In a cycle of 12 h the numerical model predicts the speed values plotted below:

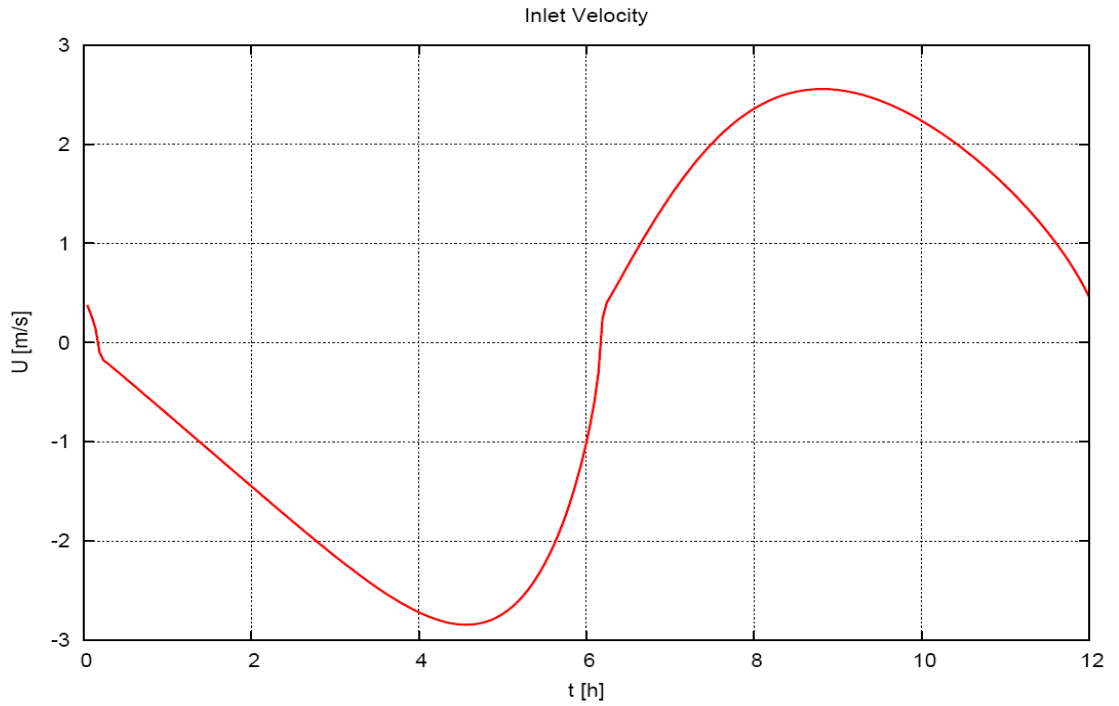


Fig. 6.11 - Trend of inlet speed throughout a tidal cycle assuming an inlet width of 4 m, a basin surface of 150000 m<sup>2</sup> and a tidal amplitude of 1.9 m.

6. A novel solution: designing artificial inlets connecting tidal estuaries to small inland basins

It's next possible to calculate the available theoretical power, in the same way as we have done when studying the behaviour of tidal estuaries.

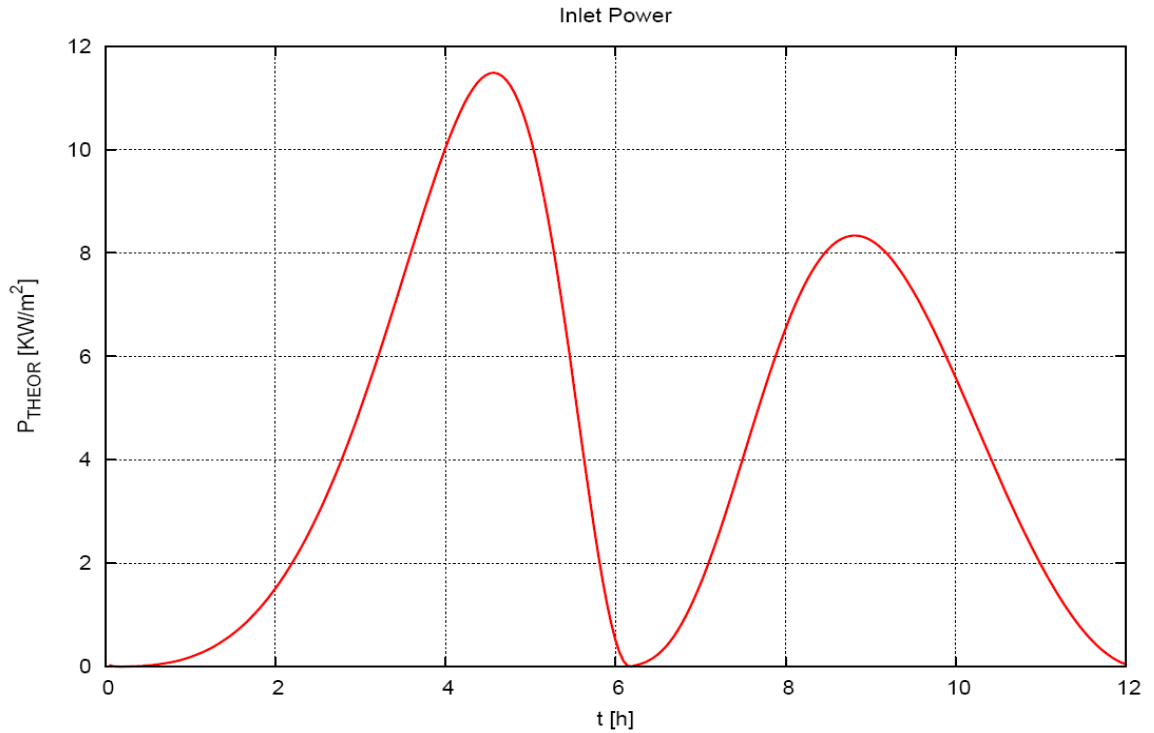


Fig. 6.12 - The theoretical power per unit of area of the turbine is plotted as a function of time in a tidal cycle

We see that the available power obtained in this situation is much higher than the one obtained for tidal estuaries; in the previous range of velocities it is possible to install a Gorlov turbine that has a high efficiency (35%) but needs velocities larger than 1.5 m/s (cut in speed) to generate electricity.

6. A novel solution: designing artificial inlets connecting tidal estuaries to small inland basins

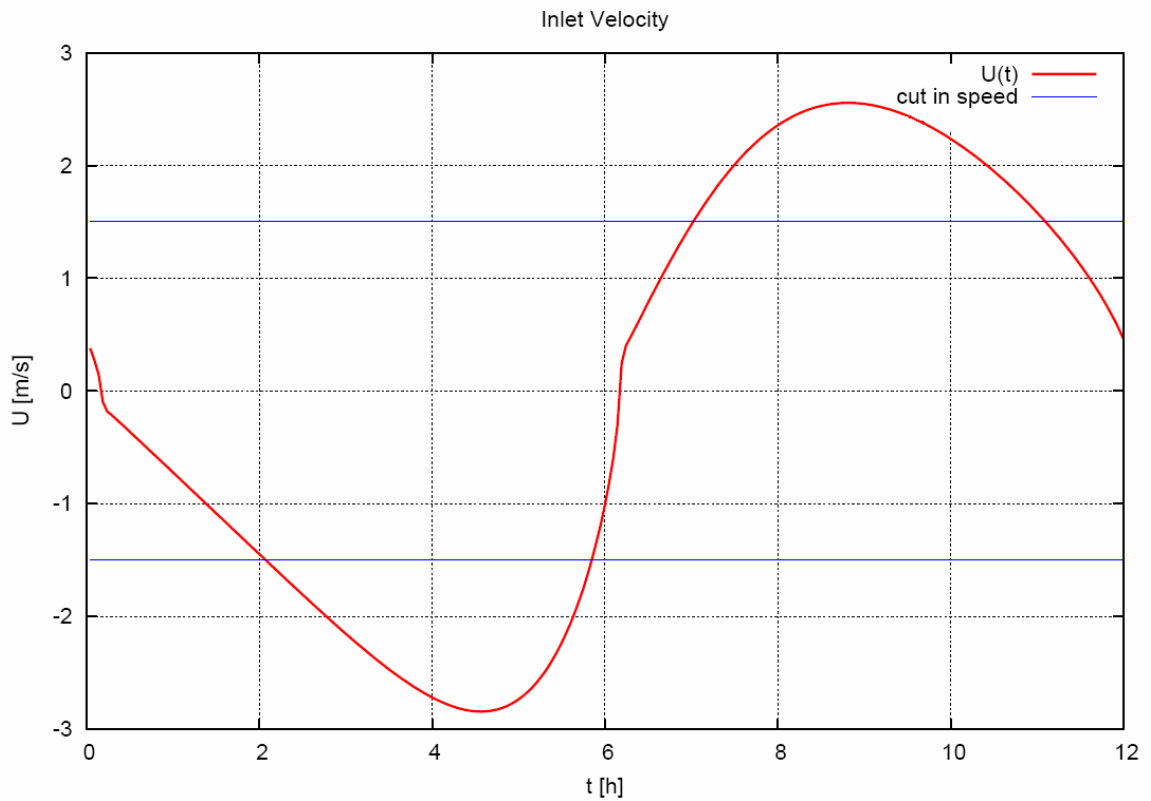


Fig. 6.13 - Dependence of inlet speed on time in a tidal cycle (red line). The cut in speed of a Gorlov turbine is also shown (blue line).

With the average amplitude considered, we see that speeds exceed 1.5 m/s for at least 8 hours in a tidal cycle. This means that it is possible to determine an energy output of 45.5 KWh in a cycle with an average value of about 4 KWh.

6. A novel solution: designing artificial inlets connecting tidal estuaries to small inland basins

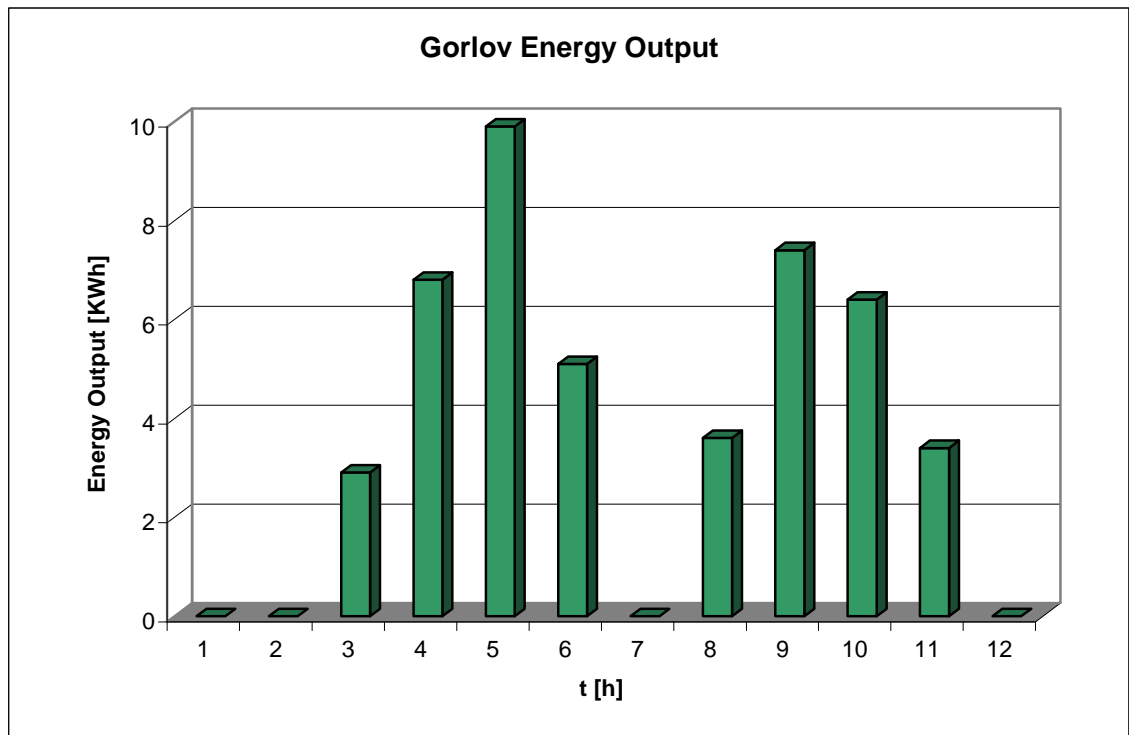


Fig. 6.14 - Energy output produced by a Gorlov turbine over a tidal cycle for the setting considered herein.

The annual energy output has been calculated adopting the annual average tidal amplitude of the analyzed site. We next consider the effects of the monthly variation of tidal amplitude simulating the two extreme cases of the maximum and minimum amplitude in Bissau, i.e. assuming the values:

- $a_0 \text{ max} = 2.5 \text{ m}$ ;
- $a_0 \text{ min} = 1.25 \text{ m}$ .

6. A novel solution: designing artificial inlets connecting tidal estuaries to small inland basins

The results are shown in the graph below.

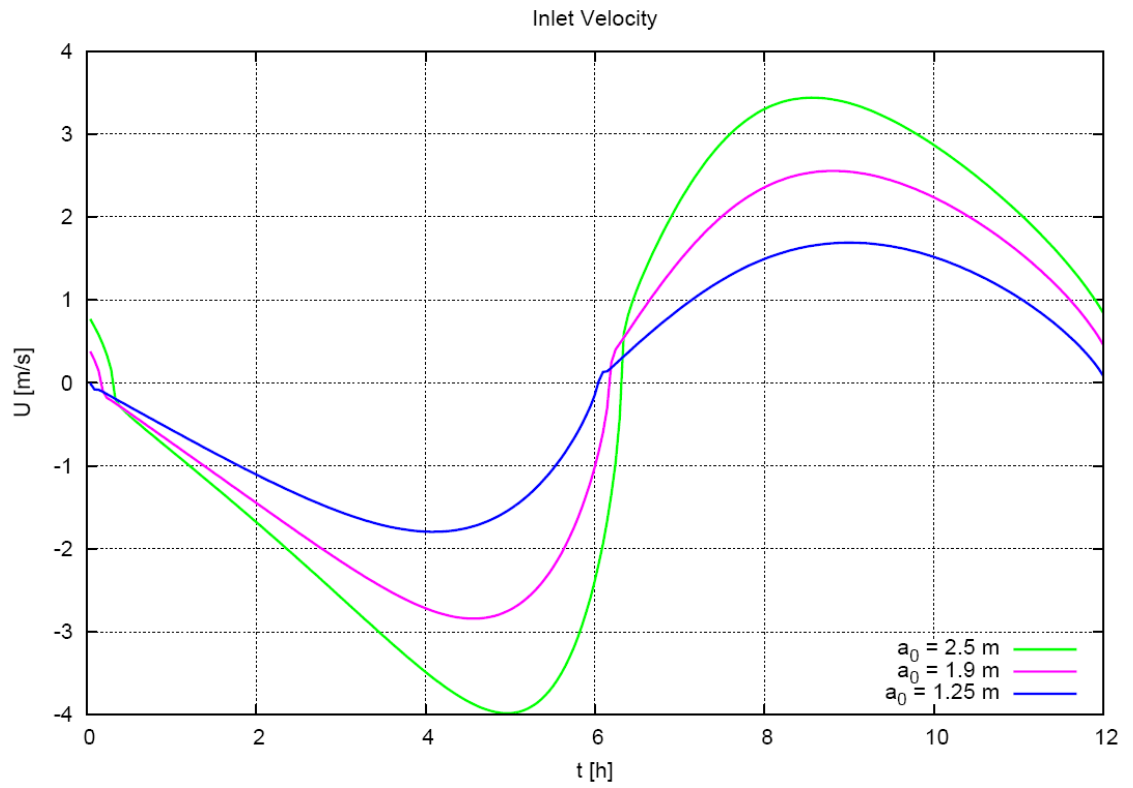


Fig. 6.15 - Dependence of inlet speed on time in a tidal cycle: comparison between the results obtained for different values of tidal amplitude.

6. A novel solution: designing artificial inlets connecting tidal estuaries to small inland basins

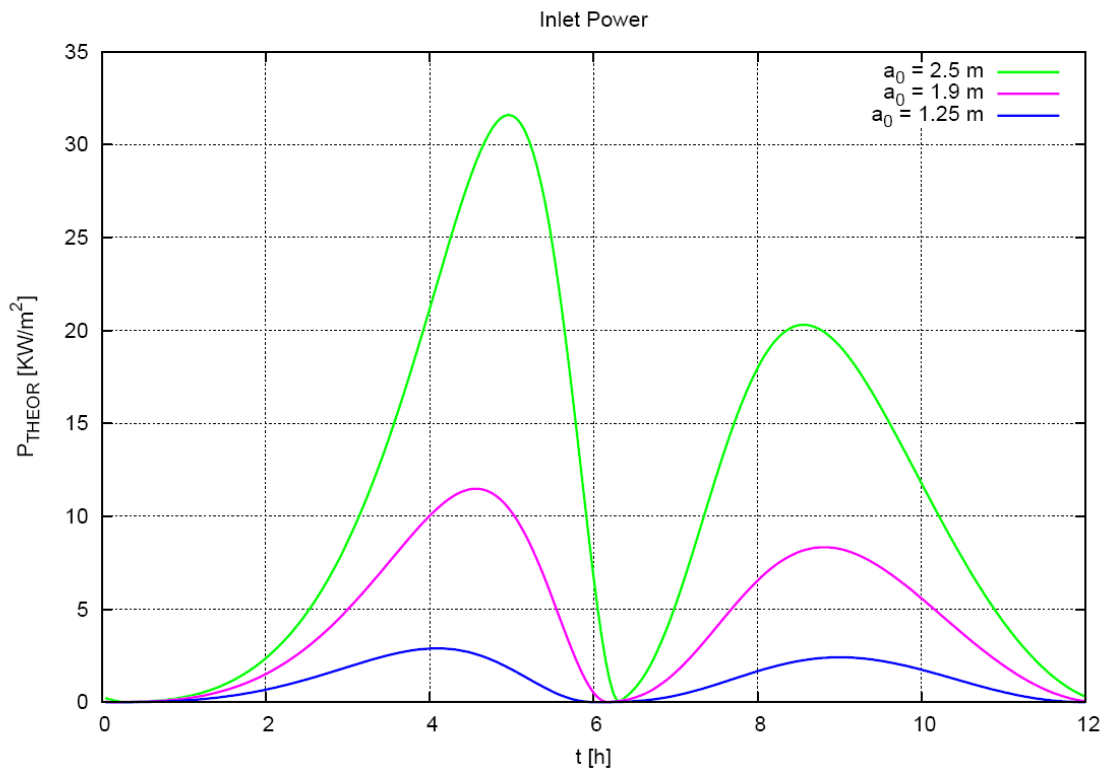


Fig. 6.16 - Dependence of inlet speed on time in a tidal cycle.: comparison between the results obtained for different values of tidal amplitude.

It is important to emphasize that, while speeds increase linearly with amplitude, the power output has a cubic dependence on flow speed. With the maximum amplitude considered, speeds remain larger than 1.5 m/s for 10 hours in a cycle, leading to an energy output of 117.4 KWh and an average value of about 9.8 KWh.

6. A novel solution: designing artificial inlets connecting tidal estuaries to small inland basins

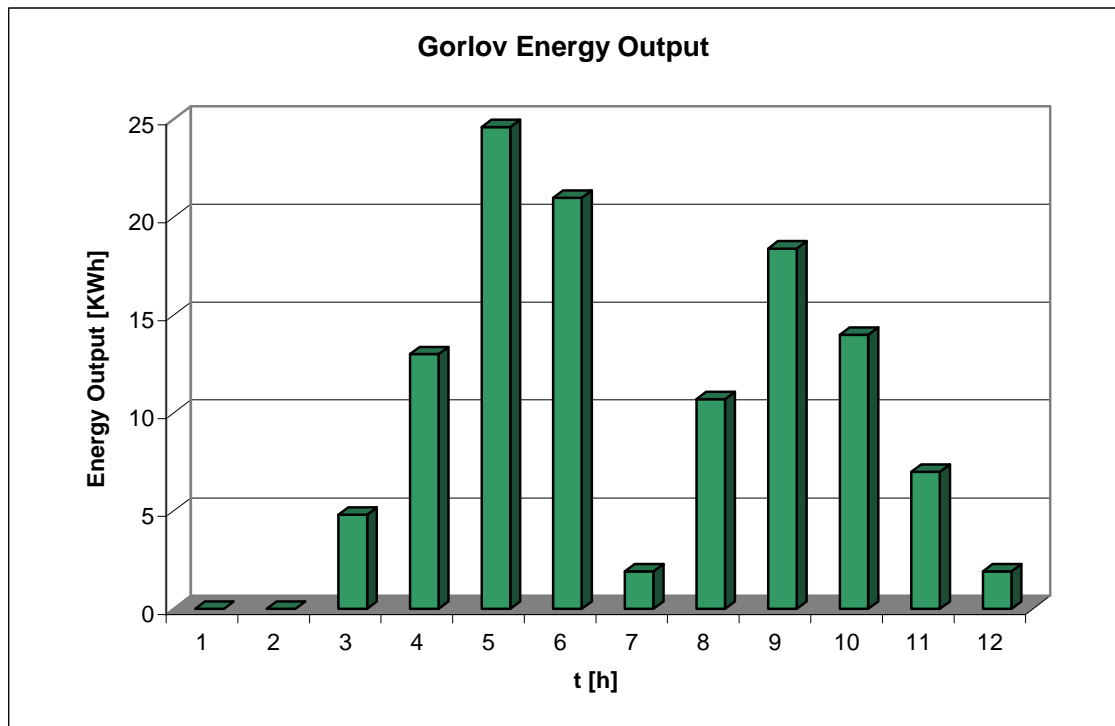


Fig. 6.17 - Energy output produced by a Gorlov turbine over a tidal cycle considering the maximum tidal amplitude.

On the other hand the minimum amplitude reduces the period in which the turbine generates electricity to only 4 hours in a cycle, leading to a total energy output in a cycle of 8.4 KWh and an average of only 0.7 KWh.

6. A novel solution: designing artificial inlets connecting tidal estuaries to small inland basins

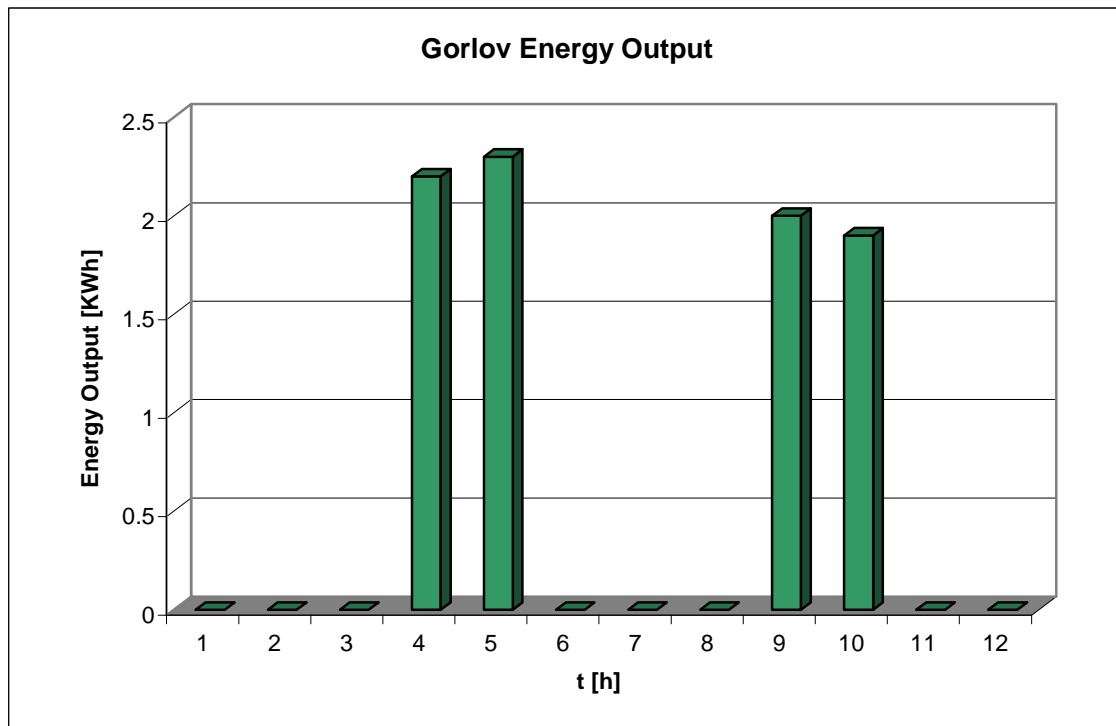


Fig. 6.18 - Energy output produced by a Gorlov turbine over a tidal cycle considering the minimum tidal amplitude.

We remark that due to the non linear dependence of the energy on the tidal amplitude, the mean of the energy outputs calculated with maximum and minimum amplitudes:

$$\frac{9.8+0.7}{2} = 5.25 \text{ KWh}$$

is larger than the one calculated with the annual average amplitude (4 KWh).

Consequently the monthly average energy output would result slightly greater than that previously evaluated and should be estimated simulating a period of at least 14 days.

*6. A novel solution: designing artificial inlets connecting tidal estuaries to small inland basins*

Finally, noting the positive effects of an amplitude of 2.5 m on the power output, it appears to be worth investigating the existence of a suitable overflow area in the inland branch of Rio Geba, where the amplitude is larger than in Bissau.

This investigation must be done on site, because of the low resolution of satellite images in the inland areas of Guinea-Bissau, as shown in the image below.



*Fig. 6.19 - Satellite image of possible overflow areas along the Rio Geba (© Google 2007).*

### 6.5 Comparison with a more refined numerical model

The simplified model shown in sect. 6.2.4 gives accurate results for small values of the ratio between average amplitude and depth ( $\varepsilon \ll 1$ ). In our case study the latter ratio is equal to 0.4.

In order to check the previous values of water velocities in the inlet, and prevent over estimation of the power output we make a comparison between the simplified model described above and a more refined numerical model that solves the classical 2-D depth averaged shallow water equations for the fluid phase.

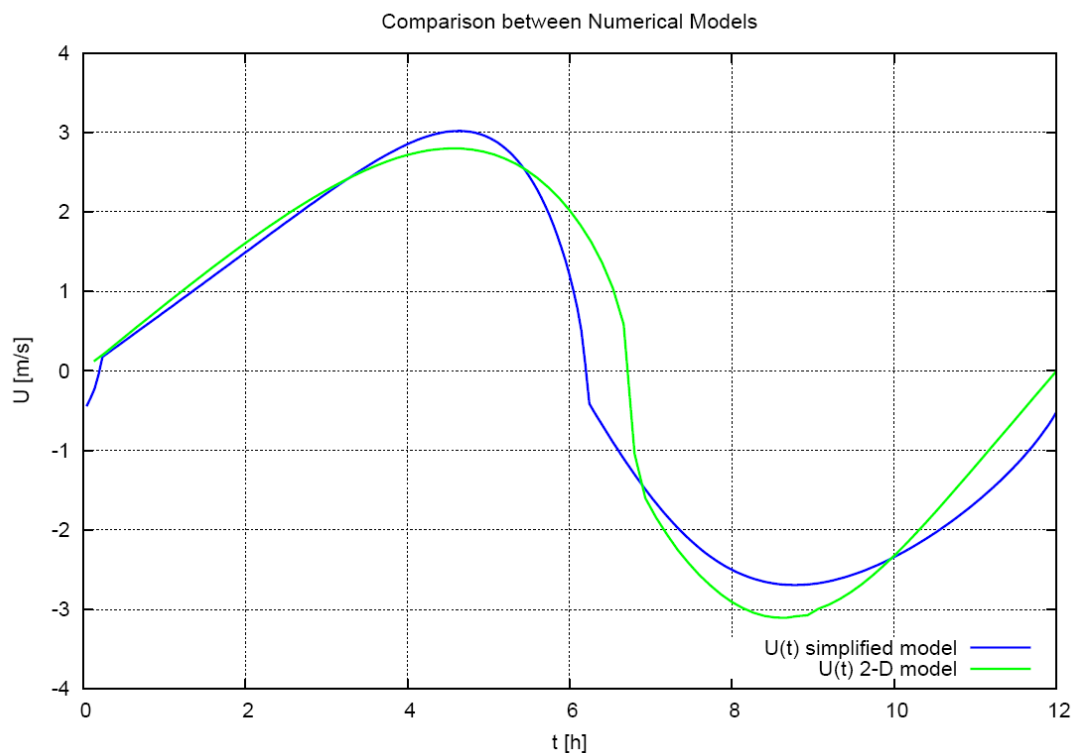


Fig. 6.20 - Comparison between flow speeds obtained by the simplified 1-D model and the 2-D complete model.

Agreement between the speeds given by the two models is reasonable, which suggests that we can consider our estimate of power production correct.

## **7. Preliminary considerations about energy storage and power supply in Guinea-Bissau**

### **7.1 Introduction**

The major hurdle to be overcome for the exploitation of tidal energy is no doubt the fluctuating character of the power output. Up to now our considerations have been focused on aspects related to power production. In this chapter we move to consider the problem of energy storage.

Basically two possibilities must be considered to obtain a fairly constant power output:

- installation of a storage system;
- employ an additional power source.

### **7.2 Installation of a storage system**

The predictability and regularity of the supply fluctuations from a tidal current plant should lend itself to effective matching with storage systems as it will be possible to predict, in advance, just how much storage capacity might be needed.

Therefore energy could be stored during periods of generating excess and released at times when the demand exceeds supply; then it would become necessary to design energy supply systems that do not need to maintain a fossil capacity.

The economics of a combined energy generation and storage system are highly dependent on a wide range of factors. One of the most crucial of them is the amount of energy storage required to balance the fluctuations in supply so as to allow the combined system to supply a constant base load.

The area of electrical energy storage has been extensively studied for both large scale, (i.e. grid connected systems) and for remote area systems, (i.e. not grid connected). Most of the work of evaluating storage systems has focused on the engineering aspects of a particular storage system. Although the economic benefits have been shown to be large, especially in markets where the cost of storage capacity is equivalent to the cost of replacement capacity.

The existing storage technologies consist of pumped hydro, batteries, compressed air energy storage, superconducting magnetic energy storage, capacitive energy storage and

## 7. Preliminary considerations about energy storage and power supply in Guinea-Bissau

flywheels.

Energy storage on a large scale is already commonly utilised through pumped hydro systems but this solution is not suitable for many countries. In dry regions compressed air storage plants have been developed and shown to be efficient. Capacitors have also been used for large-scale short burst storage systems as they offer a very high energy density; capacitive energy storage can also be used to damp out the electromagnetic oscillations. Battery energy storage systems can be efficiently used to store large amounts of power in either a central system or in a distributed manner throughout the grid for areas with poor infrastructure.

There is evidence that combined current turbine and storage systems could yield a potential economic benefit if the cost of the storage systems falls below that of equivalent fossil systems, especially in remote areas.

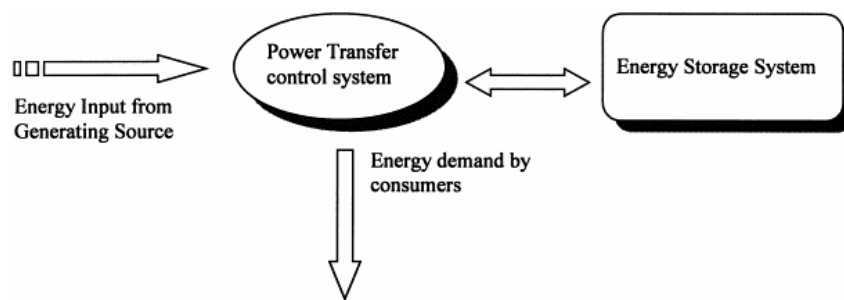


Fig. 7.1 - Schematic representation of a combined supply/storage system (I.G. Bryden et al., 2000)

### 7.3 Employ of an additional power source

The tidal resource is variable, but there is no prospect of lengthy periods for which there is no incoming energy flux; so these fluctuations can be smoothed out using an additional power source, e.g. photovoltaic cells or batteries, but more typically using fossil fuel generation.

In the absence of an energy storage capacity, the variability of a single tidal current generation system means that it could not replace a fossil fuel generation plant. It is necessary to maintain a standing reserve capacity, which must be available to meet the maximum demand.

Energy sources that cannot guarantee to deliver energy when required are referred to as

## *7. Preliminary considerations about energy storage and power supply in Guinea-Bissau*

soft sources to distinguish them from hard sources that can deliver energy whenever required. Most sources of renewable energy, such as wind, wave and tidal must be considered soft.

It means that in the absence of any storage system, it is essential to have a combination of hard and soft supplies.

### **7.4 Supply of tidal energy in Guinea-Bissau**

In the developing country Guinea-Bissau, the connection to an electrical grid can be realized only if the tidal power plant is situated near the capital Bissau (as we have seen for the medium size barrage system) and if it is joined to a traditional electrical plant which provides energy when the tidal one is not working.

Anyway we remark that it is found that to facilitate the integration of the system to the grid, a short-term energy storage is whatever needed.

As an alternative, if we regard as small streams power installations, which could be situated in many parts of the country, such as the islands or the inland estuaries, where there is no electrical grid, it is necessary to consider that energy output needs to be stored in order to supply the fluctuation in energy output.

Another solution might be to deliver the tidal energy to marginal applications which may accept an oscillating supply, such as refrigerators, pumping systems providing fresh water, or any other similar customer.

## **8. Tentative cost analysis.**

### **8.1 Introduction**

Let us now make an approximate cost analysis in order to get some feeling on whether tidal power installations can be considered as economically feasible. One way of evaluating the economics and competitiveness of such systems is to compare the costs of electrical generation with the prices that customers pay for electricity. It becomes increasingly relevant that local communities might be interested to invest in small local systems. The location of these communities and the lack of grid hook up in those locations, along with the proximity of tidal energy sources, might be a decisive factor: ocean energy could then compete with diesel generation or might, in the presence of the latter, complement it.

### **8.2 Cost of energy in Guinea Bissau**

At present most energy produced in Guinea Bissau derives from imported oil products, creating difficulties to economy due to dependence from other countries, and problems for the environment and human health, due to emissions of GHG gases.

The cost of 1 KWh produced by a diesel generator depends on the price of the generator and on the cost of gasoline, that is not constant throughout the years, but it is assumed to increase quickly in relation with the rate of petroleum production.

In this thesis, we analyze a common diesel generator (“Ashwameg” brand stationary) with a power output of 3 KWh and a consumption of 1.13 l/h: assuming that 1 l of diesel in Guinea Bissau costs about 1 euro (2007), the cost of 1 KWh ranges about 0.38 €, neglecting the price of the generator, its installation and maintenance.

Hence, if we consider a generator working 12 hours a day, the annual cost of energy produced by the generator is about 1650 €.

It is now possible to make a comparison between the costs of power produced by tidal plants and by diesel generators.

### **8.3 Generic factors influencing the costs of a barrage tidal power plant**

The economics of a barrage power plant is absolutely site-specific, and depends critically upon the topography, geology and many other factors of each individual site. These determine the size of the plant and the costs of development, which are themselves variable depending upon how the resource is developed, for example with or without storage, at high or low load factor.

This system is capital-intensive, and usually long lived, with civil works typically lasting 100 years or more. With a zero fuel cost, and typically low maintenance and operation costs, the primary economic problems arise from the high interest rates and the demand for short payback periods.

Possible consumption of local power and shorter construction times for small schemes may make them more economic than larger schemes.

### **8.4 Generic factors influencing the costs of a tidal stream power plant**

The cost per unit energy output generated by any system is influenced by:

- *fixed costs*, which represent the cost of the generation hardware, support structure, connection of the system to the grid and any other costs, such as those related to installation, which must be covered prior to the operation of the system;
- *operation and maintenance costs (O&M)*, which represent the incomplete costs of servicing, repair and, where appropriate, rental and fuel cost which, of course, are not an issue for a pure renewable system.

The economics associated with tidal streams power installations is uncertain because there have been, to date, no long term commercial-scale demonstrations of a meaningful number of systems and no large-scale devices have been built. Currently available are only many prototypes, which include all the additional costs involved in such a stage. Sources of cost data are hence difficult to find.

Other similar (or close to) areas of activities in offshore engineering could provide data that would help to calculate the capital costs of tidal energy systems.

Furthermore, as regards the particular context of Guinea-Bissau, some other factors influence the cost analysis of this kind of plants:

- the installation in shallow water, requiring less sophisticated mounting structures, (including less costly mounting related personnel and equipment costs) could reduce costs;
- the designs that hold all electrical components out of the water, reducing the need for expensive seals, perhaps reducing maintenance intervals, and reduce scheduled servicing costs due to easier access could reduce costs;
- the installation near to the shore could reduce costs due to reduced costs of connection with the electricity network;
- the installation in salt water could increase costs because of the effect of corrosion;
- debris management could increase costs.

In general the cost allocation of capital for a generic tidal stream farm is as follows:

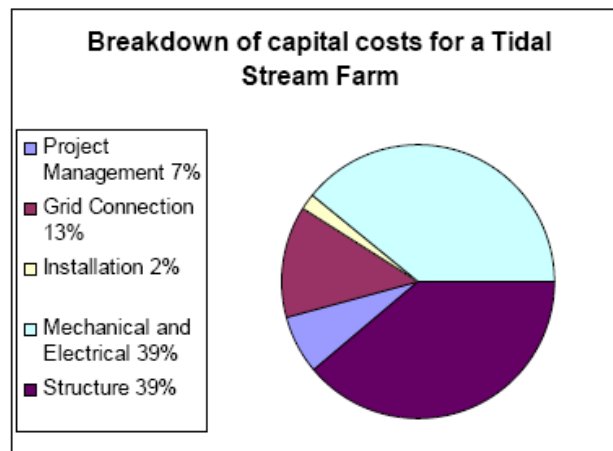


Fig. 8.1 - Costs for a tidal stream farm (© Verdant Power Canada ULC, 2006).

## 8.5 Cost estimates

A possible approach to approximate cost estimate can be made from similar projects. Adjustments must obviously be made to take care of relative sizes or other characteristics. Finding remotely related systems is more likely because of the scarcity

of ocean energy systems.

In the particular case of the Enermar system (Kobold turbine), the following figure shows the quota-weight for each step of project according with its costs.

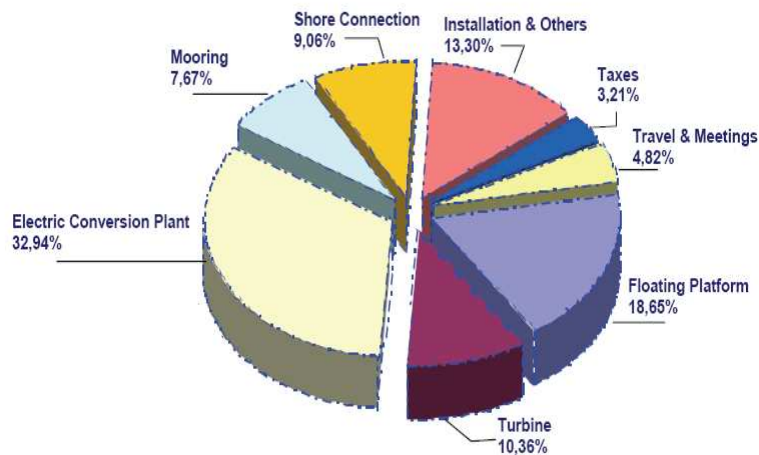


Fig. 8.2 - Quota-weight for each step of project according with its costs for the Enermar project (Ponte di Archimede S.p.A. – 2007).

The Kobold system is built in place and hence the costs will vary depending on the site. However, as an example we consider a plant that is going to be built in Indonesia, that costs \$US 180 000 (the price in Guinea Bissau should not be very different from this). The plant would be designed for the specific site, so some improvements of the performance mentioned earlier can be expected.

The Kobold technology is currently focusing on marine current exploitations and hence the flow needs to reach 3 m/s for the system to be feasible, depth no more than approximately 50 meters and distance to the shore less than 1000 meters.

This means that in Guinea Bissau this kind of system cannot be considered economically feasible because in our study we found that water velocities reach 1.6 m/s. Anyhow, it would be necessary to perform field measurement campaigns to investigate if there are local conditions that could reach 3 m/s.

As concerns Gorlov turbines, a project, in particular, is focusing on a tidal system with 100 Megawatts capacity. This massive system will consist of approximately 100 Lucid

## *8. Tentative cost analysis*

Walls (see figure 2...) and will end up costing approximately \$ US 2.2 million per MW. Depending on local rates for electricity it is anticipated that the system could pay for itself in as little as 6 years. This includes maintenance costs which are estimated to be between 10 and 15% of the cost of the system every 5 years, or \$ US 220-330,000 per year.

On a much smaller scale a small floating system with a maximum capacity of 8 KW is currently under development. As a single prototype the unit is relatively expensive, approximately \$US 3,200/kW or \$US 25,000. However, this unit is intended for consumer-level sale and, in quantity, it isn't unreasonable to suspect the cost could lower as much as 30% , in which case it would be comparable to the system mentioned above.

Finally, we try to estimate the cost of the installation in Bubaque (see sect. 5.9); considering that a Darrieus turbine, 3 m in diameter and 2.5 m in height, would cost about 16000 € and assuming that this value represents 39% of the total cost (see figure 8.), the tidal stream farm could cost about 41000 €

Multiplying the average energy output by the number of hours in a year, we find that the turbine could produce about 10000 KWh/year, and 100000 KWh in 10 year, meaning a cost of 0.41 €/KWh; considering that the turbine should be replaced every 20 years, making a comparison with the cost of 1 KWh produced by the diesel generator (0.38 €/KWh), we deduce that the system could pay for itself in about 10 years.

## 9. Conclusions

In conclusion, the investigations and the numerical simulations performed on the Guinea-Bissau network of estuaries and tributaries has allowed us to study different feasible schemes for tidal installations.

The strategic sites which we have identified for the construction of a barrage tidal plant are summarized below:

- near the village of Fanhè, where the annual average tidal range reaches 4.4 m and there is a basin with a surface area of about 29000 m<sup>2</sup>, a small plant producing an average 34 KW is feasible; after several simulations we have also identified the more efficient regulation law (which allows to obtain the maximum energy in a tidal cycle) and we have assessed the working conditions of the turbine to be installed;
- near the capital Bissau (average tidal range of 3.8 m, basin area of 1.12 km<sup>2</sup> and a barrage of 150 m in length) we propose a plant whose power production is on average 940 KW;
- on the landward share of Rio Geba, where the tidal range reaches a maximum value of 6.8 m, we consider the possibility of building a 2 km long barrage across the entire estuary, in order to install a plant of 50 MW, energy that could well meet the needs of the whole country.

As far as the analysis concerning the possibility of producing electricity with the simple installation of one or more free flow turbines, among the various proposed technologies, we choose to adopt a Darrieus turbine 3 m in diameter, because such prototype is one of the few already on the market and it can work even with low velocities.

We obtain the following results:

- along the Rio Geba the turbine would allow an average power output of 0.67 KW in the cross section of the capital Bissau (considering the maximum amplitude) and 0.71 KW in Porto Gole;
- along the Rio Mansoa, velocities do not reach high values (power output would reach a value of 0.37 KW close to Fanhè), therefore we do not deem appropriate the installation of a free flow turbine;
- close to Bubaque, in a narrow channel between 2 islands of the Arquipelago Dos

Bijagos, where on-site measurement of water speed revealed values higher than along the estuaries, the power output per turbine would reach 1.26 KW and could supply the small hotels located in the neighbourhood.

In spite of the fact that this type of installations could seem at first of little interest in terms of power output, we must consider that this energy is clean and free of any environmental impact; moreover, we emphasize the possibility of installing more turbines, taking into account the elevated width and depth of channels; a careful field measurement campaign is certainly needed to verify whether places where higher values of velocity than those obtained by numerical simulations can be found.

In the concluding part of the thesis a model of an inlet which connects a tidal estuary to a lagoon or an overflow area and sought conditions close to theoretical resonance are analysed. We remark that this novel idea allows a greater production of electricity than in the previous case, but with the same reduced environmental impact. Considering an inlet 5 m in depth and 4 m in width (available on site or artificially built) connected to a basin of 150000 m<sup>2</sup>, the installation of a single Gorlov turbine (1 m in diameter and 2.5 m in height) leads to an average power output of 4 KW with an amplitude of 1.9 m and of 8.4 KW with an amplitude up to 2.5 m.

In conclusion we can state that our analysis demonstrates that in Guinea-Bissau there is a great amount of tidal power to be exploited in order to meet the energy demand of the country through the use of this renewable source.

Certainly the results we obtained are preliminary and are based on some simplified schemes which will have to be validated through detailed sets of field measurement, in order to obtain water levels, velocities, accurate information about bathymetry, topography and geology of the sites. The availability of the latter information will lead to a more reliable estimate of power production and to a better evaluation of costs.

Finally, we remark that the shortage of tidal power plants around the world and the lack of technical information about free-flow turbines and low-head turbines, due to their recent development, makes it difficult to provide a complete overview of such a kind of installations.

## *9. Conclusions*

This notwithstanding we are confident that the results we have obtained might be useful for the O.N.L.U.S PS 76 to suggest the inclusion of a section dedicated to tidal power in the “five-year energy plan” of Guinea-Bissau . Moreover, it might allow access to funds that European Union allocate for the improvement of renewable energies in developing countries.

## References

*Intergovernmental Panel on Climate Change (IPCC)*. Climate Change 2007: Synthesis Report, , Fourth Assessment Report.

*Paper Prepared for Renewable Energy Network for the 21st Century (REN21) by The United Nations Environment Programme (UNEP)*. The Role of Renewable Energy in a Carbon-Constrained World.

*International Energy Agency (IEA)*. World Energy Outlook 2005. ISBN: 92-64-109-1094-98 – 2005.

*International Energy Agency (IEA)* . Energy Statistics.

*Y. Accad, C. L. Pekeris*. Solution of the Tidal Equations for the  $M_2$  and  $S_2$  Tides in the World Oceans from a Knowledge of the Tidal Potential Alone. *Philosophical Transactions of the Royal Society of London. Series A, Mathematical and Physical Sciences*, Vol. 290, No. 1368 (November 28, 1978), pp. 235-266.

*Department of Oceanography, Naval Postgraduate School*. Navy Operational Ocean Circulation and Tide Models. 1 University Circle, Monterey, CA 93943-5001.

*L.B. Bernshstein*. Tidal energy for electric power plants. *Israel program for scientific translation. Gerusalem, 1965*.

*P. Clark, R. Klossner, L. Kologe*. Tidal Energy, CAUSE 2003: Final Project.

*Waterpower Laboratory*. Publications. Norway.

*US Army Corps of Engineers Commander*. Engineer manuals. *USACE Publication Depot, 2803 52nd Ave. Hyattsville, MD*.

*C. G. Pandya*. With policies both in US and Europe planning for a systematic exploitation of renewable energy on a strategic scale, the stage is all set now for the fuller development of tidal power on a world wide scale. *Center for Environmental Planning & Technology, Ahmedabad, India. 2006*.

*G. Bryden, S. Naik, P. Fraenkel and C. R. Bullen*. Matching tidal current plants to local flow conditions. *Energy*, Vol. 23, No. 9, September 1998 , pp. 699-709(11).

*J. A. Clarke, A. D. Grant and C. M. Johnstone*. Output Characteristics of Tidal Current Power Stations. *Renewable Energy*, Vol. 30, Issue 11, September 2005, pp. 1713-1731.

*A. N. Gorban, A. M. Gorlov, V. M. Silantyev*. Limits of the Turbine Efficiency for Free Fluid Flow, *ASME Journal of Energy Resources Technology*, 123, pp.311-317. 2001.

- A. M. Gorlov. Helical turbine for hydropower.
- D. P. Coiro, S. Melone, F. Montella. Energia pulita dalle correnti marine: aspetti tecnici ed economici.
- L. Guittet, M. Kusulja, T. Maitre. Setting up of an experiment to test vertical axis water turbines.
- Verdant Power Canada ULC. Technology Evaluation of Existing and Emerging Technologies Water Current Turbines for River Applications.
- Office for the coordination of humanitarian. 2006 flash appeal, Guinea-Bissau.
- Comunicação nacional inicial da Guiné-Bissau sobre as mudanças climáticas.
- Guinea-Bissau-Water And Energy Project. 1997.
- Investment Conference in Construction & Civil Engineering Central & West Africa. Sector profile.
- S. Diop. La cote ouest-africaine, du Saloum à la Mellacorie. Paris: Institut français de recherche scientifique pour le développement en coopération. ORSTOM, 1990.
- Central Intelligence Agency (CIA). The World factbook.
- G. Seminara. Dispense delle lezioni, A.A. 2002-03. Università degli Studi di Genova - D.I.C.A.T.
- I. Mantica. Lezioni di costruzioni idrauliche, appunti tratti dalle lezioni tenute nell' A.A. 1992/93. Università degli Studi di Ancona - Istituto di Idraulica.
- G. Vignoli. Modelling the morphodynamics of tidal Channels. Università degli Studi di Trento, Italia, February 2005 ISBN: 88-8443-086-0.
- S. Lanzoni, G. Seminara. Long term evolution and morphodynamic equilibrium of tidal channels. *Journal of geophysical research*, vol. 107, no. c1,10.1029/2000jc000468, 2002.
- N. Tambroni, P. K. Stansby and G. Seminara. Modelling the morphodynamics of tidal inlets.
- N. Tambroni and G. Seminara. Are inlets responsible for the morphological degradation of Venice Lagoon? *Journal of geophysical research*, vol. 111, F03013, doi: 10.1029/2005JF000334, 2006.
- E. Marchi. Sulla stabilità delle bocche lagunari a marea. *Rend. Fis. Acc. Lincei 1*, 137–150, 1990.

## References

*E. Baddour.* Energy from waves and tidal currents. *Institute for Ocean Technology. National Research Council, August 2004.*

*I.G. Bryden, D.M. Macfarlane.* The utilization of short term energy storage with tidal current generation system. *Energy 25 (2000) 893-907.*

*Ponte di Archimede S.p.A.* Kobold turbine in the Strait of Messina, appraisal of environmental macro/micro economics, realizing wider socio-economic benefit. *2007 Report.*

*Verdant Power Canada ULC.* Technology evaluation of existing and emerging technologies. Water current turbines for river applications. *2006.*

## **Ringraziamenti**

Per concludere vorremmo ringraziare le molte persone che ci hanno aiutato nella realizzazione di questa tesi, che hanno creduto in questo progetto un po' "ambizioso", che ci hanno fornito informazioni tecniche sulle varie tecnologie da noi studiate o che semplicemente si sono interessate al nostro lavoro.

In primis dobbiamo ringraziare il Prof. Michele Bolla Pittaluga per la sua disponibilità, per l'entusiasmo e il coinvolgimento con cui ci ha seguito.

In secondo luogo vorremmo ringraziare il Prof. Giovanni Seminara per l'interesse e la fiducia che ha dimostrato nel nostro lavoro.

Naturalmente grazie a Danilo Marra che ci ha introdotto a questo lavoro e ci ha messo in contatto con PS 76; un grazie particolare a Nicoletta Tambroni per averci fornito i codici numerici utilizzati nell'analisi degli inlet, indispensabili alla realizzazione di buona parte del lavoro.

Grazie, poi a tutti gli "amici" sparsi per il mondo, che hanno gentilmente risposto alle nostre domande: Josh Thomas e Edward Kurth (Lucid Energy Technologies LLC), Helena Eriksson (Ponte di Archimede International S.p.a), Steve Gregory (Alternative Hydro Solutions Ltd) e tutti gli ingegneri del forum EnergeticAmbiente.it.

Grazie infine ai genitori, agli amici e ai compagni di studio che ci hanno sostenuto (e a volte sopportato) in questi intensi anni di studio!





